Step Efficient Synthesis of 3,4-Dioxygenated Quinolones Enabled by Aryne Chemistry

Inaugural Dissertation
to obtain the academic degree
Doctor rerum naturalium (Dr. rer. nat.)

Submitted to the Department of Biology, Chemistry, Pharmacy
of Freie Universität Berlin

By
Johannes Schwan
from Berlin

June 2020

Hereby, I declare that the submitted thesis is my own work and was prepared autonomously without the help of other sources than the ones cited and acknowledged. The work was not submitted to any prior doctoral procedure.

Johannes Schwan, June 2020

The following work was carried out within the research group of Prof. Dr. MATHIAS CHRISTMANN from February 2015 until December 2019 at the Institute of Chemistry and Biochemistry of the Freie Universität Berlin.

Date of Disputation: 01.10.2020

1st reviewer: Prof. Dr. MATHIAS CHRISTMANN
(Institute of Chemistry and Biochemistry, Freie Universität Berlin)
2nd reviewer: Prof. Dr. PHILIPP HERETSCH
(Institute of Chemistry and Biochemistry, Freie Universität Berlin)

„Das Reich der Freiheit beginnt in der Tat erst da, wo das Arbeiten, das durch Not und äußere Zweckmäßigkeit bestimmt ist, aufhört."

– Karl Marx

Parts of this dissertation have been published in:

Schwan, J.; Christmann, M. *Chem. Soc. Rev.* **2018**, *47*, 7985–7995.

Schwan, J.; Kleoff, M.; Hartmayer, B.; Heretsch, P.; Christmann, M. *Org. Lett.* **2018**, *20*, 7661–7664.

Schwan, J.; Kleoff, M.; Heretsch, P.; Christmann, M. *Org. Lett.* **2020**, *22*, 675–678.

Content

Danksagung

Zunächst möchte ich mich bei Herrn Professor Mathias Christmann bedanken. In Ihrem Arbeitskreis haben Sie mir die Möglichkeit gegeben, ein spannendes Thema selbstbestimmt und frei zu bearbeiten. Auch möchte ich mich bei Ihnen für Ihr Vertrauen bedanken, wodurch es mir möglich war, Flowchemie in Ihrer Arbeitsgruppe als neue Synthesetechnik zu etablieren. Dies wäre ohne die Anschaffung von kostspieligem Equipment nicht möglich gewesen. Außerdem möchte ich Ihnen meinen besonderen Dank für Ihre Rücksichtnahme auf meine Familienplanung aussprechen. Es ist leider auch heute nicht selbstverständlich, dass ein Arbeitsgruppenleiter mit so viel Verständnis und Unterstützung auf das Elternwerden einer seiner Mitarbeiter reagiert. In diesem Zusammenhang möchte ich Ihnen ebenfalls dafür danken, dass sie mir meine Mechaniker-Eskapaden an meinem Bulli haben durchgehen lassen.

Weiterhin möchte ich Professor Philipp Heretsch danken – nicht nur für die Übernahme des Zweitgutachtens, sondern auch für die freundschaftliche und konstruktive Zusammenarbeit, sei es beim Überarbeiten der Manuskripte oder bei präparativen Problemen im Labor.

Mein Dank gilt darüber hinaus allen Mitarbeitern der Arbeitsgruppen Christmann und Heretsch sowie insbesondere meinen Forschungspraktikanten und Bachelorstudenten: Bence Hartmayer, Niklas Pontesegger, Klaus Omoregbee, Dilcan Dirican und Jan-Marwin Wollschläger.

Außerdem möchte ich Dr. Reinhold Zimmer für sein stets offenes Ohr für Probleme und Klagen, sowie die vielen Korrekturarbeiten und zahllosen Bestellungen danken, die Du in den Jahren für mich durchgeführt hast.

Einen weiteren wichtigen Baustein für den erfolgreichen Abschluss meiner Projekte lieferte Christiane Groneberg. Durch Deine Expertise gelang es Dir, fast alle meine kleinen und größeren Trennprobleme zu lösen. Ebenso möchte ich dem gesamten Team der NMR- und MS-Core Facility für Ihre zahllosen Analysen danken.

Weiterhin möchte ich der DFG für mein einjähriges Stipendium zu Beginn meiner Promotion danken.

Einen besonderen Platz in dieser Arbeit nimmt Merlin Kleoff ein. Ohne Dich wäre diese Promotion in dieser Form sicher nicht möglich gewesen. Durch unsere vielen gemeinsamen Projekte sind wir zusammen auch persönlich gewachsen und konnten beide viel voneinander lernen. Du bist als Forschungspraktikant in einer dunklen Stunde meiner Promotion zu mir gekommen und zusammen haben wir das Ruder herumreißen können. Ich bin sehr stolz auf unsere gemeinsame Arbeit.

Neben den vielen Helfern an der Uni möchte ich aber auch meinen privaten Unterstützern danken. Meine Familie gab mir in den vergangenen Jahren meines Studiums und meiner Promotion stets Rückhalt und Unterstützung, ohne die ich diese Promotion nicht hätte durchführen können. Dabei

haben meine Eltern sicher so manche ruhelose Stunde durchleben müssen, ob Ihr Sohn denn nun irgendwann noch seine Promotion wird abschließen können. An Eurem Vertrauen zu mir hat es Euch aber nie gemangelt.
Zuletzt möchte ich meiner Frau Jill danken. Auch ohne Dich wäre diese Promotion nicht möglich gewesen. Schon vor der Geburt unserer Tochter hast Du mir stehts den Rücken frei gehalten und mich aufgebaut, wenn ich von der Arbeit nichts mehr wissen wollte. Aber vor allem jetzt, wo unsere Tochter rund um die Uhr unsere Aufmerksamkeit fordert, wäre das Schreiben dieser Arbeit ohne Dich undenkbar gewesen.

Abbreviations

AIBN	azobisisobutyronitrile
API	active pharmaceutical ingredient
BPR	back-pressure regulator
Boc	tert-butyloxycarbonyl
cat.	catalyst
Da	Damköhler number
DBU	1,8-diazabicyclo[5.4.0]undec-7-ene
DFT	density functional theory
DMAP	4-dimethylaminopyridine
DMF	dimethylformamide
DMSO	dimethylsulfoxide
DOS	design-of-experiment
E	electrophile
ECD	electronic circular dichroism
EDDA	ethylenediamine diacetate
EU	European Union
Eq.	equation
d.r.	diastereomeric ratio
Het	heteroatom
HMDS	hexamethyldisilazane
HOMO	highest occupied molecular orbital
Imid.	imidazole
IUPAC	International Union of Pure and Applied Chemistry
LLS	längste lineare Sequenz or longest linear sequence
LUMO	lowest unoccupied molecular orbital
NBS	*N*-bromosuccinimide
NRPS	non-ribosomal peptide synthetase
Nu	nucleophile
OY	overall yield
ox.	oxidation
TBAF	tetrabutylammonium fluoride
TBDPSCl	tert-butyldiphenylsilyl chloride
TBS	tert-butyldimethylsilyl

TEMPO	(2,2,6,6-tetramethylpiperidin-1-yl)oxyl
THC	tetrahydrocannabinol
THF	tetrahydrofuran
TMS	trimethylsilyl

Zusammenfassung

Die vorliegende Arbeit beschreibt die Synthese von 3,4-dioxygenierten Chinolinon-Naturstoffen. Zunächst wurden repräsentative Naturstoffsynthesen bezüglich ihrer Stufeneffizienz analysiert.[1] Hierzu wurde ein Farbschema entwickelt, mit dessen Hilfe die Stufeneffizienz einer Synthese grafisch veranschaulicht werden kann. So konnten einige besonders erfolgreiche Strategien zur stufeneffizienten Naturstoffsynthese identifiziert werden. Dazu zählen die retrosynthetische Teilung des Zielmoleküls in möglichst gleich große und komplexe Fragmente, das Vermeiden von nicht-strategischen Redoxmanipulationen und die Minimierung von Austauschreaktionen funktioneller Gruppen, als auch die Verwendung von milden Methoden, welche mehrere Bindungen innerhalb eines einzelnen Schrittes knüpfen.

Die so gewonnenen Erkenntnisse wurden auf die Naturstoffklasse der 3,4-dioxygenierten Chinolinone übertragen. Es wurden eine diastereoselektive Aldol-Zyklisierung und eine Arin-Insertion in ein unsymmetrisches Imid als geeignete Methoden zur Darstellung der Chinolinon-Naturstoffe identifiziert (Schema 1a).[2]

So wurde das Zielmolekül aus zwei ähnlich großen Fragmenten aufgebaut. Zugleich konnten durch die Arin-Insertion zwei Kohlenstoff–σ-Bindungen in einem Schritt geknüpft werden. Die Durchführung der Arin-Insertion im kontinuierlichen Flussreaktor verkürzte die Reaktionszeit auf wenige Minuten, wohingegen längere Reaktionszeiten und geringere Ausbeuten bei der Durchführung im Kolben beobachtet wurden. Weiterhin erlaubte die Synthesestrategie eine Variation sowohl des Arins als auch des Imids, wodurch eine Vielzahl verschiedener 3,4-dioxygenierter Chinolinon-Naturstoffe synthetisiert werden konnte. Insgesamt wurden sieben Naturstoffe in einer bis drei Stufen dargestellt. Diese umfassen (±)-Peniprechinolon, (±)-Aflachinolone E und F, (±)-6-Deoxyaflachinolon E, die (±)-Chinolinone A und B, sowie (±)-Aniduchinolon C (Schema 1b).[2]

Die gewählte Synthesestrategie folgt dem Idealitäts-Prinzip und nutzt fast ausschließlich Reaktionen, die in strategischen Bindungsschlüssen resultieren.

Schema 1. Synthese von 3,4-dioxygenierten Chinolinonen via Arin-Insertion in unsymmetrische Imide.

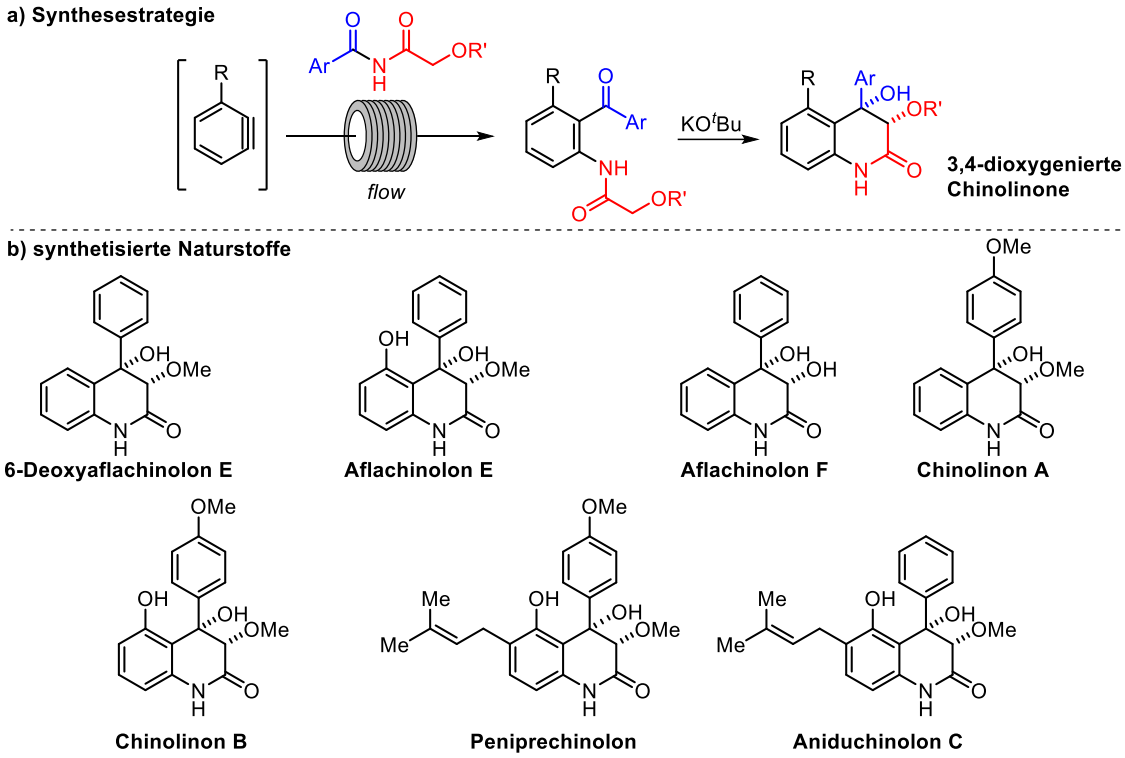

Durch die zuvor entwickelte Arin-Strategie konnten die zytotoxischen Yaechinolone J1 und J2 in nur fünf Stufen in der längsten linearen Sequenz (LLS) dargestellt werden (Schema 2).[3] Das Chromen-Motiv wurde bereits im ersten Schritt durch eine organokatalytische Tandem-KNOEVENAGEL-Electrozyklisierung von 2-Bromresorcin und Citral aufgebaut. Das so erhaltene Chromen **1** wurde anschließend doppelt silyliert, einer retro-BROOK-Umlagerung unterzogen und anschließend mit Trifluormethansulfonsäureanhydrid abgefangen. Der so erhaltene Arin-Precursor **2** wurde anschließend in Gegenwart von Cäsiumfluorid mit dem Imid **3** umgesetzt. Die Insertion verlief mit guter Regioselektivität von 3 : 1 für das gewünschte Isomer **4**. Die Naturstoffe Yaechinolon J1 und J2 wurden abschließend durch eine Aldol-Zyklisierung erhalten, wobei jedoch keine Diastereoselektivität bezüglich des quaternären Stereozentrums an C-3“ beobachtet wurde.

Schema 2. Fünf-Stufen Synthese von Yaechinolon J1 und J2.

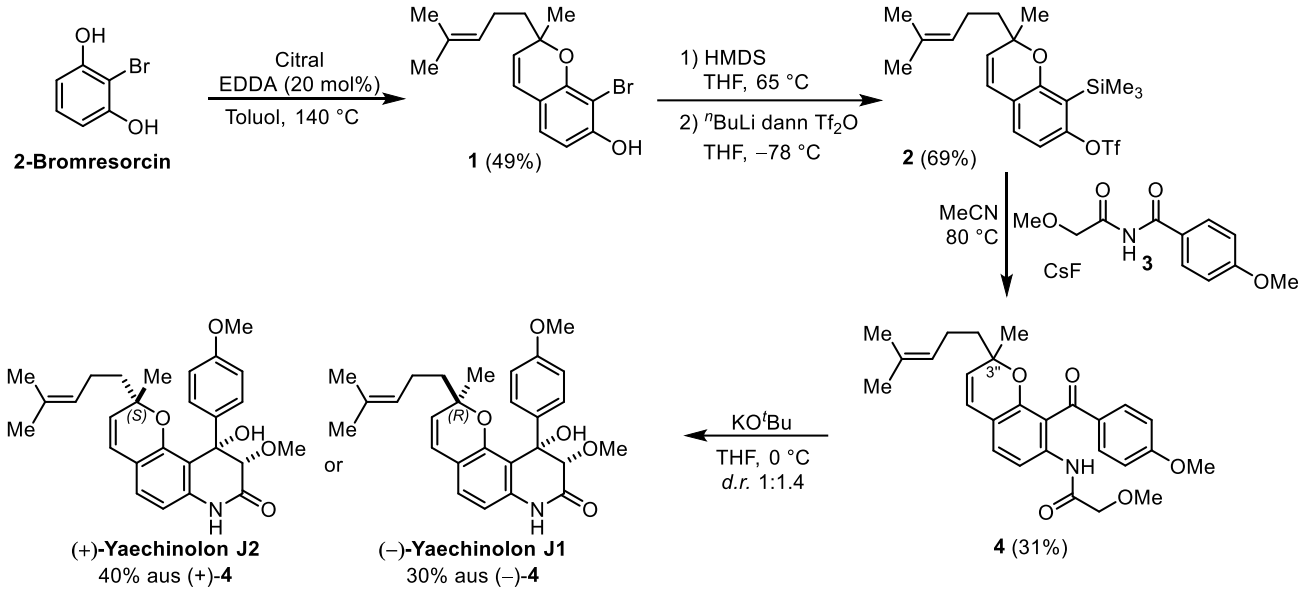

Abstract

In the present thesis, the step efficient synthesis of 3,4-dioxygenated quinolinones is described. Initially, step efficient syntheses of other natural products were analyzed by using a color-coded flow chart presentation.[1] Thus, particularly powerful strategies were identified. These included disconnection in equally sized and complex substructures, avoidance of non-strategic redox- and functional group interconversions, as well as the usage of functional group tolerant transformations capable of forging multiple bonds in a single step.

By applying these principles to the natural product class of 3,4-dioxygenated quinolinones, an aryne insertion into an unsymmetric imide followed by a diastereoselective aldol reaction was recognized (Scheme 1a). The target was thus built up from two equally sized molecules whilst the aryne insertion yielded two new carbon – σ-bonds in a single step. When performed in continuous flow, the reaction proceeded within minutes, while lower yields and longer reaction times were observed in batch. Furthermore, both aryne and imide could easily be varied so that a multitude of differently substituted 3,4-dioxygenated quinolinones were synthesized. In total, seven natural products, including (±)-peniprequinolone, (±)-aflaquinolones E and F, (±)-6-deoxyaflaquinolone E, (±)-quinolinones A and B, and (±)-aniduquinolone C were synthesized in one to three steps (Scheme 1b).[2]

Scheme 1. Synthesis of 3,4-dioxygenated quinolinones via aryne insertions into unsymmetric imides.

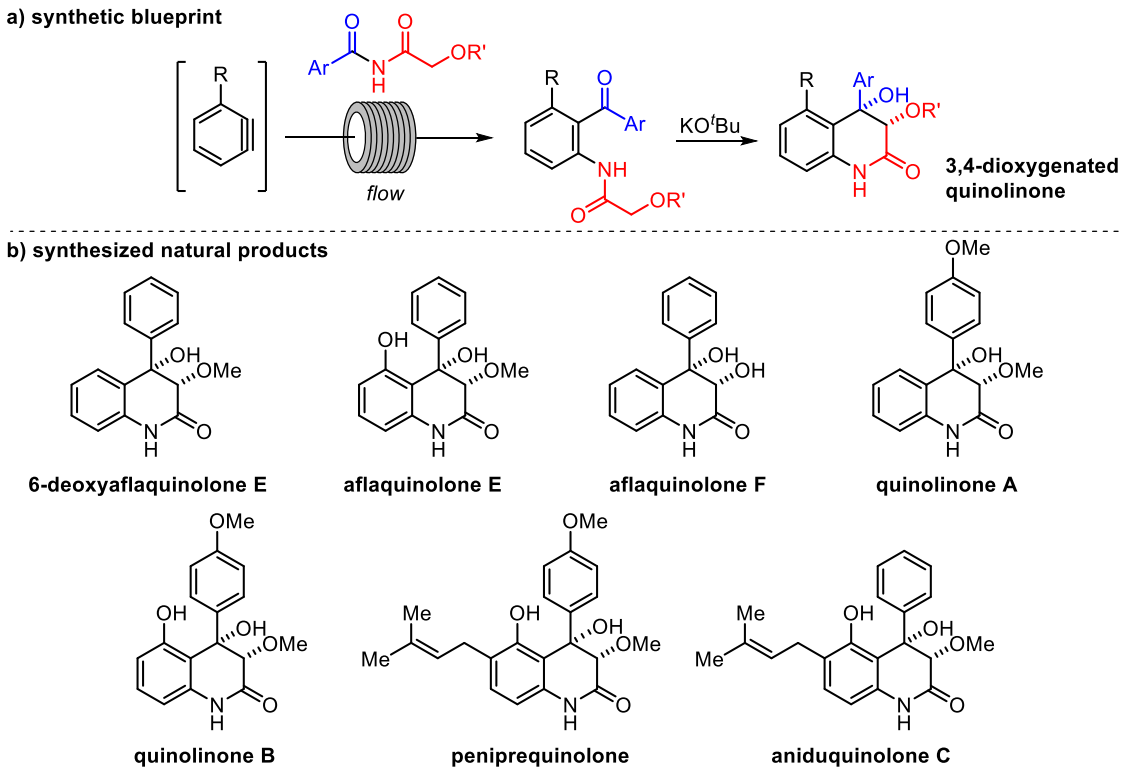

Following this synthetic blueprint, a step efficient synthesis of yaequinolones J1 and J2 was realized. Using the previously developed aryne strategy, the cytotoxic yaequinolones J1 and J2 were synthesized in only five steps in the LLS (Scheme 2).[3] The chromene motif was installed in the first step by an organocatalytic tandem KNOEVENAGEL electrocyclization of citral and 2-bromoresorcinol. The resulting chromene **1** was then transformed to the aryne precursor **2** via double silylation followed by a retro-BROOK rearrangement and quenching with triflic anhydride. The aryne insertion of imide **3** proceeded with good regioselectivity of 3:1 in favor of the desired regioisomer **4**. The final aldol cyclization delivered yaequinolones J1 and J2, albeit with no diastereoselectivity regarding the quaternary stereocenter at C-3''.

The approach adheres to the ideality principle, using almost exclusively strategic bond-forming reactions.

Scheme 2. Five-step synthesis of yaequinolones J1 and J2.

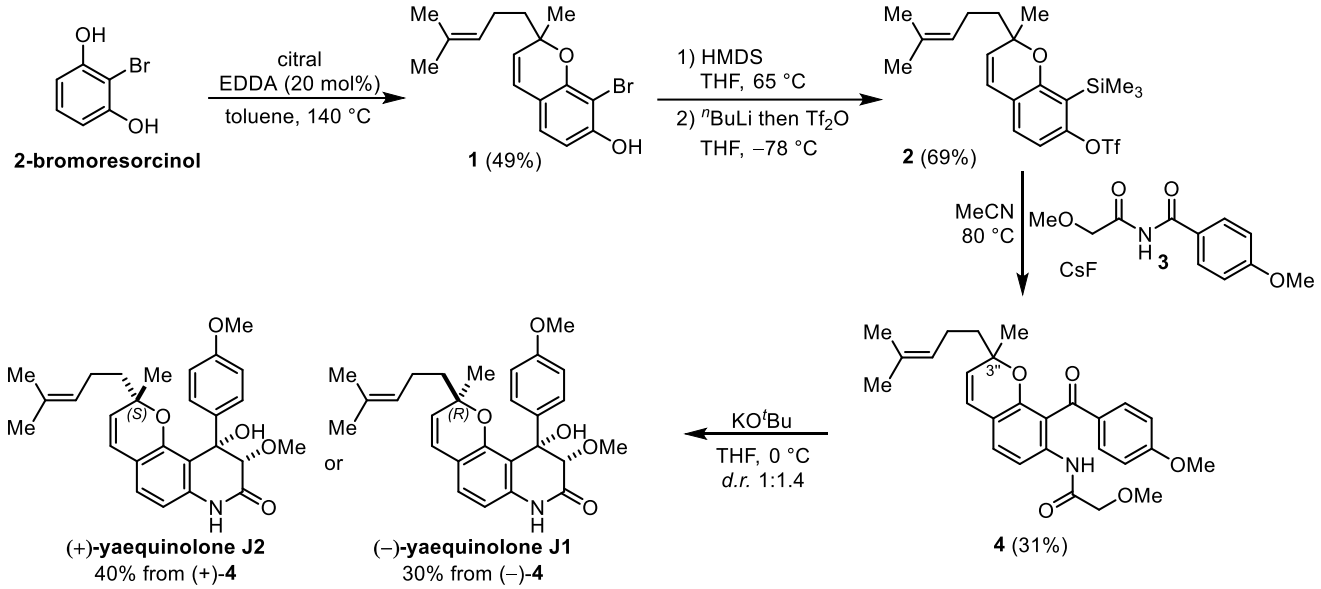

1. Natural Product Synthesis – General Aspects

Mankind has been using plant extracts, ferments and other natural materials since thousands of years for the treatment of numerous diseases and complaints, but also as drugs in religious and social contexts or as toxins to kill prey or rivals. In most cases, the biological activities of these materials can be traced back to small molecules. These molecules are serving a specific function for their producing organism that is not necessarily related to its growth or survival but rather fulfills other functions, such as being part of a molecular defense mechanism or to attract sexual partners for reproduction, to only name a few. These small molecules are called natural products.[4] Famous examples of natural products include strychnine, an alkaloid found in the seeds of the poison-nut tree (S*trychnos nux-vomica*)[5] or tetrahydrocannabinol (THC),[6] the main active ingredient of cannabis (Figure 1). Natural products constitute a gigantic pool of structural diversity, that makes them irreplaceable for modern drug discovery: From the 1,562 new drugs approved between 1981 and 2014, 65% were based on or inspired by natural products.[7]

Figure 1. Structures and producing organisms of two famous natural products: (−)-Δ⁹-*trans*-tetrahydrocannabinol and (−)-strychnine.

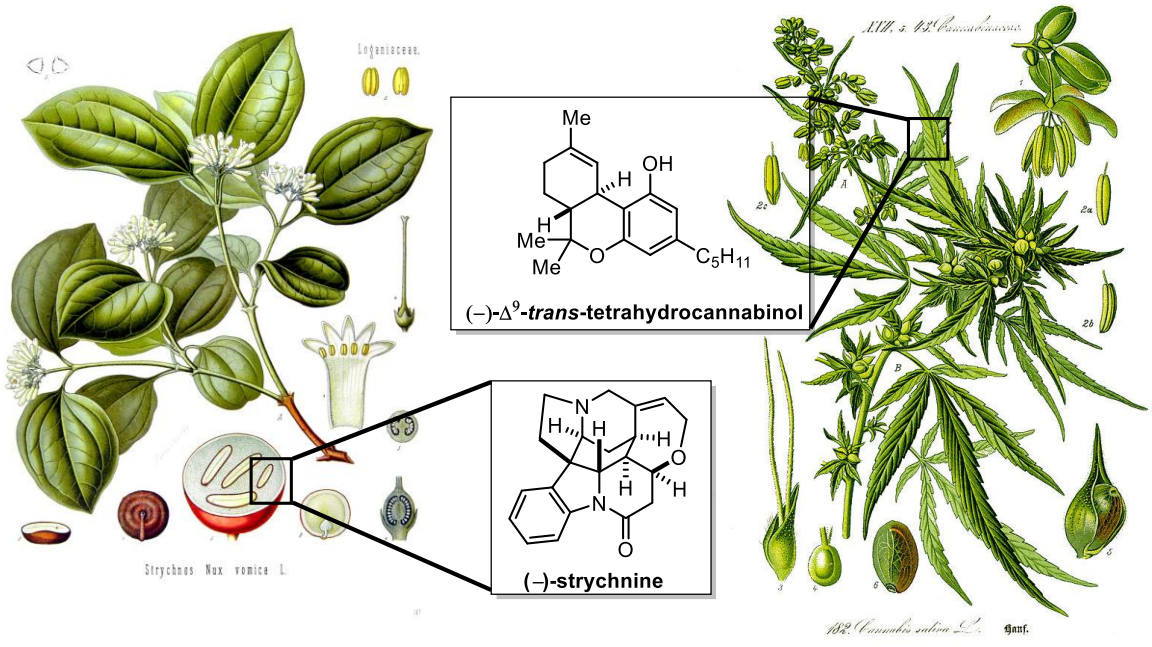

Apart from their importance for drug development, their synthesis in the laboratory has been a key research field of organic chemistry since the early 20th century until today.[8] Being able to synthesize a natural product can be advantageous for several reasons. The amount of natural product that can be isolated from the producing organism is usually quite low, which makes its production uneconomic. An illustrative example is the discovery of taxol, one of the most important drugs in chemotherapy. Taxol was first isolated in 1967 from the bark of the pacific jew tree (*Taxus brevifolia*).[9] In order to obtain 1 kg of taxol, 3,000 of the rare pacific jew trees had to be harvested. Only due to the development of a semisynthetic route, it was possible to satisfy the global demand in a much cheaper and more sustainable way.

Another benefit of natural product synthesis is the possibility to derivatize the target structure to access structures which cannot be made from the natural product itself. This greatly facilitates pharmacological research and can help to better understand the mode of action of a certain natural product or affect its pharmacological properties.

Another possible reason for synthesizing a natural product is the exact elucidation of its structure. Even though this function is largely supplanted by analytical methods today, it still plays a crucial role, as it can be seen from the large number of natural products, whose structures have been revised by means of total synthesis.[10]

Despite the described benefits of natural product synthesis, some of the work that has been conducted in the past cannot be rationalized by these criteria. An example of a natural product that has been synthesized multiple times and that hardly meets any of the above stated reasons for natural product synthesis is the toxic alkaloid strychnine. The structure of strychnine was confirmed in 1951 by X-ray crystallography,[11] three years before its first total synthesis by WOODWARD was realized.[12] The complex alkaloid is readily available by isolation (up to 1.5 wt% in the seeds of *Strycnos nux-vomica)*, so production of larger quantities is easiest by cultivating the plant. Further syntheses could potentially provide new opportunities to derivatize the core structure in order to improve its pharmacological properties, but due to the high toxicity of strychnine, its application in medicine is limited. Nevertheless, strychnine has been synthesized by more than a dozen different research groups.[13] The reason for the numerous published syntheses of strychnine could simply be explained by the academic challenge of such an endeavor. Designing and conducting syntheses of complex molecules such as strychnine can advance the science of chemical synthesis as a whole; be it by inventing new chemical transformations or by developing new synthetic strategies.

Natural product synthesis is even regarded as a form of art by some practitioners of the field, often described with adjectives uncommon in natural sciences (e.g. “elegant”, “creative”, or “beautiful molecular architecture”).[8,14] When awarded with the Nobel Prize in Chemistry in 1965, A. FREDA

(Member of the Nobel Prize Committee) introduced R. B. WOODWARD with the words: "It is sometimes said that organic synthesis is at the same time an exact science and a fine art. Here, nature is the uncontested master, but I dare say that the prize-winner of this year, Prof. WOODWARD, is a good second."[15] This underscores the perception of synthesis as a form of art but also makes a comparison in terms of quality. However, the quality of art is hard to measure and greatly depends on the personal preference of the viewer (or listener). This is also true for natural product synthesis, where over the last three decades, different metrics have evolved to evaluate the efficiency of synthetic strategies.

2. Step Efficiency as the Key Metric in Natural Product Synthesis

2.1 Metrics of Synthetic Efficiency

Due to the growing arsenal of synthetic methods available to today's chemist, natural product synthesis is shifting its focus from how to make a target molecule towards how to make it in the most ''efficient'' way.[16] The metrics of synthetic efficiency are depending on the objective – a process chemist trying to make a compound on scale will have different priorities than a medicinal chemist aiming for structural diversity or a PhD student trying to synthesize a natural product for the first time.[1] Thus, different guidelines on how to rationalize natural product syntheses and how to measure efficiency have evolved, namely:[a]

- E-factor
- Atom economy
- Overall yield
- Redox economy
- Ideality or step efficiency

The E-factor is widely used in industry (not only chemical), and compares the output material to the sum of all waste, including reagents, solvents and reaction aids, such as filter- or column materials (eq. 1).[17]

$$E = \frac{\sum m(waste)}{m(product)} \qquad \text{(eq. 1)}$$

Typical E-factors of the chemical industry are depicted in table 1. As it can be seen, the E-factor of pharmaceuticals (which reflect natural products best) is the highest, meaning that very little product is obtained in comparison to the amount of waste that is generated. Although useful in industrial settings, the E-factor is of limited utility when it comes to natural product synthesis. The amount of waste per gram of natural product is typically not documented, at least in academia.

[a]The list is not comprehensive and summarizes strategies such as process mass intensity (PMI) or reaction mass efficiency under the term E-factor.

Also, the scale of a reaction drastically influences its E-factor. Furthermore, it is nearly impossible to implement the E-factor already at the planning stage of a natural product synthesis, as little information on yields, type of workup, concentration, etc. are available and are hard to predict.

Table 1. E-factors in the chemical industry[17b]

Industry Segment	t per annum	E-factor
Oil refining	$10^6 – 10^8$	<0.1
Bulk chemicals	$10^4 – 10^6$	<1–5
Fine chemicals	$10^2 – 10^4$	5–50
Pharmaceuticals	$10 – 10^3$	25– >100

Another metric often used to evaluate a synthesis or a method is atom economy. This metric compares the number of atoms in the product to the number of atoms on the left side of the reaction arrow. Thus, a step is regarded as atom economic, if all atoms of starting material and reagents end up in the product of the reaction.[18] A classic example of a reaction with perfect atom economy is the DIELS ALDER reaction. While this approach is useful when considering the efficiency of synthetic methods, it can be misleading in the context of natural product synthesis. For instance, the WITTIG reaction is considered to be a reaction with poor atom economy as it transfers only a small number of carbon atoms to the target while forming equimolar amounts of triphenylphosphine oxide (Ph_3PO) as a byproduct. However, it is a very powerful method to form carbon–carbon double bonds and can potentially save steps and improve the overall yield.

The overall yield is the most common way to compare synthetic efficiency. As yields are usually stated in scientific publications of natural product syntheses, the overall yield can easily be calculated in case it is not explicitly addressed. It also directly refers to the claim of the synthetic community, that synthetic natural products deliver better accessibility than natural sources can provide. The overall yield is also linked to the number of steps in the LLS, as it drops exponentially with the number of steps (figure 2).[19]

Figure 2. Exponential decrease of the overall yield with the number of steps at an average yield of 70% per step.

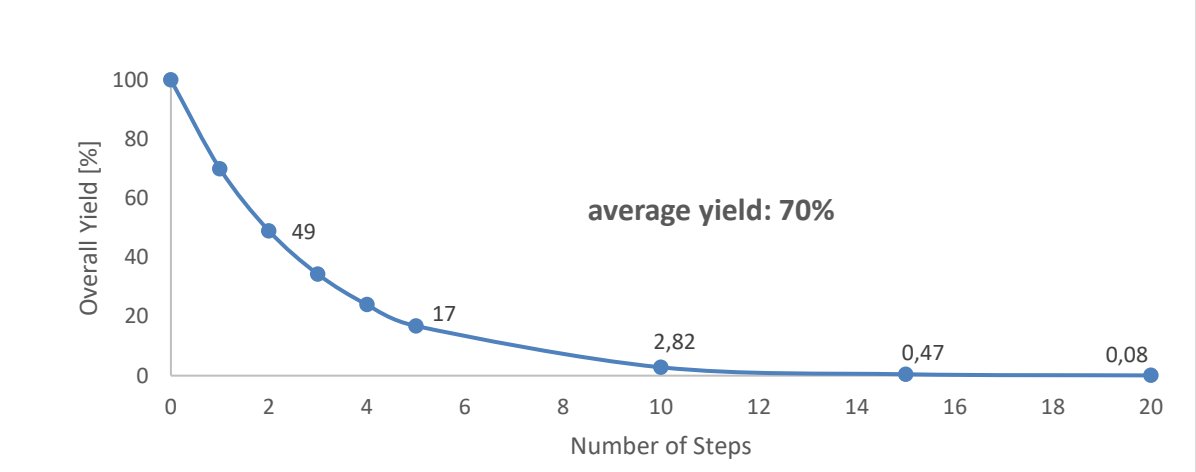

In order to achieve a high overall yield, two strategies can be employed: One is the use of well established methods that are known to deliver good yields, such as click reactions. The other strategy is to minimize the number of steps. The later strategy is considered to be more important, since the step count influences the overall yield exponentially (*vide supra*). Furthermore, both strategies can contradict each other, as step efficient methods (e.g. those forming multiple bonds at the same time) often deliver poorer yields compared to high yielding classical methods that may require protection groups or other additional steps.

Redox economy directly contributes to step-efficiency. It refers to the endeavors to reduce the number of non-strategic (those that do not set stereochemistry or are not skeleton-building) or corrective oxidation and reduction steps.[20] In an extreme case, a synthesis may be free of any redox reactions. Such syntheses are called *isohypsic*.[21] Redox economy does not forbid the use of redox reactions per se, but aims to yield a synthesis in which the oxidation state is either steadily increasing or decreasing from the starting material towards the final product (Figure 3).

Figure 3. Schematic view of redox economy in a synthetic sequence.[20]

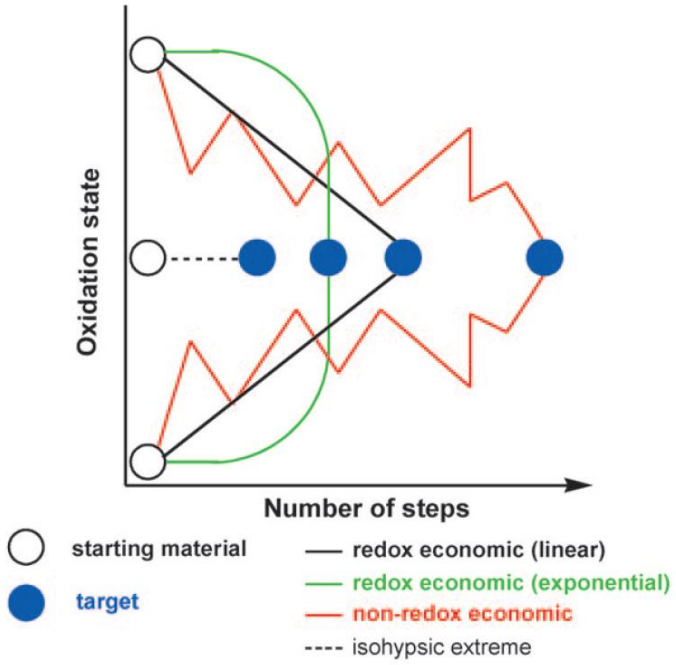

There is a plethora of skeleton-forming reactions available that do not require redox manipulations. These include rearrangements, most transition metal catalyzed cross couplings, and pericyclic reactions. On the other hand, redox steps can quickly accumulate when accessing aldehydes, the classically preferred starting point for skeleton-forming reactions, such as organometallic additions or aldol reactions (Scheme 3). Due to its high reactivity, aldehydes are usually generated directly prior to the construction reaction by either oxidation of primary alcohols or oxidative cleavage of 1,2-diols or by the reduction of an ester. The reduction of esters is more common but not straight forward. Often, the ester is first reduced to the primary alcohol, which is then oxidized to the aldehyde, resulting in two redox steps to arrive at the desired oxidation state. In contrast, WEINREB amides[22] and thioesters[23] can readily be reduced to aldehydes and should therefore be preferred whenever they can be incorporated in the starting material. Other more redox-economic aldehyde-precursors are available, e.g. terminal alkynes or alkenes, that can be hydrated[24] or hydroformylated.[25] An even more redox economic method is the hydrogen-mediated C–C bond formation.[26] Here, the carbonyl is only a transient species that is formed *in situ* and directly consumed in an enantioselective C–C bond formation. The overall reaction is redox neutral as it starts with a primary alcohol and ends with a secondary alcohol, whilst forming a new stereocenter.

Scheme 3. Comparison of different strategies for C–C bond formations via aldehydes.

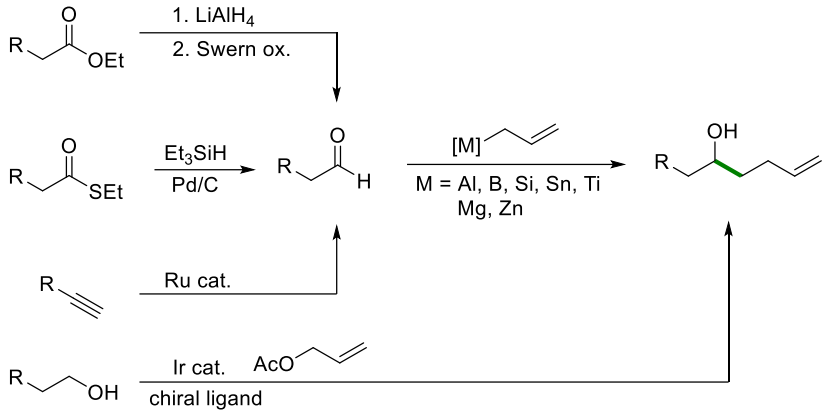

The most holistic strategy for the evaluation of synthetic efficiency is step economy.[16,27] This strategy simply aims at reducing the number of steps needed to reach a synthetic target to a minimum. In other words, all steps that do not form bonds present in the target should be avoided. A more tangible approach is provided by the ideality principle. The term was first coined by HENDRICKSON[21] and later specified by BARAN and GAICH.[28] There, steps are classified into desirable steps (C–C and C–Het-bond formations and strategic redox reactions) and undesirable steps (protection group manipulations, non-strategic redox reactions and functional group interconversions). When comparing the number of desirable steps to the total number of steps, a numeric value for the ideality of a synthesis can be derived. For biosynthetic sequences, this value often reaches 100% ideality, meaning that Nature is capable of using exclusively construction reactions without any intermediary functional group interconversions or non-strategic redox reactions. This has yet to be realized in natural product synthesis. Typical ideality values of modern syntheses are ranging between single digit values to values of 60% and more in some cases. In general, the more complex the target molecule, that means, the more functional groups and stereocenters are present, the lower is the ideality value of its synthesis. This is due to the fact that with increasing functionality, the requirements for functional group tolerant methods are also growing. Hence, it becomes gradually more difficult to design such syntheses without the use of protection groups and functional group interconversions.

When comparing different syntheses regarding their step count, one must first define what is considered as a single step. This seemingly trivial question has erupted in controversial discussions in recent years.[29] The IUPAC defines an elementary reaction step as the pathway between two local minima on the reaction ordinate.[30] This definition stands in contrast to the commonly encountered step counting performed by practitioners of the field and seems more suitable for the discussion of reaction mechanisms. A more practical definition considers a step as the sum of all transformations that happen within the same flask and that is terminated by a purification procedure.[26,31] This way of counting can be skewed by the telescoping of single

transformations into one-pot procedures. Although synthetic efficiency benefits from telescoping, it does not overcome the exponential loss of yield with the number of steps. Hence, a definition between these two extremes shall be used.

Furthermore, none of the above-mentioned strategies deliver a spatial differentiation of a synthetic sequence, meaning that the evaluation considers the synthesis as a whole. While this might be useful when comparing existing syntheses, it is less helpful when planning a synthesis. Therefore, the concept of ideality shall be transformed into a graphical synthetic flow chart, where each step is symbolized by an icon of a certain color (Scheme 4). Those colors are referring to the different step-classifications of the ideality principle. This allows the planner to identify those sequences of high ideality and those parts of the synthesis, that require redesigning. By examining different step-efficient syntheses of the past, particularly successful strategies shall be identified. Those might include the separation of the target molecule into equally sized substructures and the usage of methods that can form multiple bonds in a single step.

Scheme 4. Flow-Chart Presentation of the synthesis of (–)-englerin A by Christmann and co-workers.[32]

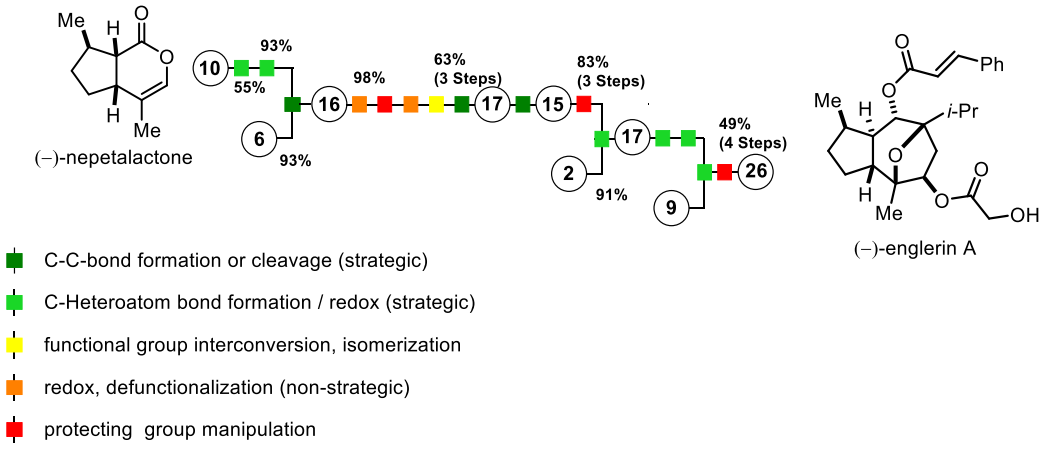

2.2 Arynes in the Context of Step Efficient Synthesis

A good example of methodology capable of forming multiple bonds at the same time is the field of aryne chemistry.[33] Once regarded as peculiarities, arynes have gained substantial attention as valuable building blocks in recent years.[34] They are formally obtained by the removal of two adjacent substituents from an aromatic ring leading to a highly strained alkyne within a six-membered ring.[35] Due to the fact that the alkyne moiety cannot adopt a linear geometry, one π-bond is formed by the overlap of two sp^2-orbitals outside the aromatic ring, making this bond extremely weak, causing a HOMO-LUMO gap of only 1.5 eV, and resulting in a partial radical character.[35,36] Originally, arynes were prepared under harsh conditions from aryl halides and a strong base, such as sodium amide, resulting in poor functional group tolerance (scheme 5, left side). In the following decades, more and more precursors have been developed that allow aryne-formation to occur under milder conditions. The most successful and most widely used aryne precursors today are 2-(trimethylsilyl)phenyl trifluoromethanesulfonates, also referred to as KOBAYASHI aryne precursors.[37] The trimethylsilyl (TMS) group can easily be cleaved by a fluoride source (such as TBAF), causing the resulting phenyl anion to eliminate trifluoromethanesulfonate under formation of a triple bond. Besides from the KOBAYASHI aryne precursor, arynes can be generated from hypervalent iodine compounds such as **5** that can easily be prepared from *o*-bis(trimethylsilyl)benzene (**6**), iodobenzene diacetate and triflic acid.[38] Following the same principle as the KOBAYASHI aryne precursor, fluoride can induce cleavage of the C–Si-bond followed by elimination of the iodonium residue to form the formal triple bond. Apart from these methods, aryne generation from aryl bromides with strong bases is still used as a viable way of aryne generation with less sensitive substrates.[39]

Scheme 5. Summary of the most common ways to generate arynes

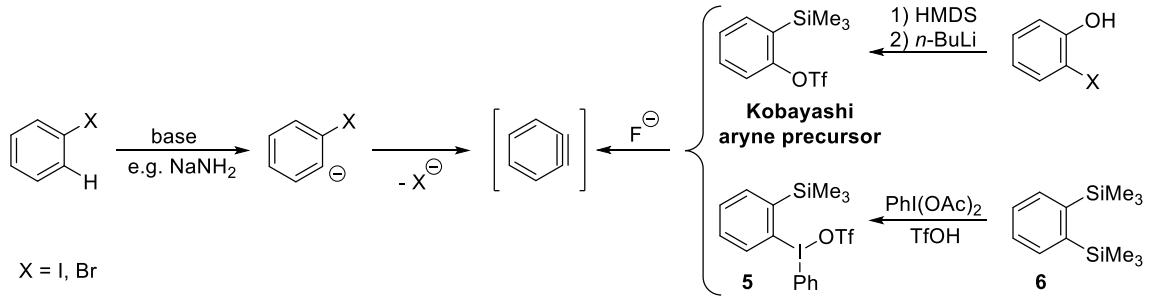

The high reactivity of arynes allows them to undergo several different reactions, rendering them as versatile building blocks. There are two main types of reactions arynes can undergo:

- Pericyclic reactions, including Diels-Alder reactions, [2+2] cycloadditions, 1,3- and 1,4-dipolar cycloadditions, and ene reactions
- Nucleophilic additions to arynes (and subsequent insertions into σ-bonds)

Arynes undergo several pericyclic reactions in an inter- or intramolecular mode that found numerous applications in organic synthesis.[40] Due to the high electrophilic character of arynes, the [4+2] addition is observed with a very wide range of dienes including extremely unreactive ones, such as benzene-derivatives.[41] Intramolecular Diels-Alder reactions of arynes were successfully applied in the synthesis of several natural products, such as lycorines[42] and phenanthridones.[43]

If a suitable nucleophile (Nu) is available, the aryne is readily attacked. The initially formed carbanion at the adjacent carbon is then either quenched by a proton to yield the arylated addition product, or can be trapped with external or internal electrophiles (E, Scheme 6, path a).[44] Soft nucleophiles (e.g. thiols) are particularly reactive, but also alcohols, amines, carbon nucleophiles (e.g. GRIGNARD-reagents), and even amides are adding to arynes.[44]

If nucleophile Nu and electrophile E are part of the same molecule and directly connected by a σ-bond, the overall outcome of the reaction is usually a formal insertion of the aryne into the Nu–E-σ-bond (Scheme 6, path b). Important examples of σ-bond insertions include the insertion into the σ-C–CO_2R bond of β-ketoesters,[45] and into the σ-C–N-bond of amides and urea-derivatives.[46] These reactions allow the simultaneous formation of two adjacent carbon-carbon or carbon-heteroatom-bonds in a single step and are therefore of great value for the step efficient synthesis of natural products.[47]

Scheme 6. Different modes of nucleophilic attacks on arynes. a) Nucleophilic attack followed by quenching with an external electrophile;[48] b) σ-bond insertion.[46]

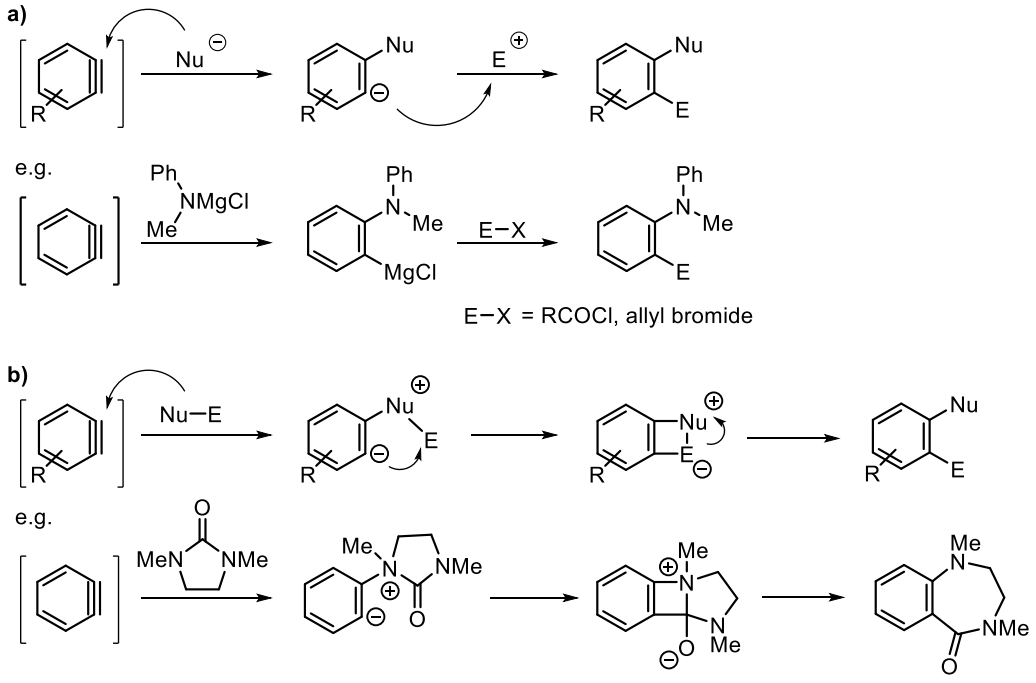

One example of a step efficient synthesis utilizing an aryne-insertion is the synthesis of cossonidine by SARPONG and co-workers.[49] The aryne insertion into a β-ketoester is used to construct a key 6-7-6 tricycle (**7**), thereby enlarging the cyclopentanone to a cycloheptanone (Scheme 7). As it can be seen in this example of a diterpenoid alkaloid, aryne chemistry can also be applied to natural products without benzene rings in their structure. Here, the benzene ring introduced by the aryne is later reduced by a BIRCH reduction.

Scheme 7. Retrosynthetic analysis of cossonidine by SARPONG et al. based on an aryne insertion into a C–C σ-bond of a β-ketoester.

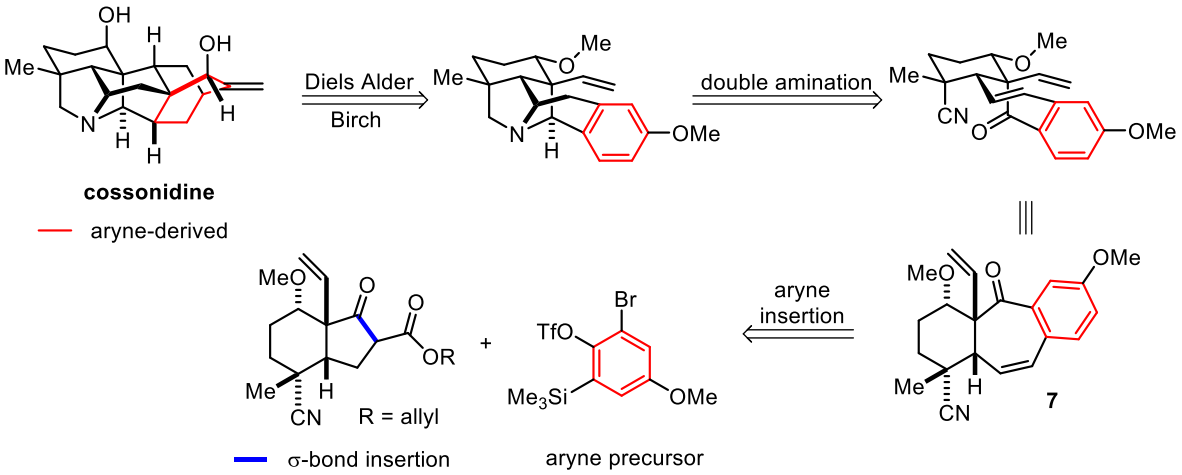

Although the KOBAYASHI aryne precursor itself is neither highly reactive nor explosive (as other aryne precursors are), the *in situ* formed aryne is a highly energetic intermediate that requires strict temperature control and rapid mixing to suppress side reactions.[50] Both requirements can be achieved using flow chemistry, yet there are only a few examples of arynes being generated in flow.[51]

2.3 Flow Chemistry as an Enabling Tool for Step Efficient Synthesis

Technology should serve mankind in order to enhance or facilitate the ability to reach a goal. In chemistry, microfluidic technologies emerged as a tool in order to aid chemists in the synthesis of molecules.

The concepts of continuously operating reactors were first used by process chemists but were then also adopted and expanded by research groups in academia and became known as flow chemistry.[52] Thus, flow chemistry has become an important tool in both industry and academia that offers a variety of advantages compared to batch reactions, such as a) improved heat and mass transfer; b) efficient radiation of photoreactions; c) increased capacity to run serial reactions and d) rapid mixing, to only name a few.[53]

Flow chemistry uses channels or tubing to conduct a chemical reaction in a continuous fashion rather than in a flask (batch-reaction). Conducting a reaction in flow offers unique control over reaction parameters such as time, temperature, pressure, stoichiometry, and mixing, thus enhancing reactivity or in some cases enabling new reactions impossible in batch.[53,54] A basic flow reaction of two reactants A and B features two pumps for the reagents, a mixing unit (e.g. a T-piece) and a reactor, consisting of a tube with a defined length and internal volume. At the end of the reactor, the mixture is either quenched or collected and submitted to further workup (Scheme 8). A back-pressure regulator (BPR) may be used if higher pressures than ambient pressure are required.

Scheme 8. Stages of a standard two-feed continuous flow reaction (adapted from ref. [53]).

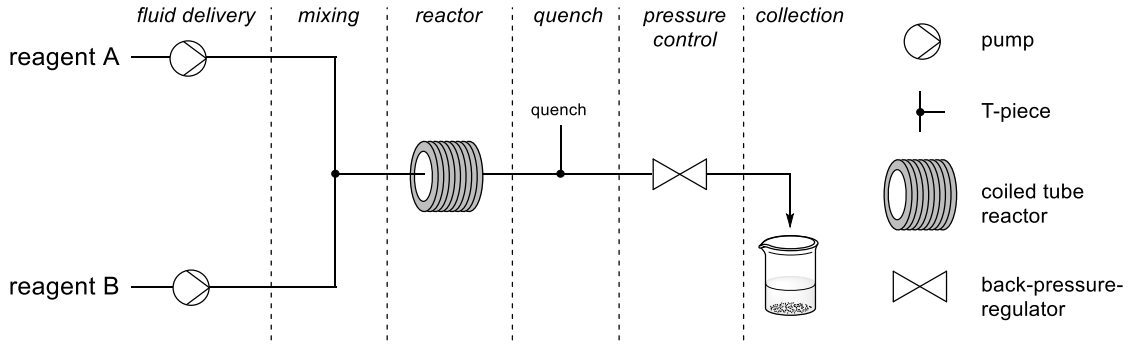

Although flow chemistry is not a “one-fits-all” solution to synthesis, there are certain reactions that can benefit from conducting them in flow (*vide supra*). Reactions that are highly exothermal are better controlled in flow due to the improved ratio of surface area to reactor volume and the resulting superior heat transfer.[55] Not only does this suppress side reactions, it also allows for a safe scale-up. Exothermal reactions pose a significant safety-concern during scale-up (risk of thermal run-away). As the scale of a reaction in a continuous flow-setup is primarily depending

on the duration of the run, scale-up is simply performed by operating the system for a longer amount of time, without changing any intrinsic reaction parameters, such as reactor volume or mixing. Due to the small reactor volumes of micro-fluidic flow-setups (µL- to mL-range), handling of dangerous compounds such as explosives is generally safer compared to large-volume batch reactors.[56] Multiphasic reactions (liquid–liquid and gas–liquid) also benefit from a flow-setup as the ratio of interfacial surface area to volume is increased. This interfacial surface area is crucial for phase transfer and can be rate-limiting.[53]

Another advantage of flow reactor tubing is its small diameter, which is beneficial in photoreactions. Photochemistry requires efficient irradiation of the reaction mixture. However, the light intensity drops exponentially with the path length l (LAMBERT-BEER Law, eq. 2).

$$log \frac{I_0}{I} = \varepsilon c l \qquad \text{(eq. 2)}$$

Thus, when irradiating a batch-reaction, only the outermost part of the reaction mixture is exposed to light, whereas the inner part of the flask stays essentially dark. Although this deficit can be overcome to some extent by rapid stirring, scale-up of photoreactions in batch usually results in extended reaction times, which can lead to increased side-reactions and diminished yields. A recent example of using a photochemical flow-setup is the semi-synthesis of the antimalarial drug and natural product artemisinin by SEEBERGER and co-workers.[57] The authors describe the oxidation of dihydroartemisinic acid to artemisinin using singlet-oxygen which is generated by a photosensitizer in flow (Scheme 9). Thus, the reaction combines two advantages of flow chemistry: A biphasic reaction (gas–liquid) and a photochemical reaction.

Scheme 9. Flow synthesis of the antimalarial drug artemisinin by SEEBERGER et al.

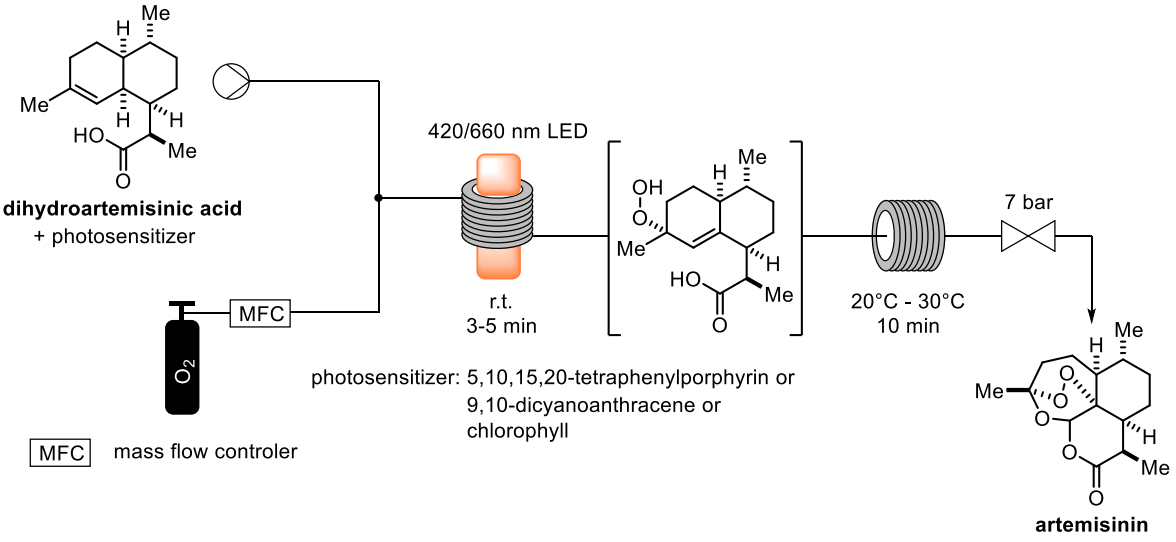

Another important aspect of flow chemistry in the context of step-efficient synthesis is the possibility to automate optimization studies. Due to the technological governance of a flow-setup, multi-dimensional design-of-experiment (DOS) studies can easily be conducted.[58] As challenging transformations in natural product synthesis usually require tedious optimization of single parameters, automatization can streamline and accelerate optimization significantly.[54b,59]
Furthermore, it can be advantageous to use flow chemistry when the reaction is very fast or involving highly reactive intermediates, such as arynes. In those cases, efficient mixing of reagents is crucial to obtain selectivity. Tube reactors have much shorter diffusion times and achieve mixing much faster compared to batch reactors. Mixing can be quantified by the DAMKÖHLER number (Da), a dimensionless unit that compares the reaction rate to the rate of mass transfer by diffusion.[60] For Da < 1, mixing is complete before the reaction occurs. When Da > 1, the reaction is faster than mass transport, resulting in concentration gradients with adverse effects on the outcome of the reaction. Both scenarios are depicted in figure 4, where two reagents A and B are reacting to the desired product C, that can form a side-product S with unreacted B.[53]

Figure 4. a) Reactions, where the Damköhler number is < 1; homogeneity is reached before the reaction produces significant amounts of product. b) When the reaction is much faster than mixing, resulting in the Damköhler number being > 1, thus local concentrations of B and C result in the formation of side product C (adapted from ref. [53]).

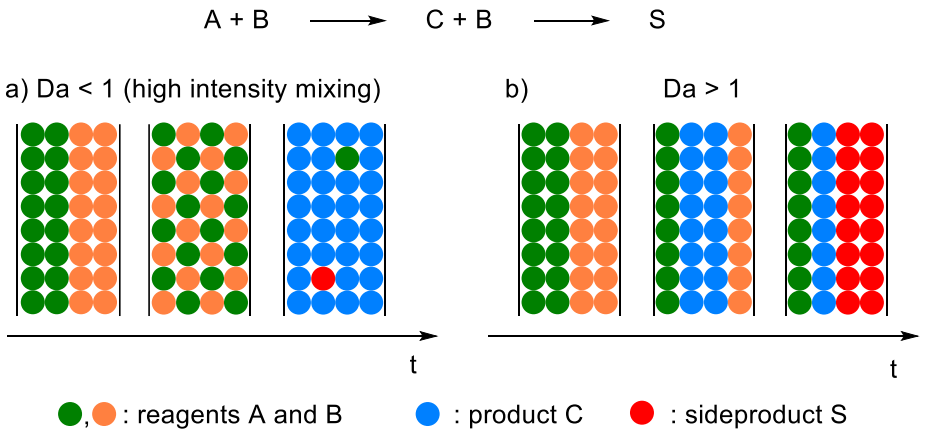

An example of a fast reacting intermediate is benzyne. Surprisingly, there are only few cases, where arynes were deliberately formed in flow.[51] In a study by YOSHIDA and co-workers, benzyne was generated by iodine-lithium exchange of 1-bromo-2-iodobenzene in a micro-flow reactor.[51c] The aryne was then attacked by an aryl-lithium reagent and the resulting phenyl-anion was trapped with different electrophiles (Scheme 10). The reactor was thus performing three consecutive and very fast intermolecular reactions with an overall reaction time of 3.83 s. The observed yields were ranging from 50% up to 73% whereas in the batch protocol, no product was formed.

Scheme 10. Aryne arylation performed in flow by YOSHIDA et al.

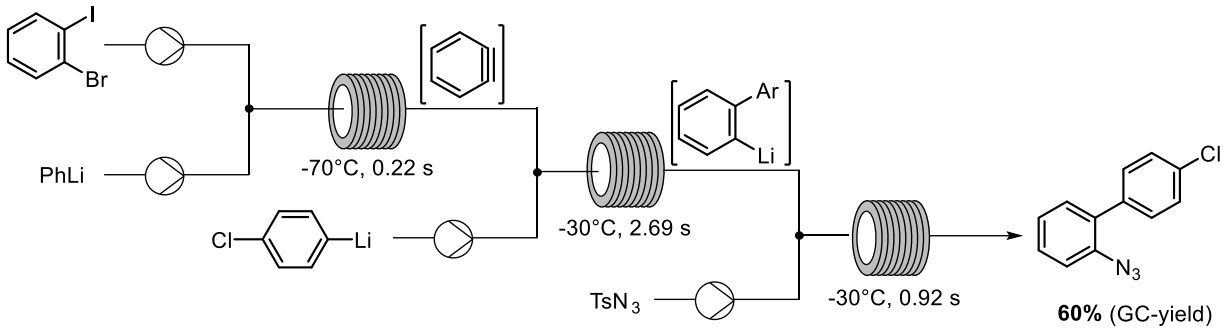

3. Quinolone Natural Products

3.1 Quinolone as a Privileged Structure in Antibiotics

Quinolones are bicyclic *N*-heterocycles consisting of a pyridinone fused to a benzene- or pyridine ring. In addition, all synthetic anti-infective quinolones are bearing a carboxylic acid at C3. Antibacterial quinolones represent one of the most important class of anti-infective agents in modern medicine, with more than 800 million patients treated.[61] Their anti-bacterial properties were discovered unintentionally, when quinolone **8** was formed as an impurity in the manufacturing process of the antimalarial drug chloroquine.[62] Due to its narrow antimicrobial spectrum, quinolone **8** was never commercialized, however it served as a lead structure that eventually resulted in the development of nalidixic acid, the first commercial quinolone antibiotic. Over the course of the following decades, quinolone antibiotics matured into a diverse compound class for the treatment of various infective diseases. Within the field of anti-infectives, the number of clinical introductions of quinolone drugs over the past five decades is only surpassed by the number of clinical introductions of β-lactames.[61a] Representative members of quinolone antibiotics in clinical practice are depicted in scheme 11.

Scheme 11. Representative quinolone-antibiotics in clinical use.

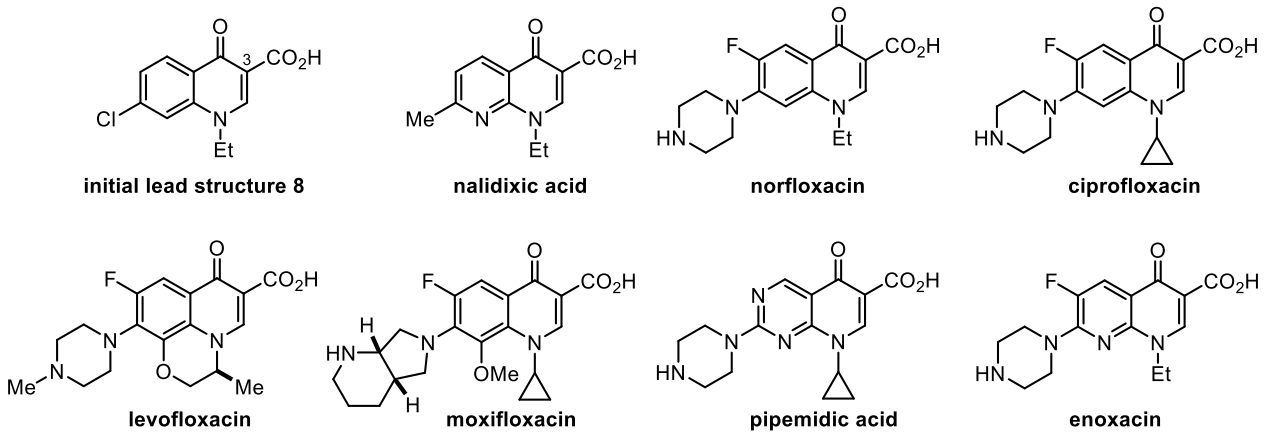

Quinolone antibiotics are targeting the bacterial topoisomerase II and IV.[63] These enzymes are dictating the proper DNA topology and thus are vital for protein biosynthesis, DNA replication, and repair.[64]

Resistance was comparatively slow to develop but is increasing in recent years. Furthermore, long-lasting severe side effects of quinolones compromising tendons, muscles, and the nervous system

have been observed. Most recently, their approval for the treatment of various infective diseases within the EU has been withdrawn by the European commission.[65] Therefore, the understanding of the underlying mechanisms causing these side effects as well as the development of new quinolone agents with a better safety profile is of great importance.

Although the development of quinolone antibiotics started with the accidental discovery of synthetic **8**, quinolone natural products have been used unknowingly at least since the late 19th century. In fact, quinolone natural products were the active pharmaceutical ingredients (API) of the very first clinically used antibiotic, pyocynanase.[66] Pyocynanase was an extract of *Pseudonomas aeruginosa* used by EMMERICH and LÖW to treat multiple infective diseases. Its active ingredient was believed to be an enzyme but was later found to be a mixture of pyocyanin and 2-alkyl-4-hydroxy-quinolones.[67]

Whereas synthetic anti-infective quinolones are solely 4-quinolones (the carbonyl group at C4), both 2- and 4-quinolones have been isolated from natural sources. Their reported biological activities are very broad.

3.2 3,4-Dioxygenated Quinolinones – Biosynthetic Origin and Biological Activities

Quinolone natural products are abundant alkaloids isolated from plant, microbial, and animal sources.[68] In comparison, the number of quinolones isolated from filamentous fungi is relatively small. However, with more fungal genomes being sequenced, it became evident that in fungi, most natural product-encoding genome clusters remain silent under conventional laboratory conditions. Thus, the diversity of fungal natural products has only been scratched at its surface.[69]

One example of (hidden) diversity in fungal secondary metabolites is the class of 3,4-dioxygenated quinolinones (further referred to as quinolinones). They are produced by both terrestrial and marine fungi, of the genera *Aspergillus* and *Penicillium*. Their general structure is depicted in scheme 12. Structurally, they can be subdivided in 4'-OMe-quinolinones (scheme 12, **a**) and those without the 4'-methoxy substituent (scheme 12, **b**). The 3,4-diol motif is almost exclusively *cis*-configured, with yaequinolone A_1 being the only exception. The absolute configuration of the diol has barely been investigated, solely by the means of electronic circular dichroism (ECD) spectroscopy, indicating a 3*S*,4*S* configuration. For yaequinolones J1 and J2, the 3*S*,4*S*-configuration was recently confirmed via asymmetric total synthesis.[70] Due to the lack of information on the absolute configuration of most quinolinones, depicted configurations in scheme 12 are referring to relative configurations. Apart from the *cis*-diol motif, many quinolinones are also bearing a phenylic hydroxyl group at C5. Structural diversity is further increased by a variety of isoprenyl-substituents at C6.

Although naturally occurring 2-quinolinones have been known long before, including precursors of 3,4-dioxygenated quinolinones, the first 3,4-dioxygenated quinolinones were isolated in 1995, when NAKAYA examined the toxicity of extracts from *Penicillium* sp. NTC-47 against brine shrimp.[71] This culminated in the isolation of the first 3,4-dioxygenated 5-hydroxyquinolinones NTC-47A and NTC-47B. The later was rediscovered in 2006 and renamed quinolinone B.[72] The structure of NTC-47A was proposed to possess a ten-membered unsaturated cyclic phenyl ether, although no spectroscopic data was reported. At the same time, Kimura studied the extracts of *Penicilium* sp. no. 410 and isolated penigequinolones A and B, both bearing an unprecedented 1,4-tetrasubstituted pyran substituent within the isoprenoid side chain at C6.[73] Over the next two decades, more than 24 quinolinones were discovered (scheme 12),[74] most of them as a result of bioactivity-guided screenings. The observed biological activities include toxicity (usually against brine shrimp), pollen-growth inhibition, nematicidal properties, cytotoxicity as well as anti-viral activities, to only name a few.

Scheme 12. Overview of 3,4-dioxygenated quinolones with and without 4'-OMe-substituent.

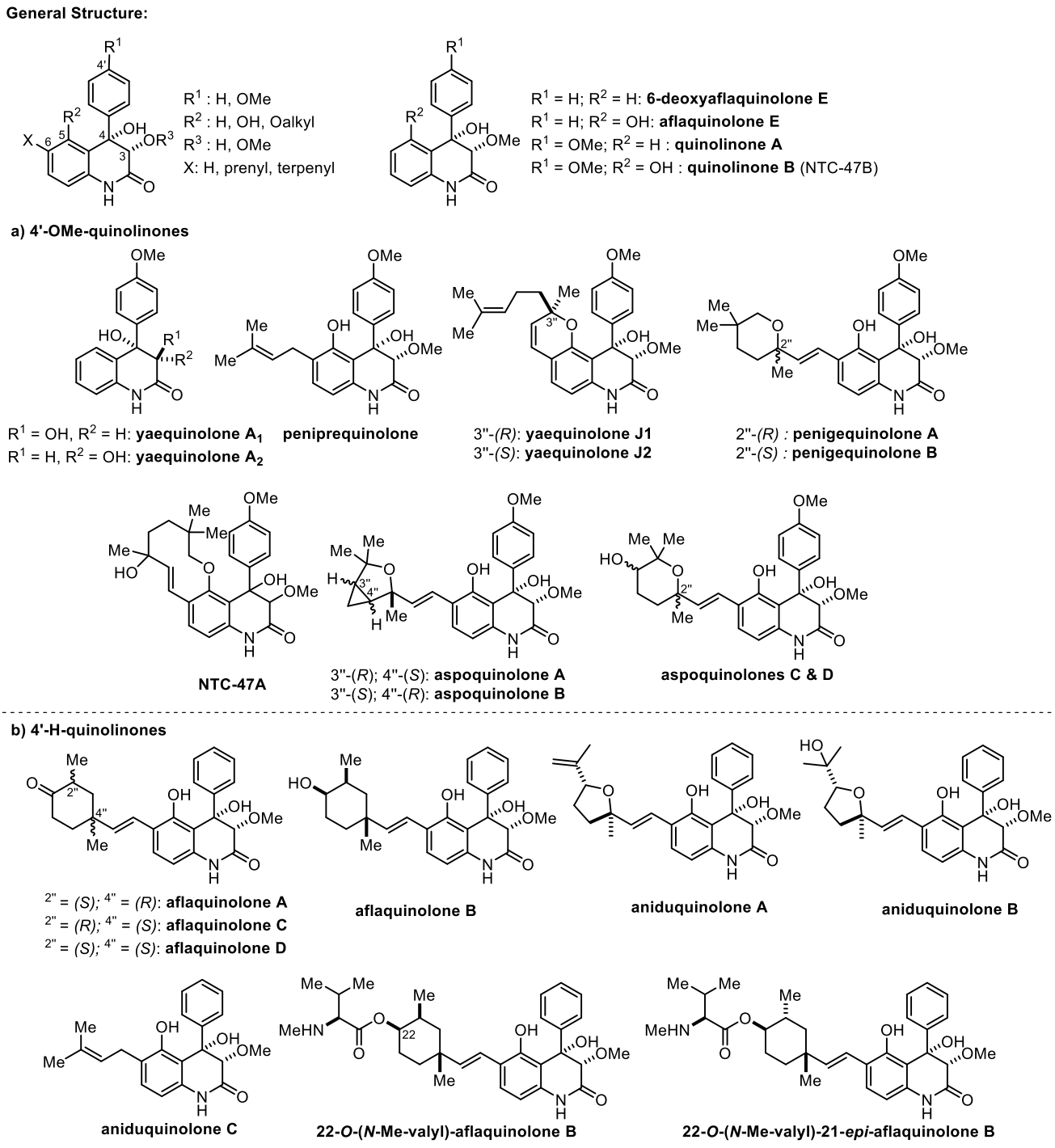

The biosynthetic pathway leading to 3,4-dioxygenated quinolinones begins with the synthesis of cyclopeptin or 4-methoxycyclopeptin, adducts of anthranilic acid and either *O*-methyl-*L*-thyrosine[75] or phenylalanine,[76] produced by the non-ribosomal peptide synthetase (NRPS)(Scheme 13, **a**). Cylopeptin is then first desaturated and subsequently oxidized by the Iron(II)/α-ketoglutarate-dependent dioxygenase AsqJ. The exact mechanism was elucidated by

GROLL, KAILA and HINTERMANN by co-crystalizing different substrates with AsqJ and subsequent DFT calculations.[77] They found that *N*-methylation of cyclopeptin is crucial for the activity of AsqJ, inducing molecular strain that fine-tunes π-stacking interactions at the active site. The thus formed spiro-epoxide **9** spring-loads the 6,7-bicyclic scaffold and induces a non-enzymatic rearrangement to form the quinolinone viridicatin or 4'-methoxyviridicatin, respectively (Scheme 13, b and c), under the formation of methyl isocyanate.[78] The biosynthesis is believed to continue by methylation of the 3-hydroxyl group followed by hydration of the enol ether to yield the 3,4-diol motif, although no details on the involved enzymes and mechanisms are known. Downstream processing into the final natural products may involve prenylation and double prenylation as well as additional oxidation steps.[79]

With this knowledge in hand, SCHERLACH and HERTWECK analyzed the recently sequenced genome of *Aspergillus nidulans*.[80] They found three copies of genes encoding for anthranilic acid synthase, the enzyme producing the starting material for the biosynthesis of quinolinones. Until then, no quinolinones have been isolated from *Aspergillus nidulans*, prompting the authors to assume that these genes so far have been silent under conventional culturing conditions. A panel of extracts prepared from 40 different culture conditions finally resulted in the isolation of four new quinolinones, aspoquinolones A–D, with unprecedented terpene side chains.[75]

So far, only three 3,4-dioxygenated quinolinones were synthesized by means of total synthesis. The synthesis of yaequinolone A_2, one of the simplest quinolinones, by PAN et al. was reported in 2009,[81] whereas an asymmetric synthesis of yaequinolones J1 and J2 was reported by HANESSIAN et al. in 2018.[70]

Scheme 13. (a) Biosynthetic origin of 3,4-dioxygenated quinolinones from anthranilic acid; (b) Crystal structure of the Iron(II)/α-ketoglutarate-dependent dioxygenase AsqJ with the bound substrate[77] and (c) the corresponding oxidation and rearrangement catalysed by AsqJ.

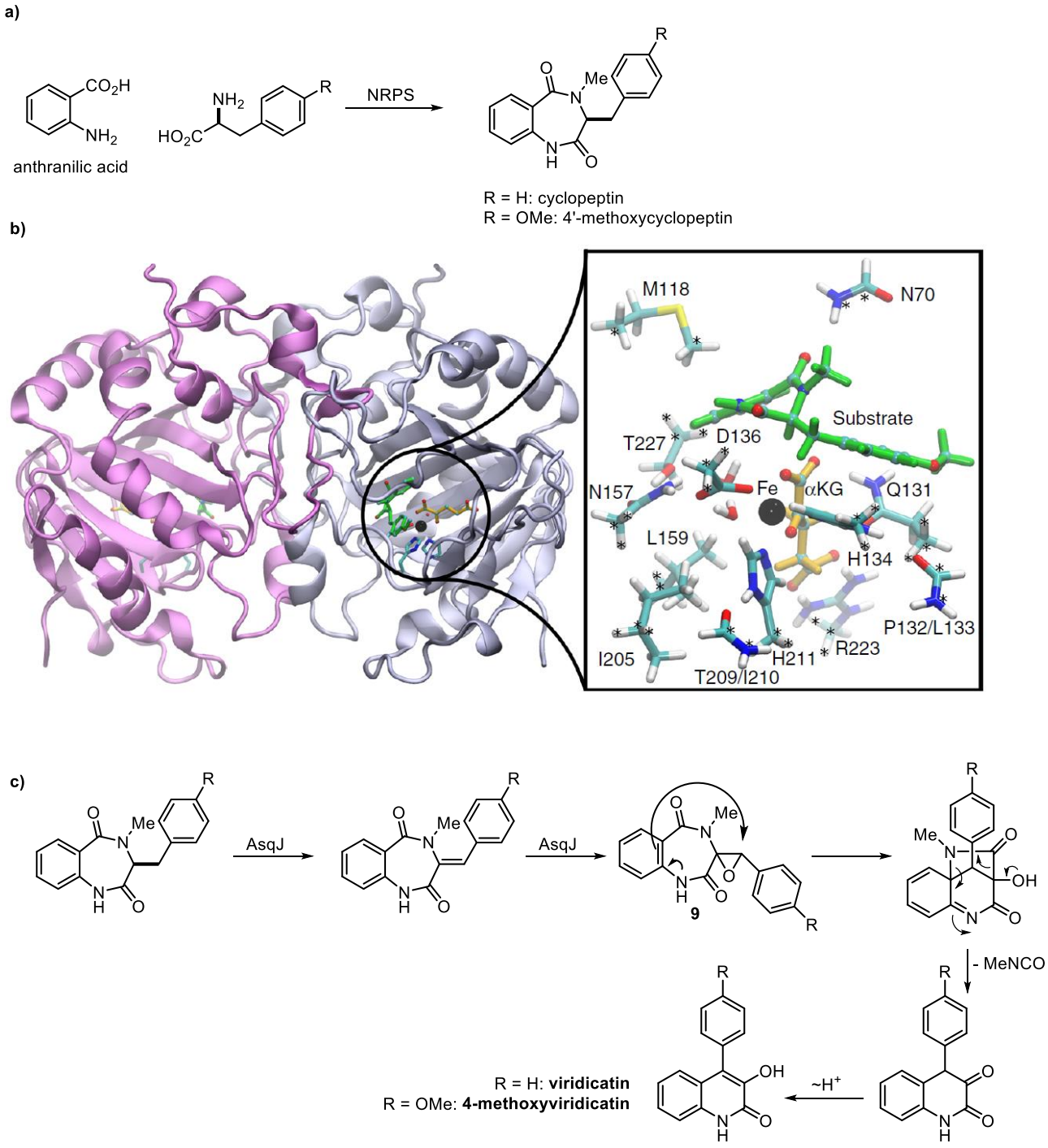

3.3 Yaequinolones J1 and J2 – Hanessian's Synthesis in the Context of Step Efficiency

Yaequinolones J1 and J2 were isolated in 2005 as novel 3,4-dioxygenated quinolinones from *Penicilium* sp.[82] Both compounds possess a terpene sidechain at C6, that cyclized to form a pyran with the phenolic hydroxy group of C5. They only differ in the configuration of the stereogenic center at C3'', which makes them epimers. Biosynthetically, the terpene side chain is introduced stepwise via two prenylation events.[79] Both compounds were initially found to be toxic against brine shrimp and were thus characterized as insecticides.[83] In 2018, HANESSIAN and coworkers disclosed the first asymmetric total synthesis of both natural products and determined their absolute configuration by single crystal X-ray diffraction of a late intermediate (Scheme 14).[70] Furthermore, both compounds were found to be cytotoxic against a melanoma A357 cell line (EC_{50} = 3.38 μM for yaequinolone J2) as well as a colorectal HCT116 cell line (EC_{50} = 3.38 μM for yaequinolone J1). The synthesis starts from 2-methyl-3-nitrophenol and builds the pyran motif early in the synthesis by an *ortho*-CLAISEN-rearrangement of alkyne **10**,[84] derived from the starting material in six steps. The benzylic methyl group is first brominated, substituted, and later oxidized to benzaldehyde **11**. The glycol side chain that later forms the 3,4-dioxygenated quinolinone is then introduced in a diastereoselective aldol reaction with the use of an EVANS' oxazolidinone as a chiral auxiliary.[85] This reaction is described to be highly stereoselective with regards to the stereocenters at C3 and C4, but is unselective with regards to the C3'' stereocenter. Thus, a 1:1 mixture of diastereomers is formed. Since both configurations at C3'' are leading to the epimeric natural products, the synthetic strategy is divergent and gives access to both natural products. The newly formed C4-stereocenter is then destroyed by oxidation to benzoketone **12**, which subsequently undergoes a diastereoselective GRIGNARD-addition with GRIGNARD-reagent **13,** thereby introducing the remaining skeletal carbon atoms and reformation of the C4 stereocenter. After several protection group- and redox manipulations, yaequinolones J1 and J2 are formed by lactamization and cleavage of the Boc-protected amide.

Scheme 14. Asymmetric total synthesis of yaequinolones J1 and J2 by HANESSIAN et al.

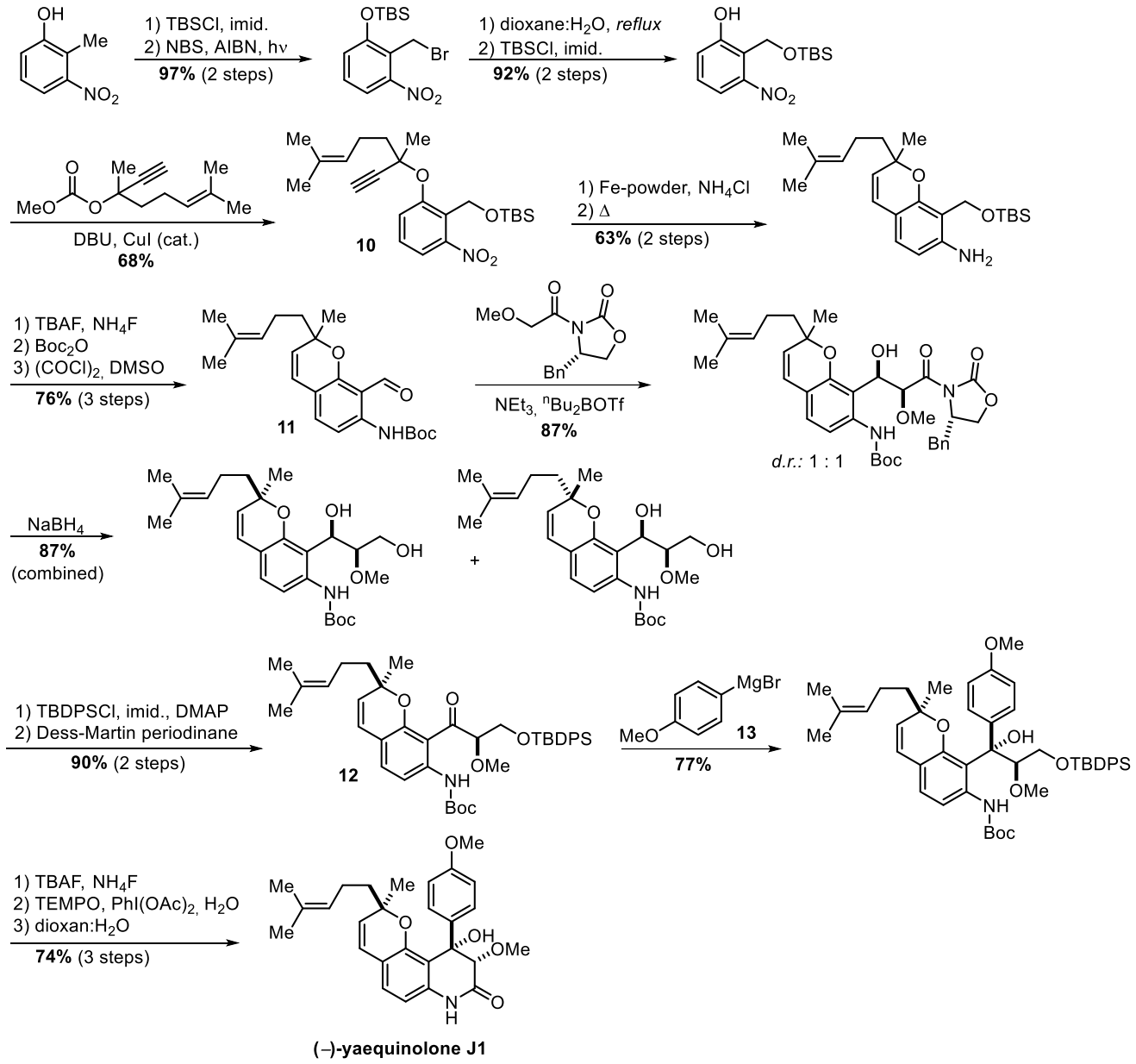

In total, the route requires 18 steps (LLS) to reach yaequinolones J1 and J2. From the perspective of step efficiency, the employed strategy suffers from a relatively high amount of functional group interconversions and protection group manipulations. Those steps are necessary because the route relies on non-catalytical methods to achieve enantioselectivity, the use of reagents with low functional group tolerance (e.g. GRINGNARD-reagent **13**), and classic carbonyl chemistry with poor redox economy. If one looks at the flow chart presented in scheme 15, the lack of step efficiency becomes immediately evident. Hence, a more step efficient access to yaequinolones J1 and J2 is needed to facilitate the exploration of their biological activities.

Scheme 15. Flowchart representation of HANESSIAN'S synthesis of yaequinolones J1 and J2

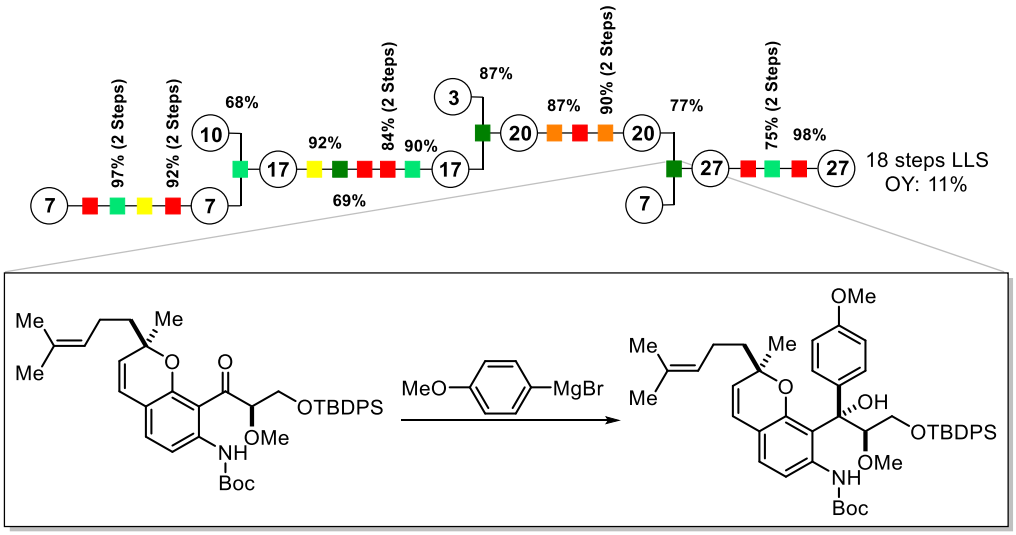

4. Scientific Goal

By analyzing representative examples of step efficient natural product syntheses of the recent years, the most successful strategies shall be identified. This includes the development of a suitable definition of a single synthetic step as well as the conception of a color-coded flow chart presentation, applicable to any given synthesis. The color-code will be based on the different types of transformations defined by the ideality principle (Scheme 16).

Scheme 16. Color-code of different types of transformations according to the ideality principle.

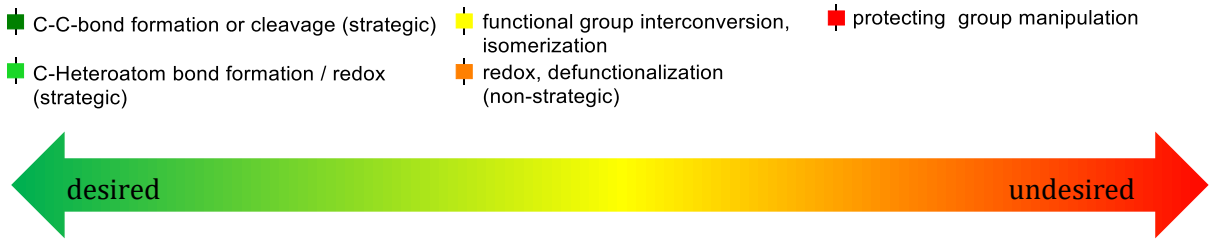

Following these guidelines, a step efficient and divergent strategy towards 3,4-dioxygenated quinolinones shall be derived. The strategy is based on a highly diastereoselective aldol cyclization of benzophenone **4**. This benzophenone will be derived from a suitable aryne precursor **2** and an unsymmetric imide **3**. If the insertion proceeds with the desired regioselectivity, this would allow for the rapid formation of the correct substitution pattern on the aromatic ring and simultaneously install the required amide residue needed for the final aldol cyclization. It also makes the synthesis divergent since different aryne precursors can be combined with different imides to access a multitude of natural products with the same strategy (Scheme 17). Difficulties in controlling the highly reactive aryne intermediate shall be overcome by using flow chemistry.

Scheme 17. Retrosynthetic analysis of 3,4-dioxygenated quinolinones based on the aryne insertion into unsymmetric imides.

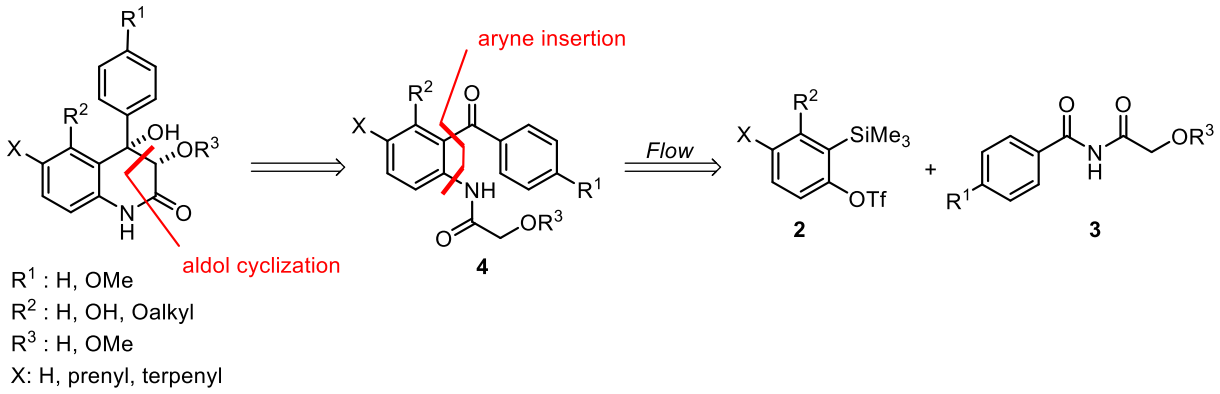

Following this blueprint, a step efficient synthesis of yaequinolone J1 and J2 shall be derived. The corresponding aryne precursor **2** should already bear the chromene motif to effectively protect the hydroxyl group adjacent to the aryne triple bond. In order to install the chromene, an organocatalytic tandem KNOEVENAGEL electrocyclization of citral and 2-bromoresorcinol is envisaged (Scheme 18).

Scheme 18. Retrosynthetic analysis of yaequinolones J1 and J2.

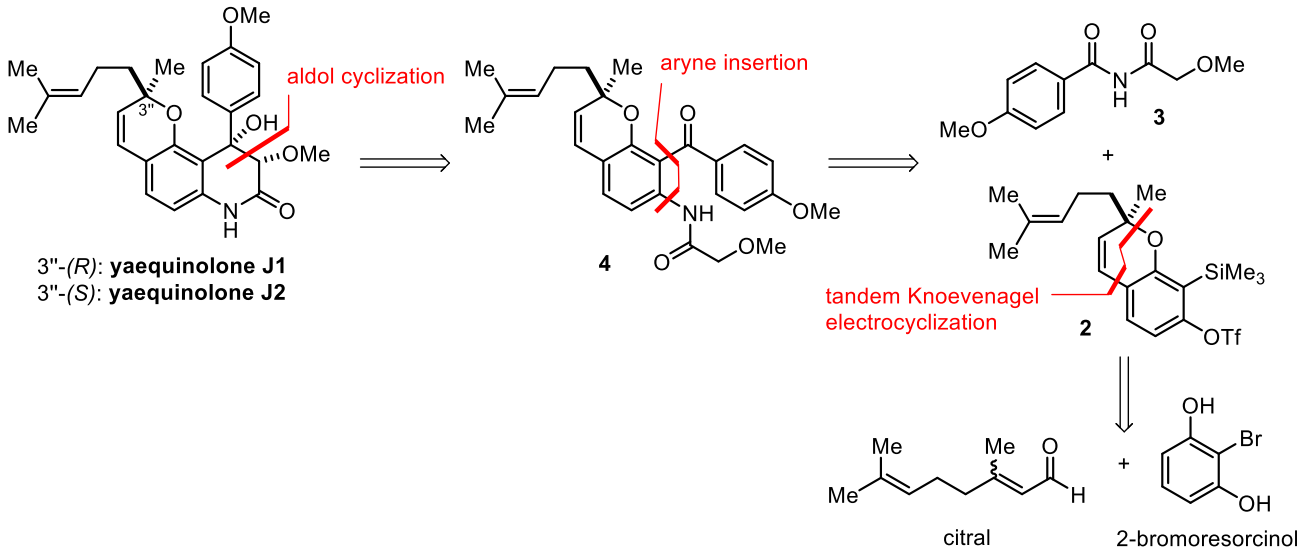

5. Publications

5.1 Enabling strategies for step efficient syntheses

JOHANNES SCHWAN and MATHIAS CHRISTMANN

Chem. Soc. Rev. **2018**, *47*, 7985–7995 (https://doi.org/10.1039/C8CS00399H)
Reprinted with permission from: http://xlink.rsc.org/?DOI=C8CS00399H

Abstract:
The field of natural product total synthesis has reached the point where synthetic efficiency has become more important than merely defining a viable (yet less ideal) route to the target molecule. Synthetic efficiency is best represented by the number of steps it takes to finish the target molecule from readily available starting materials, as by reducing the number of steps, all other factors of synthetic efficiency are influenced positively. By comparing several total syntheses from the recent years, the most successful strategies for step efficient syntheses will be highlighted. Each synthesis will be presented using a color-coded synthetic flowchart, in which each step is categorized by a colored box. Five categories of transformations are defined and rated according to their synthetic value. Each class will be signified by different colors so that the reader can quickly see which parts of the synthesis are productive and those that are not.

Author Contribution:
J. SCHWAN developed the definition of a single step in a multi-step synthesis in cooperation with M. CHRISTMANN. The color-coded flow chart was invented by M. CHRISTMANN and substantiated by J. SCHWAN. The discussed syntheses were selected, discussed, and color-coded by J. SCHWAN. The resulting rules for designing step efficient syntheses were developed by J. SCHWAN in cooperation with M. CHRISTMANN. The draft of the manuscript was provided by J. SCHWAN and revised by M. CHRISTMANN.

5.2 Synthesis of Quinolinone Alkaloids via Aryne Insertion into Unsymmetric Imides in Flow

JOHANNES SCHWAN, MERLIN KLEOFF, BENCE HARTMAYER, PHILIPP HERETSCH and MATHIAS CHRISTMANN

Org. Lett. **2018**, *20*, 7661–7664 (https://doi.org/10.1021/acs.orglett.8b03392)

Abstract:

A general strategy for the synthesis of 3,4-dioxygenated quinolin-2-one natural products is reported. The key step is a regioselective insertion of arynes into unsymmetric imides. When performed in continuous flow, the reaction proceeds within minutes, while lower yields and longer reaction times are observed in batch. The resulting N-acylated 2-aminobenzophenones were transformed to (±)-peniprequinolone, (±)-aflaquinolones E and F, (±)-6-deoxyaflaquinolone E, (±)-quinolinones A and B, and (±)-aniduquinolone C in 1−3 steps.

Author Contribution:

J. SCHWAN and M. KLEOFF developed the retrosynthetic analysis to 3,4-dioxygenated quinoline-2-ones. J. SCHWAN investigated the aryne insertion in flow. B. HARTMAYER investigated and conducted the CLAISEN-rearrangement followed by the olefin metathesis leading to (±)-peniprequinolone and (±)-aniduquinolone C as a research intern under the guidance of J. SCHWAN. The manuscript was provided by J. SCHWAN and M. KLEOFF and revised by P. HERETSCH and M. CHRISTMANN.

5.3 Five-Step Synthesis of Yaequinolones J1 and J2

JOHANNES SCHWAN, MERLIN KLEOFF, PHILIPP HERETSCH and MATHIAS CHRISTMANN

Org. Lett. **2020**, *22*, 675–678. https://doi.org/10.1021/acs.orglett.9b04455

Abstract:

A concise synthesis of yaequinolones J1 and J2 is reported. The route is based on the aryne insertion into the σ-C–N bond of an unsymmetric imide followed by a diastereoselective aldol cyclization of the resulting N-acylated aminobenzophenone. The chromene motif is generated in the first step by an organocatalytic tandem KNOEVENAGEL electrocyclization of citral and 2-bromoresorcinol. The approach adheres to the ideality principle, using almost exclusively strategic bond-forming reactions.

Author Contribution:

J. SCHWAN developed the retrosynthetic analysis to yaequinolones J1 and J2. The tandem KNOEVENAGEL electrocyclization as well as the aryne insertion were investigated and optimized by J. SCHWAN. All experiments were performed by J. SCHWAN. The manuscript was provided by J. SCHWAN and M. KLEOFF and revised by P. HERETSCH and M. CHRISTMANN.

6. Conclusions and Outlook

In summary, the most successful concepts of step-efficient syntheses were identified and applied to the natural product class of 3,4-dioxygenated quinolinones.

By analyzing a total of 19 syntheses of seven different natural products with the help of a color-coded flow-chart presentation, powerful strategies and methods were visualized graphically and several conclusions were made:

Convergent syntheses using large building blocks are considered superior in the construction of complex natural products compared to a more linear construction by adding one- or two-carbon fragments to a larger fragment. In the retrosynthetic analysis, disconnections should therefore divide the target in fragments of comparable size and complexity, thereby also lowering the number of C–C bond formations.

Rather than relying on classic methods that often come with the cost of low functional group tolerance, milder methods featuring a broad scope of tolerated functional groups should be applied. In this regard, non-strategic functional group interconversions and redox manipulations should be avoided.

Biomimetic approaches often allow for exceptionally short syntheses. If the biosynthesis of a natural product is known, one should consider imitating Nature's assembly strategy. In terpene synthesis, the separation of the cyclase phase from subsequent oxidation events can provide a blueprint for the chemical synthesis. This two-phase strategy can lead to concise routes with a minimum of protection group manipulations.

Furthermore, the developed flowchart presentation can assist in comparing different routes with respect to step- and redox economy. With the help of the color code, less efficient parts of a synthetic strategy can be easily distinguished from more efficient ones. Although syntheses have been compared using a flow-chart presentation and color coding the *yields*, the color coding of *classes of transformations* according to their synthetic value allows for the comparison of different routes already at the planning stage of a synthetic campaign.

To compare the efficiency of synthetic routes, the overall yield of a synthetic route was shown to be less diagnostic than the step count. In all evaluated syntheses, the amount of synthesized product was largest with the shortest synthesis although in some cases, longer sequences resulted in better overall yields. It was noted that the overall yield does not reflect labor, amount of waste, or atom- and redox economy. These factors are predominantly influenced by the number of steps.

By applying these principles to the natural product class of 3,4-dioxygenated quinolinones, an aryne insertion into an unsymmetric imide followed by a diastereoselective aldol reaction has been recognized. Thus, a general protocol for the synthesis of 3,4-dioxygenated quinolin-2-one natural products has been established. The sequence proceeds through an aryne insertion into unsymmetric imides, followed by a diastereoselective intramolecular aldol reaction. A flow protocol for the aryne insertion was developed, giving access to a small library of *N*-glycolated 2-aminobenzophenones. By this powerful disconnection, the quinolinone natural products yaequinolone J1 and J2, peniprequinolone, aflaquinolone E, F, quinolone A, B, and aniduquinolone C were synthesized in three to six steps (Scheme 19).

Future work should focus on the synthesis of quinolinone natural products with other side chains and higher oxidation levels, such as aspoquinolone A or aniduquinolone B. Furthermore, mechanistic insights on the aryne insertion and the observed regioselectivity are needed, in order to optimize the reaction even further. Also, with a small library of 3,4-dioxygenated quinolinones in hand, a bioactivity-screening should be performed in order to identify further possible applications in addition to the already known biological properties.

Scheme 19. Natural Products synthesized within this dissertation.

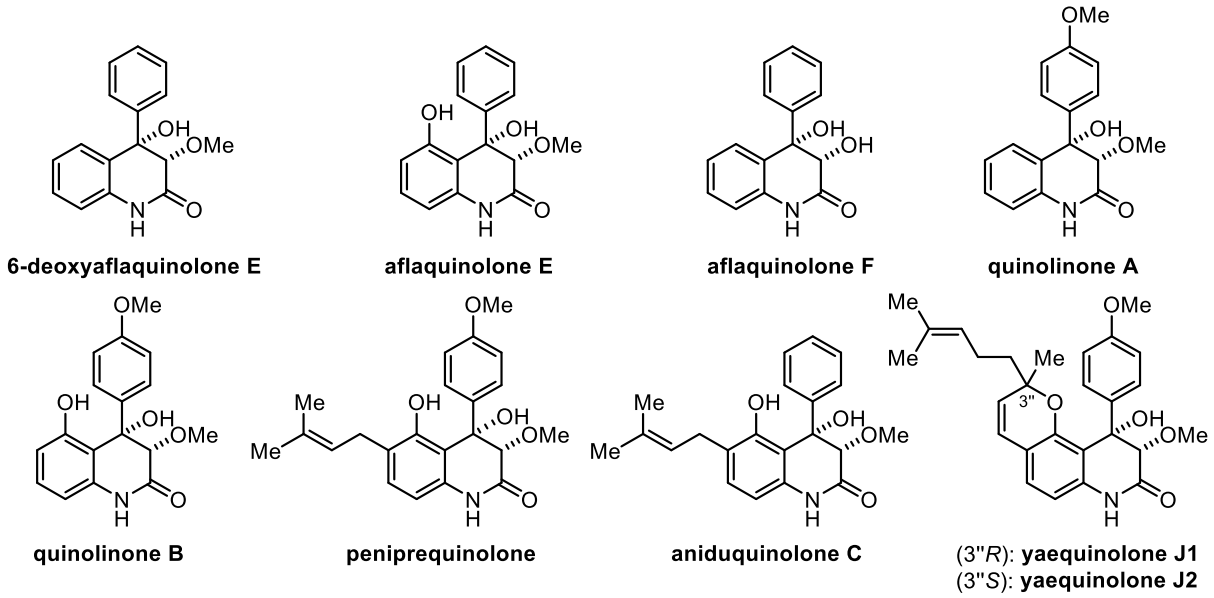

7. List of References and Illustration Credits

7.1 References

[1] Schwan, J.; Christmann, M. Enabling Strategies for Step Efficient Syntheses. *Chem. Soc. Rev.* **2018**, *47*, 7985–7995.

[2] Schwan, J.; Kleoff, M.; Hartmayer, B.; Heretsch, P.; Christmann, M. Synthesis of Quinolinone Alkaloids via Aryne Insertions into Unsymmetric Imides in Flow. *Org. Lett.* **2018**, *20*, 7661–7664.

[3] Schwan, J.; Kleoff, M.; Heretsch, P.; Christmann, M. Five-Step Synthesis of Yaequinolones J1 and J2. *Org. Lett.* **2020**, *22*, 675–678.

[4] Lemke, T. L.; Williams, D. A. *Foye's Principles of Medicinal Chemistry*, 3rd ed.; Lippincott Williams & Wilkins: Philadelphia, 2008.

[5] Buckingham, J. *Bitter Nemesis; The Intimate History of Strychnine*; CRC Press: Boca Raton, 2008.

[6] Carlini, E. The Good and the Bad Effects of (−) trans-delta-9-tetrahydrocannabinol (Δ^9-THC) on Humans. *Toxicon* **2004**, *44*, 461–467.

[7] Newman, D. J.; Cragg, G. M. Natural Products as Sources of New Drugs from 1981 to 2014. *J. Nat. Prod.* **2016**, *79*, 629–661.

[8] Nicolaou, K. C.; Vourloumis, D.; Winssinger, N.; Baran, P. S. The Art and Science of Total Synthesis at the Dawn of the Twenty-First Century. *Angew. Chem., Int. Ed.* **2000**, *39*, 44–122.

[9] (a) Wani, M. C. In *153rd National Meeting of the American Chemical Society*; Miamy Beach, 1967; Paper No. M-006. (b) Wani, M. C.; Taylor, H. L.; Wall, M. E.; Coggon, P.; Mcphail, A. T. Plant Antitumor Agents. VI. The Isolation and Structure of Taxol, a Novel Antileukemic and Antitumor Agent from Taxus Brevifolia. *J. Am. Chem. Soc.* **1971**, *93*, 2325–2327. (c) Nikolic, V. D.; Savic, I. M.; Savic, I. M.; Nicolic, L. B.; Stankovic, M. Z.; Marinkovic, V. D. Paclitaxel as an Anticancer Agent: Isolation, Activity, Synthesis, and Stability. *Cent. Eur. J. Med.* **2011**, *6*, 527–536.

[10] (a) Weinreb, S. M. Lepadiformine: A Case Study of the Value of Total Synthesis in Natural Product Structure Elucidation. *Acc. Chem. Res.* **2003**, *36*, 59–65. (b) Nicolaou, K. C.; Snyder, S. A. Chasing Molecules That Were Never There: Misassigned Natural Products and the Role of Chemical Synthesis in Modern Structure Elucidation. *Angew. Chem., Int. Ed.* **2005**, *44*,

1012–1044. (c) Maier, M. E. Structural Revisions of Natural Products by Total Synthesis. *Nat. Prod. Rep.* **2009**, *26*, 1105–1124. (d) Schniedel, V. M.; Hong, Y. J.; Lentz, D.; Tantillo, D. J.; Christmann, M. Synthesis and Structure Revision of Dichrocephones A and B. *Angew. Chem., Int. Ed.* **2018**, *57*, 2419–2422.

[11] Robertson, J. H.; Beevers, C. A. The crystal structure of strychnine hydrogen bromide. *Acta Crystallogr.* **1951**, *4*, 270–275.

[12] Woodward, R. B.; Cava, M. P.; Ollis, W. D.; Hunger, A.; Daeniker, H. U.; Schenker, K. The total synthesis of strychnine. *J. Am. Chem. Soc.* **1954**, *76*, 4749–4751.

[13] Cannon, J. S.; Overman, L. E. Is There No End to the Total Syntheses of Strychnine? Lessons Learned in Strategy and Tactics in Total Synthesis. *Angew. Chem., Int. Ed.* **2012**, *51*, 4288–4311.

[14] Hanessian, S. Reflections on the Total Synthesis of Natural Products: Art, Craft, Logic, and the Chiron Approach. *Pure Appl. Chem.* **1993**, *65*, 1189–1204.

[15] Nobel Lectures: Chemistry 1936–1970; Elsevier: New York, 1972; pp 96–123.

[16] Newhouse, T.; Baran, P. S.; Hoffmann, R. W. The Economies of Synthesis. *Chem. Soc. Rev.* **2009**, *38*, 3010–3021.

[17] (a) Tieves, F.; Tonin, F.; Fernández-Fueyo, E.; Robbins, J. M.; Bommarius, B.; Bommarius, A. S.; Alcalde, M.; Hollmann, F. Energising the E-Factor: The E + -Factor. *Tetrahedron* **2019**, *75*, 1311–1314. (b) Sheldon, R. A. The E Factor 25 Years on: The Rise of Green Chemistry and Sustainability. *Green Chem.* **2017**, *19*, 18–43. (c) Sheldon, R. A. Organic Synthesis – Past, Present, and Future. *Chem. Ind.* **1992**, 903–906.

[18] Trost, B. M. The Atom Economy - A Search for Synthetic Efficiency. *Science* **1991**, *254*, 1471–1477.

[19] Mulzer, J. Trying to Rationalize Total Synthesis. *Nat. Prod. Rep.* **2014**, *31*, 595–603.

[20] Burns, N. Z.; Baran, P. S.; Hoffmann, R. W. Redox Economy in Organic Synthesis. *Angew. Chem., Int. Ed.* **2009**, *48*, 2854–2867.

[21] Hendrickson, J. B. Systematic Characterization of Structures and Reactions for Use in Organic Synthesis. *J. Am. Chem. Soc.* **1971**, *93*, 6847–6854.

[22] Singh, J.; Satyamurthi, N.; Aidhen, I. S. The Growing Synthetic Utility of Weinreb′s Amide. *J. Prakt. Chem.* **2000**, *342*, 340–347.

[23] Fukuyama, T.; Lin, S. C.; Li, L. Facile Reduction of Ethyl Thiol Esters to Aldehydes: Application to a Total Synthesis of (+)-Neothramycin A Methyl Ether. *J. Am. Chem. Soc.* **1990**, *112*, 7050–7051.

[24] Hintermann, L.; Labonne, A. Catalytic Hydration of Alkynes and Its Application in Synthesis. *Synthesis* **2007**, 1121–1150.

[25] Ojima, I.; Tsai, C.-Y.; Tzamarioudaki, M.; Bonafoux, D. The Hydroformylation Reaction. In *Organic Reactions*; John Wiley & Sons, Inc.: Hoboken, NJ, USA, 2000; pp 1–354.

[26] Feng, J.; Kasun, Z. A.; Krische, M. J. Enantioselective Alcohol C–H Functionalization for Polyketide Construction: Unlocking Redox-Economy and Site-Selectivity for Ideal Chemical Synthesis. *J. Am. Chem. Soc.* **2016**, *138*, 5467–5478.

[27] Wender, P. A.; Croatt, M. P.; Witulski, B. New Reactions and Step Economy: The Total Synthesis of (±)-Salsolene Oxide Based on the Type II Transition Metal-Catalyzed Intramolecular [4+4] Cycloaddition. *Tetrahedron* **2006**, *62*, 7505–7511.

[28] Gaich, T.; Baran, P. S. Aiming for the Ideal Synthesis. *J. Org. Chem* **2010**, *75*, 4657–4673.

[29] (a) Peplow, M. *One small step...* web blog post, Royal Society of Chemistry, 2017, chemistryworld.com. (b) Baran Research Group, *11-Step Synthesis of (–)-Thapsigargin*, web blog post, 2016, openflask.blogspot.de.

[30] IUPAC Compendium of Chemical Terminology, IUPAC, Research Triangle Park, NC.

[31] Chu, H.; Smith, J. M.; Felding, J.; Baran, P. S. Scalable Synthesis of (−)-Thapsigargin. *ACS Cent. Sci.* **2017**, *3*, 47–51.

[32] Willot, M.; Radtke, L.; Könning, D.; Fröhlich, R.; Gessner, V. H.; Strohmann, C.; Christmann, M. Total Synthesis and Absolute Configuration of the Guaiane Sesquiterpene Englerin A. *Angew. Chem., Int. Ed.* **2009**, *48*, 9105–9108.

[33] Takikawa, H.; Nishii, A.; Sakai, T.; Suzuki, K. Aryne-Based Strategy in the Total Synthesis of Naturally Occurring Polycyclic Compounds. *Chem. Soc. Rev.* **2018**, *47*, 8030–8056.

[34] *Comprehensive Organic Synthesis*, 2nd ed.; Knochel, P.; Molander, G. A.; Eds.; Elsevier: Amsterdam, 2014.

[35] Clayden, J.; Greeves, N.; Warren, S. *Organische Chemie*, 2nd ed.; Springer: Heidelberg, 2013.

[36] (a) Breitmaier, E.; Jung, G. *Organische Chemie*, 6th ed.; Thieme: Stuttgart; New York, 2009. (b) Flemming, I. *Grennzorbitale und Reaktionen Organischer Verbindungen*, 2nd ed.; VCH: Weinheim, 1990.

[37] Himeshima, Y.; Sonoda, T.; Kobayashi, H. Fluoride-Induced 1,2-Elimination of O -Trimethylsilylphenyl Triflate to Benzyne under Mild Conditions. *Chem. Lett.* **1983**, *12*, 1211–1214.

[38] Kitamura, T.; Yamane, M. (Phenyl)[o-(Trimethylsilyl)Phenyl]Iodonium Triflate. A New and Efficient Precursor of Benzyne. *J. Chem. Soc. Chem. Commun.* **1995**, 983–984.

[39] a) Corsello, M. A.; Kim, J.; Garg, N. K. Total Synthesis of (-)-Tubingensin B Enabled by the Strategic Use of an Aryne Cyclization. *Nat. Chem.* **2017**, *9*, 944–949. (b) Goetz, A. E.; Silberstein, A. L.; Corsello, M. A.; Garg, N. K. Concise Enantiospecific Total Synthesis of Tubingensin A. *J. Am. Chem. Soc.* **2014**, *136*, 3036–3039. (c) Huters, A. D.; Styduhar, E. D.;

Garg, N. K. Total Syntheses of the Elusive Welwitindolinones with Bicyclo[4.3.1] Cores. *Angew. Chem., Int. Ed.* **2012**, *51*, 3758–3765.

[40] Pellissier, H.; Santelli, M. The Use of Arynes in Organic Synthesis. *Tetrahedron* **2003**, *59*, 701–730.

[41] (a) Miller, R. G.; Stiles, M. Reaction of Benzyne with Benzene and Naphthalene. *J. Am. Chem. Soc.* **1963**, *85*, 1798–1800. (b) Stiles, M.; Urs, B.; Freund, G. The Reaction of Benzyne with Benzene. *J. Org. Chem.* **1967**, *32*, 3718–3719.

[42] González, C.; Pérez, D.; Guitián, E.; Castedo, L. Synthesis of lycorines by intramolecular aryne cycloadditions. *J. Org. Chem.* **1995**, *60*, 6318–6326.

[43] González, C.; Guitián, E.; Castedo, L. Synthesis of phenanthridones, quinolinequinones and 7-azasteroids. *Tetrahedron* **1999**, *55*, 5195–5206.

[44] Peña, D.; Pérez, D.; Guitián, E. Insertion of Arynes into σ Bonds. *Angew. Chem., Int. Ed.* **2006**, *45*, 3579–3581.

[45] Tambar, U. K.; Stoltz, B. M. The Direct Acyl-Alkylation of Arynes. *J. Am. Chem. Soc.* **2005**, *127*, 5340–5341.

[46] Yoshida, H.; Shirakawa, E.; Honda, Y.; Hiyama, T. Addition of Ureas to Arynes: Straightforward Synthesis of Benzodiazepine and Benzodiazocine Derivatives. *Angew. Chem., Int. Ed.* **2002**, *41*, 3247–3249.

[47] (a) Tadross, P. M.; Stoltz, B. M. A Comprehensive History of Arynes in Natural Product Total Synthesis. *Chem. Rev.* **2012**, *112*, 3550–3577. (b) Gampe, C. M.; Carreira, E. M. Arynes and Cyclohexyne in Natural Product Synthesis. *Angew. Chem., Int. Ed.* **2012**, *51*, 3766–3778. (c) Goetz, A. E.; Shah, T. K.; Garg, N. K. Pyridynes and Indolynes as Building Blocks for Functionalized Heterocycles and Natural Products. *Chem. Commun.* **2015**, *51*, 34–45.

[48] Lin, W.; Sapountzis, I.; Knochel, P. Preparation of Functionalized Aryl Magnesium Reagents by the Addition of Magnesium Aryl Thiolates and Amides to Arynes. *Angew. Chem., Int. Ed.* **2005**, *44*, 4258–4261.

[49] Kou, K. G. M.; Pflueger, J. J.; Kiho, T.; Morrill, L. C.; Fisher, E. L.; Clagg, K.; Lebold, T. P.; Kisunzu, J. K.; Sarpong, R. A Benzyne Insertion Approach to Hetisine-Type Diterpenoid Alkaloids: Synthesis of Cossonidine (Davisine). *J. Am. Chem. Soc.* **2018**, *140*, 8105–8109.

[50] Kelleghan, A. V.; Busacca, C. A.; Sarvestani, M.; Volchkov, I.; Medina, J. M.; Garg, N. K. Safety Assessment of Benzyne Generation from a Silyl Triflate Precursor. *Org. Lett.* **2020**, *22*, 1665–1669.

[51] (a) Browne, D. L.; Wright, S.; Deadman, B. J.; Dunnage, S.; Baxendale, I. R.; Turner, R. M.; Ley, S. V. Continuous Flow Reaction Monitoring Using an On-Line Miniature Mass Spectrometer. *Rapid Commun. Mass Spectrom.* **2012**, *26*, 1999–2010. (b) He, Z.; Jamison, T. F. Continuous-

Flow Synthesis of Functionalized Phenols by Aerobic Oxidation of Grignard Reagents. *Angew. Chem., Int. Ed.* **2014**, *53*, 3353–3357. (c) Nagaki, A.; Ichinari, D.; Yoshida, J. I. Three-Component Coupling Based on Flash Chemistry. Carbolithiation of Benzyne with Functionalized Aryllithiums followed by Reactions with Electrophiles. *J. Am. Chem. Soc.* **2014**, *136*, 12245–12248. (d) Khadra, A.; Organ, M. G. In Situ Generation and Diels-Alder Reaction of Benzynes Derivatives with 5-Membered Ring Heterocycles Using a Microcapillary Flow Reactor. *J. Flow Chem.* **2016**, *6*, 293–296.

[52] McQuade, D. T.; Seeberger, P. H. Applying Flow Chemistry: Methods, Materials, and Multistep Synthesis. *J. Org. Chem.* **2013**, *78*, 6384–6389.

[53] Plutschack, M. B.; Pieber, B.; Gilmore, K.; Seeberger, P. H. The Hitchhiker's Guide to Flow Chemistry. *Chem. Rev.* **2017**, *117*, 11796–11893.

[54] (a) Yoshida, J.; Kim, H.; Nagaki, A. "Impossible" Chemistries Based on Flow and Micro. *J. Flow Chem.* **2017**, *7*, 60–64. (b) Ley, S. V.; Fitzpatrick, D. E.; Myers, R. M.; Battilocchio, C.; Ingham, R. J. Machine-Assisted Organic Synthesis. *Angew. Chem., Int. Ed.* **2015**, *54*, 10122–10136.

[55] Webb, D.; Jamison, T. F. Diisobutylaluminum Hydride Reductions Revitalized: A Fast, Robust, and Selective Continuous Flow System for Aldehyde Synthesis. *Org. Lett.* **2012**, *14*, 568–571.

[56] Kleoff, M.; Schwan, J.; Boeser, L.; Hartmayer, B.; Christmann, M.; Sarkar, B.; Heretsch, P. Scalable Synthesis of Functionalized Ferrocenyl Azides and Amines Enabled by Flow Chemistry. *Org. Lett.* **2020**, *22*, 902–907.

[57] (a) Lévesque, F.; Seeberger, P. H. Continuous-Flow Synthesis of the Anti-Malaria Drug Artemisinin. *Angew. Chem., Int. Ed.* **2012**, *51*, 1706–1709. (b) Gilmore, K.; Kopetzki, D.; Lee, J. W.; Horváth, Z.; McQuade, D. T.; Seidel-Morgenstern, A.; Seeberger, P. H. Continuous Synthesis of Artemisinin-Derived Medicines. *Chem. Commun.* **2014**, *50*, 12652–12655. (c) Triemer, S.; Gilmore, K.; Vu, G. T.; Seeberger, P. H.; Seidel-Morgenstern, A. Literally Green Chemical Synthesis of Artemisinin from Plant Extracts. *Angew. Chem., Int. Ed.* **2018**, *57*, 5525–5528.

[58] Leardi, R. Experimental Design in Chemistry: A Tutorial. *Anal. Chim. Acta* **2009**, *652*, 161–172.

[59] (a) Chatterjee, S.; Moon, S.; Hentschel, F.; Gilmore, K.; Seeberger, P. H. An Empirical Understanding of the Glycosylation Reaction. *J. Am. Chem. Soc.* **2018**, *140*, 11942–11953. (b) Chatterjee, S.; Guidi, M.; Seeberger, P. H.; Gilmore, K. Automated Radial Synthesis of Organic Molecules. *Nature* **2020**, *57*, 379–384.

[60] *Handbook of Industrial Mixing*; Paul, E. L.; Atiemo-Obeng, V. A.; Kresta, S. M.; Eds.; John Wiley & Sons, Inc.: Hoboken, NJ, USA, 2003.

[61] (a) Bisacchi, G. S. Origins of the Quinolone Class of Antibacterials: An Expanded "Discovery Story." *J. Med. Chem.* **2015**, *58*, 4874–4882. (b) Mitscher, L. A. Bacterial Topoisomerase

Inhibitors: Quinolone and Pyridone Antibacterial Agents. *Chem. Rev.* **2005**, *105*, 559–592. (c) Van Bambeke, F.; Michot, J. M.; Van Eldere, J.; Tulkens, P. M. Quinolones in 2005: An Update. *Clin. Microbiol. Infect.* **2005**, *11*, 256–280.

[62] Lesher, G. Y.; Froelich, E. J.; Gruett, M. D.; Bailey, J. H.; Brundage, R. P. 1,8-Naphthyridine Derivatives. A New Class of Chemotherapeutic Agents. *J. Med. Pharm. Chem.* **1962**, *5*, 1063–1065.

[63] Takei, M.; Fukuda, H.; Kishii, R.; Hosaka, M. Target Preference of 15 Quinolones against Staphylococcus Aureus, Based on Antibacterial Activities and Target Inhibition. *Antimicrob. Agents Chemother.* **2001**, *45*, 3544–3547.

[64] (a) Gellert, M.; Mizuuchi, K.; O'Dea, M. H.; Nash, H. A. DNA Gyrase: An Enzyme That Introduces Superhelical Turns into DNA. *Proc. Natl. Acad. Sci.* **1976**, *73*, 3872–3876. (b) Brown, P. O.; Cozzarelli, N. R. A Sign Inversion Mechanism for Enzymatic Supercoiling of DNA. *Science.* **1979**, *206*, 1081–1083. (c) Kato, J.; Nishimura, Y.; Imamura, R.; Niki, H.; Hiraga, S.; Suzuki, H. New Topoisomerase Essential for Chromosome Segregation in E. Coli. *Cell* **1990**, *63*, 393–404.

[65] Implementing decision of the European commission "Über die Zulassungen für die Humanarzneimittel Chinolon- und Fluorchinolon- Arzneimittel zur systemischen Anwendung und zur Inhalation" C(2019)2050, 11.03.2019

[66] (a) Hutchings, M.; Truman, A.; Wilkinson, B. Antibiotics: Past, Present and Future. *Curr. Opin. Microbiol.* **2019**, *51*, 72–80. (b) Emmerich, R.; Löw, O. Bakteriolytische Enzyme als Ursache der Erworbenen Immunität und die Heilung von Infektionskrankheiten durch Dieselben. *Zeitschrift für Hyg. und Infekt.* **1899**, *31*, 1–65.

[67] Hays, E. E.; Wells, I. C.; Katzman, P. A.; Cain, C. K.; Jacobs, F. A.; Thayer, S. A.; Doisy, E. A.; Wade, J. Antibiotic Substances Produced by Pseudomonas Aeruginosa. *J. Biol. Chem.* **1945**, *159*, 725–750.

[68] *Dictionary of Alkaloids*, 2nd ed.; Buckingham, J.; Baggaley, K. H.; Roberts, A. D., Szabó, L. F.; Eds.; CRC Press: Boca Raton, 2010

[69] Hertweck, C. Hidden Biosynthetic Treasures Brought to Light. *Nat. Chem. Biol.* **2009**, *5*, 450–452.

[70] Vece, V.; Jakkepally, S.; Hanessian, S. Total Synthesis and Absolute Stereochemical Assignment of the Insecticidal Metabolites Yaequinolones J1 and J2. *Org. Lett.* **2018**, *20*, 4277–4280.

[71] Nakaya, T. Anti-Brine Shrimp Substances Produced by Penicillium Sp. NTC-47. *Seikatsu Eisei* **1995**, *39*, 141–143.

[72] Uchida, R.; Imasato, R.; Tomoda, H.; Omura, S. Yaequinolones, New Insecticidal Antibiotics Produced by Penicillium Sp. FKI-2140. *J. Antibiot.* **2006**, *59*, 652–658.

[73] Kimura, Y.; Yoshinari, T.; Shimada, A.; Hamasaki, T. Isofunicone, a Pollen Growth Inhibitor Produced by the Fungus, Penicillium Sp. *Phytochemistry* **1995**, *40*, 629–631.

[74] For a review of 3,4-dioxygenated quinolones, see: Simonetti, S. O.; Larghi, E. L.; Kaufman, T. S. The 3,4-Dioxygenated 5-Hydroxy-4-Aryl-Quinolin-2(1*H*)-One Alkaloids. Results of 20 Years of Research, Uncovering a New Family of Natural Products. *Nat. Prod. Rep.* **2016**, *33*, 1425–1446.

[75] Scherlach, K.; Hertweck, C. Discovery of Aspoquinolones A-D, Prenylated Quinoline-2-one Alkaloids from Aspergillus Nidulans, Motivated by Genome Mining. *Org. Biomol. Chem.* **2006**, *4*, 3517–3520.

[76] (a) Walsh, C. T.; Haynes, S. W.; Ames, B. D.; Gao, X.; Tang, Y. Short Pathways to Complexity Generation: Fungal Peptidyl Alkaloid Multicyclic Scaffolds from Anthranilate Building Blocks. *ACS Chem. Biol.* **2013**, *8*, 1366–1382. (b) Luckner, M.; Winter, K.; Reisch, J. Zur Bildung von Chinolinalkaloiden in Pflanzen. *Eur. J. Biochem.* **1969**, *7*, 380–384.

[77] (a) Bräuer, A.; Beck, P.; Hintermann, L.; Groll, M. Structure of the Dioxygenase AsqJ: Mechanistic Insights into a One-Pot Multistep Quinolone Antibiotic Biosynthesis. *Angew. Chem., Int. Ed.* **2016**, *55*, 422–426. (b) Mader, S. L.; Bräuer, A.; Groll, M.; Kaila, V. R. I. Catalytic Mechanism and Molecular Engineering of Quinolone Biosynthesis in Dioxygenase AsqJ. *Nat. Commun.* **2018**, *9*, 1168.

[78] (a) White, J. D.; Dimsdale, M. J. The Conversion of Cyclopenin into Viridicatin. *J. Chem. Soc. D Chem. Commun.* **1969**, 1285–1286. (b) Luckner, M.; Winter, K.; Nover, L.; Reisch, J. Thermische Spaltung und Massenspektrometrie der Benzodiazepinalkaloide (-)-Cyclopenin und (-)-Cyclopenol. *Tetrahedron* **1969**, *25*, 2575–2588. (c) Luckner, M.; Winter, K.; Reisch, J. Zur Bildung von Chinolinalkaloiden in Pflanzen. 4. Über den Wirkungsmechanismus des Fermentes Cyclopenase. *Eur. J. Biochem.* **1969**, *7*, 380–384.

[79] Zou, Y.; Zhan, Z.; Li, D.; Tang, M.; Cacho, R. A.; Watanabe, K.; Tang, Y. Tandem Prenyltransferases Catalyze Isoprenoid Elongation and Complexity Generation in Biosynthesis of Quinolone Alkaloids. *J. Am. Chem. Soc.* **2015**, *137*, 4980–4983.

[80] Galagan, J. E.; Calvo, S. E.; Cuomo, C.; Ma, L. J.; Wortman, J. R.; Batzoglou, S.; Lee, S. I.; Baştürkmen, M.; Spevak, C. C.; Clutterbuck, J. et al. Sequencing of Aspergillus Nidulans and Comparative Analysis with A. Fumigatus and A. Oryzae. *Nature* **2005**, *438*, 1105–1115.

[81] Li, X.; Huo, X.; Li, J.; She, X.; Pan, X. A Concise Synthesis of (±)-Yaequinolone A2. *Chin. J. Chem.* **2009**, *27*, 1379–1381.

[82] Uchida, R.; Imasato, R.; Shiomi, K.; Tomoda, H.; Ōmura, S. Yaequinolones J1 and J2, Novel Insecticidal Antibiotics from Penicillium Sp. FKI-2140. *Org. Lett.* **2005**, *7*, 5701–5704.

[83] (a) Kempter, C.; Roos, U.; Schorderet Weber, S.; Ebinger, Y.; Glaser, S. *U.S.* 2014, US8648091B2. (b) Gauvry, N.; Kempter, C.; Pautrat, F.; Roos, U. *PTC Int. Appl.* 2014, WO2014044615A1.

[84] (a) Martín Castro, A. M. Claisen Rearrangement over the Past Nine Decades. *Chem. Rev.* **2004**, *104*, 2939–3002. (b) Koch, M.; Elomri, A.; Michel, S.; Tillequin, F. A Novel Synthesis of 6-Demethoxyacronycine. *Heterocycles* **1992**, *34*, 799–807.

[85] (a) Heravi, M. M.; Zadsirjan, V.; Farajpour, B. Applications of Oxazolidinones as Chiral Auxiliaries in the Asymmetric Alkylation Reaction Applied to Total Synthesis. *RSC Adv.* **2016**, *6*, 30498–30551. (b) Evans, D. A.; Bartroli, J.; Shih, T. L. Enantioselective Aldol Condensations. 2. Erythro-Selective Chiral Aldol Condensations via Boron Enolates. *J. Am. Chem. Soc.* **1981**, *103*, 2127–2129.

7.2 Illustration Credits

Figure 1, p. 1

a) Downloaded and adapted for free from: https://de.wikipedia.org/wiki/Datei:Strychnos_nux-vomica_-_K%C3%B6hler%E2%80%93s_Medizinal-Pflanzen-266.jpg (Accessed: 23.03.2020)

b) Downloaded and adapted for free from: https://commons.wikimedia.org/wiki/File:Illustration_Cannabis_sativa0_clean.jpg (Accessed: 23.03.2020)

Figure 2, p. 7

Created using Microsoft Excel (Version 2003)

Figure 3, p. 8

Reprinted with permission from (Burns, N. Z.; Baran, P. S.; Hoffmann, R. W. *Angew. Chem., Int. Ed.* **2009**, *48*, 2854–2867.): Copyright © 2009 WILEY-VCH Verlag GmbH & Co. KGaA, Weinheim (Licence No. 4794661485930)

Figure 4, p. 16

Created using ChemDraw 16 and adapted from Plutschack, M. B.; Pieber, B.; Gilmore, K.; Seeberger, P. H. *Chem. Rev.* **2017**, *117*, 11796–11893.

Scheme 13, p. 24

(b) Crystal structure of AsqJ reprinted with permission of: (Mader, S. L.; Bräuer, A.; Groll, M.; Kaila, V. R. I. Catalytic Mechanism and Molecular Engineering of Quinolone Biosynthesis in Dioxygenase AsqJ. *Nat. Commun.* **2018**, *9*, 1168.) https://www.nature.com/articles/s41467-018-03442-2 published under creative commons attribution 4.0 license http://creativecommons.org/licenses/by/4.0/ .

Appendix

Supporting Information – Synthesis of Quinolinone Alkaloids via Aryne Insertion into Unsymmetric Imides in Flow

Synthesis of Quinolinone Alkaloids via Aryne Insertions into Unsymmetric Imides in Flow

Johannes Schwan, Merlin Kleoff, Bence Hartmayer, Philipp Heretsch* and Mathias Christmann*

Freie Universität Berlin, Institut für Chemie und Biochemie, Takustraße 3, 14195 Berlin, Germany

Supporting Information

General Methods

Analytical data were obtained with the help of the following equipment:

NMR spectroscopy: ^{1}H and ^{13}C NMR spectra were acquired on a JEOL ECX 400 (400 MHz), JEOL ECP 500 (500 MHz) and a Bruker Avance 700 (700 MHZ) in the reported deuterated solvents. The chemical shifts were reported relative to the deuterated solvents' residual shifts. The multiplicities of the signals are reported using the following abbreviations: s = singlet, d = doublet, t = triplet, q = quartet, p = quintet, br = broad.

The spectra were processed with the software MestRec 9.0.

Mass spectra were obtained on a ESI-FTICR-MS: Ionspec QFT-7 (Agilent/Varian), or a HR-EI-MS: Autospec Premier (Waters).

GC-MS were recorded on a GC system Agilent Technologies 7890-A series/Mass selective detector, Agilent Technologies 5975 C (column: HP-5MS (J&W Scientific, Agilent); 30 m, 0.250 mm i.D., Film 0.25 µm).

IR spectroscopy: IR Spectra were recorded on a JASCO FT/IR-4100 spectrometer. Characteristic absorption bands are reported in wavelengths $\tilde{\nu}$ in cm^{-1} and were analyzed with the software Spectral Manager from JASCO.

Melting points were measured on a Thermovar (Reichert) and are not corrected.

Chromatography: Reaction progress was monitored by thin layer chromatography (silica gel 60 F 254, E. Merck) using UV light (λ = 254 nm) for visualization or vanillin staining agent (170 mL methanol, 20.0 ml conc. acetic acid, 10.0 mL conc. sulfuric acid, 1.0 g vanillin).

Flash column chromatography was performed using silica gel M60 from Macherey & Nagel (particle size: 40–63 µm).

HPLC was conducted on a modular Knauer HPLC system with a UV detector at 254 nm and differential refractometer on a 4 x 250 mm column packed with Nucleosil 50-5 from Machery-Nagel.

Flow Reactions: Flow reactions were performed in 1/16 inch PTFE tubing with an inner diameter of 1.0 mm. The tubing was embedded in an aluminum block from ThalesNano and heated with an IKA stirring plate. A stainless steel T-piece from Vici or a static mixer from Upchurch Scientific was used for mixing. Fittings were either coned 10/32 stainless steel fittings from Upchurch scientific or flat bottom 1/4-28 gripper fittings from Dibafit. A kdScientific syringe pump (model no. KDS 200CE) was used to pump the reagents through the reactor.

Reagents and Solvents: Reactions with air or moisture sensitive substances were carried out under an argon atmosphere with the help of the Schlenk technique. All other reagents and solvents were used as purchased from commercial suppliers unless otherwise noted. Anhydrous solvents were purified with the solvent purification system MB-SPS-800 (Braun). Dry acetonitrile was purchased from Acros Organics in AcroSeal©-bottles under argon atmosphere with molecular sieves (4 Å). HPLC-grade acetonitrile was purchased from Fischer Scientific. The solvents used for column chromatography (ethyl acetate, pentane) and work up were purified from commercially available technical grade solvents by distillation under reduced pressure with the help of rotatory evaporators (Heidolph or IKA) at 40 °C bath temperature.

Benzamides,[1] benzyloxy acetic acid,[2] benzyloxyacetyl chloride[3] and 3-hydroxy-2-(trimethylsilyl)phenyl triflate[4] were prepared according to literature procedures.

Compound names are derived from Chemdraw and are not necessarily identical with the IUPAC nomenclature.

Room temperature refers to 23 °C.

Synthesis of Compounds

_N_-(2-Methoxyacetyl)-benzamide (4a)

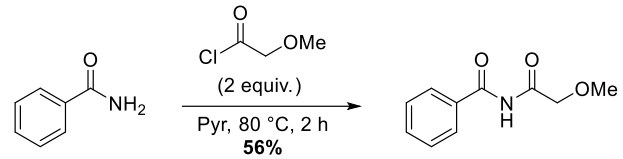

Benzamide (2.00 g, 16.5 mmol, 1 equiv.) was dissolved in anhydrous pyridine (26 mL) and 2-methoxyacetyl chloride (3.01 mL, 33.0 mmol, 2 equiv.) was added in one portion at room temperature. The yellow mixture was stirred in a sealed tube at 80 °C for 2 hours. After cooling to room temperature, the mixture was concentrated under reduced pressure to 1/4 of its original volume and diluted with NH_4Cl (sat. aq., 50 mL) and EtOAc (50 mL). The organic layer was separated and the aqueous layer was extracted with EtOAc (3 × 50 mL). The combined organic layers were washed with NH_4Cl (sat. aq., 3 × 150 mL) and NaCl (sat. aq., 100 mL), dried ($MgSO_4$), filtered, and concentrated under reduced pressure. The crude product was purified by column chromatography (silica gel, *n*-pentane/EtOAc = 1:1) affording the title compound (**4a**, 1.77 g, 9.17 mmol, 56%) as a colorless solid.

R_f = 0.41 (*n*-pentane/EtOAc = 1:1); **m.p.:** 103 **°C -** 105 °C; **^{1}H NMR** (500 MHz, $CDCl_3$): δ = 9.44 (s, 1H), 7.86 (d, *J* = 7.4 Hz, 2H), 7.58 (t, *J* = 7.4 Hz, 1H), 7.48 (t, *J* = 7.7 Hz, 2H), 4.38 (s, 2H), 3.49 (s, 3H) ppm; **^{13}C NMR** (126 MHz, $CDCl_3$): δ = 171.1, 165.2, 133.4, 132.5, 129.0, 127.9, 73.1, 59.5 ppm; **IR** (neat): $\tilde{\nu}$ = 3378, 3280, 3168, 3071, 2990, 2963, 2938, 2920, 2825, 2748, 2600, 1909, 1771, 1709, 1685, 1636, 1602, 1584, 1555, 1508, 1465, 1448, 1396, 1384, 1346, 1327, 1310, 1287, 1250, 1239, 1196, 1169, 1120, 1090, 1069, 1031, 1012, 1002, 973, 933, 907, 842, 818, 805, 751, 701 cm^{-1}; **HRMS** (ESI): m/z calculated for $C_{10}H_{11}NNaO_3^+$ ($[M+Na]^+$): 216.0631; found: 216.0641.

4-Methoxy-_N_-(2-methoxyacetyl)-benzamide (4b)

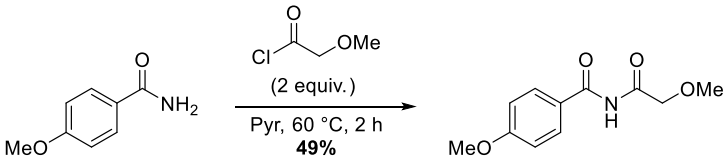

4-Methoxybenzamide (2.00 g, 13.2 mmol, 1 equiv.) was dissolved in anhydrous pyridine (20 mL) and 2-methoxyacetyl chloride (1.50 mL, 16.5 mmol, 2 equiv.) was added at room temperature. The orange mixture was stirred in a sealed tube at 60 °C for 2 hours. After cooling to room temperature, the solvent was removed under reduced pressure. The residue was suspended in $NaHCO_3$ (sat. aq., 250 mL) and EtOAc (250 mL). The organic layer was separated and the aqueous layer was extracted with EtOAc (3 × 100 mL). The combined organic layers were washed with NaCl (sat. aq., 2 × 400 mL), dried (Na_2SO_4), filtered and concentrated under reduced pressure. The crude product was recrystallized from hot EtOAc affording the title compound (**4b**, 1.45 g, 6.48 mmol, 49%) as a colorless solid.

R_f = 0.42 (*n*-pentane/EtOAc = 1:2); **m.p.:** 153 °C - 156 °C; **^{1}H NMR** (400 MHz, DMSO-d_6): δ = 11.00 (s, 1H), 7.94 (d, *J* = 8.8 Hz, 2H), 7.03 (d, *J* = 8.9 Hz, 2H), 4.44 (s, 2H), 3.83 (s, 3H), 3.34 (s, 3H) ppm; **^{13}C NMR** (101 MHz, DMSO-d_6): δ = 172.9, 165.7, 163.0, 130.7, 124.6, 113.8, 72.8, 58.5, 55.6 ppm; **IR** (neat):

$\tilde{\nu}$ = 3390, 3291, 3169, 3094, 3080, 3014, 2970, 2942, 2843, 1769, 1710, 1685, 1645, 1618, 1607, 1574, 1517, 1458, 1422, 1394, 1311, 1254, 1182, 1146, 1124, 1025, 849, 809, 764 cm^{-1}; **HRMS** (ESI): m/z calculated for $C_{11}H_{13}NNaO_4^+$ ([M+Na]$^+$): 246.0737; found 246.0738.

4-bromo-*N*-(2-methoxyacetyl)-benzamide (4c)

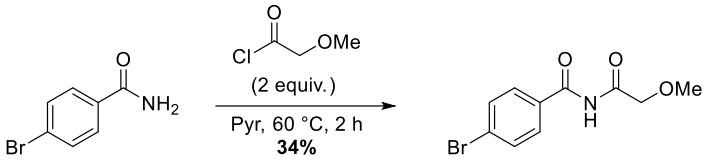

C_7H_6BrNO (200.04) $C_{10}H_{10}BrNO_3$ (272.10)

4-Bromobenzamide (150 mg, 0.992 mmol, 1 equiv.) was dissolved in anhydrous pyridine (1.6 mL) and 2-methoxyacetyl chloride (0.181 mL, 1.99 mmol, 2 equiv.) was added at room temperature. The orange mixture was stirred in a sealed tube at 60 °C for 2 hours. After cooling to room temperature, the solvent was removed under reduced pressure. The residue was suspended in $NaHCO_3$ (sat. aq., 20 mL) and EtOAc (20 mL). The organic layer was separated and the aqueous layer was extracted with EtOAc (3 × 20 mL). The combined organic layers were washed with NaCl (sat. aq., 2 × 50 mL), dried (Na_2SO_4), filtered, and concentrated under reduced pressure. The crude product was purified by column chromatography (silica gel, *n*-pentane/EtOAc 2:1) to afford the title compound (**4c**, 74.0 mg, 0.332 mmol, 34%) as a colorless solid.

R_f = 0.30 (*n*-pentane/EtOAc = 1:2); **m.p.:** 139 °C - 141 °C; **^{1}H NMR** (500 MHz, $CDCl_3$) δ = 9.37 (s, 1H), 7.73 (d, *J* = 8.1 Hz, 2H), 7.64 (d, *J* = 8.2 Hz, 2H), 4.35 (s, 2H), 3.51 (s, 3H) ppm; **^{13}C NMR** (126 MHz, $CDCl_3$) δ = 170.7, 164.5, 132.4, 131.5, 129.5, 128.6, 73.0, 59.6 ppm; **IR** (neat): $\tilde{\nu}$ = 3240, 3196, 3160, 2970, 2952, 2926, 2823, 1731, 16696, 1591, 1524, 1502, 1479, 1400, 1386, 1257, 1232, 1202, 1136, 1110, 1069, 1012, 939, 907, 840, 818, 772, 763, 744, 717, 684, 661 cm^{-1}; **HRMS** (ESI): m/z calculated for $C_{10}H_{10}BrNO_3Na^+$ ([M+Na]$^+$): 293.9736; found: 293.9745.

***N*-(2-(Benzyloxy)acetyl)benzamide (4d)**

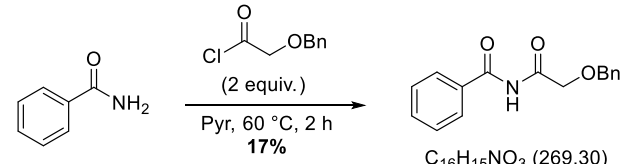

C_7H_7NO (121.14) $C_{16}H_{15}NO_3$ (269.30)

Benzamide (800 mg, 6.60 mmol, 1 equiv.) was dissolved in anhydrous pyridine (11 mL). Benzyloxyacetyl chloride (2.44 g, 13.2 mmol, 2 equiv.) was added and the mixture was stirred in a sealed tube at 60 °C for 2 hours. After cooling to room temperature, the solvent was removed under reduced pressure. The residue was dissolved in EtOAc (10 mL) and $NaHCO_3$ (sat. aq., 10 mL), the layers were separated, and the aqueous layer was extracted with EtOAc (3 x 10 mL). The combined organic layers were washed with NaCl (sat. aq., 2 x 10 mL) and dried ($MgSO_4$). The solvents were removed under reduced pressure. The crude product was recrystallized from boiling EtOAc affording the title compound (**4d**, 300 mg, 1.10 mmol, 17%) as colorless crystals.

m.p.: 109 °C **-** 113 °C; **^{1}H NMR** (700 MHz, $CDCl_3$) δ = 9.32 (s, 1H), 7.82 – 7.80 (m, 2H), 7.60 (td, *J* = 7.3, 1.3 Hz, 1H), 7.50 – 7.47 (m, 2H), 7.39 (s, 2H), 7.38 (d, *J* = 1.6 Hz, 2H), 7.36 – 7.33 (m, 1H), 4.70 (s, 2H), 4.43 (s, 2H) ppm; **^{13}C NMR** (176 MHz, $CDCl_3$) δ = 170.5, 165.0, 136.8, 133.5, 132.6, 129.2,

128.8, 128.5, 128.2, 127.8, 73.9, 70.5 ppm; **IR** (neat): $\tilde{\nu}$ = 3284, 2951, 2922, 2868, 1712, 1688, 1599, 1582, 1500, 1469, 1406, 1390, 1373, 1324, 1304, 1244, 1216, 1115, 1102, 1072, 1028, 1001, 975, 949, 933, 908, 872, 862, 841, 822, 800, 785, 757, 702, 657 cm^{-1}; **HRMS** (ESI): *m/z* calculated for $C_{16}H_{15}NNaO_3^+$ ([M+Na]$^+$): 292.0944; found: 292.0951.

3-(Benzyloxy)-2-(trimethylsilyl)phenyl trifluoromethanesulfonate (**3b**)

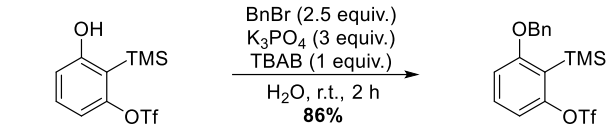

$C_{10}H_{13}F_3O_4SSi$ (314.35) $C_{17}H_{19}F_3O_4SSi$ (404.48)

3-Hydroxy-2-(trimethylsilyl)phenyl trifluoromethanesulfonate (500 mg, 1.59 mmol, 1 equiv.) was suspended in water (15 mL) and benzyl bromide (0.472 mL, 3.98 mmol, 2.5 equiv.), tetrabutylammonium bromide (513 mg, 1.59 mmol, 1 equiv.) and K_3PO_4 (1.01 g, 4.77 mmol, 3 equiv.) were added at room temperature. The suspension was stirred vigorously for 2 hours, diluted with water, and extracted with EtOAc (3 x 50 mL). The combined organic layers were dried (Na_2SO_4), filtered, and concentrated under reduced pressure. The crude product was purified by column chromatography (silica gel, *n*-pentane/EtOAc = 20:1) to afford the title compound (**3b**, 555 mg, 1.37 mmol, 86%) as a colorless oil.

R_f = 0.83 (*n*-pentane/EtOAc = 10:1); **^{1}H NMR** (500 MHz, $CDCl_3$) δ = 7.41 (m, 4H), 7.39 – 7.32 (m, 2H), 6.97 (d, *J* = 8.4 Hz, 1H), 6.89 (d, *J* = 8.4 Hz, 1H), 5.09 (s, 2H), 0.34 (s, 9H) ppm; **^{13}C NMR** (126 MHz, $CDCl_3$) δ = 164.8, 154.9, 136.2, 131.7, 128.8, 128.4, 127.9, 121.2, 118.8 (q, *J* = 320.6 Hz), 113.1, 110.6, 71.1, 1.1 ppm; **^{19}F NMR** (376 MHz, $CDCl_3$) δ = -73.98 ppm; **IR** (neat): $\tilde{\nu}$ = 3067, 3036, 2954, 2901, 2876, 1594, 1565, 1434, 1417, 1247, 1207, 1160, 1137, 1116, 1024, 934, 842, 826, 785, 735 cm^{-1}; **HRMS** (ESI): m/z calculated for $C_{17}H_{19}F_3O_4SSiK$ ([M+K]$^+$): 443.0357, found 443.0378.

3-(Allyloxy)-2-(trimethylsilyl)phenyl trifluoromethanesulfonate (**3c**)

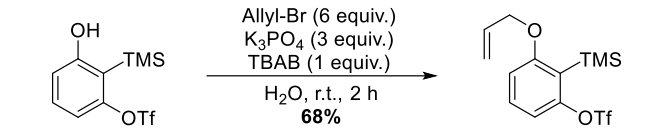

$C_{10}H_{13}F_3O_4SSi$ (314.35) $C_{13}H_{17}F_3O_4SSi$ (354.42)

3-Hydroxy-2-(trimethylsilyl)phenyl trifluoromethanesulfonate (1.47 g, 4.66 mmol, 1 equiv.) was suspended in water (150 mL). Allyl bromide (2.42 mL, 28.0 mmol, 6.0 equiv.), tetrabutylammonium bromide (1.50 g, 4.66 mmol, 1.0 equiv.) and K_3PO_4 (2.97 g, 14.0 mmol, 3 equiv.) were added at room temperature. The suspension was stirred vigorously for 1 hour, diluted with water (50 mL), and extracted with EtOAc (3 x 50 mL). The combined organic layers were dried (Na_2SO_4), filtered, and concentrated under reduced pressure. The crude product was purified by column chromatography (silica gel, *n*-pentane) to afford the title compound (**3c**, 1.12 g, 3.16 mmol, 68%) as a colorless oil.

R_f = 0.65 (*n*-pentane); **^{1}H NMR** (500 MHz, $CDCl_3$) δ = 7.34 (t, *J* = 8.4 Hz, 1H), 6.94 (d, *J* = 8.4 Hz, 1H), 6.81 (d, *J* = 8.3 Hz, 1H), 6.09 – 5.98 (m, 1H), 5.45 – 5.35 (m, 1H), 5.34 – 5.30 (m, 1H), 4.56 (d, *J* = 5.4 Hz, 2H), 0.38 (s, 9H) ppm; **^{13}C NMR** (126 MHz, $CDCl_3$) δ = 164.6, 154.8, 132.7, 131.7, 121.2, 118.8 (q, *J* = 320.6 Hz), 118.5, 113.0, 110.6, 69.7, 1.1 ppm; **^{19}F NMR** (376 MHz, $CDCl_3$) δ = -72.77 ppm; **IR** (neat): $\tilde{\nu}$ = 3089, 2988, 2955, 2901, 2865, 1595, 1565, 1436, 1420, 1362, 1247, 1206, 1160, 1140, 1117, 1057,

1034, 996, 939, 924, 894, 837, 787, 769, 738, 712, 693, 668 cm^{-1}; **HRMS** (ESI): m/z calculated for $C_{13}H_{17}F_3O_4SSiNa^+$ ([M+Na]$^+$): 377.0461, found: 377.0461.

General Procedure for the Optimization of the Aryne Insertion in Flow

A stock solution of **3a** and **4a** at the indicated concentrations was loaded onto a 1 mL sample loop. A second stock solution of tetrabutylammonium difluorotriphenylsilicate at the indicated concentration was loaded on a second 1 mL sample loop. Both loops were connected to two syringes in a syringe pump and the stock solutions were combined at a T-piece or static mixer, as indicated in table S1. The reaction was pushed through a 4 mL reaction coil at the reported flow rate and temperature and collected afterwards. The results are summarized in Table S1.

Table S1. Analysis of main parameters for the synthesis of benzophenone **5a** and acetophenone **7a**

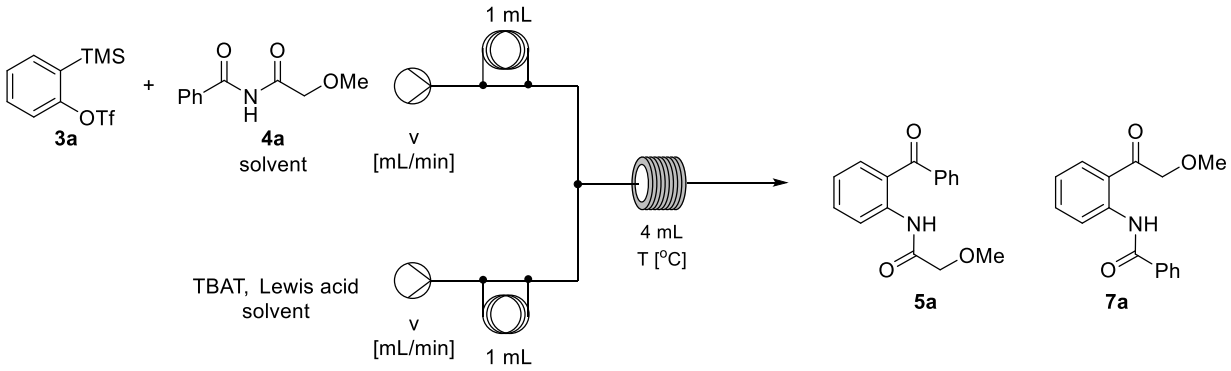

Entry	v [ml/min]	Residence time [min]	Lewis acid	C_{Imid} [mol/L]	C_{Arin} [mol/L]	C_{TBAT} [mol/L]	T [°C]	**5a : 7a**[a]	Solvent/cond.	**5a**[a] [%]
1	0.5	4	none	0.05	0.06	0.10	55	-	no workup	32
2	0.5	4	none	0.05	0.06	0.10	55	-	aq. workup	42
3	0.5	4	none	0.05	0.06	0.10	55	-	wet MeCN, no workup, static mixer	31
4	0.5	4	none	0.05	0.06	0.10	55	-	static mixer, dry MeCN	36
5	0.2	10	none	0.05	0.06	0.10	55	-	wet MeCN, no workup, static mixer	32
6	0.2	10	none	0.05	0.06	0.10	65	-	wet MeCN, no workup, static mixer	32
7	0.2	10	none	0.05	0.08	0.10	55	-	wet MeCN, no workup, static mixer	26
8	0.2	10	none	0.09	0.05	0.10	55	-	wet MeCN, no workup, static mixer	24
9	0.5	4	none	0.05	0.08	0.10	80	-	wet MeCN, no workup, static mixer	42
10	0.5	4	none	0.025	0.04	0.05	55	2.7 : 1	PhMe/MeCN (1:1)	31

11	0.5	4	none	0.025	0.04	0.05	80	4.2 : 1	PhMe/MeCN (1:1); 40 psi BPR[d]	42
12	0.2	10	none	0.025	0.04	0.05	65	3.1 : 1	PhMe/MeCN (1:1), static mixer	32
13	0.5	4	none	0.05	0.08	0.1	55	2.5 : 1	THF	20
14	0.5	4	none	0.04	0.08	0.1	80	4.1 : 1	wet MeCN; 40 psi BPR	36
15	0.5	4	none	0.04	0.08	0.1	90	4.2 : 1	wet MeCN; 40 psi BPR	35
16	0.5	4	none	0.04	0.08	0.1	100	4.0 : 1	wet MeCN; 40 psi BPR	40
17	0.5	4	$Sc(OTf)_3$	0.1	0.15	0.18	65	-	dry MeCN	<5[b]
18	0.5	4	$MgCl_2$	0.1	0.15	0.18	65	-	dry MeCN	<5[b]
19	0.5	4	$BF_3{\cdot}OEt_2$	0.1	0.15	0.18	65	-	dry MeCN	<5[b]
20	0.5	4	$AlCl_3$	0.1	0.15	0.18	65	-	dry MeCN	<5[b]
21	0.5	4	$Ti(OiPr)_4$	0.1	0.15	0.18	65	-	dry MeCN	<5[b]
22	0.5	4	$Ti(OiPr)_4$	0.1	0.15	0.18	65	-	dry MeCN	<5[b]
23	0.5	4	none	0.1	0.15	0.18	65	2.9 : 1[c]	wet MeCN	52[c]
24	0.2	10	none	0.05	0.06	0.075	65	3.3 : 1[b]	dry MeCn	42[c]
25	0.2	10	none	0.05	0.06	0.075	80	3.8 : 1[b]	dry MeCN	39[c]

[a]The ratio of **5a**:**7a** as well as the yield of **5a** were determined via GC-MS with acetanilide as standard. An aliquot of the reactor output (100 µL or 500 µL) was taken, diluted to yield a volume of 900 µL, and treated with a solution of acetanilide (100 µL, 0.05 M). [b]Determined by ^{1}H NMR integration. [c]Isolated yield. [d]BPR: back pressure regulator.

General Procedure for the Aryne Insertion in Flow (GP1)

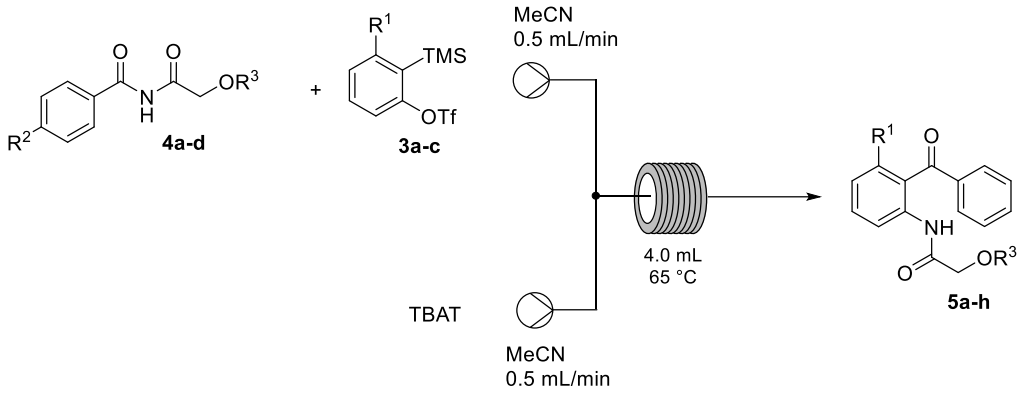

A stock solution of aryne precursor (**3a**–**c**, 0.150 M in acetonitrile, 1.5 equiv.) and imide (**4a**–**d**, 0.100 M in acetonitrile, 1.0 equiv.) were pumped simultaneously with a stock solution of tetrabutylammonium difluorotriphenylsilicate (0.180 M in acetonitrile, 1.8 equiv.), both at a rate of 0.5 mL/min. The stock solutions were combined at a T-piece to react in a 4.0 mL PTFE coil, preheated to 65 °C. The reaction mixture was collected, concentrated under reduced pressure, and purified by column chromatography to afford the *ortho*-aminobenzophenones **5a**–**h**. The constitutional isomer ratio was deduced by ^{1}H NMR integration of the crude reaction product.

***N*-(2-Benzoylphenyl)-2-methoxyacetamide (5a)**

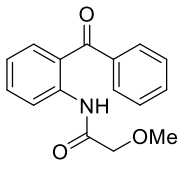

5a $C_{16}H_{15}NO_3$ (269.30)

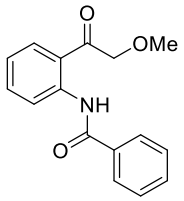

7a $C_{16}H_{15}NO_3$ (269.30)

Compound **5a** was prepared according to **GP1** starting from **3a** (127 mg, 0.427 mmol, 1.5 equiv.) and **4a** (55.0 mg, 0.285 mmol, 1 equiv.). Column chromatography (silica gel, *n*-pentane/EtOAc = 4:1) afforded the title compound (**5a**, 40.0 mg, 0.148 mmol, 52%) as a colorless oil that solidified in the fridge and compound **7** (14.5 mg, 0.054 mmol, 19%) as a colorless solid. The isomeric ratio was determined as 2.9:1 (**5a**:**7a**).

5a:

R_f = 0.40 (*n*-pentane/EtOAc = 3:1); **^{1}H NMR** (700 MHz, $CDCl_3$): δ = 11.39 (s, 1H), 8.69 (d, *J* = 8.3 Hz, 1H), 7.73 – 7.70 (m, 2H), 7.60 – 7.54 (m, 3H), 7.47 (t, *J* = 7.8 Hz, 2H), 7.11 (td, *J* = 7.6, 1.2 Hz, 1H), 4.04 (s, 2H), 3.55 (s, 3H) ppm; **^{13}C NMR** (176 MHz, $CDCl_3$): δ 199.1, 169.2, 139.4, 138.7, 134.1, 133.5, 132.5, 130.0, 128.4, 124.3, 122.6, 121.7, 72.7, 59.8 ppm; **IR** (neat): $\tilde{\nu}$ = 3286, 3060, 3033, 2996, 2934, 2828, 2756, 2249, 1832, 1692, 1639, 1598, 1577, 1515, 1446, 1432, 1362, 1317, 1293, 1263, 1196, 1180, 1158, 1114, 1076, 1048, 1028, 987, 959, 935, 917, 880, 852, 805, 752, 728 cm^{-1}; **HRMS** (ESI): m/z calculated for $C_{16}H_{15}NNaO_3^+$ ([M+Na]$^+$): 292.0944; found: 292.0959.

7a:

R_f = 0.35 (*n*-pentane/EtOAc = 3:1); **m.p.:** 138–139 °C; **^{1}H NMR** (500 MHz, $CDCl_3$): δ = 12.57 (s, 1H), 9.02 (dd, J = 8.6, 1.1 Hz, 1H), 8.12 – 8.08 (m, 2H), 7.82 (dd, J = 8.0, 1.4 Hz, 1H), 7.64 (ddd, J = 8.7, 7.3, 1.5 Hz, 1H), 7.58 – 7.54 (m, 1H), 7.53 – 7.49 (m, 2H), 7.14 (t, J = 8.2 Hz, 1H), 4.81 (s, 2H), 3.55 (s, 3H) ppm; **^{13}C NMR** (126 MHz, $CDCl_3$): δ = 200.2, 166.2, 141.8, 135.9, 134.6, 132.2, 129.6, 129.0, 127.7, 122.6, 121.3, 119.7, 75.5, 59.7 ppm; **IR** (neat): $\tilde{\nu}$ = 3268, 3236, 3130, 3062, 2995, 2942, 2829, 1672, 1653, 1610, 1585, 1559, 1537, 1507, 1496, 1448, 1368, 1322, 1311, 1258, 1216, 1196, 1139, 1120, 1029, 978, 925, 699, 661 cm^{-1}; **HRMS** (ESI): m/z calculated for $C_{16}H_{15}NNaO_3^+$ ([M+Na]$^+$): 292.0944; found: 292.0944.

2-Methoxy-*N*-(2-(4-methoxybenzoyl)phenyl)acetamide (5b)

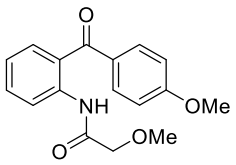

5b

$C_{17}H_{17}NO_4$ (299.33)

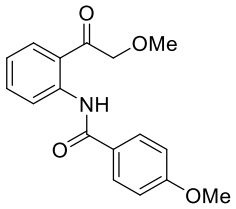

7b

$C_{17}H_{17}NO_4$ (299.33)

Compound **5b** was prepared according to **GP1** starting from **3a** (90.4 mg, 0.303 mmol, 1.5 equiv., 0.015 M) and **4b** (45.0 mg, 0.202 mmol, 1 equiv., 0.010 M). Column chromatography (silica gel, *n*-pentane/EtOAc = 3:1) afforded the title compound (**5b**, 32.8 mg, 0.122 mmol, 60%) as a slightly yellow oil. The isomeric ratio was determined as 4.6:1 (**5b**:**7b**).

5b:

R_f = 0.21 (*n*-pentane/EtOAc = 3:1); **^{1}H NMR** (500 MHz, $CDCl_3$): δ = 11.09 (s, 1H), 8.62 (dt, *J* = 8.1, 1.0 Hz, 1H), 7.78 – 7.72 (m, 2H), 7.58 – 7.52 (m, 2H), 7.16 – 7.09 (m, 1H), 6.99 – 6.93 (m, 2H), 4.03 (s, 2H), 3.89 (s, 3H), 3.53 (s, 3H) ppm; **^{13}C NMR** (126 MHz, $CDCl_3$): δ = 197.3, 169.1, 163.5, 138.8, 133.4, 132.8, 132.7, 131.1, 125.3, 122.7, 121.9, 113.7, 72.7, 59.8, 55.7 ppm; **IR** (neat): $\tilde{\nu}$ = 3310, 3006, 2931, 2840, 1687, 1633, 1597, 1578, 1510, 1447, 1419, 1315, 1306, 1293, 1253, 1196, 1172, 1154, 1110, 1026, 986, 925, 844, 788, 760, 739, 696 cm^{-1}; **HRMS** (ESI): m/z calculated for $C_{17}H_{17}NNaO_4^+$ ([M+Na]$^+$): 322.1050; found: 322.1062.

***N*-(2-(4-Bromobenzoyl)phenyl)-2-methoxyacetamide (5c)**

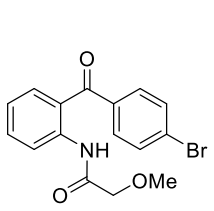

5c
$C_{16}H_{14}BrNO_3$ (348.20)

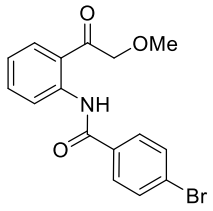

7c
$C_{16}H_{14}BrNO_3$ (348.20)

Compound **5c** was prepared according to **GP1** starting from **3a** (44.8 mg, 0.150 mmol, 1.5 equiv.) **4c** (27.2 mg, 0.100 mmol, 1 equiv.). Column chromatography (silica gel, *n*-pentane/EtOAc 3:1) afforded the title compound (**5c**, 8.10 mg, 0.023 mmol, 23%) as a slightly yellow oil. The isomeric ratio was determined as 4.5:1 (**5c**:**7c**).

5c:

R_f = 0.33 (*n*-pentane/EtOAc = 3:1); **^{1}H NMR** (500 MHz, $CDCl_3$): δ = 11.31 (s, 1H), 8.68 (dd, *J* = 8.4, 1.0 Hz, 1H), 7.67 – 7.54 (m, 5H), 7.52 (dd, *J* = 7.9, 1.6 Hz, 1H), 7.15 – 7.11 (m, 1H), 4.05 (s, 2H), 3.56 (s, 3H) ppm; **^{13}C NMR** (126 MHz, $CDCl_3$): δ = 197.9, 169.2, 139.5, 137.5, 134.4, 133.2, 131.8, 131.6, 127.7, 124.0, 122.8, 121.9, 72.7, 59.9 ppm; **IR** (neat): $\tilde{\nu}$ = 3298, 3081, 3033, 2995, 2932, 2827, 1692, 1641, 1601, 1577, 1515, 1483, 1446, 1432, 1394, 1361, 1314, 1293, 1262, 1196, 1178, 1167, 1157, 1114, 1068, 1051, 1010, 987, 959, 921, 880, 841, 783, 758, 725, 675, 654 cm^{-1}; **HRMS** (ESI): m/z calculated for $C_{16}H_{14}BrNNaO_3^+$ ([M+Na]$^+$): 370.0049; found: 370.0063.

***N*-(2-Benzoyl-3-(benzyloxy)phenyl)-2-methoxyacetamide (5d)**

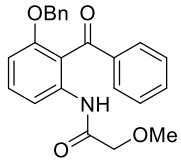

5d
$C_{23}H_{21}NO_4$ (375.42)

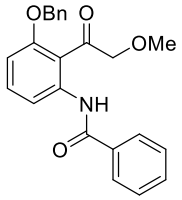

7d
$C_{23}H_{21}NO_4$ (375.42)

Compound **5d** was prepared according to **GP1** starting from **3b** (273 mg, 0.675 mmol, 1.5 equiv.) and **4a** (87.0 mg, 0.450 mmol, 1 equiv.). Column chromatography (silica gel, *n*-pentane/EtOAc = 4:1) afforded the title compound (**5d**, 59.0 mg, 0.082 mmol, 35%) as a slightly yellow oil. Additionally, **7d** (14.6 mg, 0.038 mmol, 9%) was isolated as a colorless oil. The isomeric ratio was determined as 4.9:1 (**5d**:**7d**).

5d:

R_f = 0.24 (*n*-pentane/EtOAc = 4:1); **^{1}H NMR** (700 MHz, $CDCl_3$): δ = 9.51 (s, 1H), 8.03 (dd, *J* = 8.4, 0.8 Hz, 1H), 7.80 – 7.77 (m, 2H), 7.55 (tt, *J* = 8.7, 1.3 Hz, 1H), 7.47 – 7.41 (m, 3H), 7.21 – 7.17 (m, 1H), 7.16 – 7.13 (m, 2H), 6.81 (dd, *J* = 8.4, 0.8 Hz, 1H), 6.77 (d, *J* = 7.5 Hz, 2H), 4.90 (s, 2H), 3.93 (s, 2H), 3.41 (s, 3H) ppm; **^{13}C NMR** (176 MHz, $CDCl_3$): δ = 197.1, 168.6, 157.4, 139.4, 137.1, 136.1, 133.1, 132.5, 129.4, 128.5, 128.4, 127.8, 126.8, 118.8, 115.2, 108.5, 72.4, 70.4, 59.6 ppm; **IR** (neat): $\tilde{\nu}$ = 3359, 3061, 3031, 3003, 2929, 2829, 1802, 1693, 1646, 1597, 1581, 1523, 1497, 1466, 1460, 1450, 1428,

1381, 1313, 1275, 1256, 1196, 1178, 1146, 1112, 1087, 1071, 1028, 986, 925, 875, 865, 846, 807, 782, 739 cm^{-1}; **HRMS** (ESI): m/z calculated for $C_{23}H_{21}NNaO4^+$ ([M+Na]$^+$): 398.1363; found: 398.1367.

7d:

R_f = 0.37 (*n*-pentane/EtOAc = 4:1); **^{1}H NMR** (700 MHz, $CDCl_3$): δ = 12.22 (s, 1H), 8.52 (dd, *J* = 8.5, 0.9 Hz, 1H), 8.07 – 8.03 (m, 2H), 7.56 – 7.53 (m, 1H), 7.53 – 7.48 (m, 3H), 7.46 – 7.42 (m, 4H), 7.41 – 7.38 (m, 1H), 6.80 (dd, *J* = 8.4, 1.0 Hz, 1H), 5.17 (s, 2H), 4.56 (s, 2H), 3.31 (s, 3H) ppm; **^{13}C NMR** (176 MHz, $CDCl_3$): δ = 202.6, 166.2, 160.2, 142.1, 135.5, 135.3, 134.8, 132.2, 129.0, 128.9, 128.9, 128.3, 127.7, 114.5, 113.3, 107.2, 80.3, 71.6, 59.2 ppm; **IR** (neat): $\tilde{\nu}$ = 3065, 3031, 2925, 2822, 1680, 1648, 1604, 1579, 1525, 1492, 1458, 1408, 1382, 1271, 1187, 1124, 1098, 1053, 1024, 1001, 986, 910, 847, 787, 741 cm^{-1}; **HRMS** (ESI): m/z calculated for $C_{23}H_{21}NNaO4^+$ ([M+Na]$^+$): 398.1363; found: 398.1382.

N-(3-(Benzyloxy)-2-(4-methoxybenzoyl)phenyl)-2-methoxyacetamide (5e)

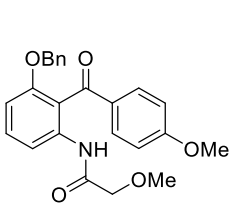

5e

$C_{24}H_{23}NO_5$ (405.45)

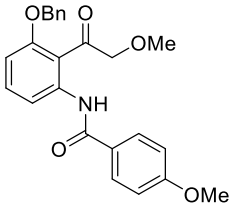

7e

$C_{24}H_{23}NO_5$ (405.45)

Compound **5e** was prepared according to **GP1** starting from **3b** (571 mg, 1.41 mmol, 1.5 equiv., 0.015 M) and **4b** (210 mg, 0.941 mmol, 1 equiv., 0.010 M). Column chromatography (silica gel, *n*-pentane/EtOAc = 3:1) afforded the title compound (**5e**, 90.6 mg, 0.122 mmol, 24%) as a slightly yellow oil. Additionally, **7e** (38.1 mg, 0.094 mmol, 10%) was isolated as a colorless oil. The isomeric ratio was determined as 2.8:1 (**5e**:**7e**).

5e:

R_f = 0.18 (*n*-pentane/EtOAc = 3:1); **^{1}H NMR** (700 MHz, CD_3CN): δ = 8.96 (s, 1H), 7.87 (dd, *J* = 8.3, 0.8 Hz, 1H), 7.76 – 7.73 (m, 2H), 7.47 (t, *J* = 8.3 Hz, 1H), 7.24 – 7.18 (m, 3H), 6.99 – 6.96 (m, 3H), 6.95 – 6.93 (m, 2H), 4.98 (s, 2H), 3.85 (s, 3H), 3.84 (s, 2H), 3.30 (s, 3H) ppm; **^{13}C NMR** (176 MHz, CD_3CN): δ = 195.8, 169.1, 165.2, 157.6, 137.4, 137.3, 132.6, 132.5, 132.2, 129.2, 128.7, 128.1, 120.7, 115.9, 114.9, 109.8, 72.7, 71.1, 59.7, 56.4 ppm; **IR** (neat): $\tilde{\nu}$ = 3360, 3062, 3034, 3009, 2935, 2840, 1691, 1645, 1593, 1509, 1461, 1382, 1280, 1254, 1173, 1145, 1111, 1070, 1028, 986, 927, 844, 793, 735, 696, 668 cm^{-1}; **HRMS** (ESI): m/z calculated for $C_{24}H_{23}NNaO_5^+$ ([M+Na]$^+$): 428.1468; found: 428.1461.

7e:

R_f = 0.30 (*n*-pentane/EtOAc = 5:2); **^{1}H NMR** (700 MHz, $CDCl_3$): δ = 12.16 (s, 1H), 8.51 (d, *J* = 8.5 Hz, 1H), 8.03 (d, *J* = 8.7 Hz, 2H), 7.49 (td, *J* = 8.5, 1.9 Hz, 1H), 7.46 – 7.37 (m, 5H), 7.00 – 6.96 (m, 2H), 6.78 (d, *J* = 8.3 Hz, 1H), 5.16 (s, 2H), 4.56 (s, 2H), 3.87 (d, *J* = 2.1 Hz, 3H), 3.31 (d, *J* = 2.0 Hz, 3H) ppm; **^{13}C NMR** (176 MHz, $CDCl_3$): δ = 202.6, 165.7, 162.8, 160.2, 142.4, 135.5, 135.3, 129.6, 129.0, 128.9, 128.3, 127.1, 114.4, 114.1, 111.6, 106.8, 80.3, 71.6, 59.2, 55.6 ppm; **IR** (neat): $\tilde{\nu}$ = 3194, 2953, 2925, 2844, 2818, 1675, 1647, 1604, 1579, 1531, 1507, 1457, 1420, 1404, 1380, 1308, 1253, 1174,

1124, 1052, 1027, 983, 907, 844, 787, 760, 744 cm^{-1}; **HRMS** (ESI): m/z calculated for $C_{24}H_{23}NNaO_5^+$ ($[M+Na]^+$): 428.1468; found: 428.1476.

***N*-(2-Benzoylphenyl)-2-(benzyloxy)acetamide (5f)**

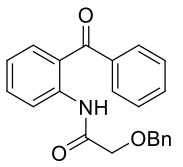

5f
$C_{22}H_{19}NO_3$ (345.40)

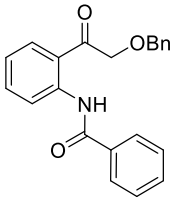

7f
$C_{22}H_{19}NO_3$ (345.40)

Compound **5f** was prepared according to **GP1** starting from **3a** (199 mg, 0.668 mmol, 1.5 equiv.) and **4d** (120 mg, 0.446 mmol, 1 equiv.). Column chromatography (silica gel, *n*-pentane/EtOAc 6:1) afforded the title compound (**5f**, 63.0 mg, 0.180 mmol, 40%) as a colorless oil. Additionally, compound **7f** (19.1 mg, 0.058 mmol, 13%) was isolated as colorless oil. The isomer ratio was determined as 4.3:1 (**5f**:**7f**).

5f:

R_f = 0.23 (*n*-pentane/EtOAc = 6:1); **^{1}H NMR** (700 MHz, $CDCl_3$): δ = 11.46 (s, 1H), 8.67 (dd, *J* = 8.4, 1.1 Hz, 1H), 7.77 – 7.74 (m, 2H), 7.62 – 7.55 (m, 3H), 7.52 – 7.45 (m, 4H), 7.37 – 7.33 (m, 2H), 7.32 – 7.28 (m, 1H), 7.15 – 7.10 (m, 1H), 4.73 (s, 2H), 4.10 (s, 2H) ppm; **^{13}C NMR** (176 MHz, $CDCl_3$): δ = 198.8, 169.2, 139.3, 138.7, 136.9, 134.0, 133.3, 132.6, 130.2, 128.7, 128.4, 128.2, 128.1, 124.6, 122.7, 121.8, 73.8, 69.8 ppm; **IR** (neat): $\tilde{\nu}$ = 3300, 3061, 3029, 2955, 2924, 2867, 1694, 1641, 1599, 1578, 1519, 1447, 1397, 1373, 1317, 1293, 1265, 1207, 1163, 1099, 1027, 1000, 974, 936, 921, 852, 805, 75 cm^{-1}; **HRMS** (ESI): m/z calculated for $C_{22}H_{19}NNaO_3^+$ ($[M+Na]^+$): 368.1257; found: 368.1263.

7f:

R_f = 0.25 (*n*-pentane/EtOAc = 6:1); **^{1}H NMR** (700 MHz, $CDCl_3$): δ = 12.51 (s, 1H), 9.02 – 9.00 (m, 1H), 8.13 – 8.09 (m, 2H), 7.81 – 7.79 (m, 1H), 7.65 – 7.61 (m, 1H), 7.60 – 7.54 (m, 1H), 7.54 – 7.51 (m, 2H), 7.41 – 7.38 (m, 2H), 7.38 – 7.35 (m, 2H), 7.33 – 7.30 (m, 1H), 7.12 (ddd, *J* = 8.0, 7.3, 1.2 Hz, 1H), 4.82 (s, 2H), 4.75 – 4.72 (m, 2H) ppm; **^{13}C NMR** (176 MHz, $CDCl_3$): δ = 200.3, 166.3, 141.8, 137.1, 135.8, 134.8, 132.2, 130.0, 129.0, 128.8, 128.3, 128.2, 127.7, 122.6, 121.3, 120.0, 73.8, 73.0 ppm; **IR** (neat): $\tilde{\nu}$ = 3276, 3243, 3062, 3030, 2925, 2857, 1664, 1607, 1583, 1525, 1496, 1450, 1365, 1305, 1256, 1213, 1188, 1168, 1144, 1121, 1094, 1053, 1028, 976, 946, 896, 869, 798, 751 cm^{-1}; **HRMS** (ESI): m/z calculated for $C_{22}H_{19}NNaO_3^+$ ($[M+Na]^+$): 368.1257; found: 368.1260.

***N*-(3-(Allyloxy)-2-benzoylphenyl)-2-methoxyacetamide (5g)**

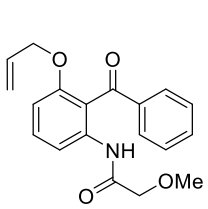

5g
$C_{19}H_{19}NO_4$ (325.36)

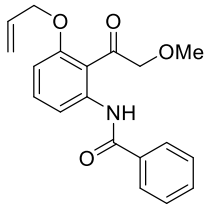

7g
$C_{19}H_{19}NO_4$ (325.36)

Compound **5g** was prepared according to **GP1** starting from **3c** (107 mg, 0.303 mmol, 1.5 equiv.) and **4a** (45.0 mg, 0.202 mmol, 1 equiv.). Column chromatography (silica gel, *n*-pentane/EtOAc = 3:1) afforded the title compound (**5g**, 12.0 mg, 0.0371 mmol, 18%) as a slightly yellow oil. The isomeric ratio was determined as 3.0:1 (**5g**:**7g**).

5g:

R_f = 0.29 (*n*-pentane/EtOAc = 3:1); **^{1}H NMR** (500 MHz, $CDCl_3$): δ = 9.52 (s, 1H), 8.01 (dd, *J* = 8.4, 0.8 Hz, 1H), 7.80 – 7.73 (m, 2H), 7.56 – 7.51 (m, 1H), 7.47 – 7.38 (m, 3H), 6.73 (dd, *J* = 8.4, 0.9 Hz, 1H), 5.53 (ddt, *J* = 17.2, 10.7, 4.9 Hz, 1H), 4.97 (dq, *J* = 10.7, 1.5 Hz, 1H), 4.87 (dq, *J* = 17.3, 1.7 Hz, 1H), 4.35 (dt, *J* = 5.0, 1.7 Hz, 2H), 3.93 (s, 2H), 3.40 (s, 3H) ppm; **^{13}C NMR** (126 MHz, $CDCl_3$): δ = 197.1, 168.6, 157.4, 139.3, 137.1, 133.1, 132.5, 132.1, 129.3, 128.4, 118.6, 117.1, 115.1, 108.6, 72.4, 69.3, 59.6 ppm; **IR** (neat): $\tilde{\nu}$ = 3356, 3066, 2951, 2922, 2850, 1696, 1648, 1597, 1584, 1522, 1468, 1422, 1370, 1362, 1314, 1277, 1197, 1178, 1145, 1114, 1076, 986, 926, 853, 808, 782, 746, 718, 702, 671, 661 cm^{-1}; **HRMS** (ESI): m/z calculated for $C_{19}H_{19}NNaO_4^+$ ([M+Na]$^+$): 348.1206; found: 348.1207.

***N*-(3-(Allyloxy)-2-(4-methoxybenzoyl)phenyl)-2-methoxyacetamide (5h)**

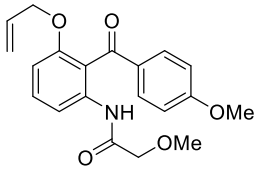

5h
$C_{20}H_{21}NO_5$ (355.39)

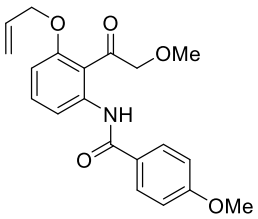

7h
$C_{20}H_{21}NO_5$ (355.39)

Compound **5h** was prepared according to **GP1** starting from **3c** (198 mg, 0.555 mmol, 1.5 equiv., 0.015 M) and **4b** (83.0 mg, 0.370 mmol, 1 equiv., 0.010 M). Column chromatography (silica gel, *n*-pentane/EtOAc = 2:1) afforded the title compound (**5h**, 39.3 mg, 0.111 mmol, 30%) as a slightly yellow oil. The isomeric ratio was determined as 4.2:1 (**5h**:**7h**).

5h:

R_f = 0.32 (*n*-pentane/EtOAc = 2:1); **^{1}H NMR** (500 MHz, $CDCl_3$): δ = 9.25 (s, 1H), 7.95 (d, *J* = 7.8 Hz, 1H), 7.78 (d, *J* = 8.5 Hz, 2H), 7.40 (t, *J* = 8.3 Hz, 1H), 6.89 (d, *J* = 8.2 Hz, 2H), 6.74 (d, *J* = 9.1 Hz, 1H), 5.65 (ddt, *J* = 17.2, 10.6, 4.9 Hz, 1H), 5.02 (dq, *J* = 10.7, 1.5 Hz, 1H), 4.96 (dq, *J* = 17.3, 1.7 Hz, 1H), 4.40 (dt, *J* = 4.8, 1.7 Hz, 2H), 3.90 (s, 2H), 3.86 (s, 3H), 3.37 (s, 3H) ppm; **^{13}C NMR** (126 MHz, $CDCl_3$): δ = 195.1, 168.5, 164.0, 156.8, 136.5, 132.4, 132.0, 131.8, 131.6, 119.5, 117.1, 115.2, 113.7, 108.7, 72.3, 69.3, 59.6, 55.7 ppm; **IR** (neat): $\tilde{\nu}$ = 3359, 3075, 2931, 2840, 1810, 1693, 1646, 1594, 1522, 1509, 1467, 1421, 1382, 1362, 1315, 1281, 1256, 1196, 1173, 1146, 1113, 1073, 1026, 986, 929, 880, 846,

817, 792, 768, 734, 709, 693, 672, 663 cm^{-1}; **HRMS** (ESI): m/z calculated for $C_{20}H_{21}NNaO_5^+$ ([M+Na]$^+$): 378.1312; found: 378.1331.

General Procedure for the Aldol Reaction (GP2)

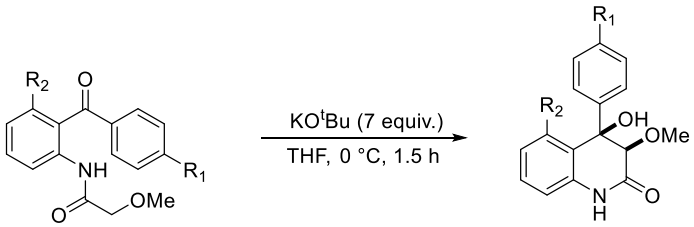

The *ortho*-aminobenzophenone (**5a**–**h**, 1 equiv.) was dissolved in anhydrous THF (50 mL/mmol substrate) and a solution of KO^{t}Bu (7 equiv., 1 M in THF) was added dropwise at 0 °C. Upon addition of KO^{t}Bu, the solution turned bright yellow. After stirring at 0 °C for 1.5 hours, water (50 mL/mmol substrate) was added to the reaction mixture. The organic layer was separated and the aqueous layer was extracted with EtOAc (3 x 50 mL/mmol substrate). The combined organic layers were dried ($MgSO_4$), filtered, and concentrated under reduced pressure. The crude products were purified by column chromatography to afford the quinolinones **6a**–**g**.

(±)–6-Deoxyaflaquinolone E (6a)

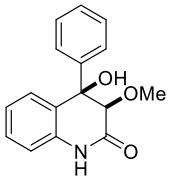

$C_{16}H_{15}NO_3$ (269.30)

6-Deoxyaflaquinolone E was prepared according to **GP2** starting from **5a** (20 mg, 0.075 mmol, 1 equiv.) and KO^{t}Bu (59 mg, 0.53 mmol, 7 equiv.). The crude product was purified by column chromatography (silica gel, CH_2Cl_2/MeOH = 100:3) to afford the title compound (**6a**, 18 mg, 0.068 mmol, 92%) as a colorless solid.

R_f = 0.21 (*n*-pentane/EtOAc = 1:1); **m.p.:** 160–165 °C; **^{1}H NMR** (700 MHz, DMSO-d_6): δ = 10.21 (s, 1H), 7.33 (m, 4H), 7.28 (dt, *J* = 8.5, 4.2 Hz, 1H), 7.24 – 7.20 (m, 1H), 6.93 – 6.90 (m, 2H), 6.88 (dd, *J* = 7.5, 1.6 Hz, 1H), 5.81 (s, 1H), 4.18 (s, 1H), 3.34 (s, 3H) ppm; **^{13}C NMR** (176 MHz, DMSO-d_6): δ = 168.4, 142.3, 136.8, 129.2, 128.7, 127.8, 127.5, 127.3, 126.7, 122.1, 115.1, 83.9, 76.7, 59.1 ppm; **IR** (neat): $\tilde{\nu}$ = 3446, 3361, 3211, 3085, 3022, 2993, 2931, 2845, 2831, 1681, 1609, 1593, 1559, 1486, 1446, 1433, 1397, 1318, 1285, 1263, 1246, 1226, 1203, 1181, 1157, 1142, 1119, 1097, 1069, 1048, 1020, 1001, 953, 940, 910, 871, 858, 824, 791, 762, 752, 704, 674, 658 cm^{-1}; **HRMS** (ESI): m/z calculated for $C_{16}H_{15}NNaO_3^+$ ([M+Na]$^+$): 292.0944; found: 292.0945. The NMR data match those reported for 6-deoxyaflaquinolone E.[5]

(±)–Quinolinone A (6b)

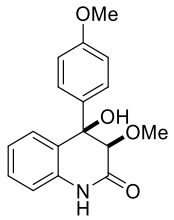

$C_{17}H_{17}NO_4$ (299.33)

Quinolinone A was prepared according to **GP2** starting from **5b** (20 mg, 0.067 mmol, 1 equiv.) and KO*t*Bu (53 mg, 0.47 mmol, 7 equiv.). The crude product was purified by column chromatography (silica gel, CH_2Cl_2/MeOH = 100:3) to afford the title compound (**6b**, 16.7 mg, 0.056 mmol, 84%) as a colorless solid.

R_f = 0.22 (*n*-pentane/EtOAc = 1:1); **m.p.:** 172–175 °C; **^{1}H NMR** (500 MHz, acetone-d_6): δ = 9.29 (s, 1H), 7.35 – 7.20 (m, 4H), 7.07 – 6.97 (m, 2H), 6.91 – 6.81 (m, 2H), 4.61 (s, 1H), 3.93 (s, 1H), 3.76 (s, 3H), 3.45 (s, 3H) ppm; **^{13}C NMR** (126 MHz, acetone-d_6): δ = 168.2, 160.3, 137.6, 134.5, 129.6, 129.0, 128.4, 123.6, 115.9, 115.9, 114.2, 85.7, 77.3, 59.4, 55.5 ppm; **IR** (neat): $\tilde{\nu}$ = 3249, 3081, 3002, 2931, 2836, 1687, 1611, 1595, 1512, 1483, 1463, 1379, 1306, 1252, 1173, 1146, 1106, 1081, 1033, 991, 942, 903, 860, 833, 812, 757 cm^{-1}; **HRMS** (ESI): m/z calculated for $C_{17}H_{17}NNaO_4^+$ ([M+Na]$^+$): 322.1050; found: 322.1047. The NMR data match those reported for Quinolinone A.[6]

***cis*-4-(4-Bromophenyl)-4-hydroxy-3-methoxy-3,4-dihydroquinolin-2(1*H*)-one (6c)**

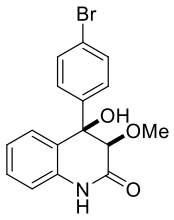

$C_{16}H_{14}BrNO_3$ (348.20)

Compound **6c** was prepared according to **GP2** starting from **5c** (8.0 mg, 0.021 mmol, 1 equiv.) and KO*t*Bu (16 mg, 0.15 mmol, 7 equiv.). The crude product was purified by column chromatography (silica gel, CH_2Cl_2/MeOH = 100:3) to afford the title compound (**6c**, 7.2 mg, 0.019 mmol, 90%) as a colorless oil.

R_f = 0.21 (*n*-pentane/EtOAc = 1:1); **^{1}H NMR** (700 MHz, CD_3OD): δ = 7.51 (d, *J* = 8.8 Hz, 2H), 7.36 – 7.33 (m, 2H), 7.28 (ddd, *J* = 8.0, 5.8, 3.0 Hz, 1H), 7.00 – 6.98 (m, 2H), 6.95 (dt, *J* = 7.9, 0.8 Hz, 1H), 4.23 (s, 1H), 3.40 (s, 3H) ppm; **^{13}C NMR** (176 MHz, $CDCl_3$): δ = 170.9, 142.4, 138.0, 132.2, 130.5, 130.2, 129.7, 129.1, 124.3, 122.7, 116.8, 85.4, 78.4, 60.6 ppm; **IR** (neat): $\tilde{\nu}$ = 3241, 3069, 2954, 2927, 2853, 2358, 1685, 1607, 1592, 1488, 1467, 1394, 1309, 1205, 1173, 1143, 989, 802, 759 cm^{-1}; **HRMS** (ESI): m/z calculated for $C_{16}H_{14}BrNO_3Na^+$ ([M+Na]$^+$): 370.0049; found: 370.0051.

***cis*-5-(Benzyloxy)-4-hydroxy-3-methoxy-4-phenyl-3,4-dihydroquinolin-2(1*H*)-one (6d)**

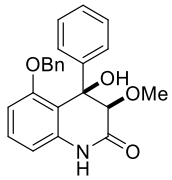

$C_{23}H_{21}NO_4$ (375.42)

Compound **6d** was prepared according to **GP2** starting from **5d** (28 mg, 0.075 mmol, 1 equiv.) and KO*t*Bu (59 mg, 0.53 mmol, 7 equiv.). The crude product was purified by column chromatography (silica gel, CH_2Cl_2/MeOH = 100:2) to afford the title compound (**6d**, 23 mg, 0.062 mmol, 84%) as a colorless oil.

R_f = 0.25 (*n*-pentane/EtOAc = 1:1); **^{1}H NMR** (700 MHz, $CDCl_3$): δ = 8.58 (s, 1H), 7.28 – 7.21 (m, 9H), 7.07 (dd, *J* = 7.6, 1.9 Hz, 2H), 6.73 (dd, *J* = 8.5, 0.9 Hz, 1H), 6.57 (dd, *J* = 8.0, 0.9 Hz, 1H), 5.29 (s, 1H), 5.05 (d, *J* = 11.5 Hz, 1H), 4.96 (d, *J* = 11.6 Hz, 1H), 3.85 (d, *J* = 1.4 Hz, 1H), 3.61 (s, 3H) ppm; **^{13}C NMR** (176 MHz, $CDCl_3$): δ = 168.0, 158.0, 142.0, 137.2, 135.7, 130.1, 128.7, 128.7, 128.4, 128.3, 127.5, 126.2, 115.2, 109.6, 108.8, 85.0, 78.4, 71.1, 59.8 ppm; **IR** (neat): $\tilde{\nu}$ = 3503, 3232, 3062, 3031, 2930, 2829, 2248, 1691, 1595, 1498, 1471, 1448, 1383, 1315, 1277, 1259, 1222, 1176, 1138, 1102, 1059, 1028, 993, 910, 846, 783, 730, 697, 654 cm^{-1}; **HRMS** (ESI): m/z calculated for $C_{23}H_{21}NNaO_4^+$ ($[M+Na]^+$): 398.1363; found: 398.1368.

***cis*-5-(benzyloxy)-4-hydroxy-3-methoxy-4-(4-methoxyphenyl)-3,4-dihydroquinolin-2(1*H*)-one (6e)**

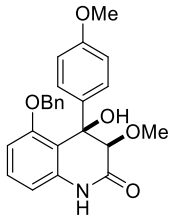

$C_{24}H_{23}NO_5$ (405.45)

Compound **6e** was prepared according to **GP2** starting from **5e** (30 mg, 0.080 mmol, 1 equiv.) and KO*t*Bu (63 mg, 0.56 mmol, 7 equiv.). The crude product was purified by column chromatography (silica gel, CH_2Cl_2/MeOH = 100:3) to afford the title compound (**6e**, 25 mg, 0.067 mmol, 84%) as a colorless oil.

R_f = 0.25 (*n*-pentane/EtOAc = 1:1); **^{1}H NMR** (700 MHz, $CDCl_3$): δ = 8.33 (s, 1H), 7.29 – 7.23 (m, 3H), 7.21 (t, *J* = 7.8 Hz, 1H), 7.16 (d, *J* = 7.5 Hz, 2H), 7.11 – 7.08 (m, 2H), 6.79 (d, *J* = 7.5 Hz, 2H), 6.71 (d, *J* = 8.4 Hz, 1H), 6.52 (d, *J* = 8.0 Hz, 1H), 5.28 (s, 1H), 5.05 (d, *J* = 11.5 Hz, 1H), 4.97 (d, *J* = 11.5 Hz, 1H), 3.80 (s, 1H), 3.76 (s, 3H), 3.59 (s, 3H) ppm; **^{13}C NMR** (176 MHz, $CDCl_3$): δ = 168.0, 159.7, 158.1, 137.1, 135.7, 133.6, 129.9, 128.8, 128.4, 127.6, 127.5, 115.4, 114.1, 109.5, 108.8, 85.2, 78.2, 71.1, 59.7, 55.4 ppm; **IR** (neat): $\tilde{\nu}$ = 3502, 3237, 3066, 3034, 2999, 2930, 2834, 1693, 1596, 1508, 1471, 1388, 1302, 1280, 1253, 1231, 1172, 1103, 1061, 1031, 993, 913, 895, 834, 778, 734, 698, 656 cm^{-1}; **HRMS** (ESI): m/z calculated for $C_{24}H_{23}NNaO_5^+$ ($[M+Na]^+$): 428.1468; found: 428.1467.

cis-3-(Benzyloxy)-4-hydroxy-4-phenyl-3,4-dihydroquinolin-2(1_H_)-one (6f)

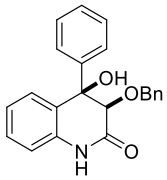

$C_{22}H_{19}NO_3$ (345.40)

Compound **6f** was prepared according to **GP2** starting from **5f** (14 mg, 0.043 mmol, 1 equiv.) and KO^{t}Bu (34 mg, 0.30 mmol, 7 equiv.). The crude product was purified by column chromatography (silica gel, CH_2Cl_2/MeOH = 100:3) to afford the title compound (**6f**, 12 mg, 0.031 mmol, 72%) as a colorless oil.
R_f = 0.23 (Pentane/EtOAc = 1:1); **^{1}H NMR** (500 MHz, CD_3OD): δ = 7.40 – 7.32 (m, 5H), 7.27 (ddd, *J* = 7.9, 6.3, 2.6 Hz, 1H), 7.20 – 7.15 (m, 3H), 7.03 – 6.99 (m, 2H), 6.99 – 6.93 (m, 3H), 4.81 (d, *J* = 11.5 Hz, 1H), 4.50 (s, 1H), 4.45 (d, *J* = 11.5 Hz, 1H) ppm; **^{13}C NMR** (176 MHz, $CDCl_3$): δ = 168.5, 140.7, 136.7, 135.7, 129.7, 128.8, 128.6, 128.6, 128.5, 128.5, 128.2, 128.1, 126.8, 124.1, 115.5, 81.1, 73.8 ppm; **IR** (neat): $\tilde{\nu}$ = 3263, 3087, 3060, 3029, 2923, 2854, 1692, 1610, 1595, 1485, 1448, 1375, 1296, 1265, 1241, 1211, 1174, 1143, 1125, 1096, 1070, 1044, 1028, 989, 936, 907, 853, 811, 753 cm^{-1}; **HRMS** (ESI): m/z calculated for $C_{22}H_{19}NO_3K^+$ ([M+K$^+$]): 384.0997; found: 384.1002.

cis-5-(Allyloxy)-4-hydroxy-3-methoxy-4-phenyl-3,4-dihydroquinolin-2(1_H_)-one (6g)

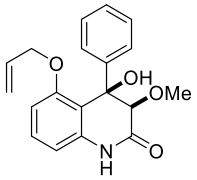

$C_{19}H_{19}NO_4$ (325.36)

Compound **6g** was prepared according to **GP2** starting from **5g** (35 mg, 0.11 mmol, 1 equiv.) and KO^{t}Bu (86 mg, 0.77 mmol, 7 equiv.). The crude product was purified by column chromatography (silica gel, CH_2Cl_2/MeOH = 100:2) to afford the title compound (**6g**, 27 mg, 0.072 mmol, 67%) as a colorless oil.
R_f = 0.23 (*n*-pentane/EtOAc = 1:1); **^{1}H NMR** (500 MHz, $CDCl_3$): δ = 8.07 (s, 1H), 7.29 – 7.26 (m, 5H), 7.22 (t, *J* = 8.2 Hz, 1H), 6.65 (dd, *J* = 8.4, 1.0 Hz, 1H), 6.52 (dd, *J* = 8.0, 0.9 Hz, 1H), 5.78 (ddt, *J* = 17.2, 10.6, 5.4 Hz, 1H), 5.34 (s, 1H), 5.21 – 5.15 (m, 2H), 4.52 – 4.41 (m, 2H), 3.84 (d, *J* = 1.4 Hz, 1H), 3.58 (s, 3H) ppm; **^{13}C NMR** (126 MHz, $CDCl_3$): δ = 167.7, 158.0, 141.9, 137.2, 132.1, 130.0, 128.7, 128.5, 126.1, 118.8, 115.0, 109.4, 108.7, 85.1, 78.4, 69.8, 59.8 ppm; **IR** (neat): $\tilde{\nu}$ = 3494, 3249, 3235, 3083, 3002, 2928, 2829, 1692, 1596, 1502, 1473, 1447, 1421, 1391, 1324, 1313, 1278, 1259, 1224, 1179, 1103, 1059, 1028, 992, 930, 887, 824, 784, 750, 731, 699, 674, 665, 654 cm^{-1}; **HRMS** (ESI): m/z calculated for $C_{19}H_{19}NO_4Na^+$ ([M+Na]$^+$): 348.1206; found: 348.1195.

cis-5-(Allyloxy)-4-hydroxy-3-methoxy-4-(4-methoxyphenyl)-3,4-dihydroquinolin-2(1*H*)-one (6h)

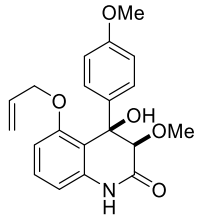

$C_{20}H_{21}NO_5$ (355.39)

Compound **6h** was prepared according to **GP2** starting from **5h** (43 mg, 0.12 mmol, 1 equiv.) and KO^{t}Bu (94 mg, 0.84 mmol, 7 equiv.). The crude product was purified by column chromatography (silica gel CH_2Cl_2/MeOH = 100:3) to afford the title compound (**6h**, 25 mg, 0.070 mmol, 58%) as a colorless oil. **R_f** = 0.23 (*n*-pentane/EtOAc = 1:1); **^{1}H NMR** (500 MHz, $CDCl_3$): δ = 8.34 (s, 1H), 7.21 (t, *J* = 8.2 Hz, 1H), 7.18 – 7.15 (m, 2H), 6.81 – 6.77 (m, 2H), 6.65 (d, *J* = 8.5 Hz, 1H), 6.51 (dd, *J* = 8.0, 0.8 Hz, 1H), 5.83 (ddt, *J* = 17.0, 10.4, 5.3 Hz, 1H), 5.40 (s, 1H), 5.25 – 5.16 (m, 2H), 4.54 – 4.44 (m, 2H), 3.81 (d, *J* = 1.5 Hz, 1H), 3.74 (s, 3H), 3.59 (s, 3H) ppm; **^{13}C NMR** (126 MHz, $CDCl_3$): δ = 167.9, 159.7, 158.0, 137.0, 133.6, 132.1, 129.8, 127.5, 118.8, 115.2, 114.1, 109.5, 108.7, 85.2, 78.2, 69.8, 59.6, 55.3 ppm; **IR** (neat): $\tilde{\nu}$ = 3697, 3251, 3237, 3196, 3101, 3087 3039, 2997, 2932, 2833, 2246, 1691, 1595, 1508, 1471, 1442, 1417, 1392, 1303, 1280, 1251, 1224, 1172, 1101, 993, 928, 912, 893, 833, 809, 779, 729, 693, 670, 661cm^{-1}; **HRMS** (ESI): m/z calculated for $C_{20}H_{21}NNaO_5^+$ ([M+Na]$^+$): 378.1312; found: 378.1317.

(±)–Aflaquinolone E (9)

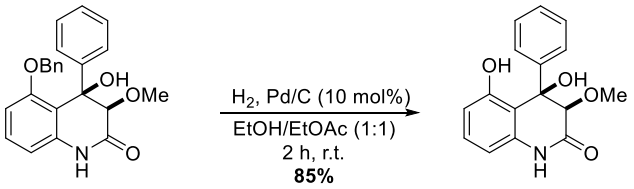

6d
$C_{23}H_{21}NO_4$ (375.42)

9
$C_{16}H_{15}NO_4$ (285.30)

To a solution of **6d** (23 mg, 0.060 mmol, 1 equiv.) in EtOH/EtOAc (1:1, 1 mL) was added Pd/C (6.4 mg, 0.0061 mmol, 10 w% Pd, 10 mol%) and the atmosphere was changed from Ar to H_2 by short evacuation and backfilling with H_2. The reaction mixture was then stirred vigorously at room temperature for 2 hours under an atmosphere of H_2. The reaction mixture was then filtered through a short pad of Celite® and concentrated under reduced pressure. The crude product was purified by column chromatography (silica gel, CH_2Cl_2/MeOH = 50:1) to afford the title compound (**9**, 15 mg, 0.051 mmol, 85%) as a colorless solid. **R_f** = 0.21 (*n*-pentane/EtOAc = 3:1); **m.p.:** 143–148 °C; **^{1}H NMR** (700 MHz, CD_3OD): δ = 7.32 – 7.29 (m, 3H), 7.29 – 7.26 (m, 2H), 7.15 (t, *J* = 8.1 Hz, 1H), 6.54 (dd, *J* = 8.3, 1.1 Hz, 1H), 6.46 (dd, *J* = 8.0, 1.1 Hz, 1H), 3.66 (s, 1H), 3.53 (s, 3H) ppm; **^{13}C NMR** (176 MHz, CD_3OD): δ = 169.1, 159.1, 140.9, 138.1, 131.0, 129.8, 129.6, 127.5, 113.2, 113.0, 108.2, 86.3, 79.9, 59.2 ppm; **IR** (neat): $\tilde{\nu}$ = 3281, 3061, 2998, 2935, 2832, 1681, 1620, 1595, 1475, 1448, 1387, 1243, 1207, 1169, 1099, 1021, 879, 791, 745, 725, 698, 659 cm^{-1}; **HRMS** (ESI): m/z calculated for $C_{16}H_{15}NNaO_4^+$ ([M+Na]$^+$): 308.0893; found: 308.0900. The NMR data match those reported for Aflaquinolone E.[7]

(±)–Quinolinone B (10)

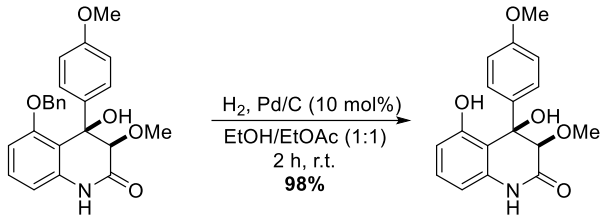

6e
$C_{24}H_{23}NO_5$ (405.45)

10
$C_{17}H_{17}NO_5$ (315.33)

To a solution of **6e** (12 mg, 0.028 mmol, 1 equiv.) in EtOAc/EtOH (1:1, 1 mL) was added Pd/C (3.0 mg, 0.0029 mmol, 10 w% Pd, 10 mol%) and the atmosphere was changed from Ar to H_2 by short evacuation and backfilling with H_2. The reaction mixture was then stirred vigorously at room temperature for 2 hours under an atmosphere of H_2. The reaction mixture was then filtered through a short pad of Celite® and concentrated under reduced pressure. The crude product was purified by column chromatography (silica gel CH_2Cl_2/MeOH = 50:1) to afford the title compound (**10**, 8.8 mg, 0.028 mmol, 98%) as a colorless oil. **R_f** = 0.60 (CH_2Cl_2/MeOH = 50:1); **^{1}H NMR** (700 MHz, acetone-d_6): δ = 9.28 (s, 1H), 9.16 (s, 1H), 7.22 (d, *J* = 8.9 Hz, 2H), 7.16 (t, *J* = 8.1 Hz, 1H), 6.88 (d, *J* = 8.9 Hz, 2H), 6.55 (dd, *J* = 8.0, 1.1 Hz, 1H), 6.49 (dd, *J* = 8.2, 1.1 Hz, 1H), 6.14 (s, 1H), 3.77 (s, 3H), 3.67 (d, *J* = 1.6 Hz, 1H), 3.50 (s, 3H) ppm; **^{13}C NMR** (176 MHz, acetone-d_6): δ = 166.5, 161.0, 159.2, 138.1, 131.9, 130.7, 128.8, 114.7, 112.5, 112.4, 107.4, 85.8, 79.6, 58.9, 55.5. ppm; **IR** (neat): $\tilde{\nu}$ = 3294, 3066, 2993, 2932, 2837, 1685, 1626, 1595, 1510, 1439, 1379, 1305, 1253, 1207, 1170, 1103, 1076, 1051, 1025, 989, 936, 884, 834, 783, 756, 716 cm^{-1}; **HRMS** (ESI): m/z calculated for $C_{17}H_{17}NNaO_5^+$ ($[M+Na]^+$): 338.0999; found: 338.1006. The NMR data match those reported for Quinolinone B.[6]

(±)–Aflaquinolone F (11)

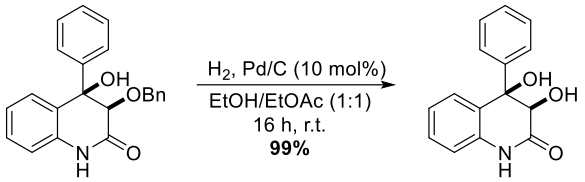

6f
$C_{22}H_{19}NO_3$ (345.40)

11
$C_{15}H_{13}NO_3$ (255.27)

To a solution of **6f** (12 mg, 0.034 mmol, 1 equiv.) in EtOAc/EtOH (1:1, 1 mL) was added Pd/C (3.6 mg, 0.0031 mmol, 10 w% Pd, 10 mol%) and the atmosphere was changed from Ar to H_2 by short evacuation and backfilling with H_2. The reaction mixture was then stirred vigorously at room temperature for 16 hours under an atmosphere of H_2. The reaction mixture was filtered through a short pad of Celite® and concentrated under reduced pressure. The crude product was purified by column chromatography (silica gel, CH_2Cl_2/MeOH = 100:3) to afford the title compound (**11**, 8.7 mg, 0.034 mmol, 99%) as a colorless oil.

R_f = 0.30 (CH_2Cl_2/MeOH = 50:1); **^{1}H NMR** (700 MHz, CD_3OD): δ = 7.53 – 7.49 (m, 2H), 7.39 (t, *J* = 7.6 Hz, 2H), 7.34 – 7.31 (m, 1H), 7.26 (td, *J* = 7.6, 1.2 Hz, 1H), 6.96 (dd, *J* = 7.9, 1.2 Hz, 1H), 6.91 (td, *J* = 7.6, 1.1 Hz, 1H), 6.73 (d, *J* = 7.8 Hz, 1H), 4.76 (s, 1H) ppm; **^{13}C NMR** (176 MHz, CD_3OD): δ = 172.6, 143.1, 138.3, 130.6, 130.1, 129.0, 128.4, 128.3, 124.0, 117.0, 78.6, 75.8 ppm; **IR** (neat): $\tilde{\nu}$ = 3294, 2954,

2922, 2853, 1727, 1707, 1606, 1464, 1376, 1282, 1248, 1116, 1031, 824, 762, 722 cm^{-1}; **HRMS** (ESI): m/z calculated for $C_{15}H_{13}NNaO_3^+$ ([M+Na]$^+$): 278.0787; found: 278.0795. The NMR data match those reported for Aflaquinolone F.[7]

***cis*-6-Allyl-4,5-dihydroxy-3-methoxy-4-phenyl-3,4-dihydroquinolin-2(1*H*)-one (12a)**

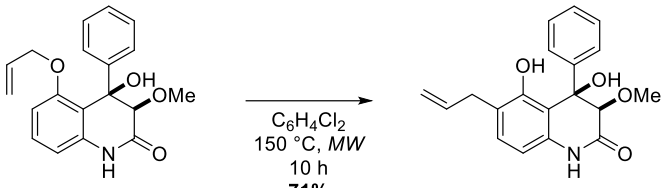

6g
$C_{19}H_{19}NO_4$ (325.36)

12a
$C_{19}H_{19}NO_4$ (325.36)

6g (14 mg, 0.040 mmol, 1 equiv.) was dissolved in 1,2-dichlorobenzene (1 mL) and heated in a microwave at 150 °C for 10 hours. The solvent was removed under reduced pressure and the crude product was purified by column chromatography (silica gel, *n*-pentane/EtOAc = 1:2) to afford the title compound (**12a**, 9.9 mg, 0.030 mmol, 71%) as a colorless oil.

R_f = 0.32 (CH_2Cl_2/MeOH = 50:1); **^{1}H NMR** (500 MHz, $CDCl_3$): δ = 8.90 (d, *J* = 0.5 Hz, 1H), 7.85 (s, 1H), 7.33 – 7.29 (m, 3H), 7.28 – 7.25 (m, 2H), 7.05 (d, *J* = 8.0 Hz, 1H), 6.32 (d, *J* = 8.0 Hz, 1H), 5.97 (ddt, *J* = 16.8, 10.1, 6.6 Hz, 1H), 5.07 – 5.02 (m, 2H), 4.60 (s, 1H), 3.69 (d, *J* = 1.5 Hz, 1H), 3.62 (s, 3H), 3.31 (qdt, *J* = 15.7, 6.7, 1.7 Hz, 2H) ppm; **^{13}C NMR** (126 MHz, $CDCl_3$): δ = 165.7, 155.7, 137.7, 136.9, 133.8, 130.8, 129.3, 129.0, 126.5, 124.4, 115.7, 110.5, 106.5, 84.3, 79.1, 59.1, 33.7 ppm; **IR** (neat): $\tilde{\nu}$ = 3465, 3290, 3074, 2954, 2924, 2869, 1683, 1638, 1622, 1602, 1505, 1493, 1463, 1449, 1421, 1378, 1346, 1272, 1223, 1174, 1102, 1077, 1036, 1027, 992, 947, 916, 892, 856, 846, 815, 754, 697, 673, 666 cm^{-1}; **HRMS** (ESI): *m/z* calculated for $C_{19}H_{19}NNaO_4^+$ ([M+Na]$^+$): 348.1206; found: 348.1216.

***cis*-6-Allyl-4,5-dihydroxy-3-methoxy-4-(4-methoxyphenyl)-3,4-dihydroquinolin-2(1*H*)-one (12b)**

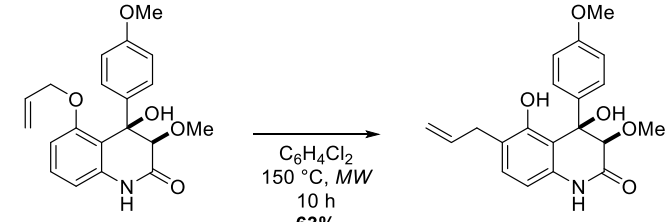

6h
$C_{20}H_{21}NO_5$ (355.39)

12b
$C_{20}H_{21}NO_5$ (355.39)

6h (39 mg, 0.11 mmol, 1 equiv.) was dissolved in 1,2-dichlorobenzene (1 mL) and heated in a microwave at 150 °C for 10 hours. The solvent was removed under reduced pressure and the crude product was purified by column chromatography (SiO_2, *n*-pentane/EtOAc = 1:2) to afford the title compound (**12b**, 25 mg, 0.070 mmol, 63%) as a colorless oil.

R_f = 0.32 (*n*-Pentane/EtOAc = 1:1); **^{1}H NMR** (400 MHz, acetone-d_6): δ= 9.45 (s, 1H), 9.25 (s, 1H), 7.28 – 7.15 (m, 2H), 7.04 (dt, *J* = 8.1, 0.7 Hz, 1H), 6.93 – 6.82 (m, 2H), 6.51 (d, *J* = 8.5 Hz, 1H), 6.23 (s, 1H), 6.01 – 5.89 (m, 1H), 5.08 – 5.00 (m, 1H), 4.96 (ddtd, *J* = 10.1, 2.0, 1.4, 0.5 Hz, 1H), 3.76 (s, 3H), 3.65 (dd, *J* = 1.5, 0.5 Hz, 1H), 3.50 (s, 3H), 3.33 – 3.20 (m, 2H) ppm; **^{13}C NMR** (126 MHz, acetone-d_6): δ = 166.4, 161.0, 156.6, 138.1, 136.3, 131.9, 130.8, 128.8, 123.2, 115.4, 114.7, 112.0, 107.1, 85.8, 79.7, 58.8, 55.5, 34.2. ppm; **IR** (neat): $\tilde{\nu}$ = 3280, 3069, 2955, 2924, 2853, 1683, 1638, 1623, 1603, 1509, 1463, 1418, 1379, 1306, 1253, 1224, 1172, 1103, 1077, 1028, 993, 944, 909, 891, 860, 830, 812, 798,

765, 754, 730, 709, 701, 687, 681, 666 cm^{-1}; **HMRS** (ESI): *m/z* calculated for $C_{20}H_{21}NNaO_5^+$ ([M+Na]$^+$): 378.1312; found: 378.1328.

(±)–Aniduquinolone C (13a)

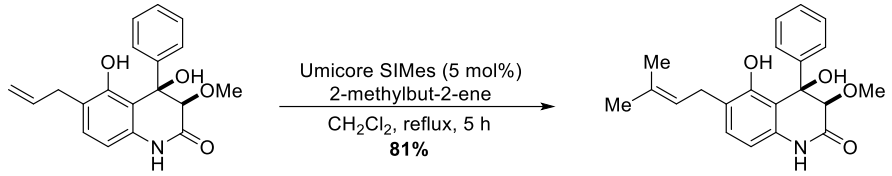

$C_{19}H_{19}NO_4$ (325.36) $C_{21}H_{23}NO_4$ (353.42)

12a (9.9 mg, 0.030 mmol, 1 equiv.) and Umicore M71 SIMes (1.1 mg, 0.0015 mmol, 5 mol%) were dissolved in CH_2Cl_2 (0.5 mL). 2-Methylbut-2-ene (0.030 mL, 0.30 mmol, 10 equiv.) was added and the reaction mixture was heated to reflux for 5 hours in a sealed tube. After cooling to room temperature, the reaction mixture was filtered through a short pad of silica gel. All volatiles were removed under reduced pressure and the crude product was purified by HPLC (EtOH/*n*-pentane = 1:10, 1 mL/min, t_r = 7.00 min) to afford the title compound (**13a**, 8.0 mg, 0.024 mmol, 81%) as a colorless oil.

R_f = 0.35 (CH_2Cl_2/MeOH 50:1); **^{1}H NMR** (700 MHz, DMSO-d_6): δ = 10.15 (s, 1H), 9.59 (s, 1H), 7.37 – 7.28 (m, 3H), 7.19 (dd, *J* = 5.8, 3.6 Hz, 2H), 6.95 (d, *J* = 7.9 Hz, 1H), 6.37 (d, *J* = 7.9 Hz, 1H), 5.24 (t, *J* = 7.4 Hz, 1H), 3.58 (s, 1H), 3.43 (s, 3H), 3.19 (dd, *J* = 15.4, 7.4 Hz, 1H), 3.08 (dd, *J* = 15.4, 7.3 Hz, 1H), 1.68 (s, 3H), 1.65 (s, 3H) ppm; **^{13}C NMR** (176 MHz, DMSO-d_6): δ = 166.1, 155.0, 140.0, 135.0, 131.3, 129.2, 128.6, 126.2, 123.0, 122.8, 110.9, 106.3, 84.4, 78.7, 58.3, 27.5, 25.6, 17.7 ppm; **IR** (neat): $\tilde{\nu}$ = 3218, 3142, 3062, 2912, 2832, 2255, 1685, 1623, 1602, 1506, 1493, 1447, 1422, 1375, 1274, 1224, 1174, 1105, 1076, 1024, 1003, 943, 902, 867, 818, 767, 734 cm^{-1}; **HRMS** (ESI): *m/z* calculated for $C_{21}H_{23}NNaO_4^+$ ([M+Na]$^+$): 376.1519; found: 376.1513. The NMR data match those reported for Aniduquinolone C.[5]

(±)–Peniprequinolone (**13b**)

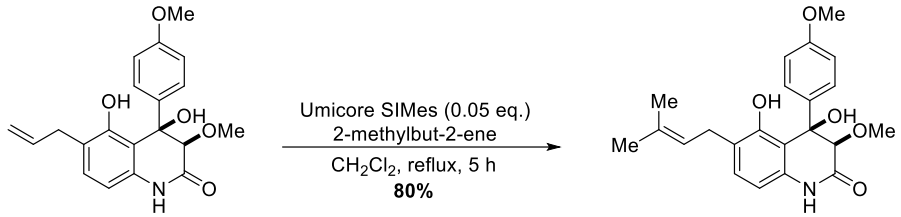

$C_{20}H_{21}NO_5$ (355.39) $C_{22}H_{25}NO_5$ (383.44)

12b (11 mg, 0.030 mmol, 1 equiv.) and Umicore M71 SIMes (1.1 mg, 0.0015 mmol, 5 mol%) were dissolved in CH_2Cl_2 (0.5 mL). 2-Methylbut-2-ene (0.030 mL, 0.30 mmol, 10 equiv.) was added and the reaction mixture was heated to reflux for 5 hours in a sealed tube. After cooling to room temperature, the reaction mixture was filtered through a short pad of silica gel. All volatiles were removed under reduced pressure and the crude product was purified by HPLC (EtOH/*n*-pentane = 1:10, 1 mL/min, t_r = 8.60 min) to afford the title compound (**13b**, 9.0 mg, 0.024 mmol, 80%) as a colorless solid.

R_f = 0.40 (CH_2Cl_2/MeOH 50:1); **m.p.:** 55 **°C -** 59°C; **^{1}H NMR** (500 MHz, $CDCl_3$): δ = 8.91 (s, 1H), 7.91 (s, 1H), 7.19 – 7.14 (m, 2H), 7.03 (d, J = 8.0 Hz, 1H), 6.84 – 6.78 (m, 2H), 6.28 (d, J = 8.0 Hz, 1H), 5.30 – 5.26 (m, 1H), 4.54 (s, 1H), 3.76 (s, 3H), 3.68 (d, J = 1.5 Hz, 1H), 3.60 (s, 3H), 3.29 (dd, J = 16.0, 7.5

Hz, 1H), 3.20 (dd, J = 16.0, 7.2 Hz, 1H), 1.74 (s, 3H), 1.68 (s, 3H) ppm; **^{13}C NMR** (126 MHz, $CDCl_3$): δ = 166.0, 160.3, 155.7, 133.3, 132.8, 130.1, 129.5, 128.0, 125.8, 122.4, 114.4, 110.5, 106.4, 84.5, 78.9, 59.0, 55.4, 27.8, 25.9, 17.9 ppm; **IR** (neat): $\tilde{\nu}$ = 3277, 3059, 2954, 2923, 2869, 2853, 1684, 1621, 1603, 1510, 1462, 1419, 1377, 1306, 1254, 1221, 1188, 1172, 1105, 1079, 1032, 989, 974, 940, 929, 903, 867, 829, 810, 767, 755, 734, 707, 698, 974, 661, 652 cm^{-1}; **HRMS** (ESI): *m/z* calculated for $C_{22}H_{25}NNaO_5^+$ ($[M+Na]^+$): 406.1625; found: 406.1627. The NMR data match those reported for Peniprequinolone.[6]

References

(1) Kang, D.; Lee, J.; Lee, H.-Y. *Org. Synth.* **2012**, *89*, 66–72.

(2) Wulischleger, C. W.; Gertsch, J.; Altmann, K. H. *Org. Lett.* **2010**, *12*, 1120–1123.

(3) Mukaiyama, T.; Shiina, I.; Iwadare, H.; Saitoh, M.; Nishimura, T.; Ohkawa, N.; Sakoh, H.; Nishimura, K.; Tani, Y.; Hasegawa, M.; Yamada, K.; Saitoh, K. *Chem. Eur. J.* **1999**, *5*, 121–161.

(4) Suguru, Y.; Ken, S.; Takako, N.; Takamitsu, H. *Chem. Lett.* **2015**, *44*, 1324–1326.

(5) An, C.-Y.; Li, X.-M.; Luo, H.; Li, C.-S.; Wang, M.-H.; Xu, G.-M.; Wang, B.-G., *J. Nat. Prod.* **2013**, *76*, 1896–1901.

(6) Hayashi, H.; Nakatani, T.; Inoue, Y; Nakayama, M.; Nozake, H.; *Biosci. Biotech. Biochem.* **1997**, *61*, 914–916.

(7) Neff, S. A.; Lee, S. U.; Asami, Y.; Ahn, J. S.; Oh, H.; Baltrusaitis, J.; Gloer, J. B.; Wicklow, D. T.; *J. Nat. Prod.* **2012**, *75*, 464–472.

NMR-Spectra

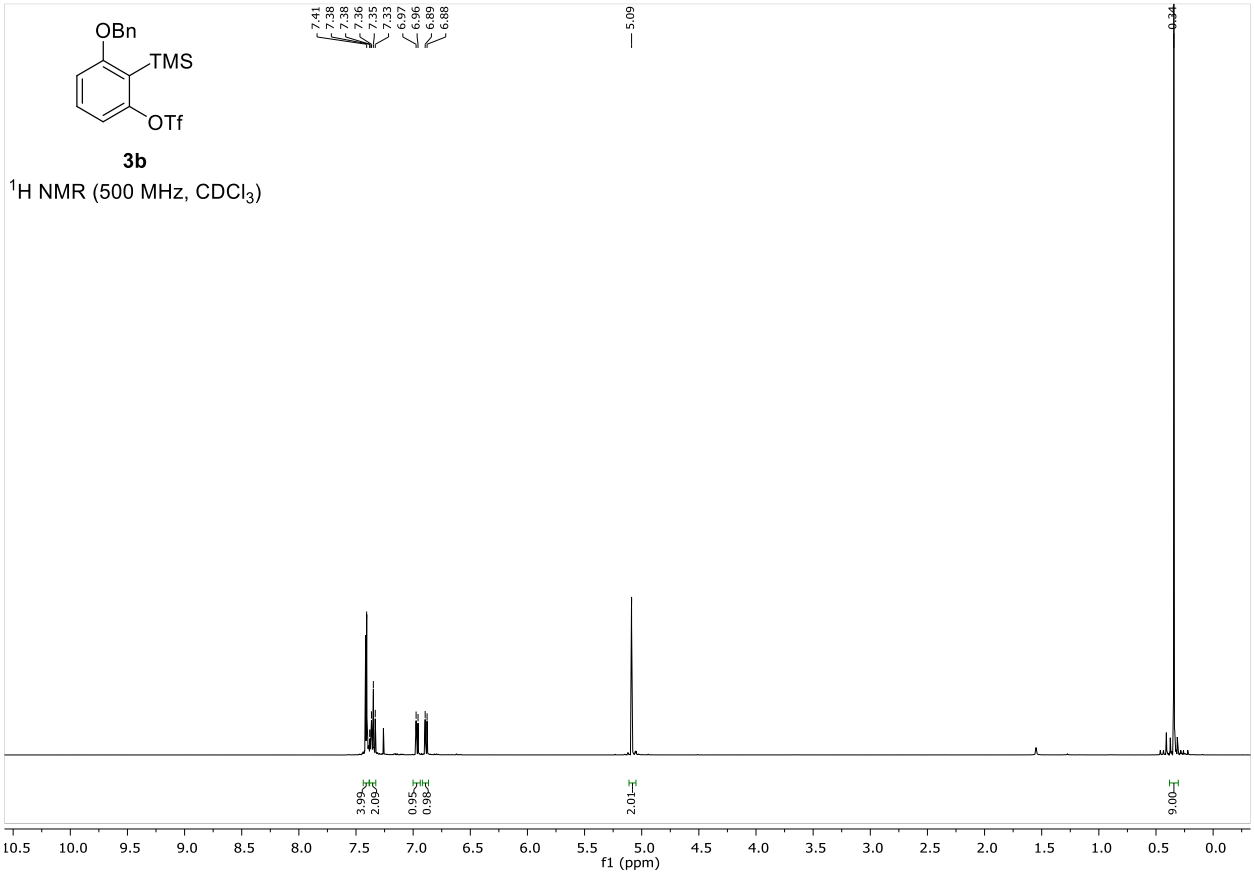
OBn
TMS
OTf
3b
1H NMR (500 MHz, CDCl3)
7.41
7.38
7.38
7.36
7.35
7.33
6.97
6.96
6.89
6.88
5.09
0.34
3.99
2.09
0.95
0.98
2.01
9.00
f1 (ppm)

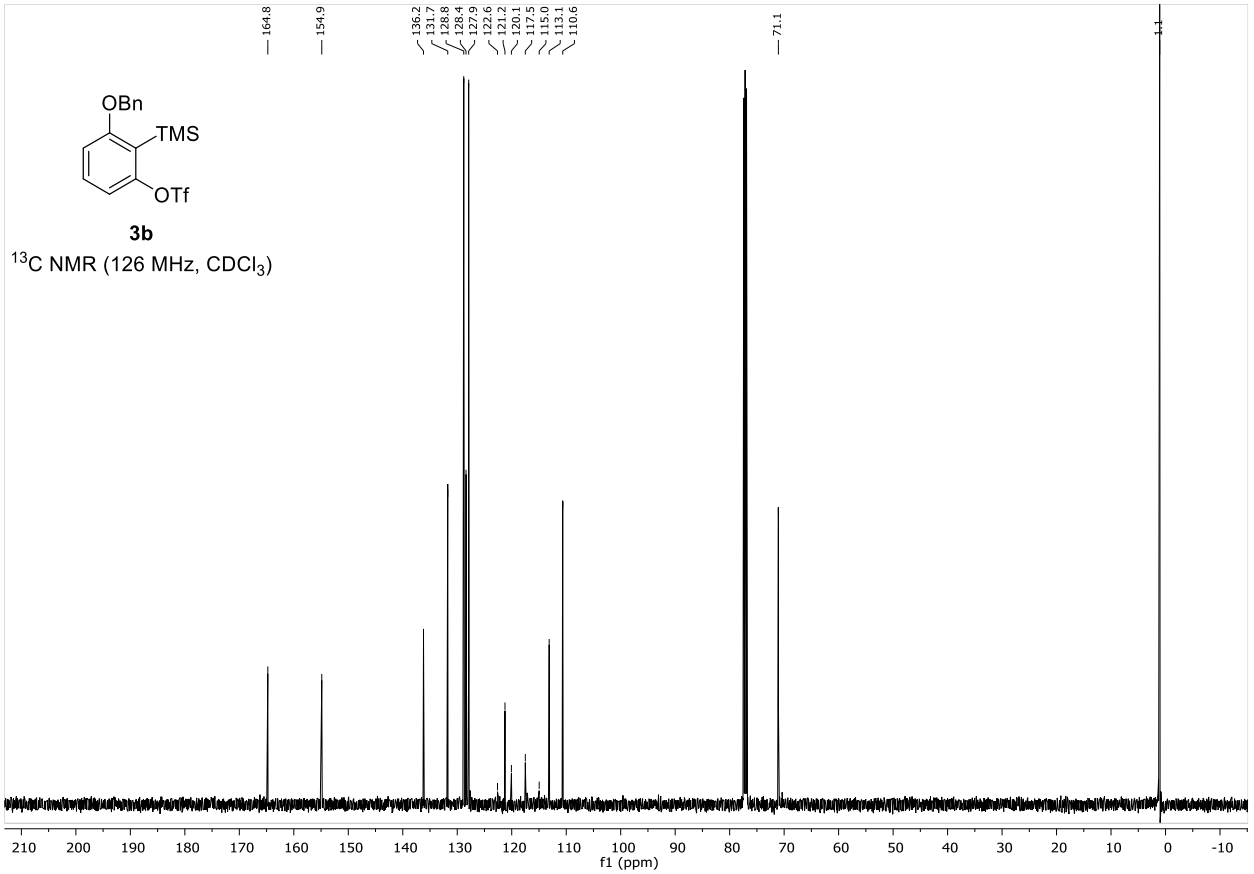
OBn
TMS
OTf
3b
13C NMR (126 MHz, CDCl3)
164.8
154.9
136.2
131.7
128.8
128.4
127.9
122.6
121.2
120.1
117.5
115.0
113.1
110.6
71.1
1.1
f1 (ppm)

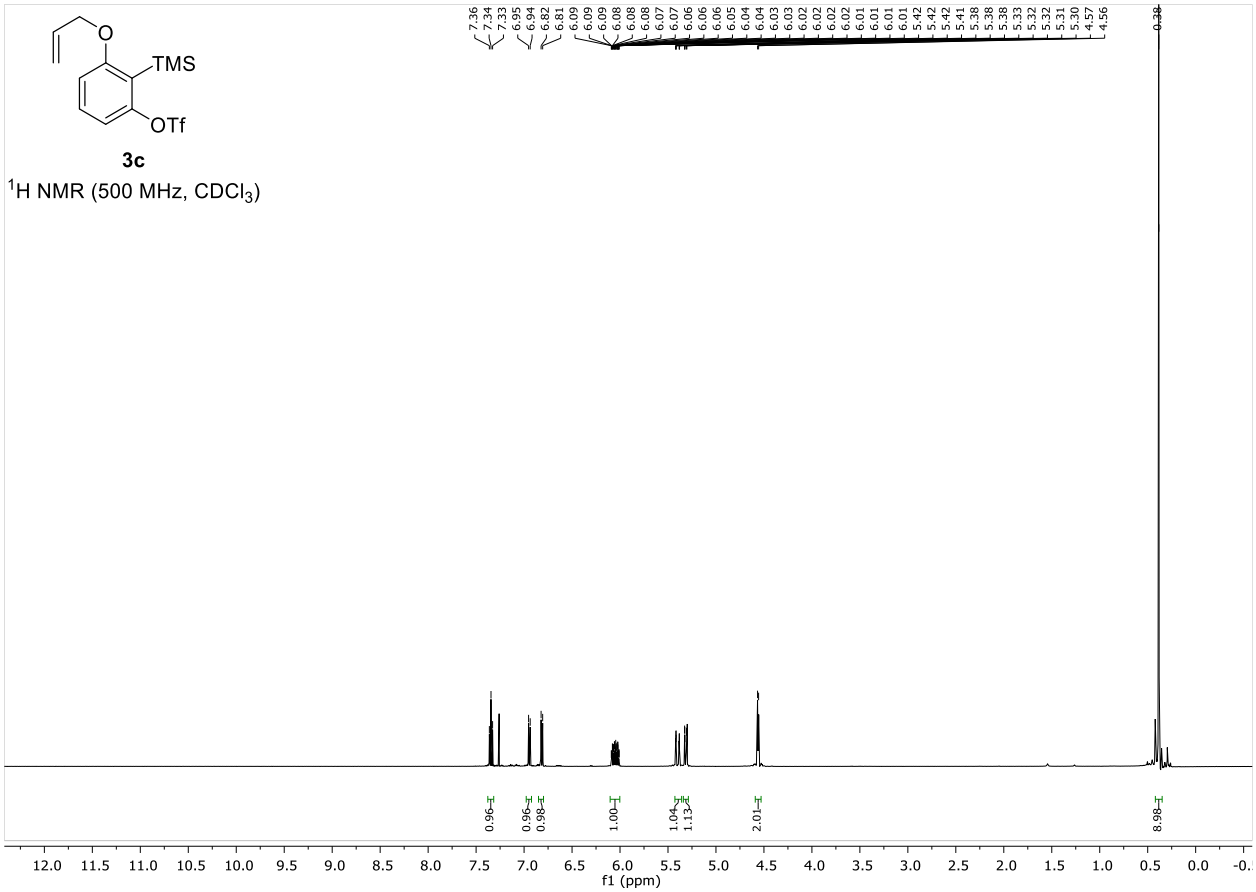
TMS
OTf
3c
1H NMR (500 MHz, CDCl3)
f1 (ppm)

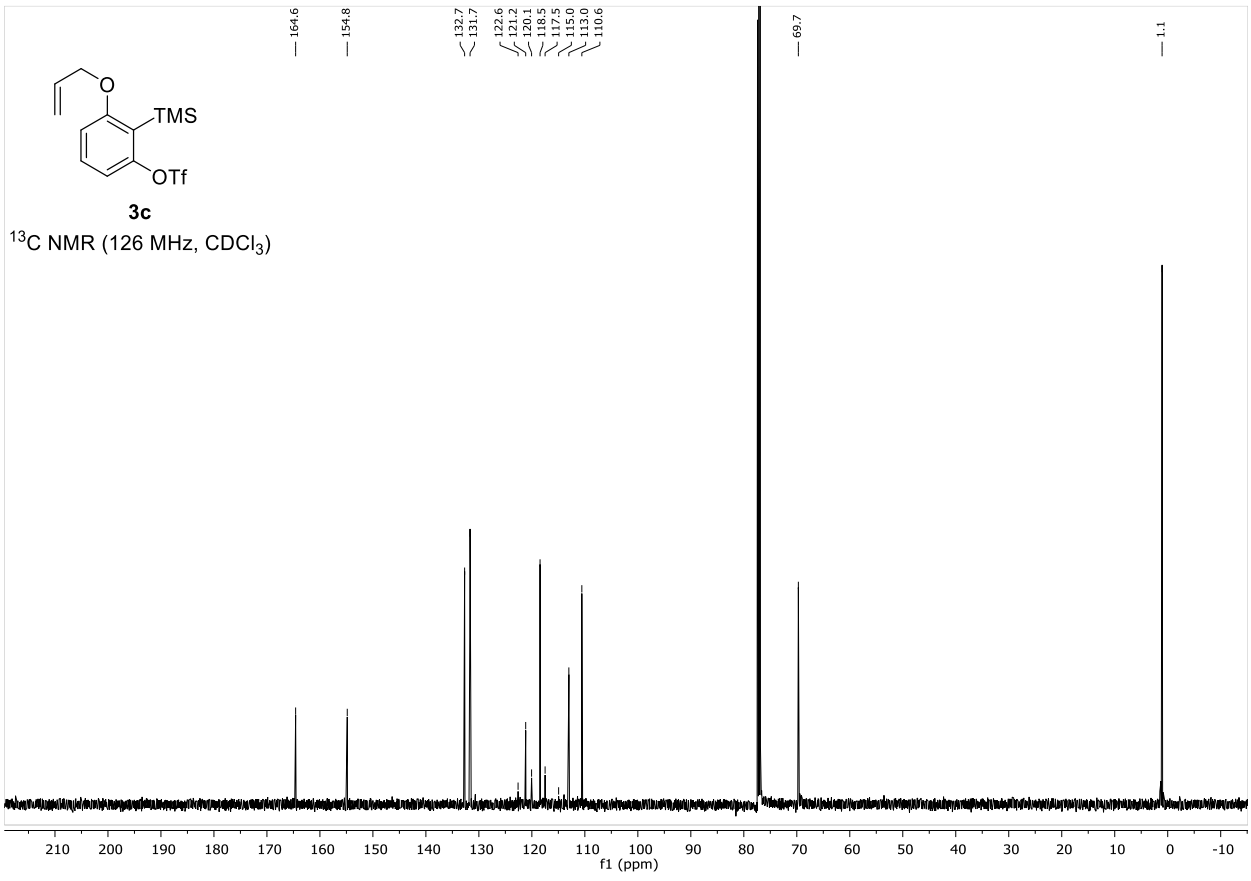
TMS
OTf
3c
13C NMR (126 MHz, CDCl3)
f1 (ppm)

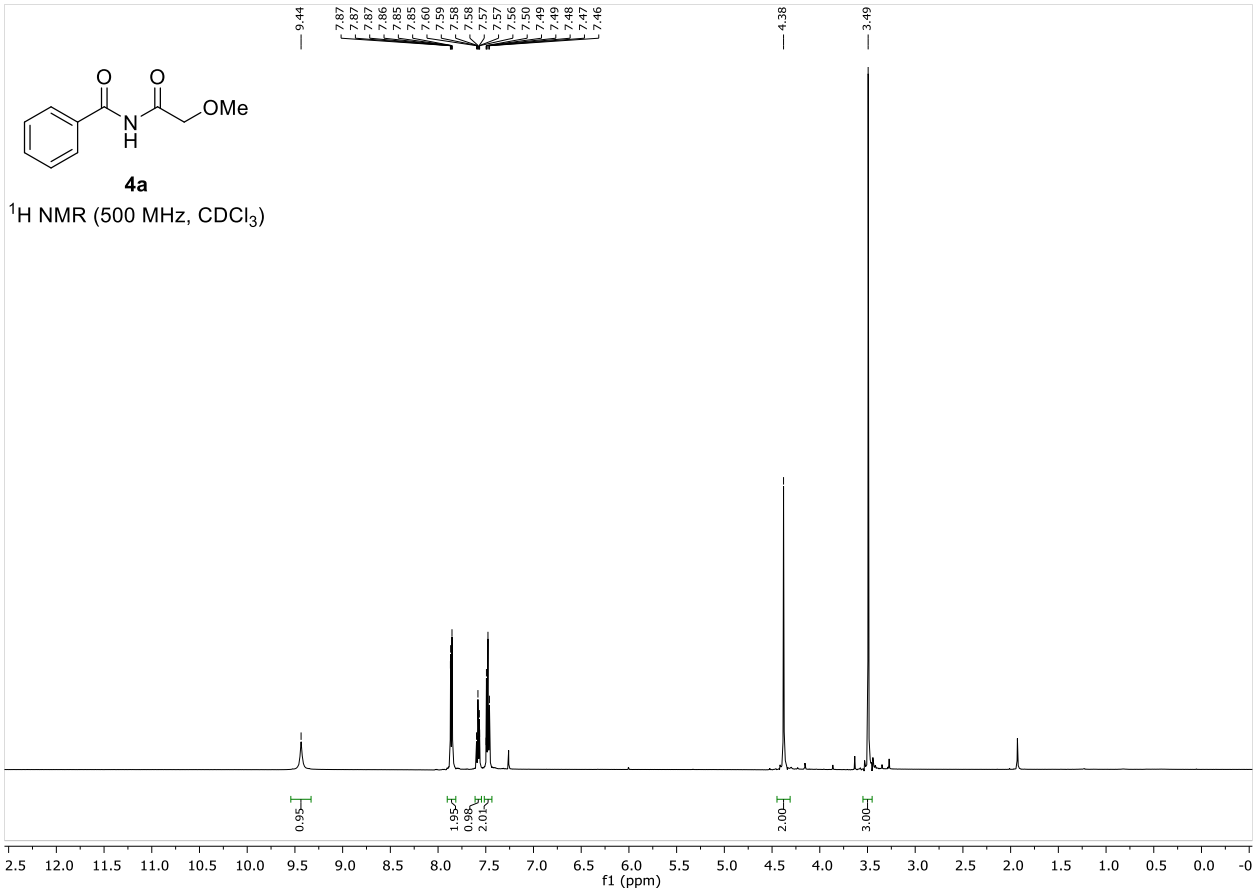
9.44
7.87
7.87
7.87
7.86
7.85
7.85
7.60
7.59
7.58
7.58
7.57
7.57
7.56
7.50
7.49
7.49
7.48
7.47
7.46
4.38
3.49
O
O
N
H
OMe
4a
1H NMR (500 MHz, CDCl3)
0.95
1.95
0.98
2.01
2.00
3.00
f1 (ppm)

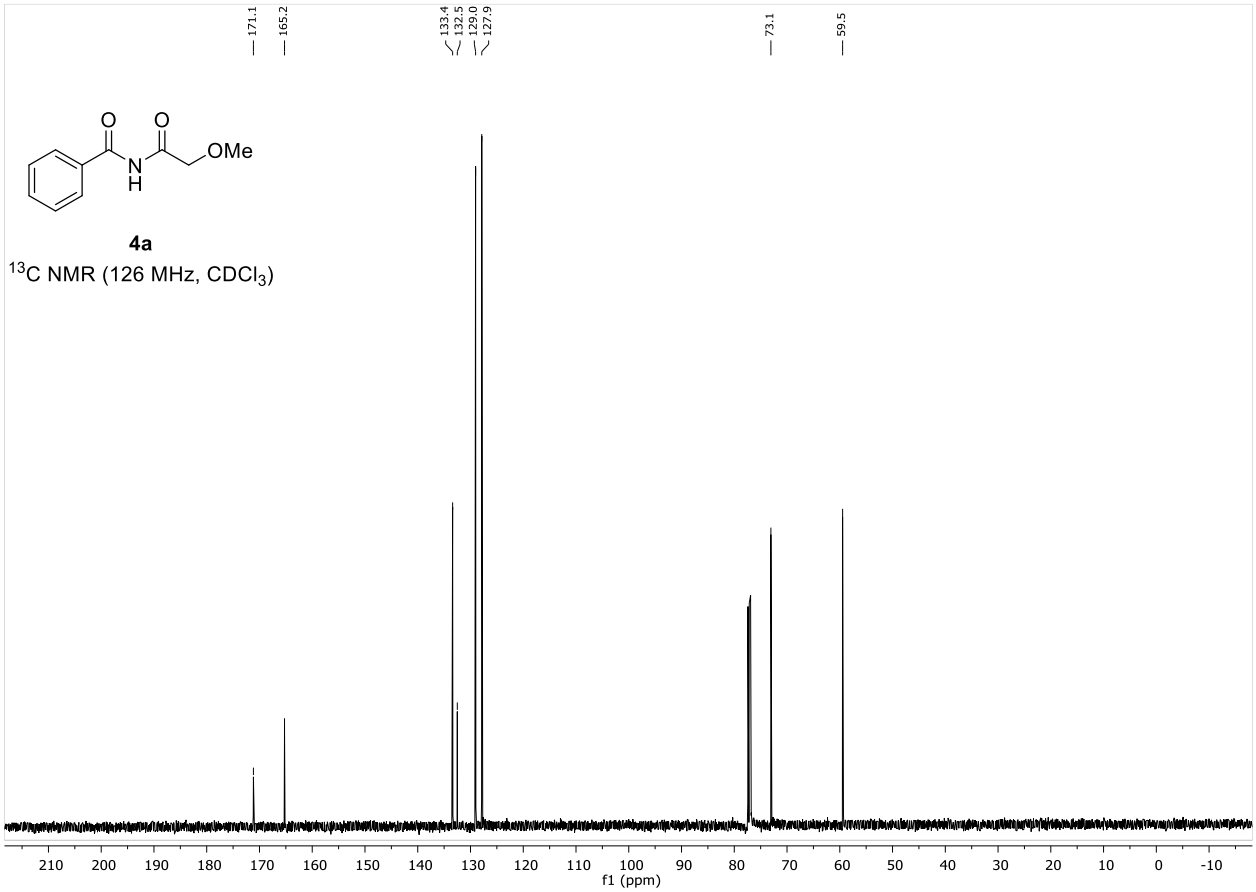
171.1
165.2
133.4
132.5
129.0
127.9
73.1
59.5
O
O
N
H
OMe
4a
13C NMR (126 MHz, CDCl3)
f1 (ppm)

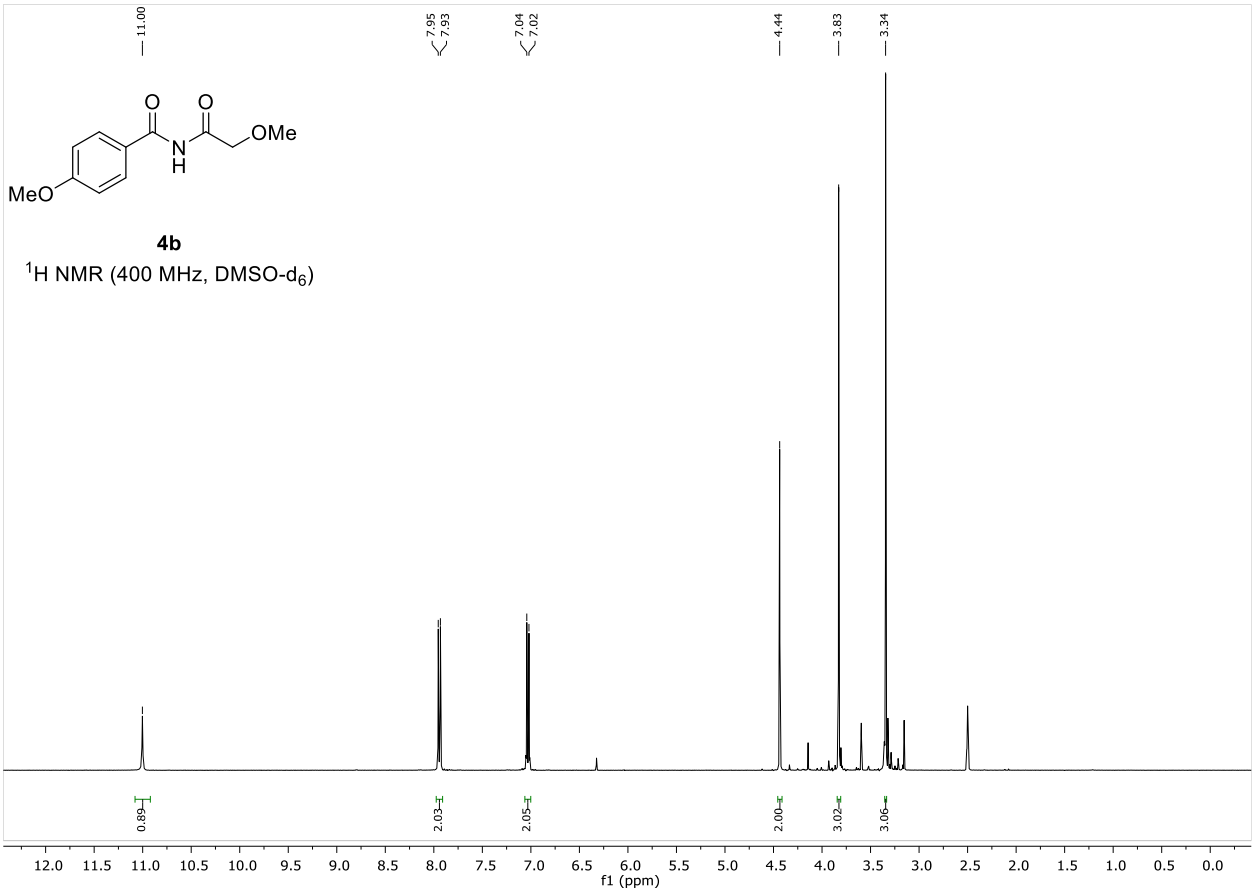

4b

^{1}H NMR (400 MHz, DMSO-d_6)

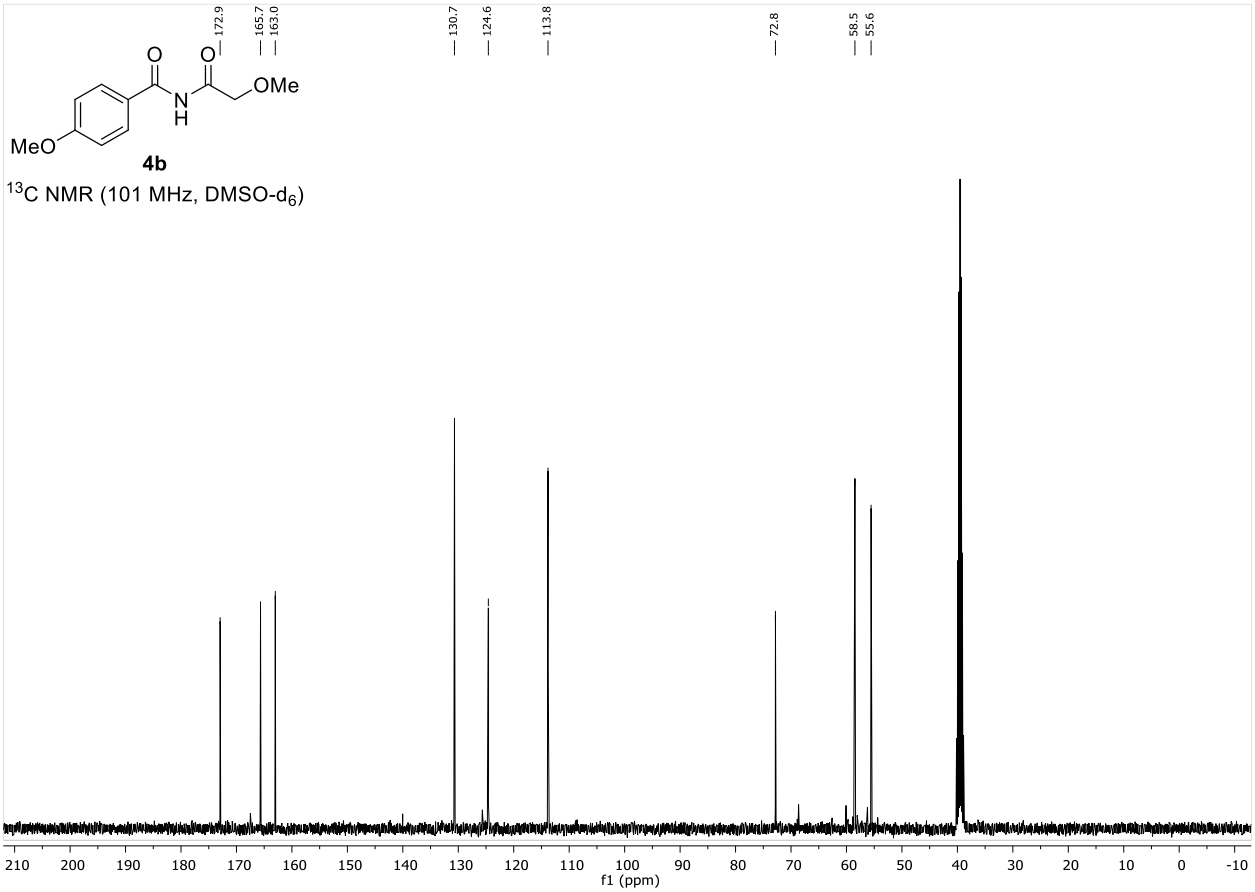

4b

^{13}C NMR (101 MHz, DMSO-d_6)

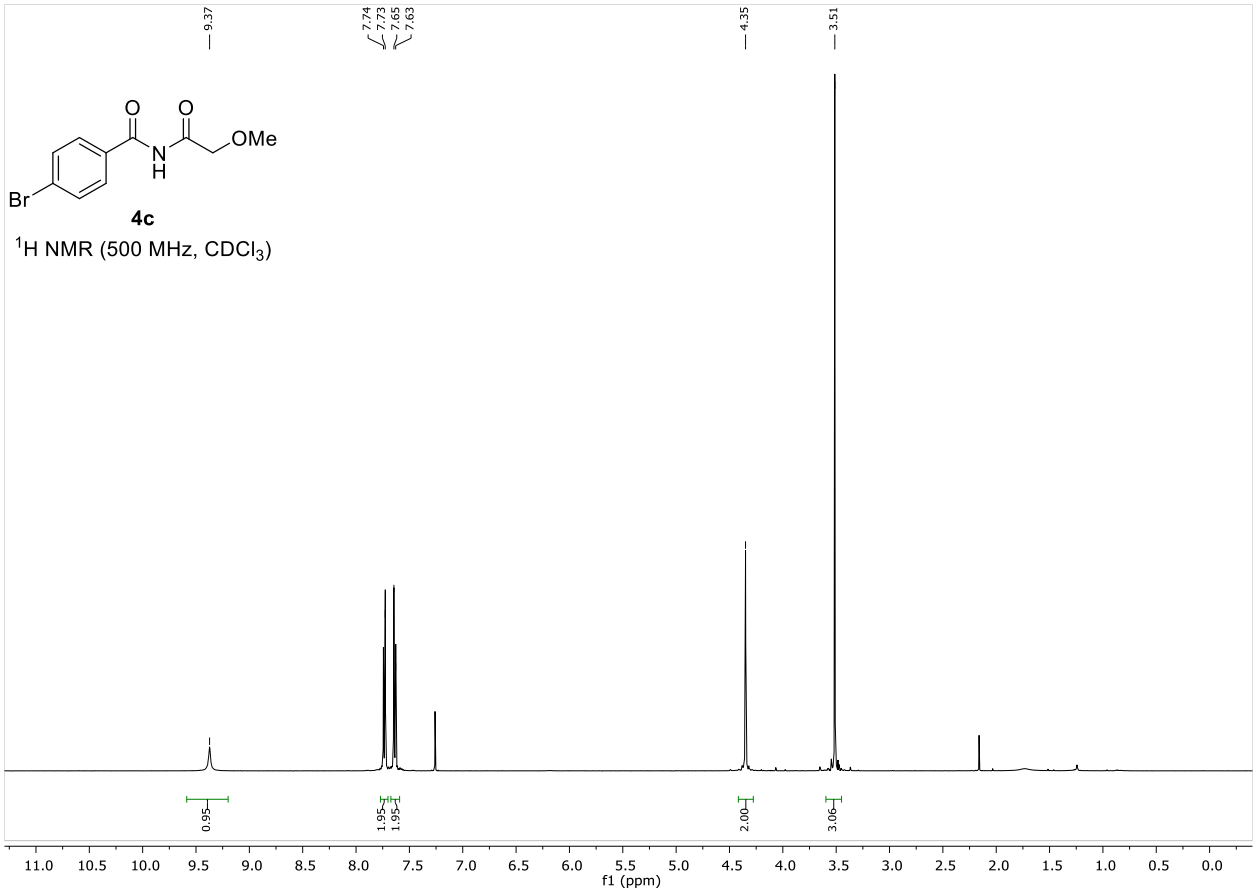

4c

^{1}H NMR (500 MHz, $CDCl_3$)

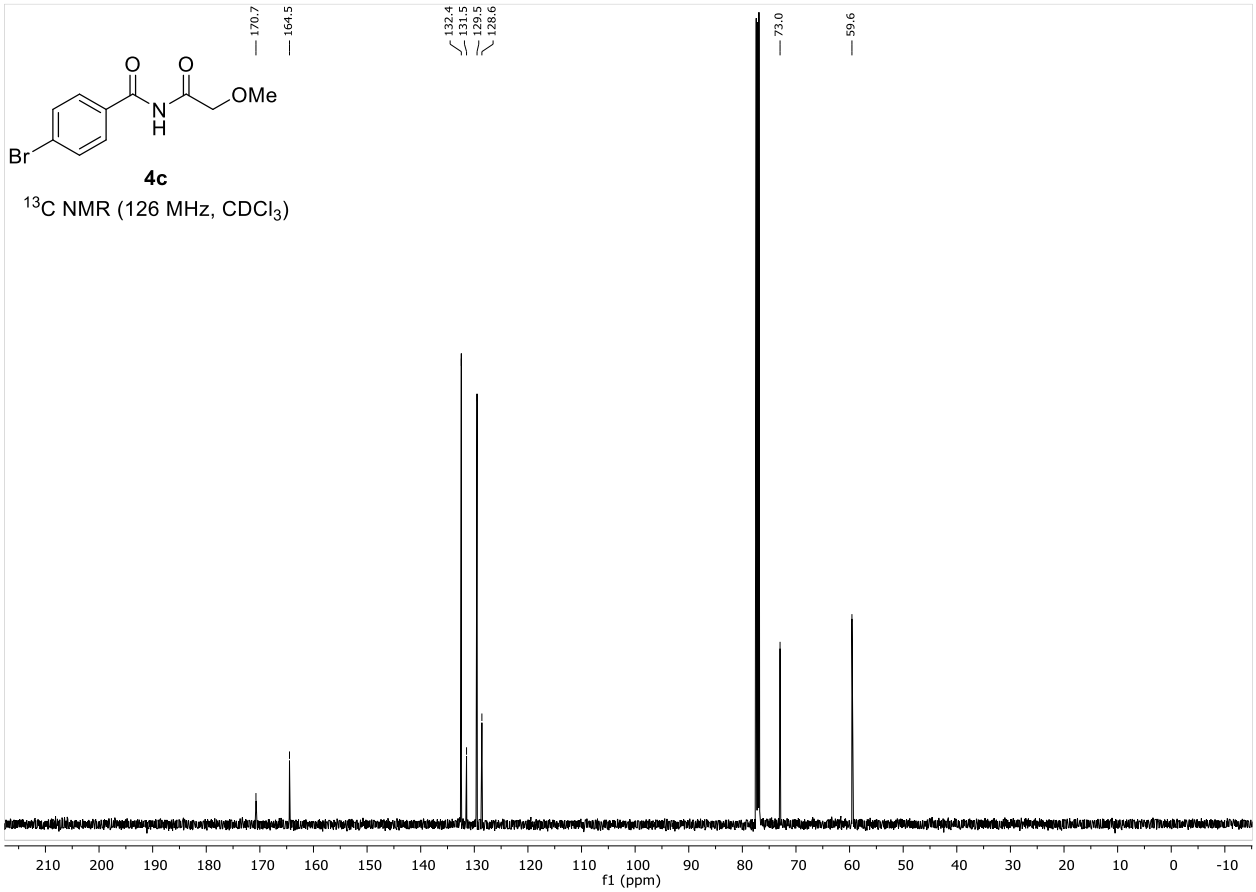

4c

^{13}C NMR (126 MHz, $CDCl_3$)

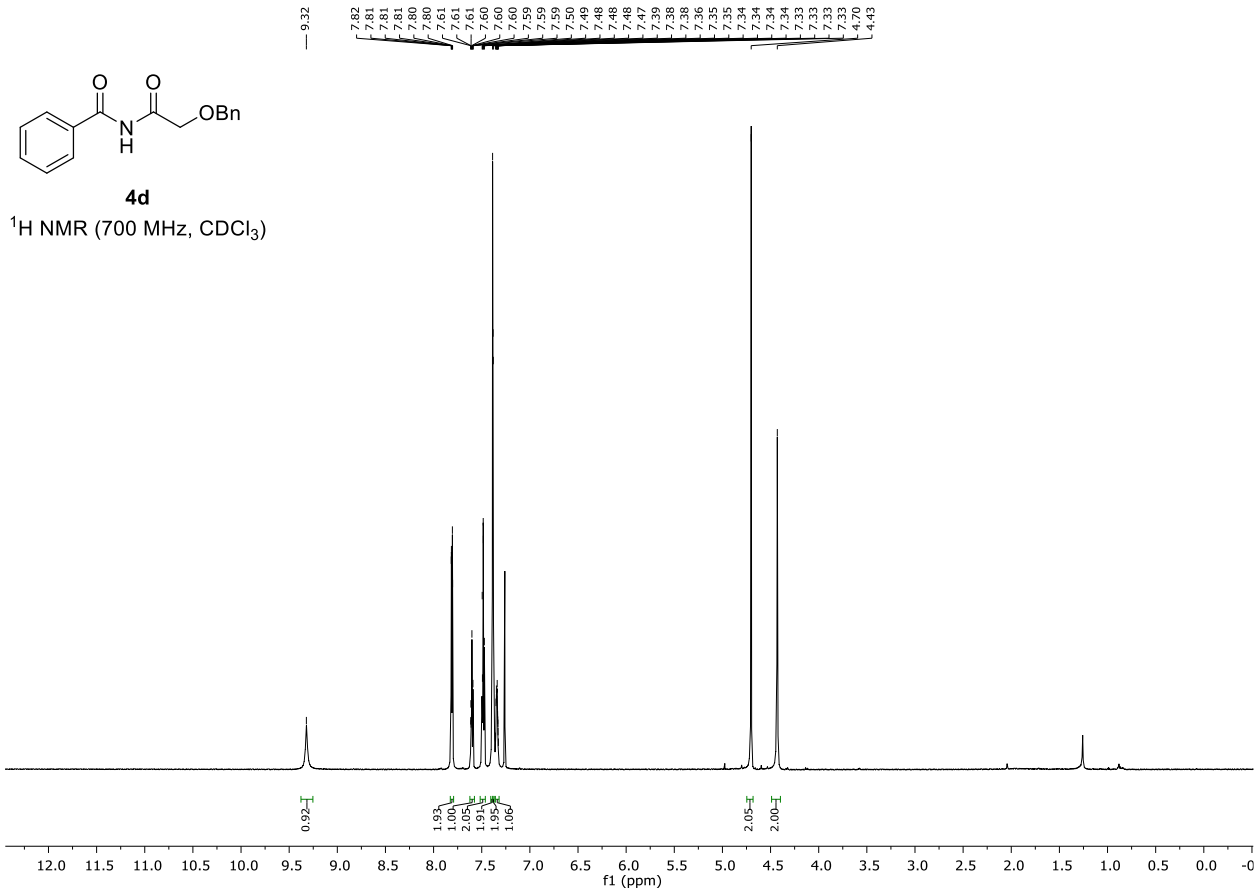
9.32
7.82
7.81
7.81
7.81
7.80
7.80
7.61
7.61
7.61
7.60
7.60
7.60
7.59
7.59
7.59
7.59
7.50
7.49
7.48
7.48
7.48
7.47
7.39
7.38
7.38
7.36
7.35
7.35
7.34
7.34
7.34
7.34
7.33
7.33
7.33
7.33
4.70
4.43
O
O
N
H
OBn
4d
1H NMR (700 MHz, CDCl3)
0.92
1.93
1.00
2.05
1.91
1.95
1.06
2.05
2.00
12.0 11.5 11.0 10.5 10.0 9.5 9.0 8.5 8.0 7.5 7.0 6.5 6.0 5.5 5.0 4.5 4.0 3.5 3.0 2.5 2.0 1.5 1.0 0.5 0.0 -0
f1 (ppm)

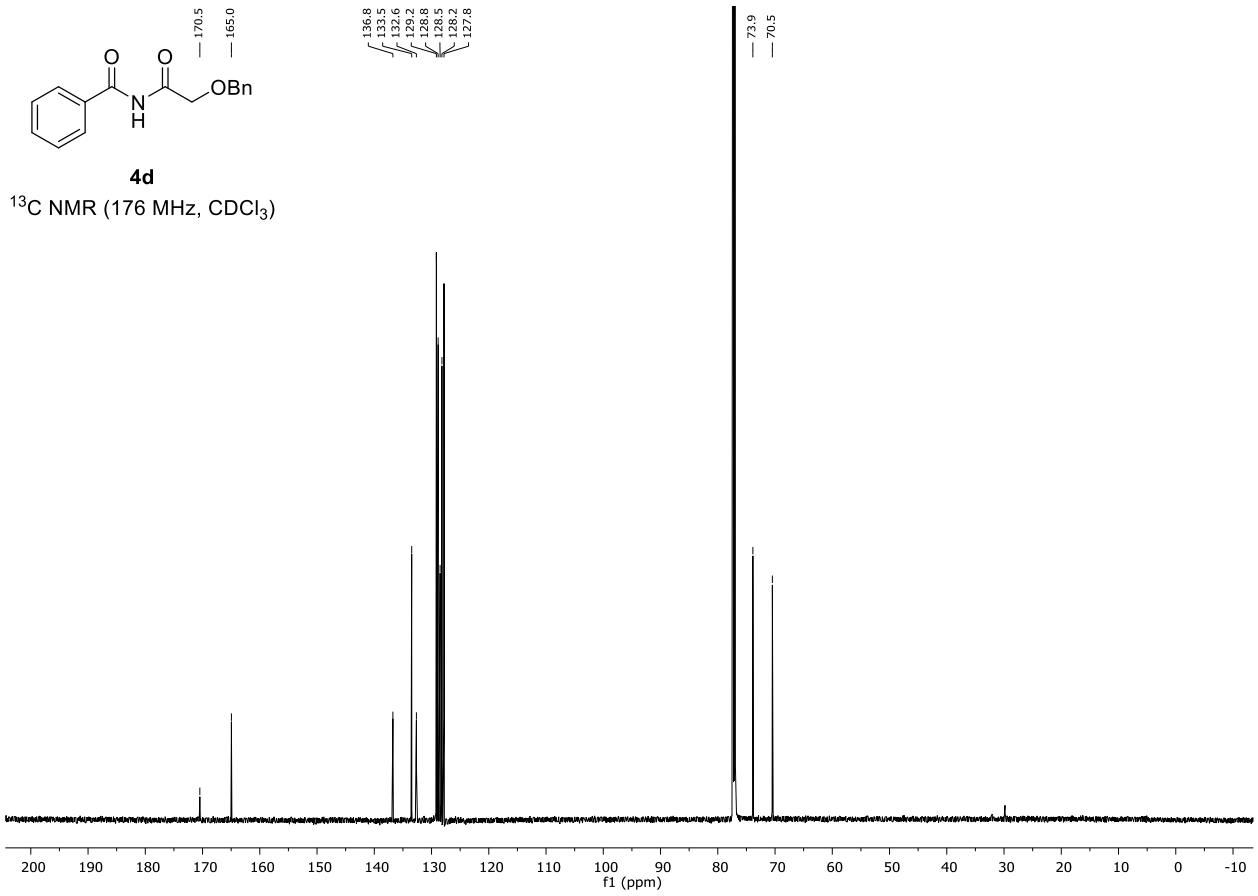
170.5
165.0
136.8
133.5
132.6
129.2
128.8
128.5
128.2
127.8
73.9
70.5
O
O
N
H
OBn
4d
13C NMR (176 MHz, CDCl3)
200 190 180 170 160 150 140 130 120 110 100 90 80 70 60 50 40 30 20 10 0 -10
f1 (ppm)

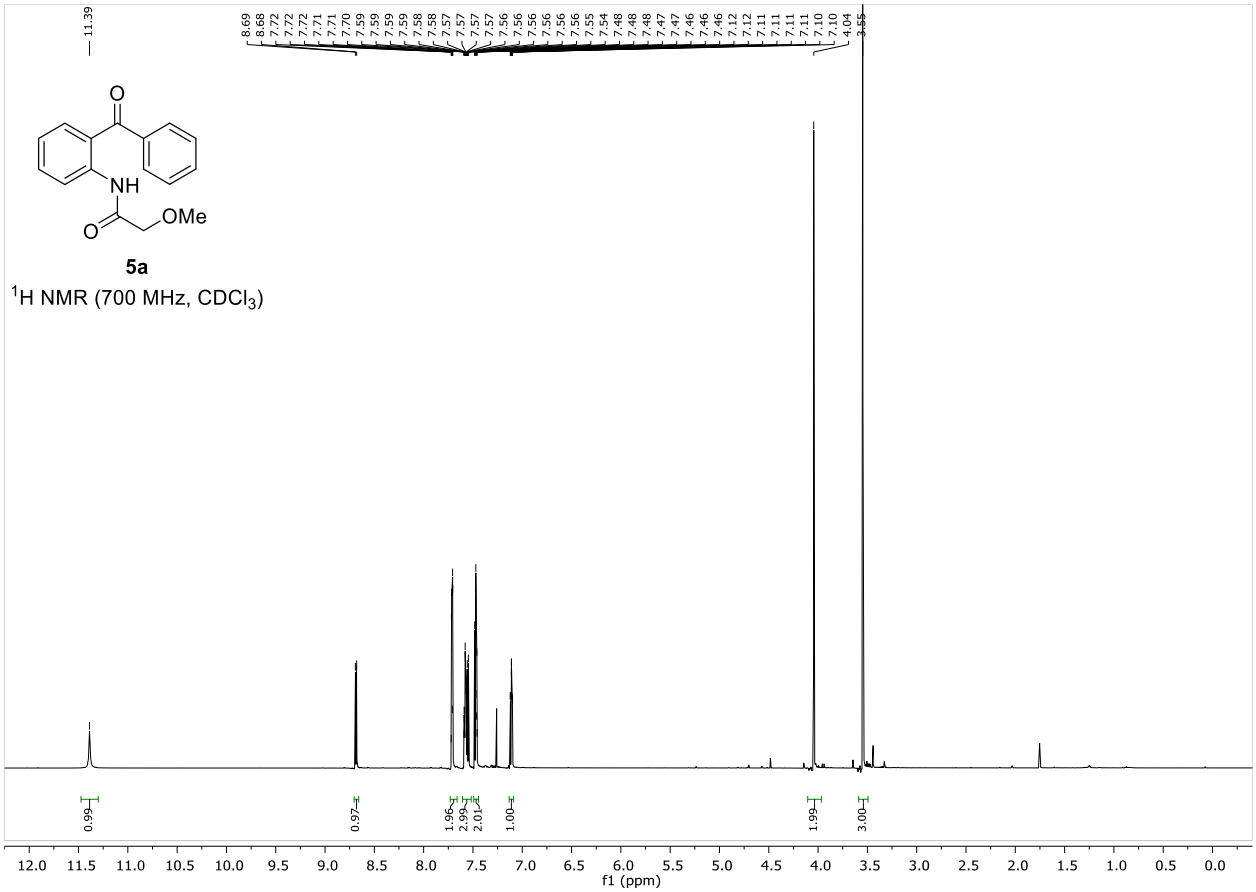

5a

^{1}H NMR (700 MHz, $CDCl_3$)

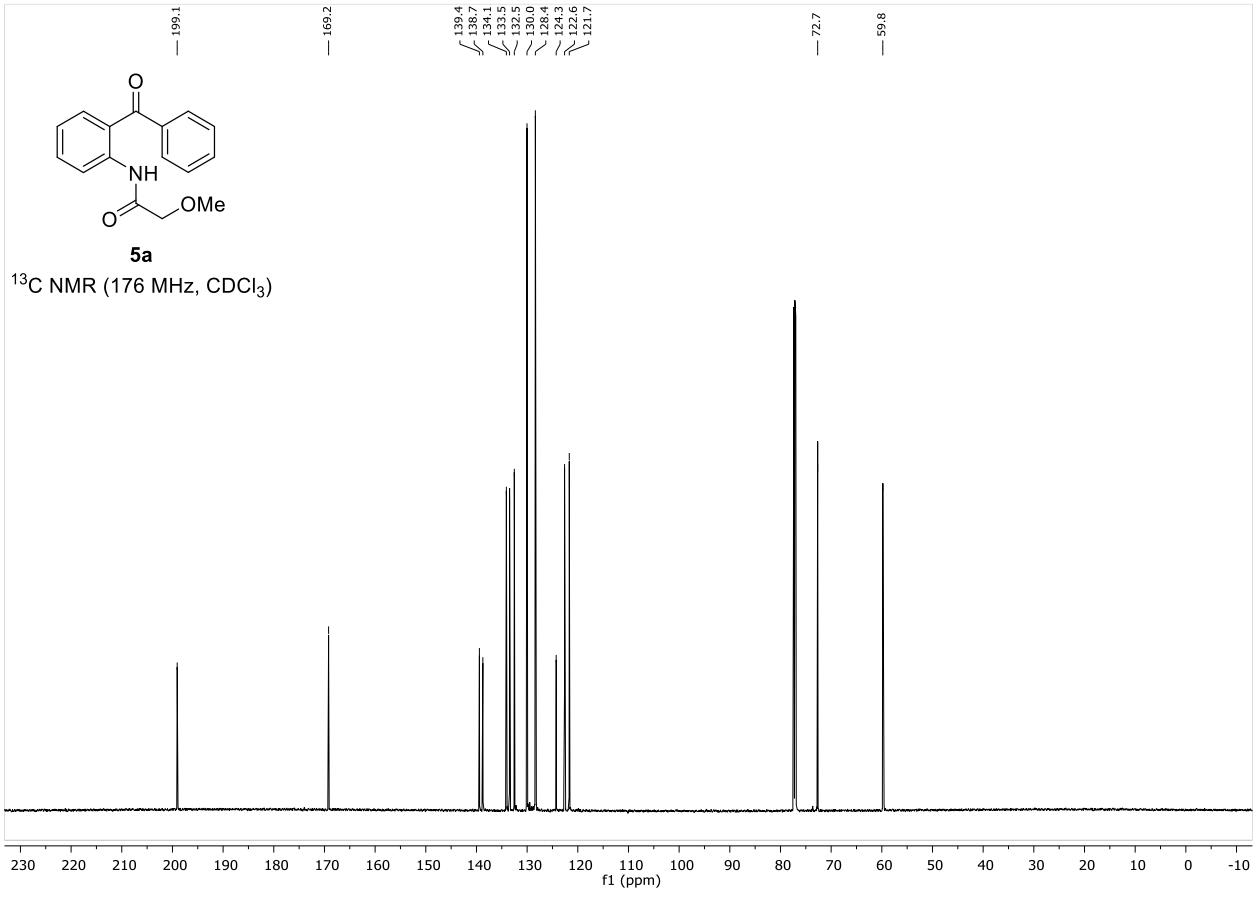

5a

^{13}C NMR (176 MHz, $CDCl_3$)

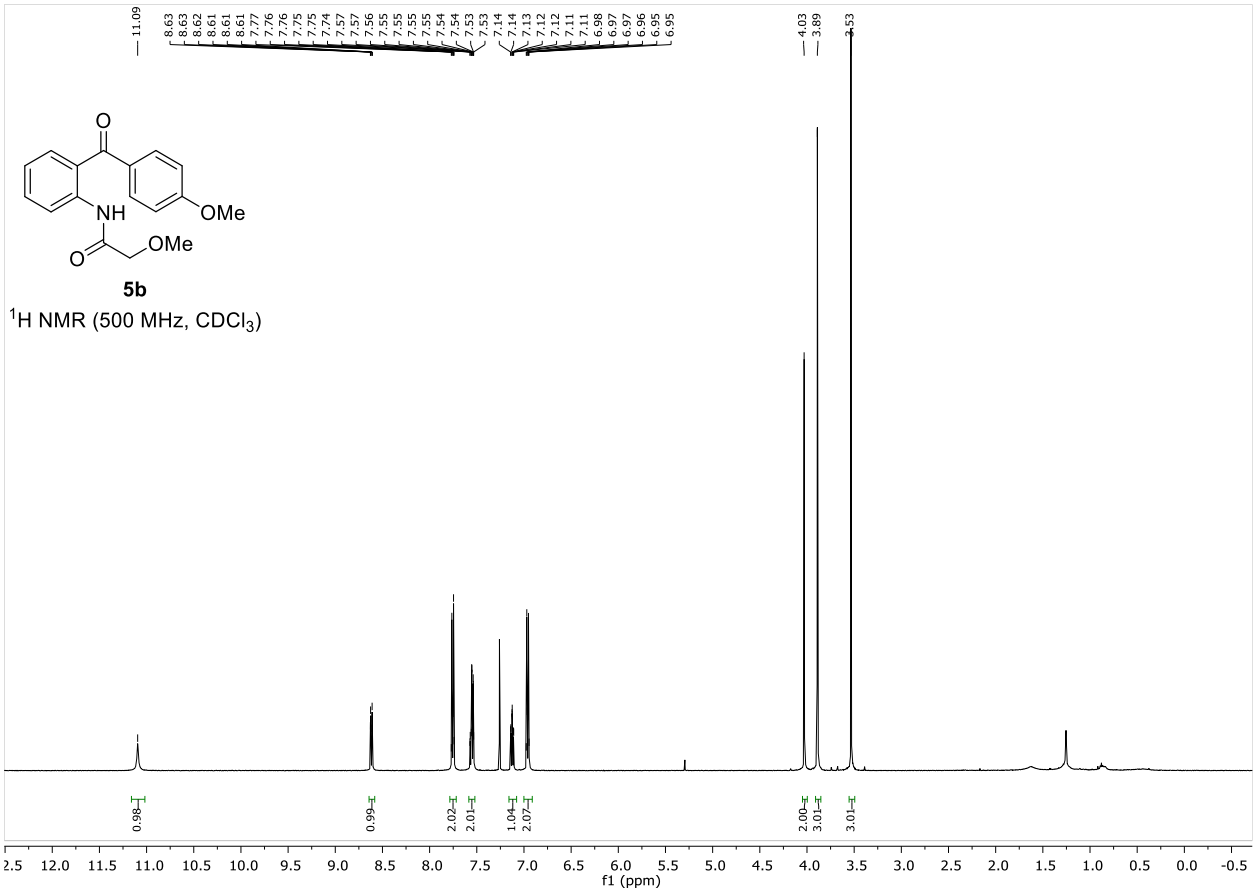

5b

^{1}H NMR (500 MHz, $CDCl_3$)

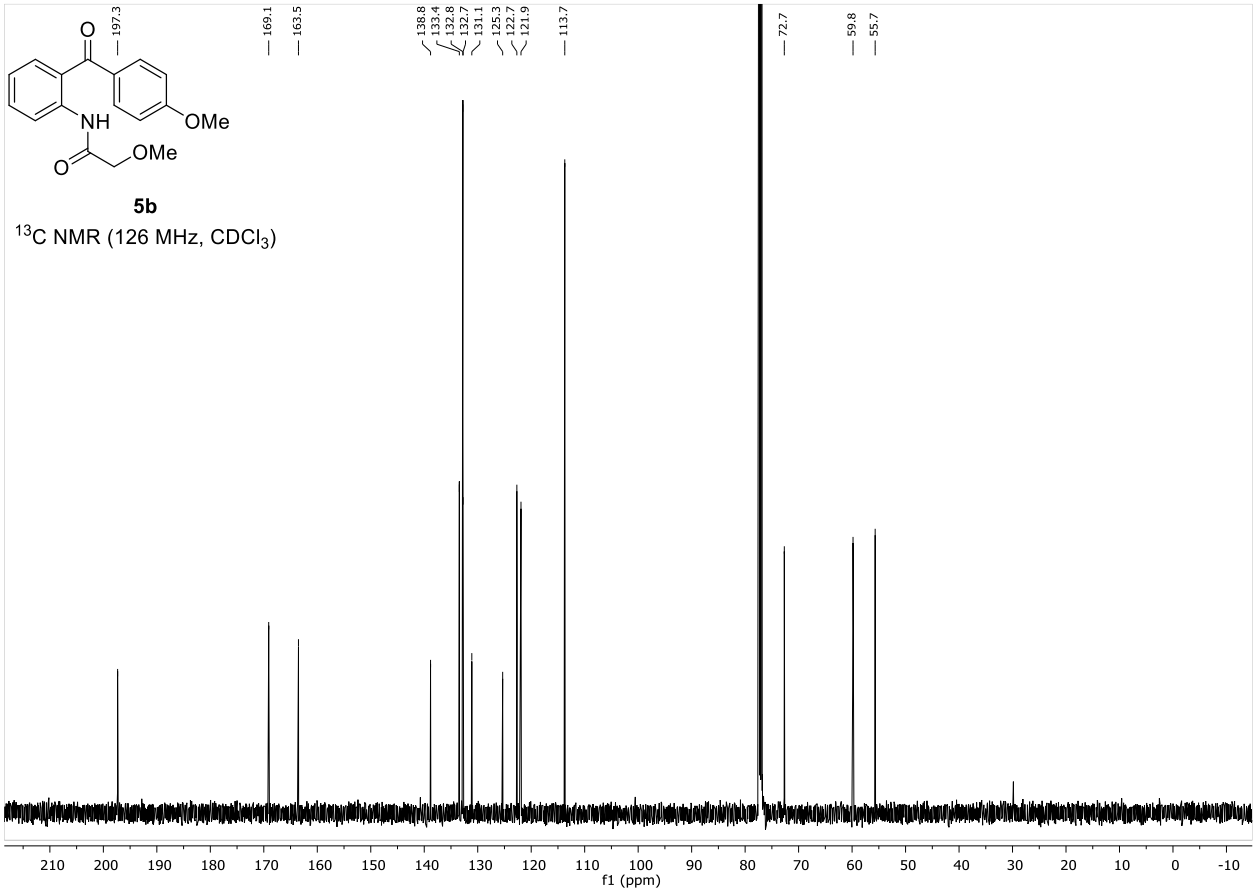

5b

^{13}C NMR (126 MHz, $CDCl_3$)

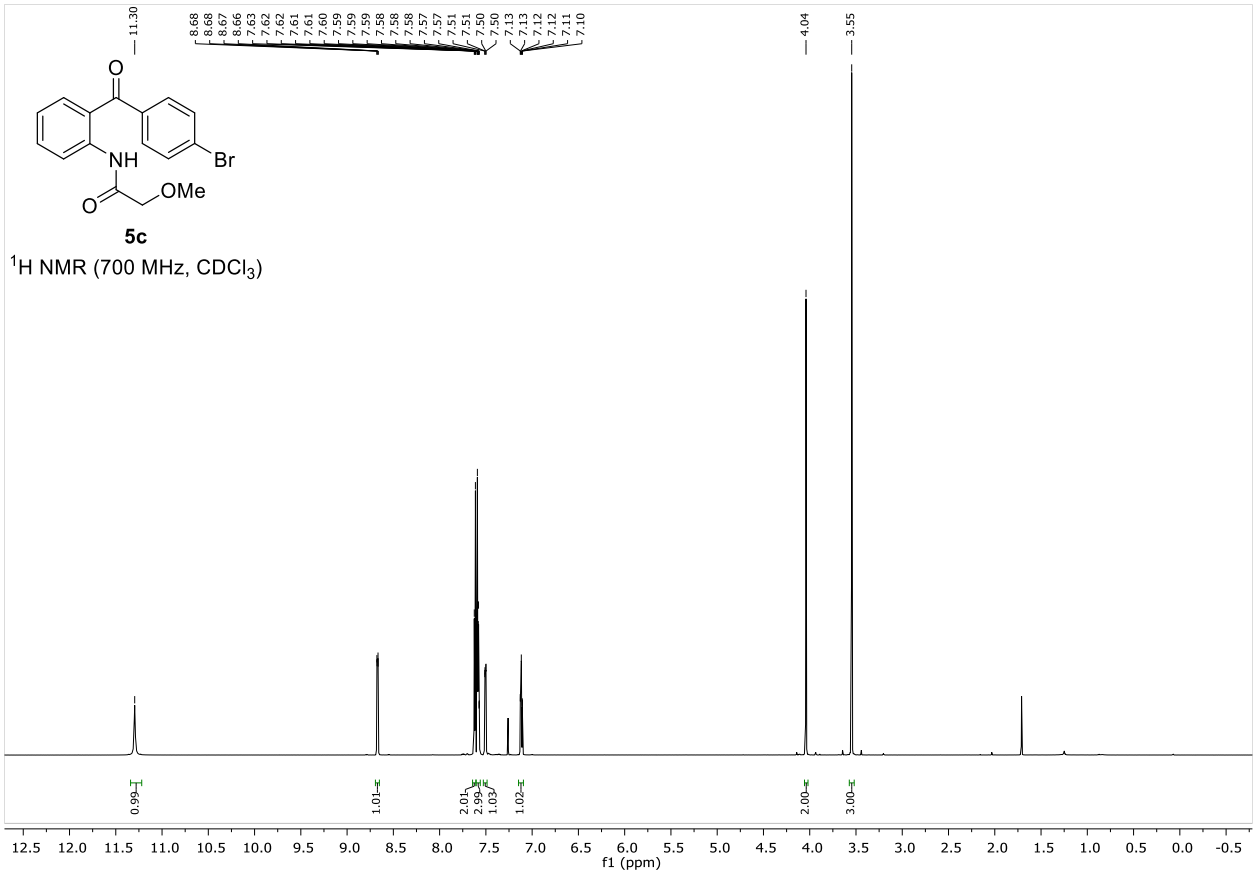

5c

^{1}H NMR (700 MHz, $CDCl_3$)

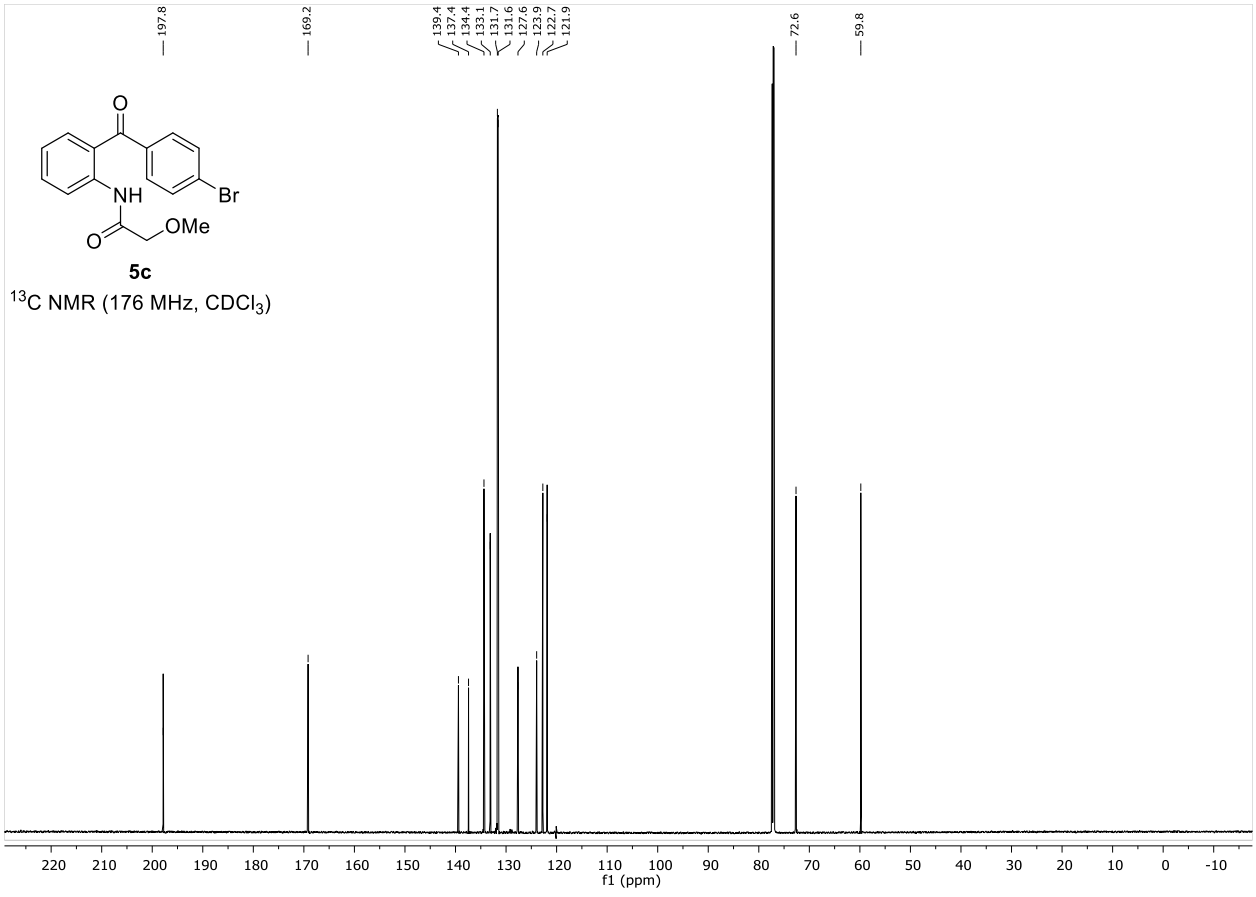

5c

^{13}C NMR (176 MHz, $CDCl_3$)

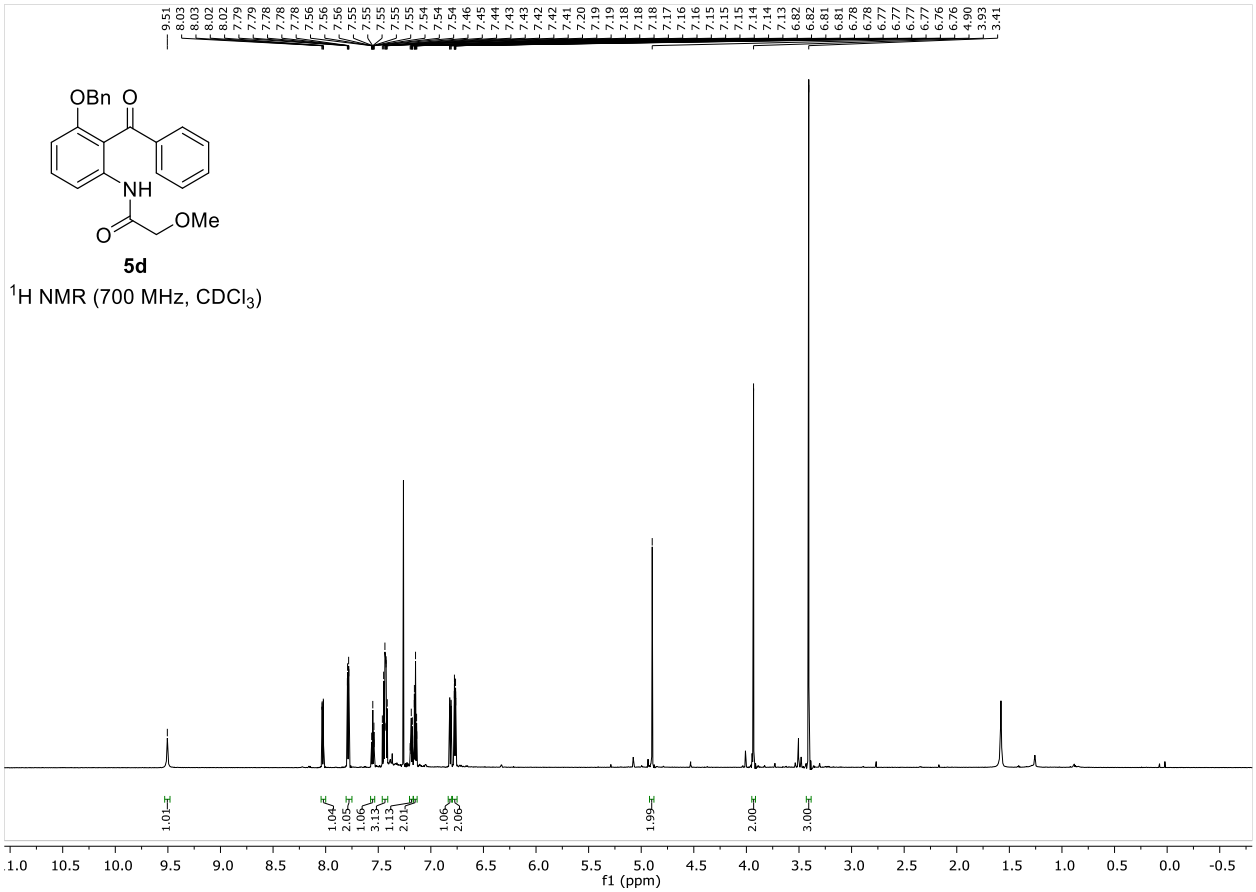

5d

^{1}H NMR (700 MHz, $CDCl_3$)

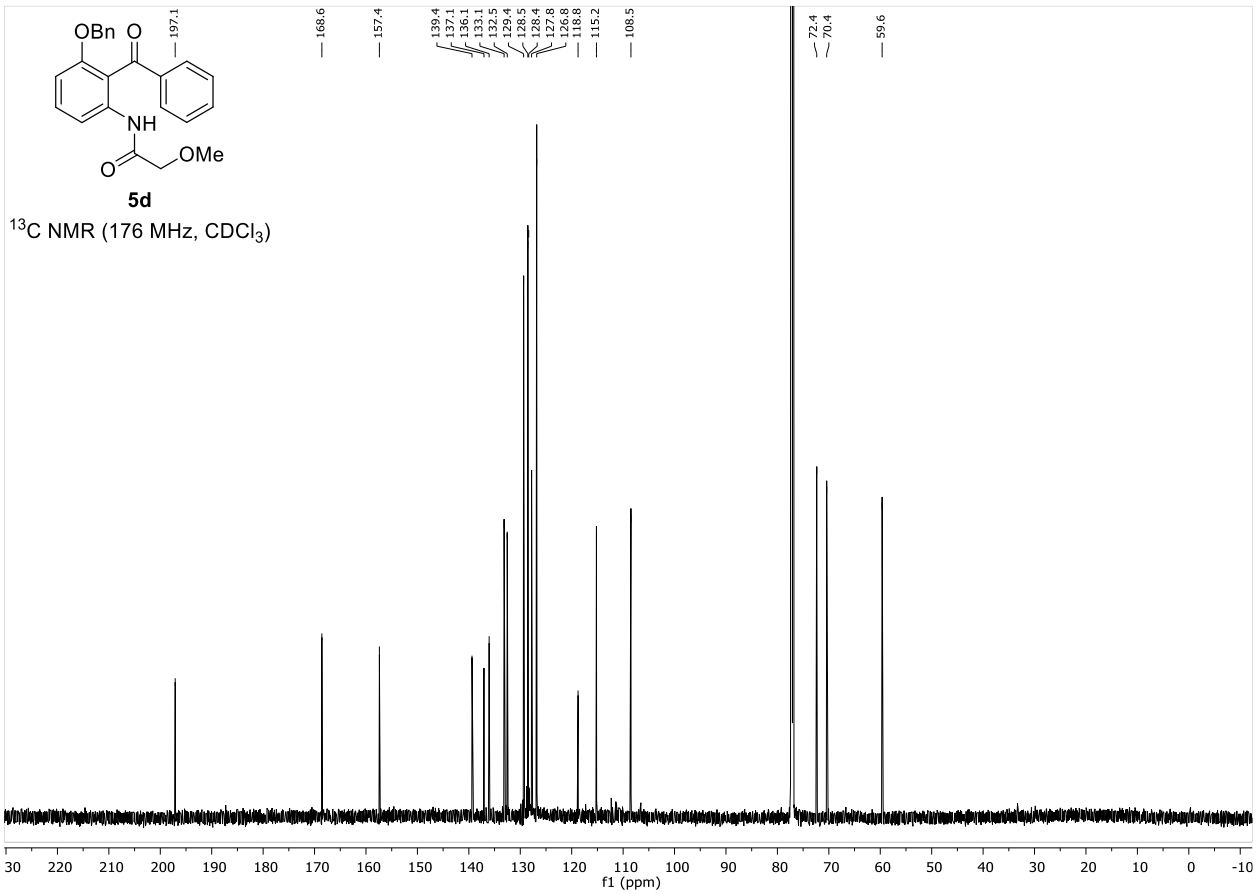

5d

^{13}C NMR (176 MHz, $CDCl_3$)

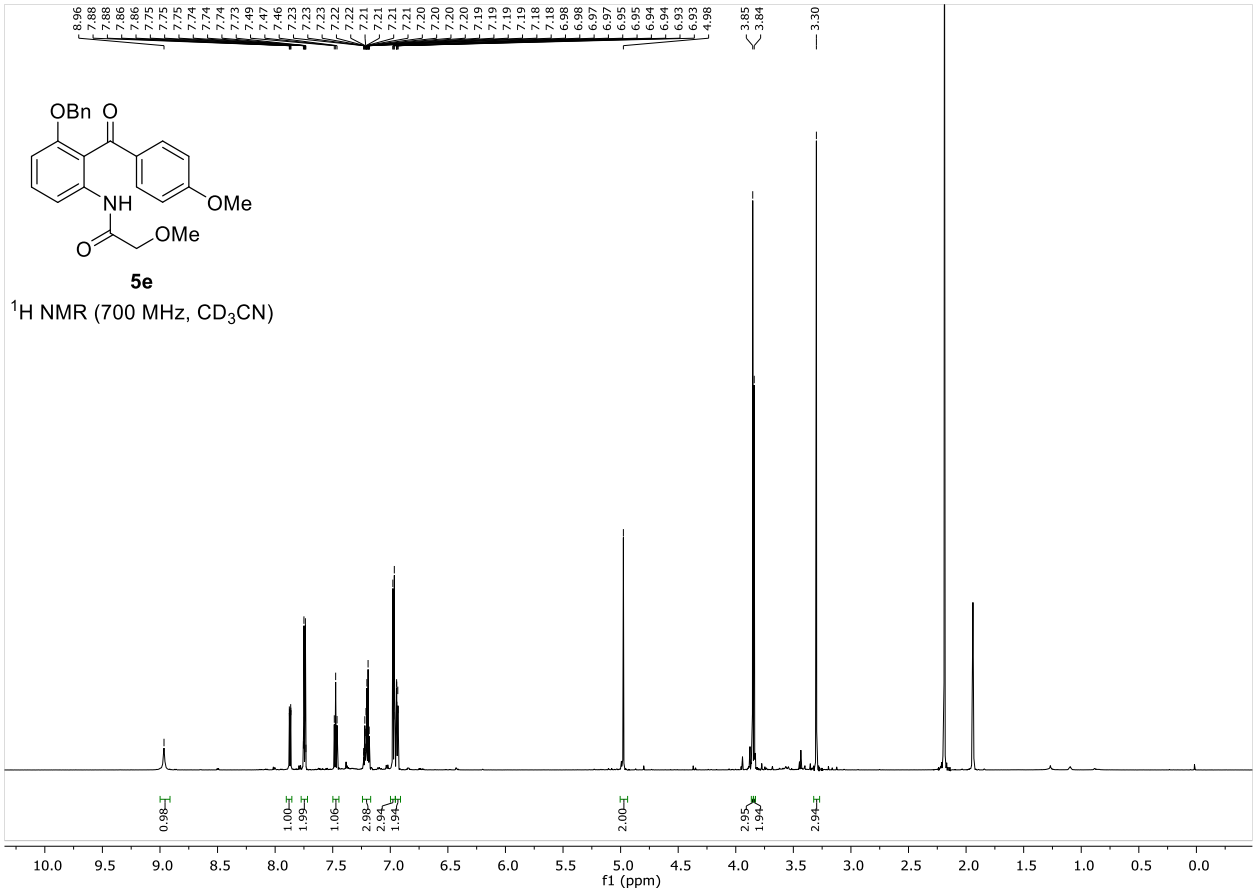
OBn O
NH
OMe
OMe
O
5e
1H NMR (700 MHz, CD3CN)
f1 (ppm)

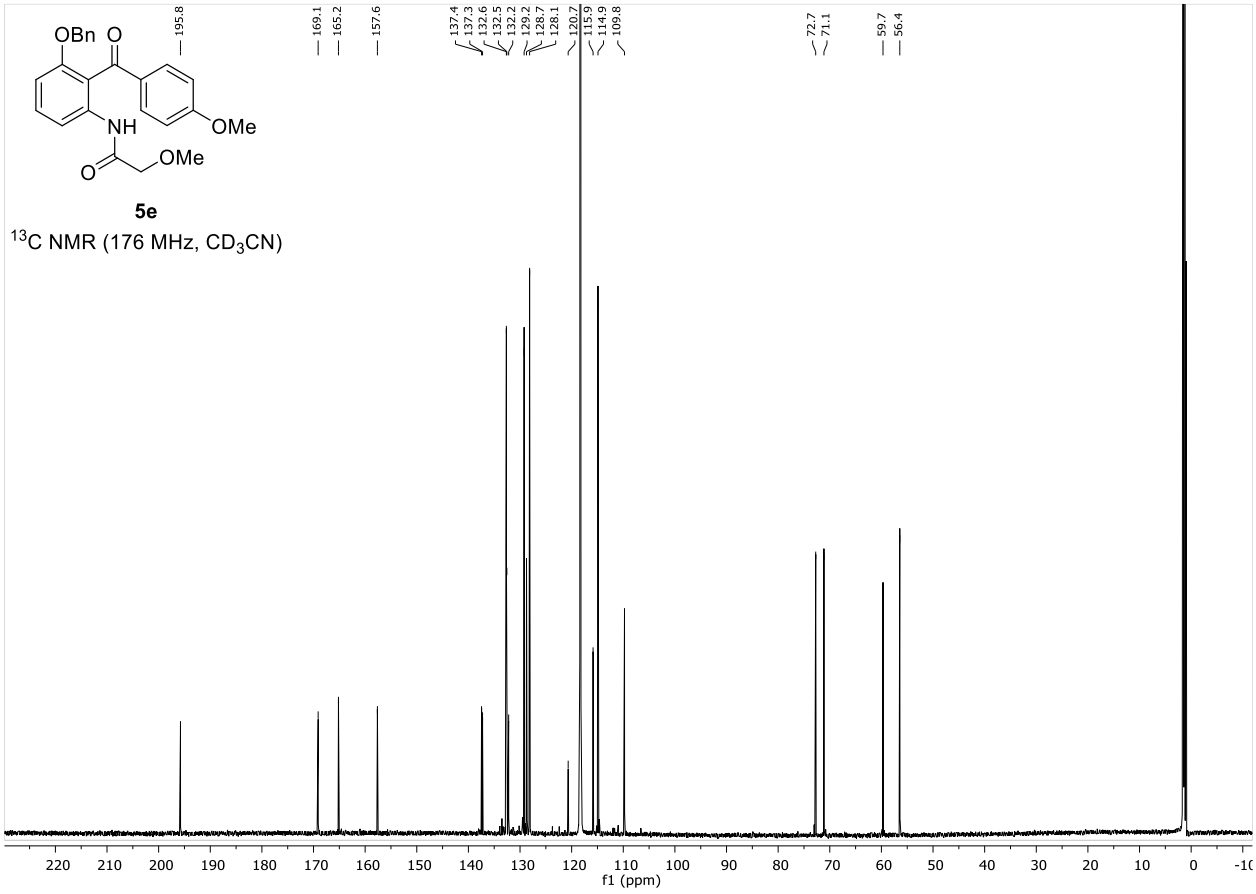
OBn O
NH
OMe
OMe
O
5e
13C NMR (176 MHz, CD3CN)
f1 (ppm)

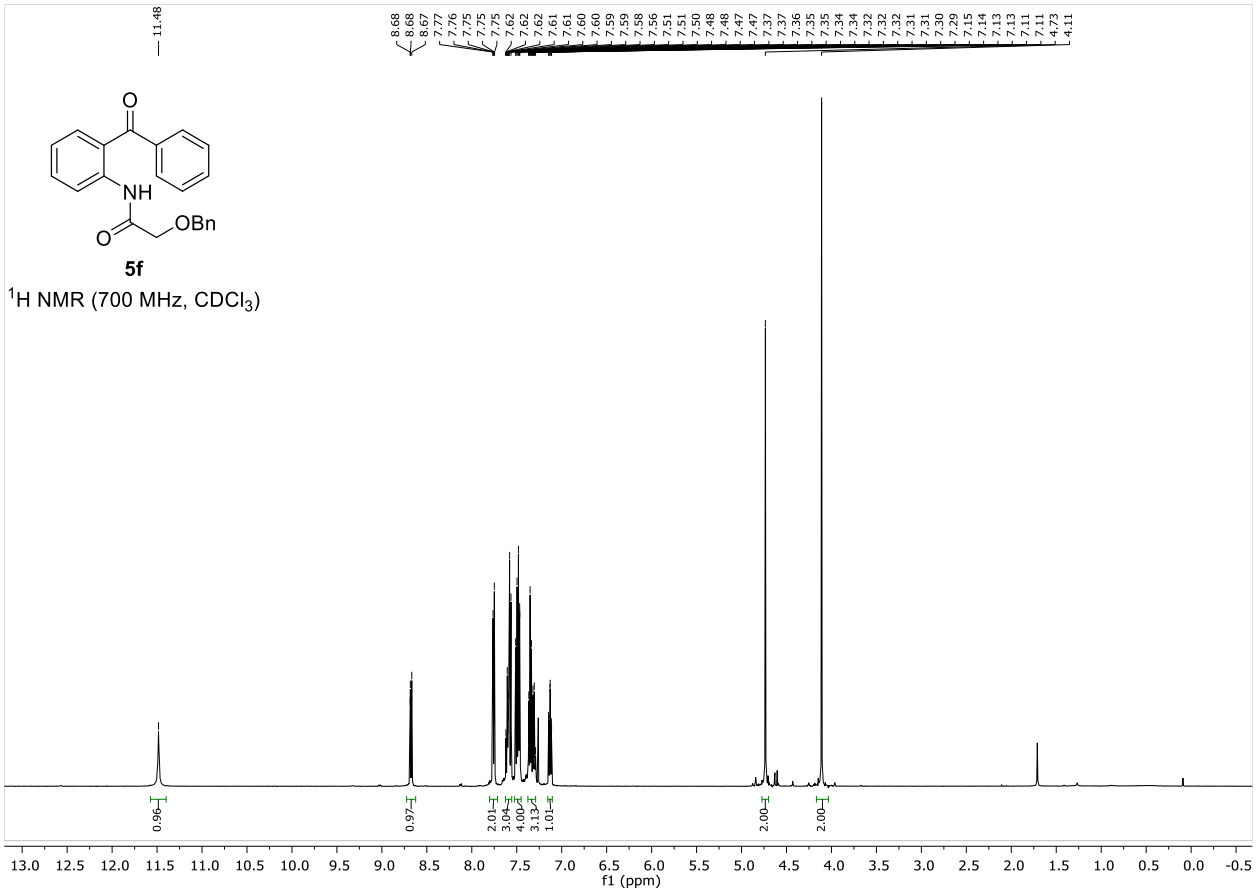

5f

^{1}H NMR (700 MHz, $CDCl_3$)

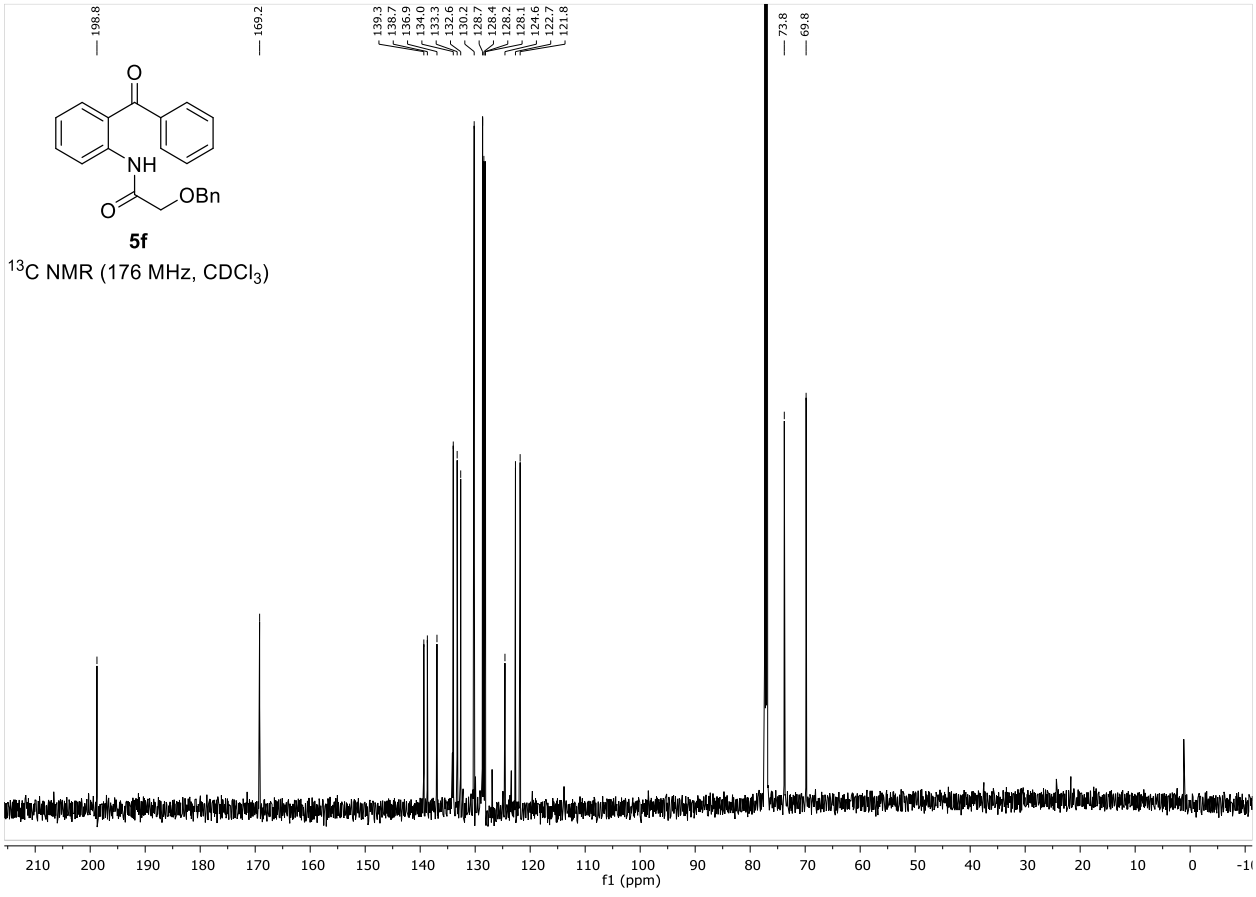

5f

^{13}C NMR (176 MHz, $CDCl_3$)

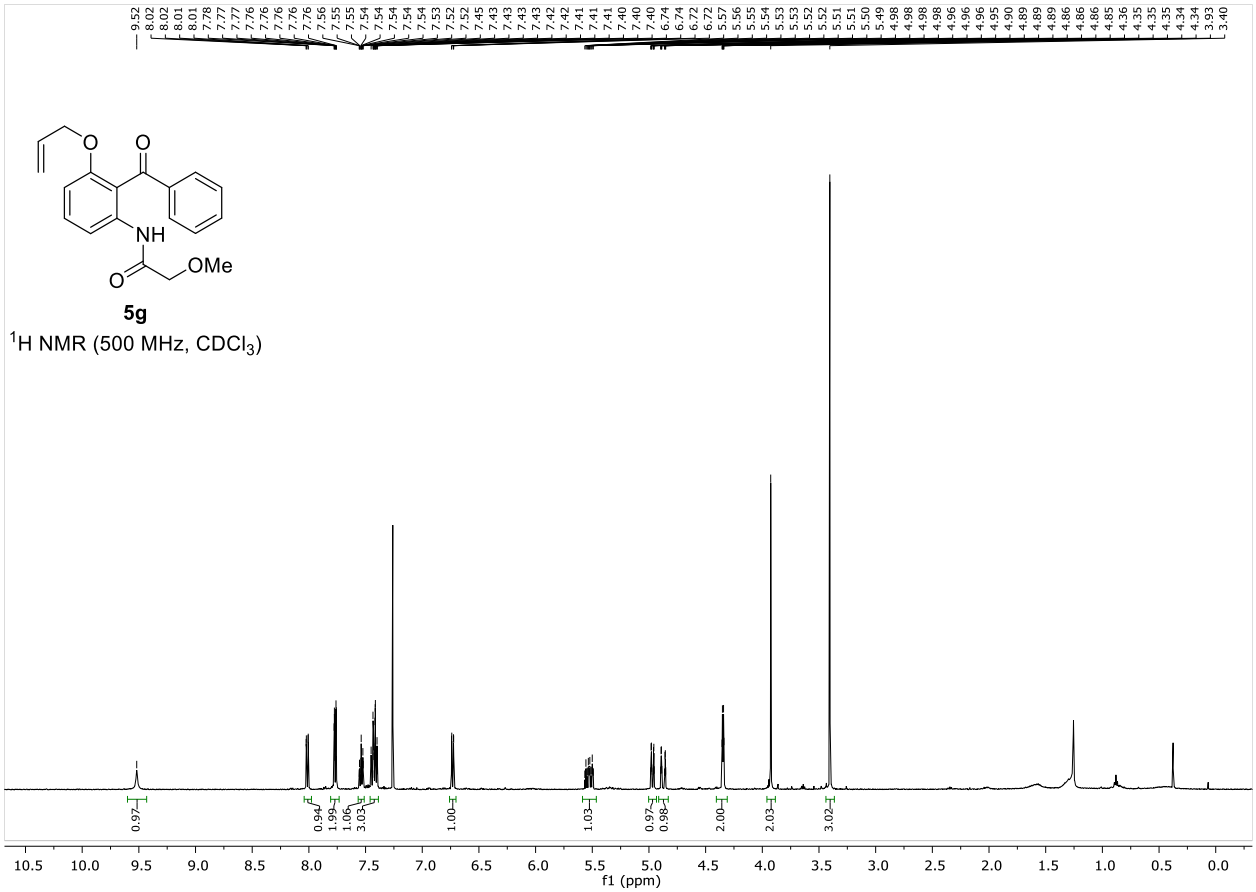
9.52 8.02 8.02 8.01 8.01 7.78 7.77 7.77 7.76 7.76 7.76 7.76 7.76 7.56 7.55 7.55 7.54 7.54 7.54 7.54 7.54 7.53 7.52 7.52 7.45 7.43 7.43 7.43 7.42 7.41 7.41 7.41 7.40 7.40 7.40 6.74 6.74 6.72 6.72 5.57 5.56 5.55 5.54 5.53 5.53 5.52 5.52 5.51 5.51 5.50 5.49 4.98 4.98 4.98 4.96 4.96 4.96 4.95 4.90 4.89 4.89 4.89 4.86 4.86 4.86 4.85 4.36 4.35 4.35 4.35 4.34 4.34 3.93 3.40
O
O
NH
O
OMe
5g
1H NMR (500 MHz, CDCl3)
0.97
0.94
1.99
1.06
3.03
1.00
1.03
0.97
0.98
2.00
2.03
3.02
10.5 10.0 9.5 9.0 8.5 8.0 7.5 7.0 6.5 6.0 5.5 5.0 4.5 4.0 3.5 3.0 2.5 2.0 1.5 1.0 0.5 0.0
f1 (ppm)

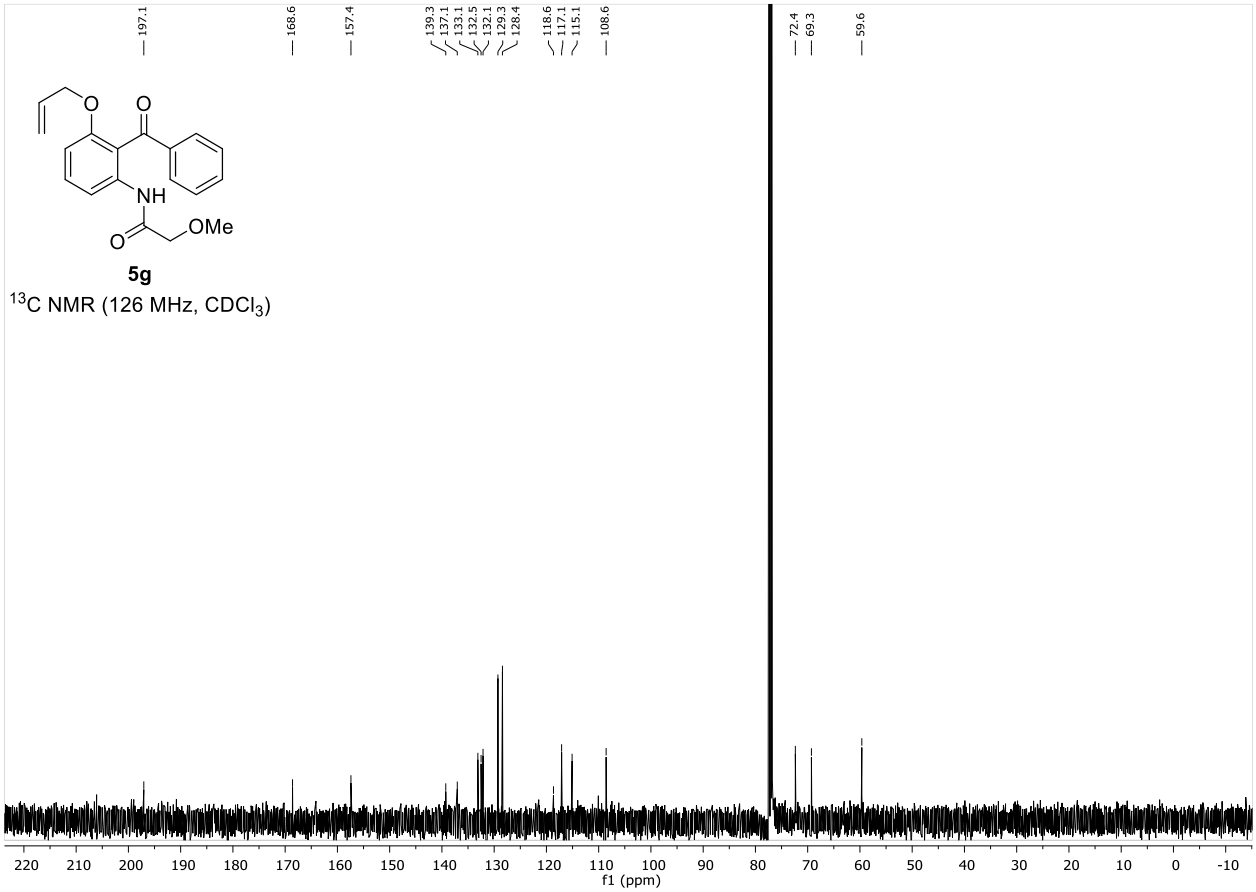
197.1
168.6
157.4
139.3
137.1
133.1
132.5
132.1
129.3
128.4
118.6
117.1
115.1
108.6
72.4
69.3
59.6
O
O
NH
O
OMe
5g
13C NMR (126 MHz, CDCl3)
220 210 200 190 180 170 160 150 140 130 120 110 100 90 80 70 60 50 40 30 20 10 0 -10
f1 (ppm)

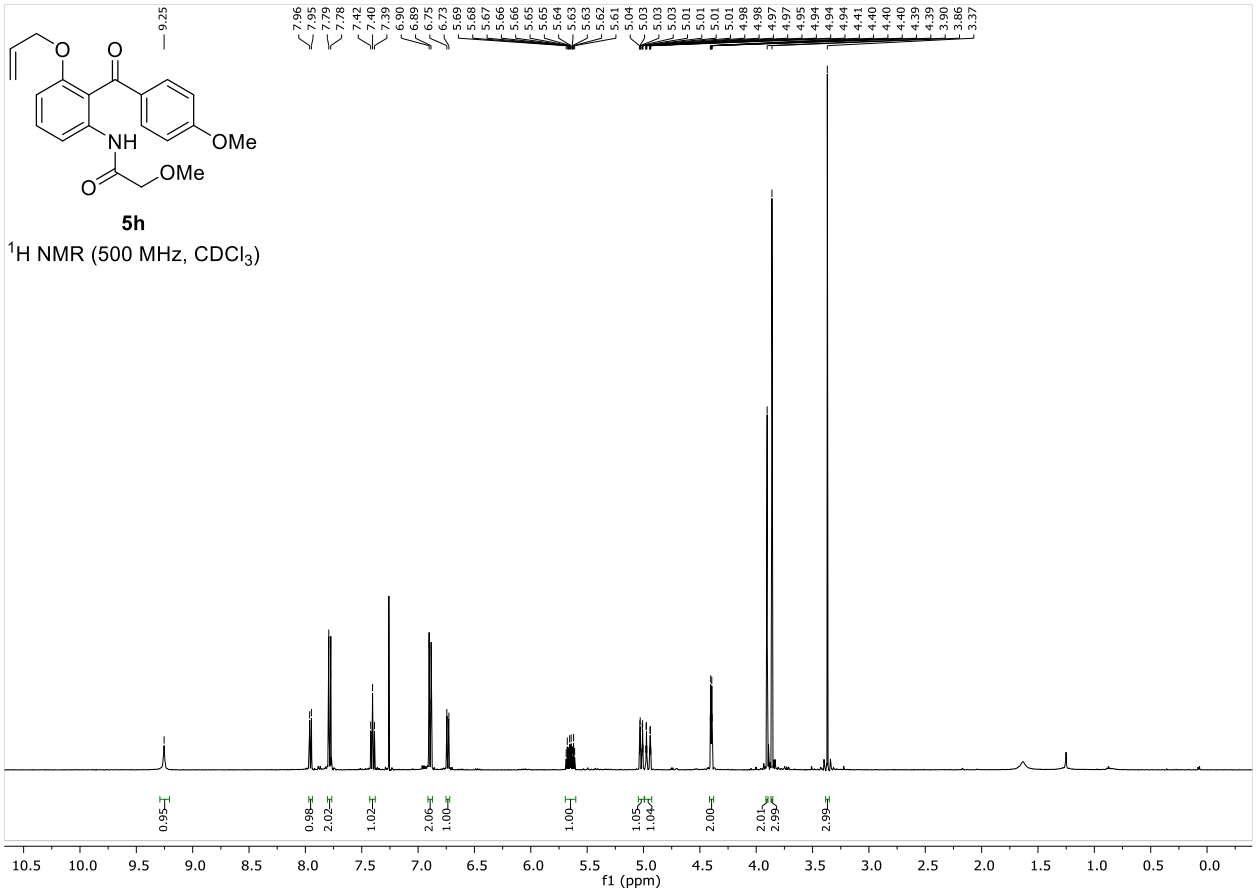

5h

^{1}H NMR (500 MHz, $CDCl_3$)

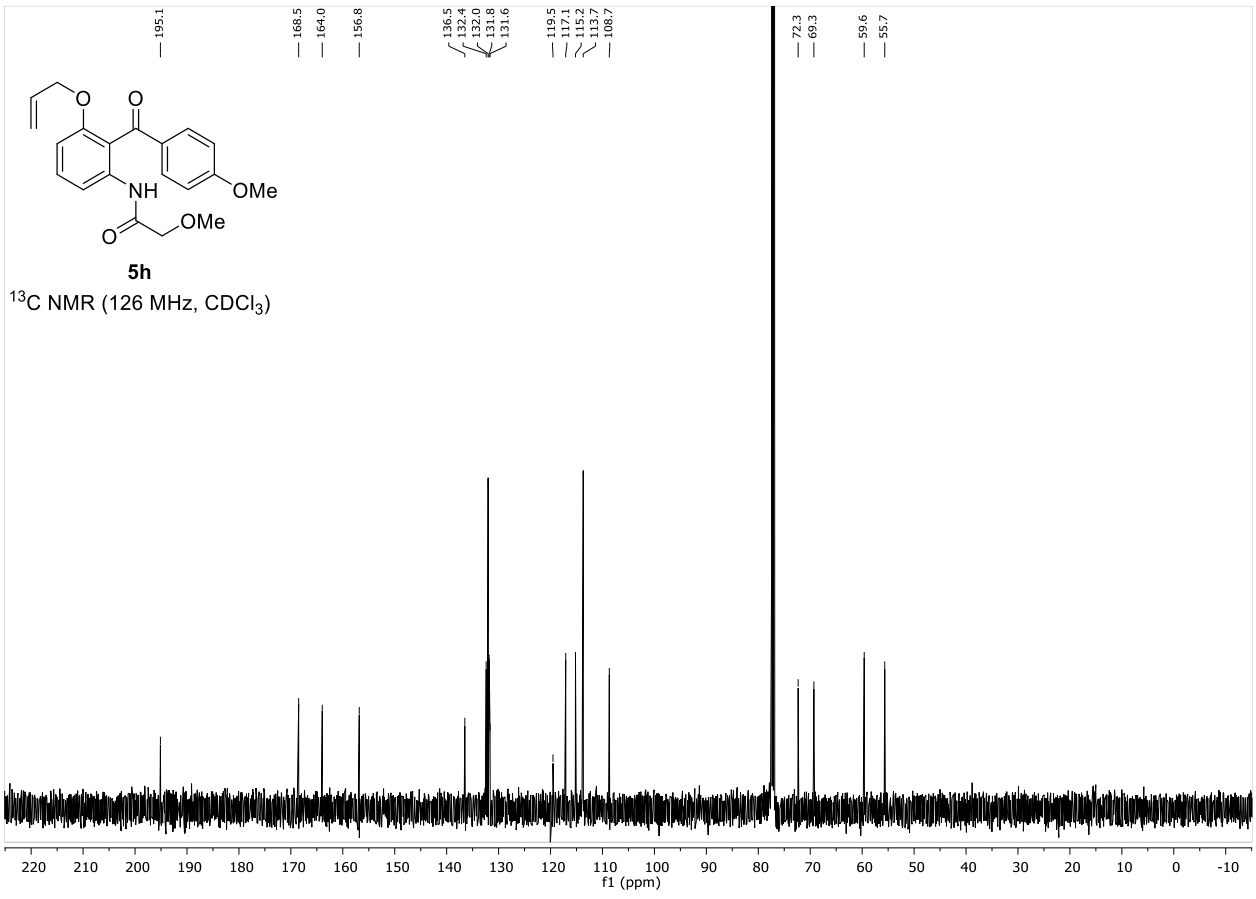

5h

^{13}C NMR (126 MHz, $CDCl_3$)

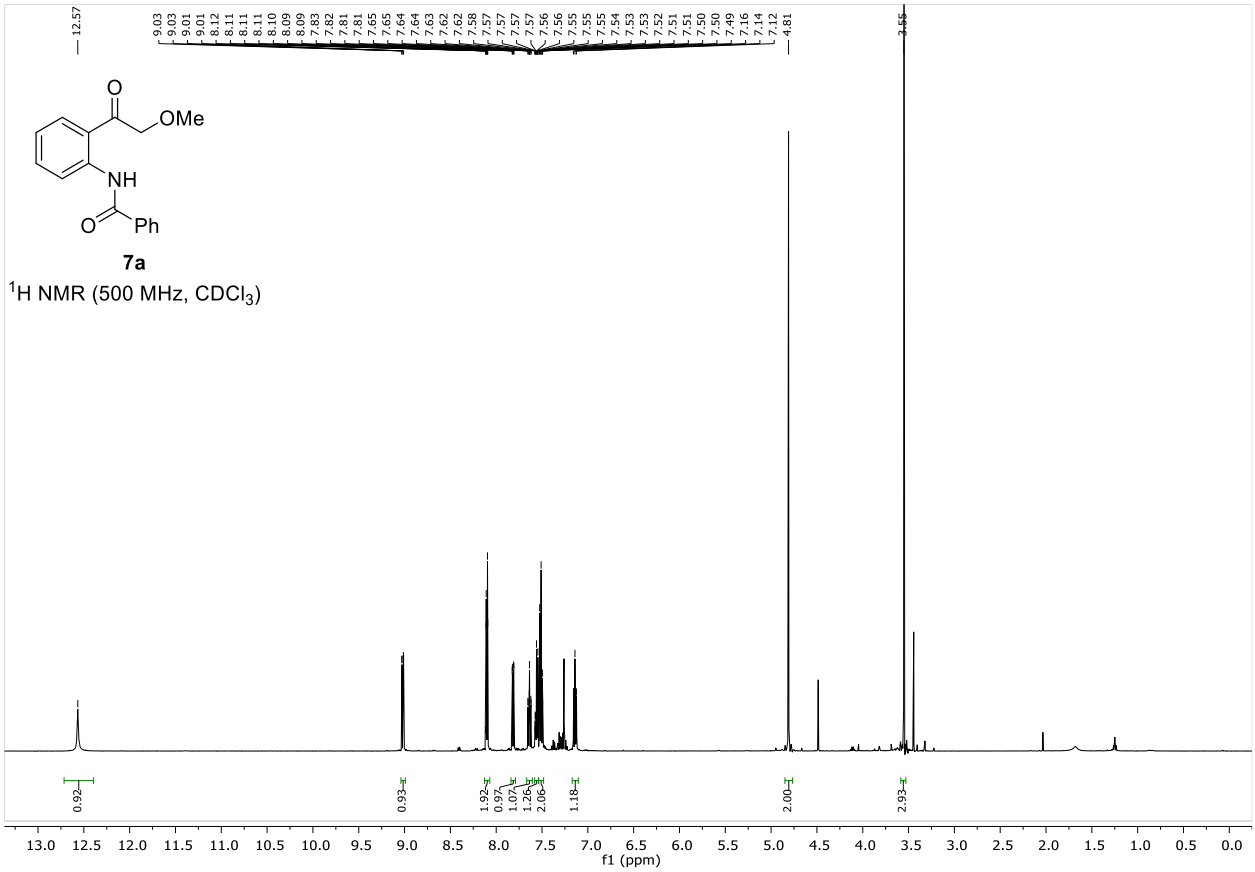
12.57
9.03
9.03
9.01
9.01
8.12
8.11
8.11
8.11
8.10
8.09
8.09
7.83
7.82
7.81
7.81
7.65
7.64
7.64
7.63
7.62
7.62
7.58
7.57
7.57
7.57
7.57
7.56
7.56
7.55
7.55
7.55
7.54
7.53
7.53
7.52
7.51
7.51
7.50
7.50
7.49
7.16
7.14
7.12
4.81
3.55
O
OMe
NH
O
Ph
7a
1H NMR (500 MHz, CDCl3)
0.92
0.93
1.92
0.97
1.07
1.26
2.06
1.18
2.00
2.93
13.0 12.5 12.0 11.5 11.0 10.5 10.0 9.5 9.0 8.5 8.0 7.5 7.0 6.5 6.0 5.5 5.0 4.5 4.0 3.5 3.0 2.5 2.0 1.5 1.0 0.5 0.0
f1 (ppm)

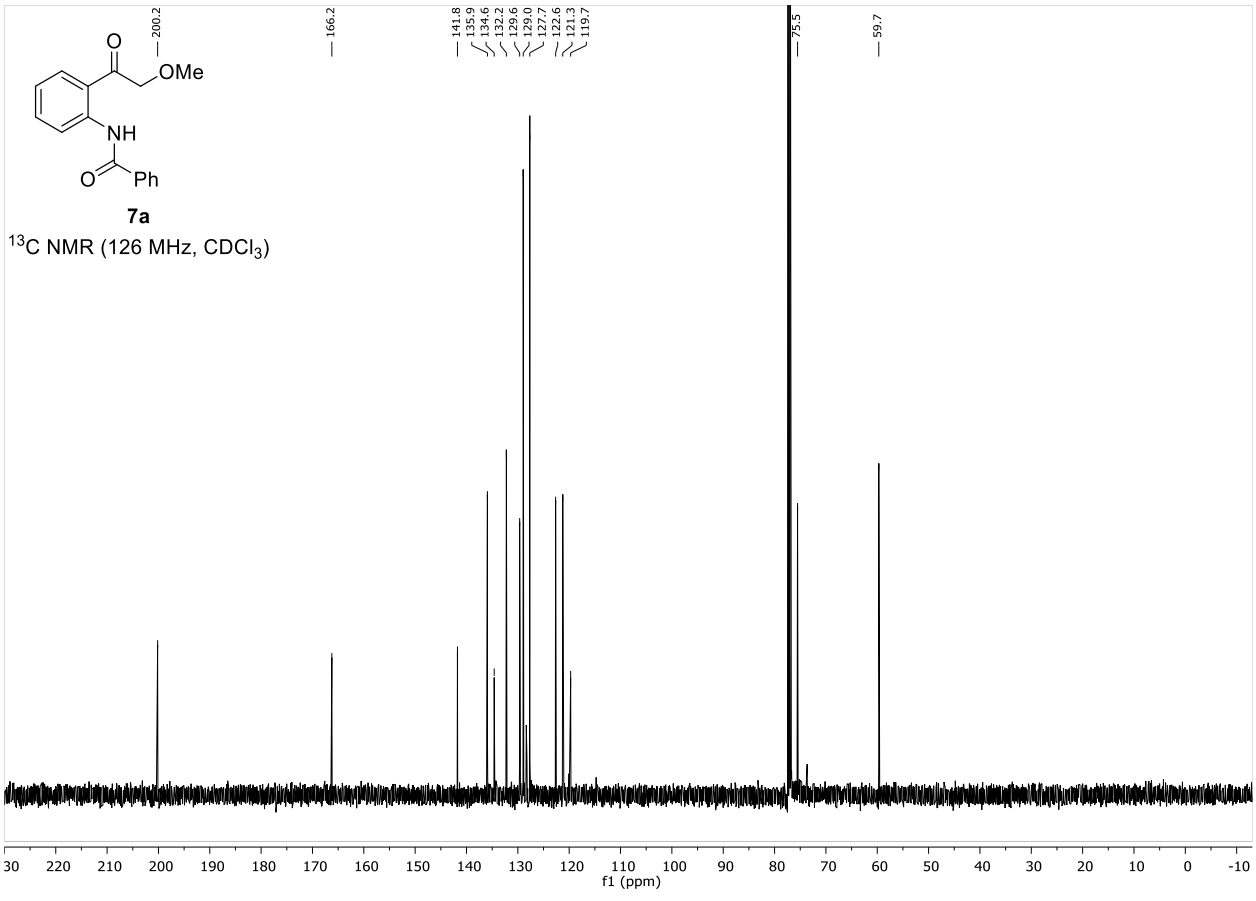
200.2
166.2
141.8
135.9
134.6
132.2
129.6
129.0
127.7
122.6
121.3
119.7
75.5
59.7
O
OMe
NH
O
Ph
7a
13C NMR (126 MHz, CDCl3)
30 220 210 200 190 180 170 160 150 140 130 120 110 100 90 80 70 60 50 40 30 20 10 0 -10
f1 (ppm)

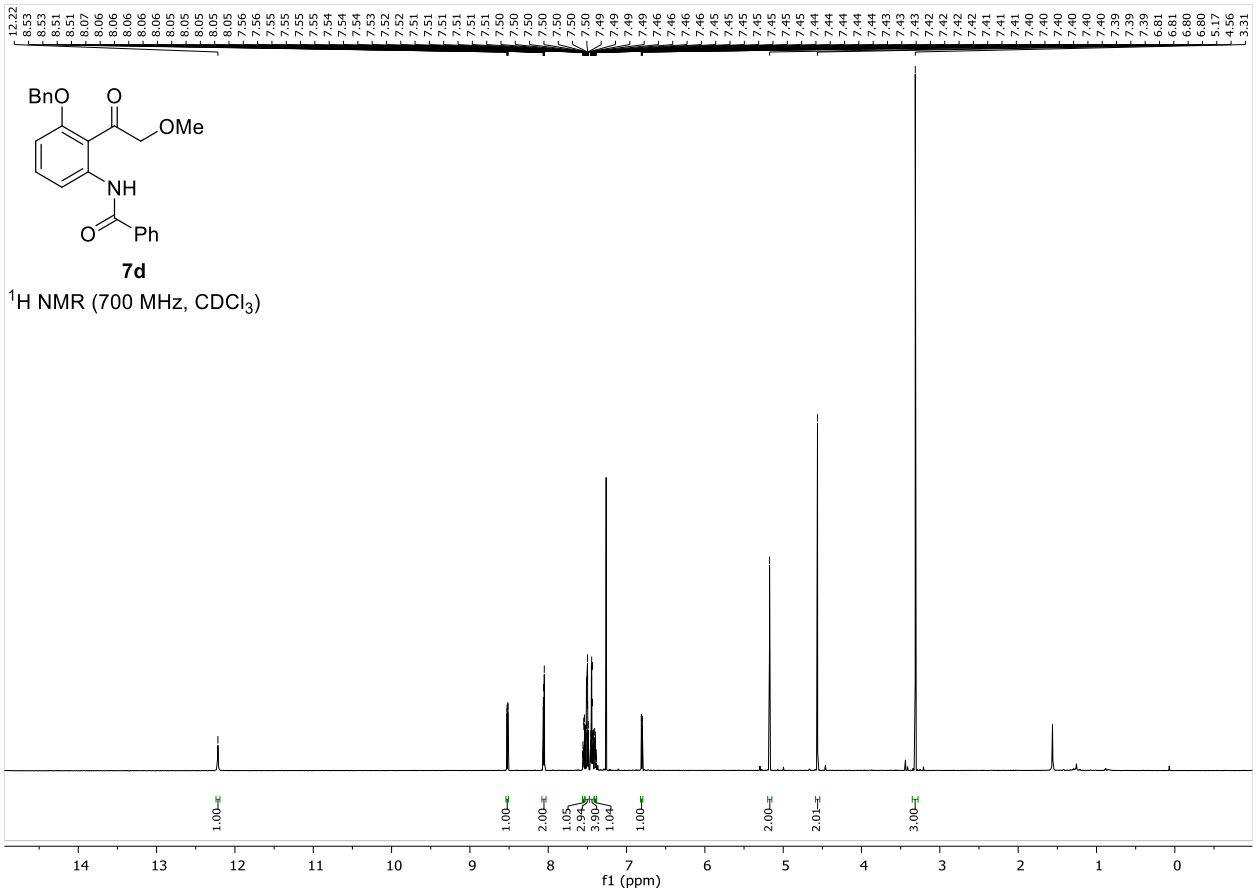

7d

^{1}H NMR (700 MHz, $CDCl_3$)

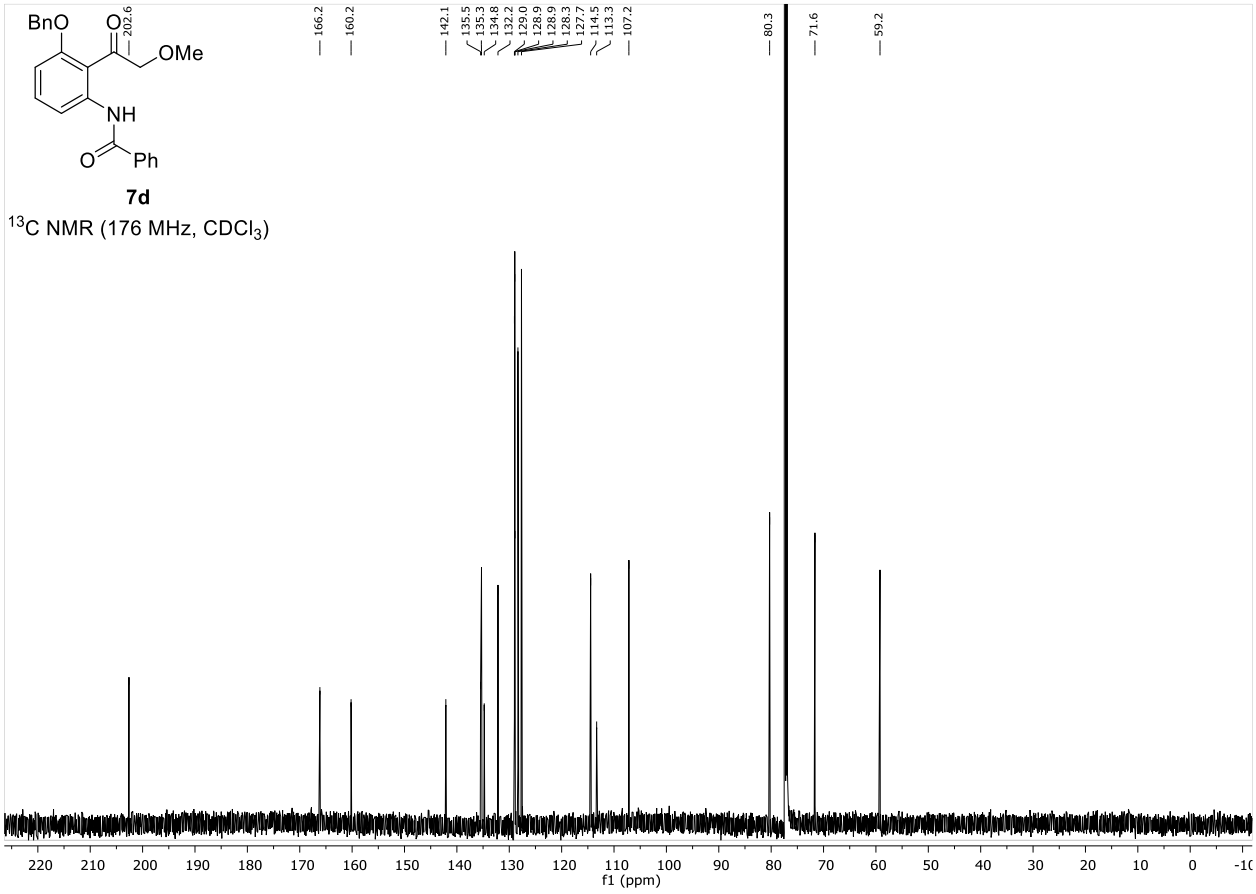

7d

^{13}C NMR (176 MHz, $CDCl_3$)

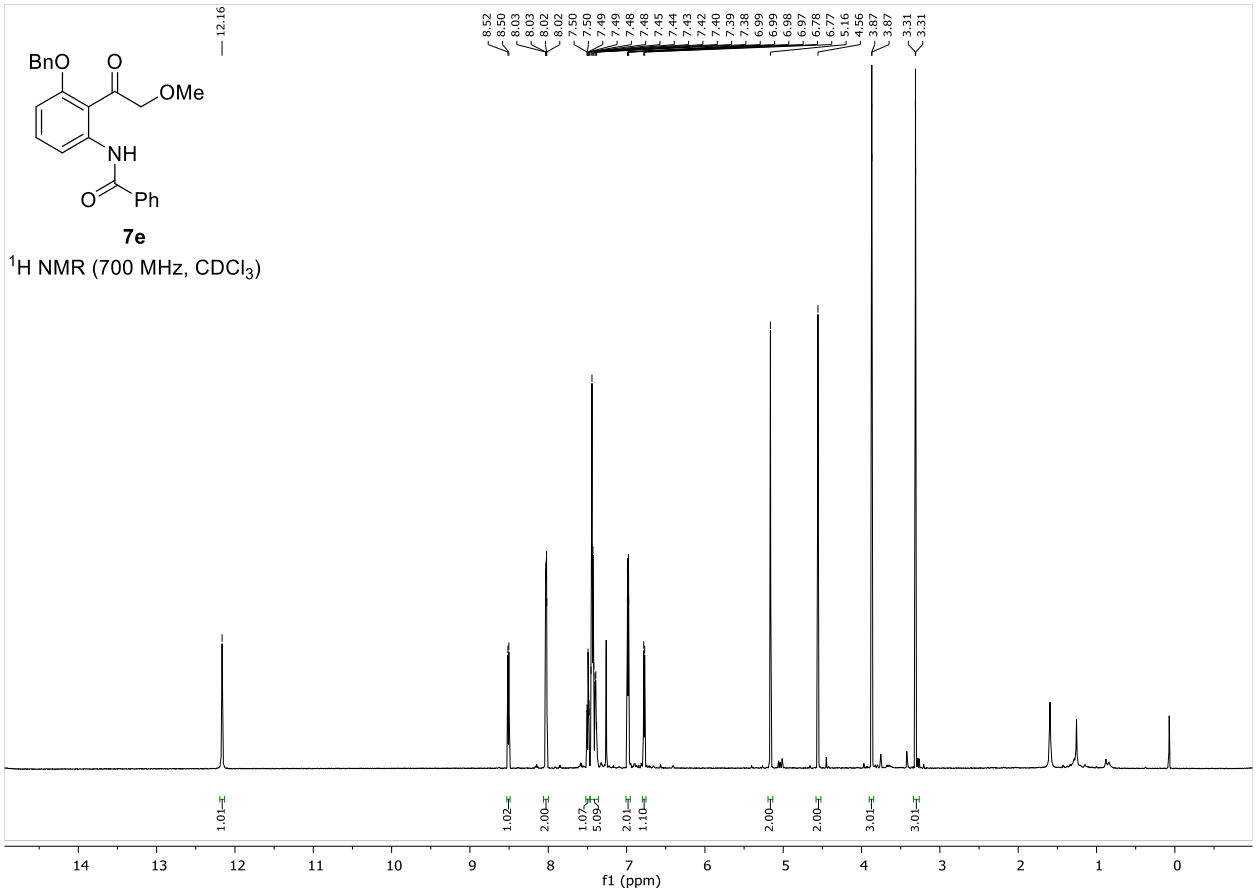
BnO
O
OMe
NH
O
Ph
7e
1H NMR (700 MHz, CDCl3)
f1 (ppm)

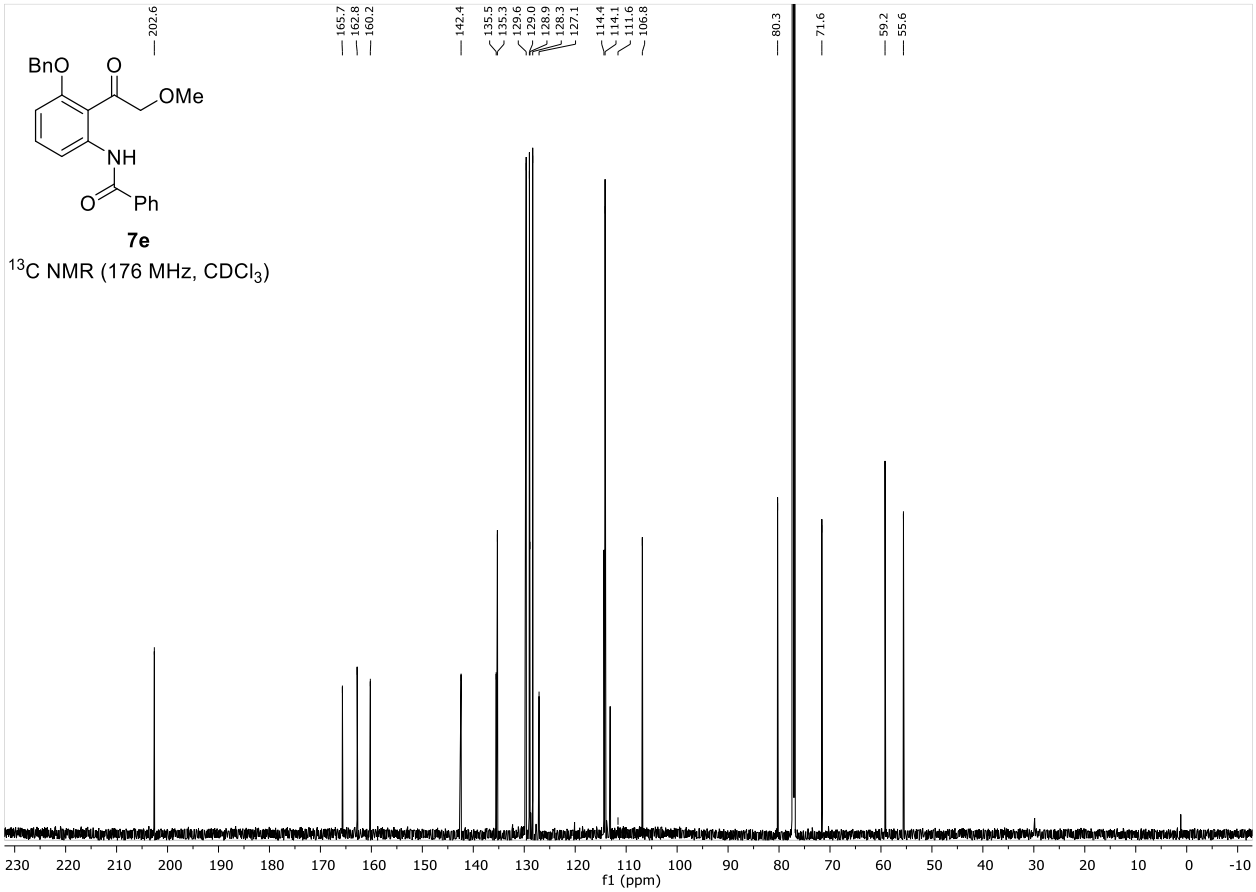
BnO
O
OMe
NH
O
Ph
7e
13C NMR (176 MHz, CDCl3)
f1 (ppm)

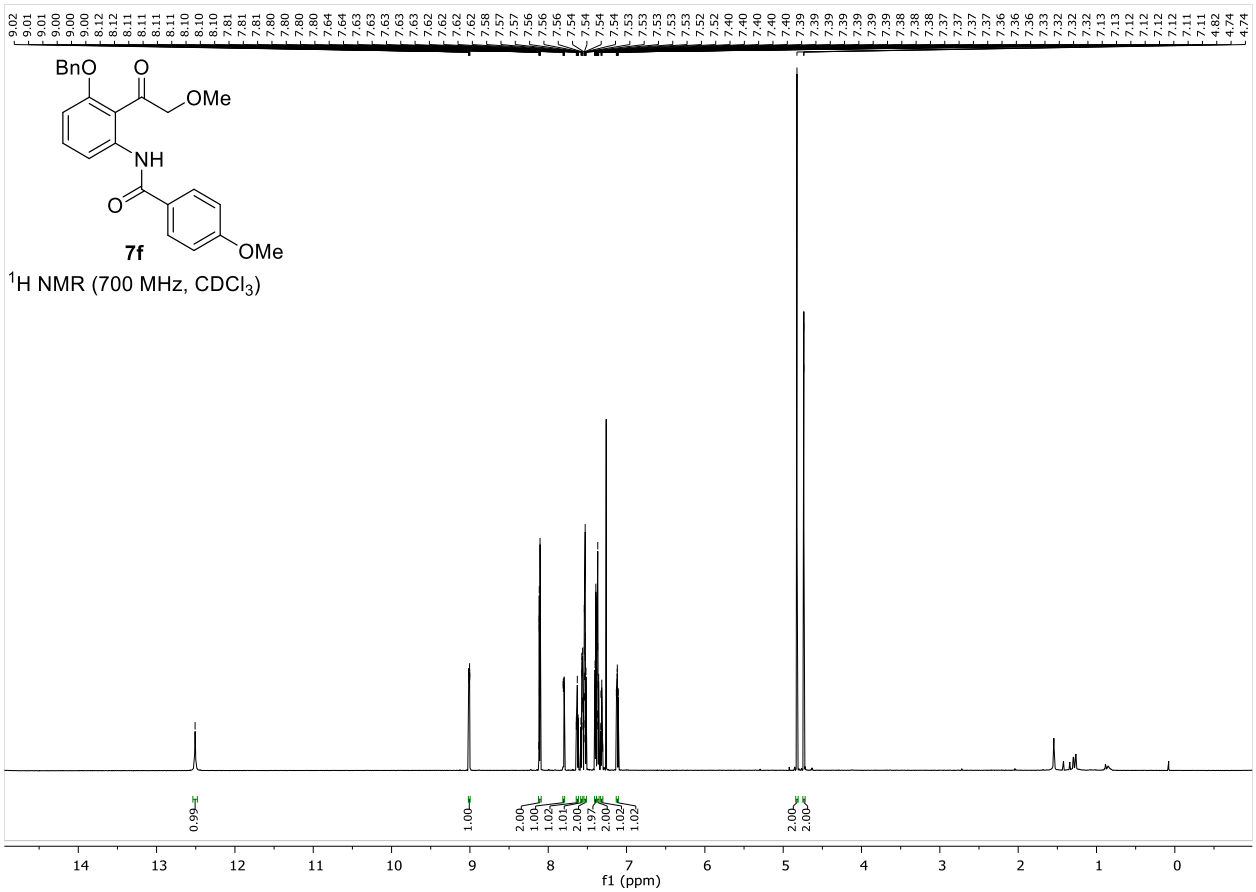
BnO
O
OMe
NH
O
OMe
7f
^{1}H NMR (700 MHz, $CDCl_3$)
f1 (ppm)

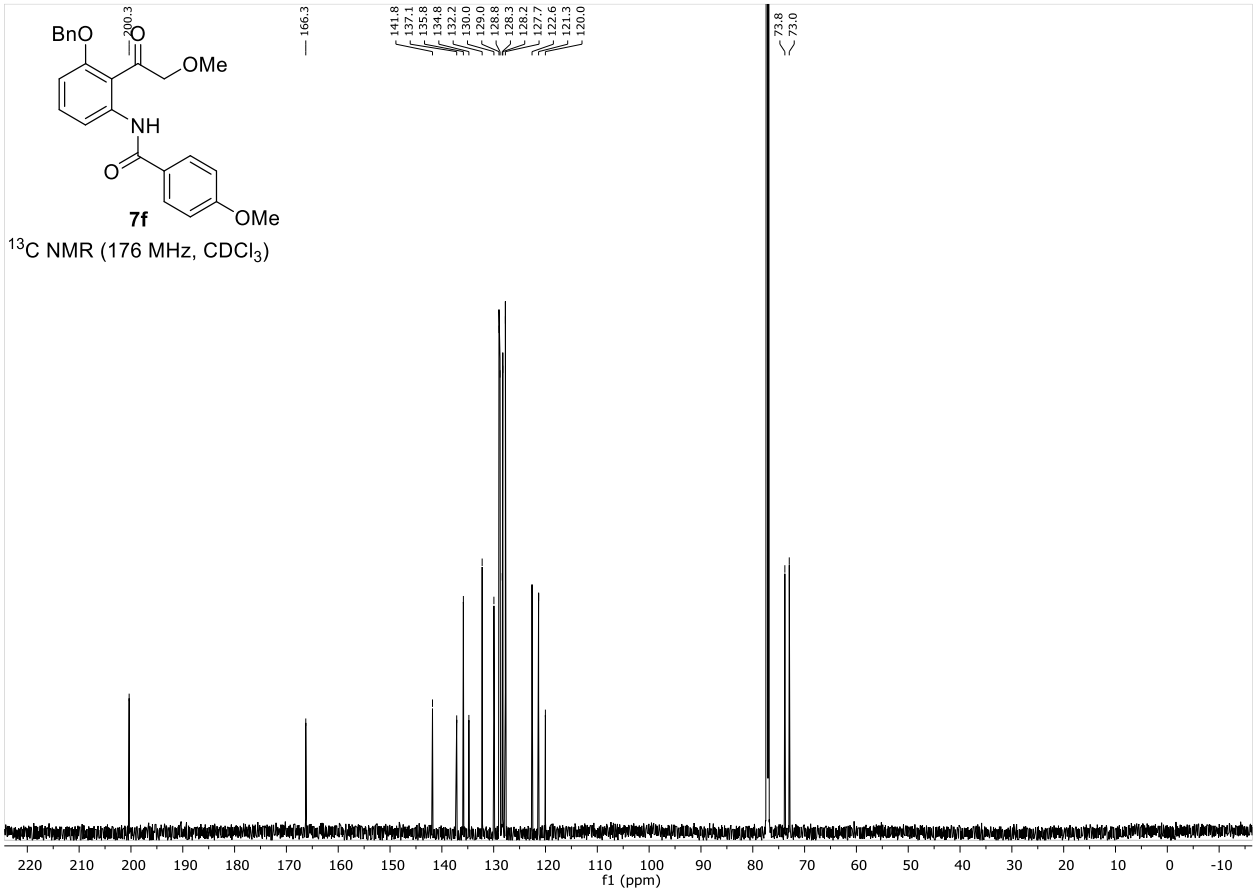
BnO
O
OMe
NH
O
OMe
7f
^{13}C NMR (176 MHz, $CDCl_3$)
f1 (ppm)

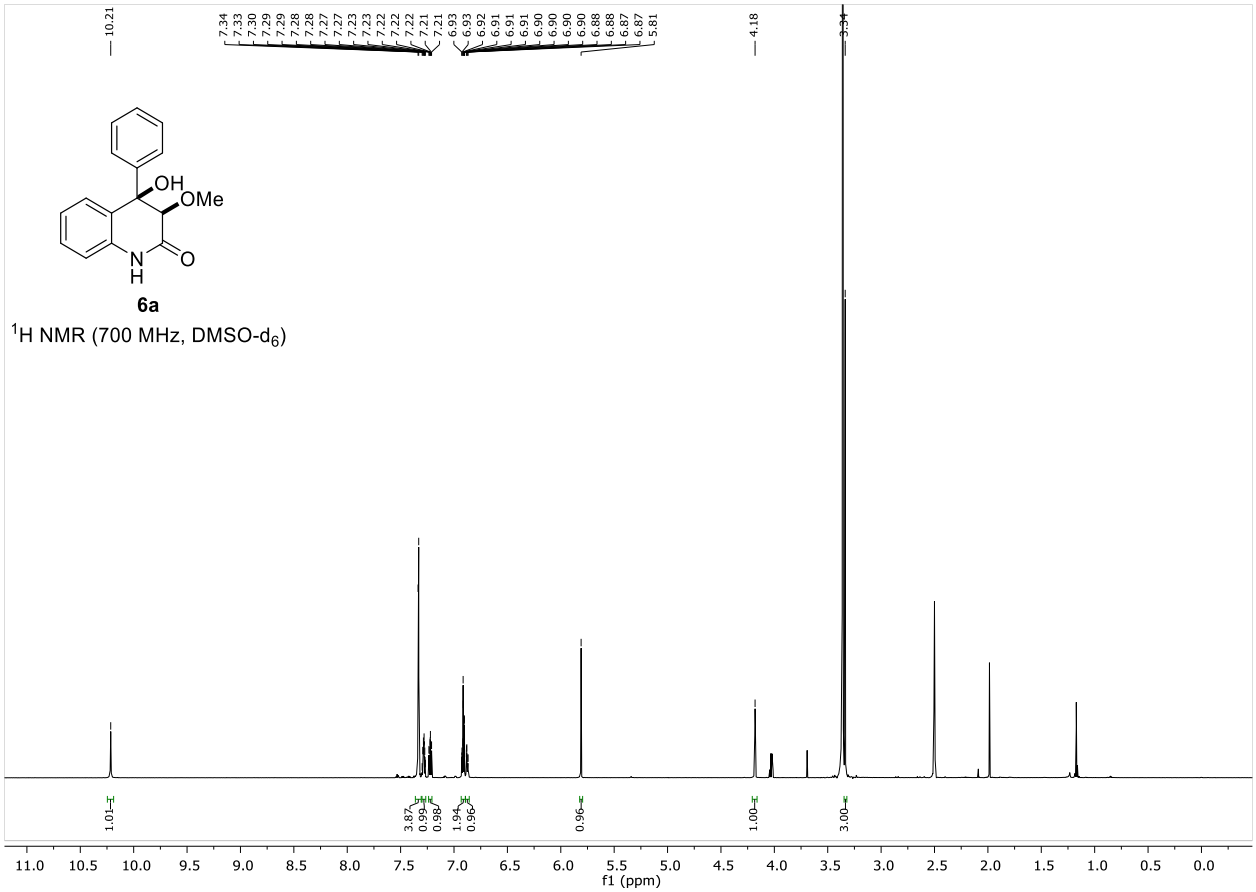

6a

^{1}H NMR (700 MHz, DMSO-d_6)

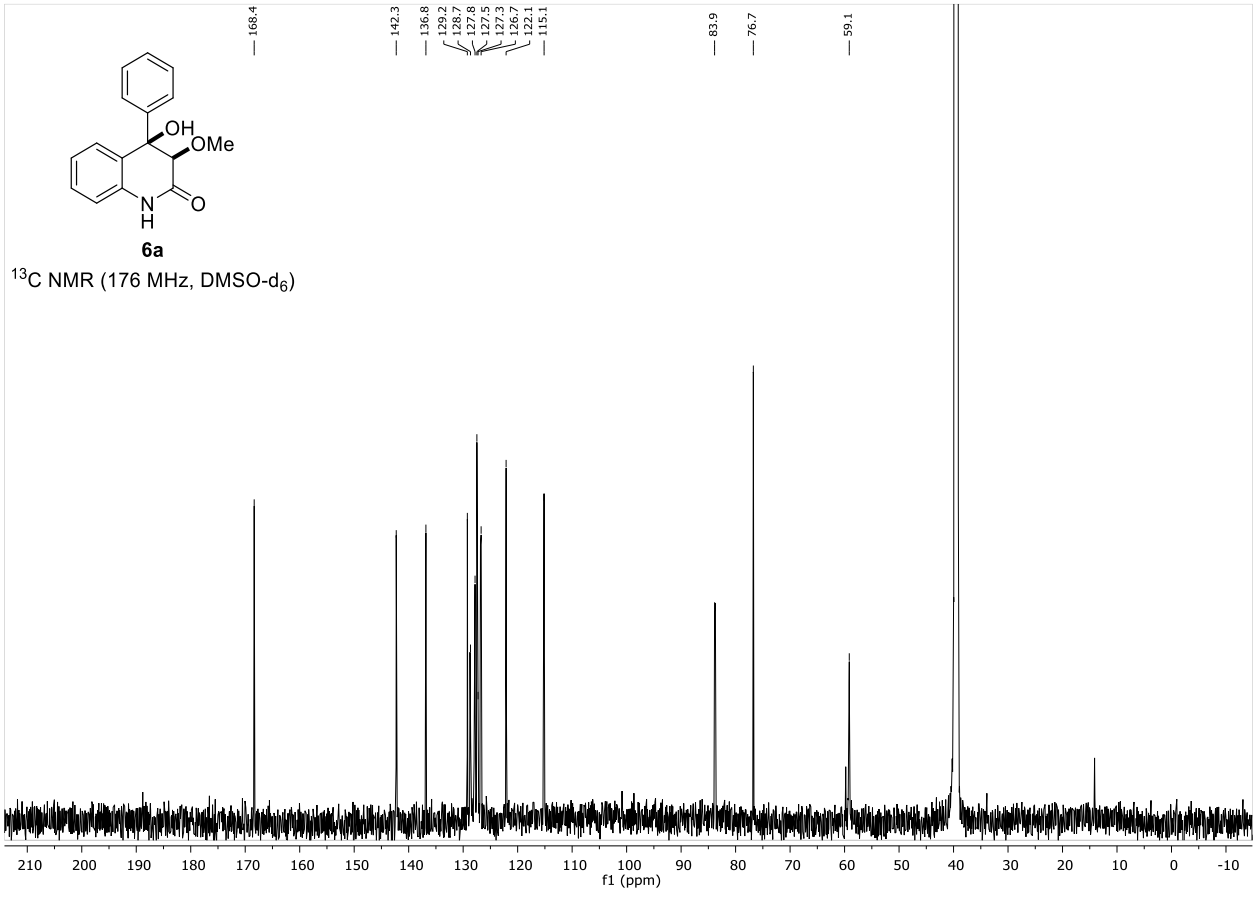

6a

^{13}C NMR (176 MHz, DMSO-d_6)

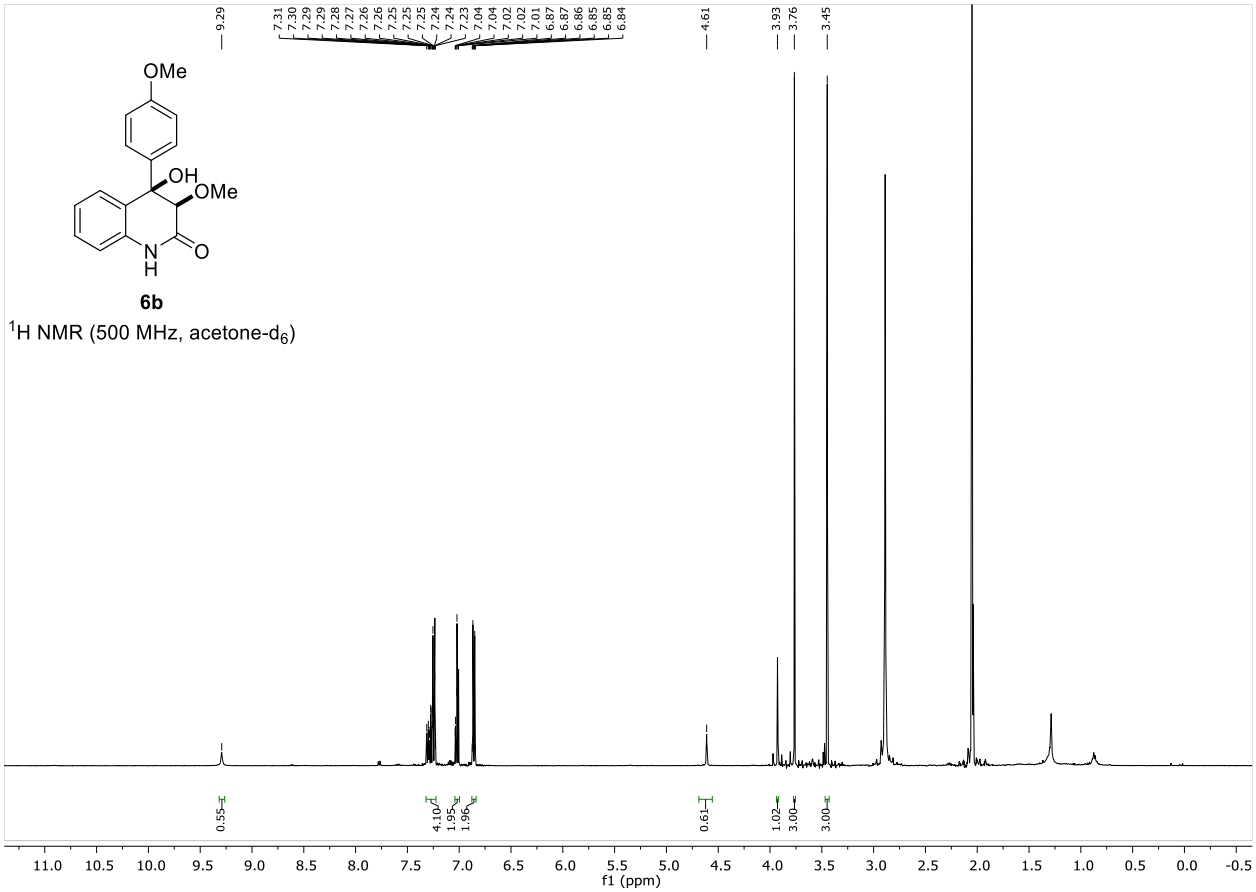

6b

^{1}H NMR (500 MHz, acetone-d_6)

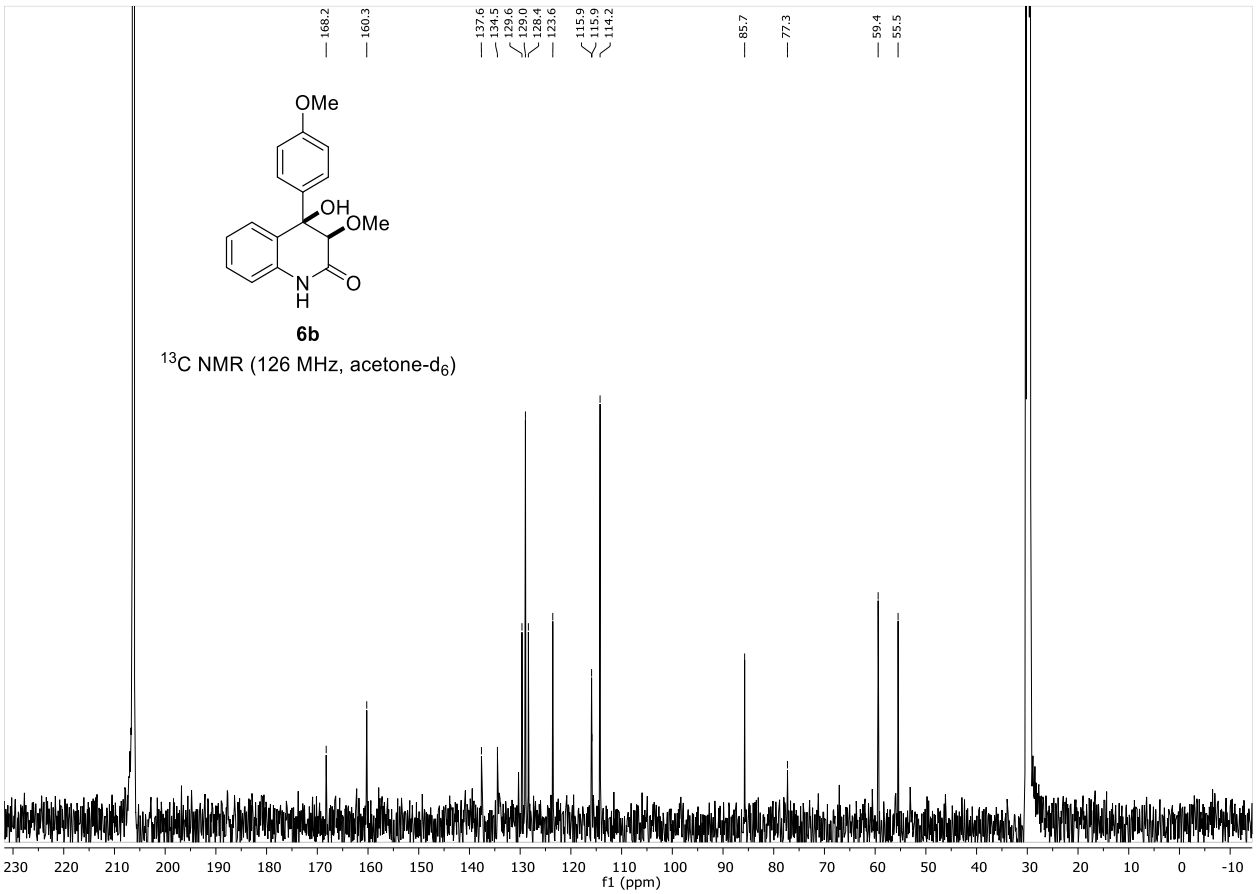

6b

^{13}C NMR (126 MHz, acetone-d_6)

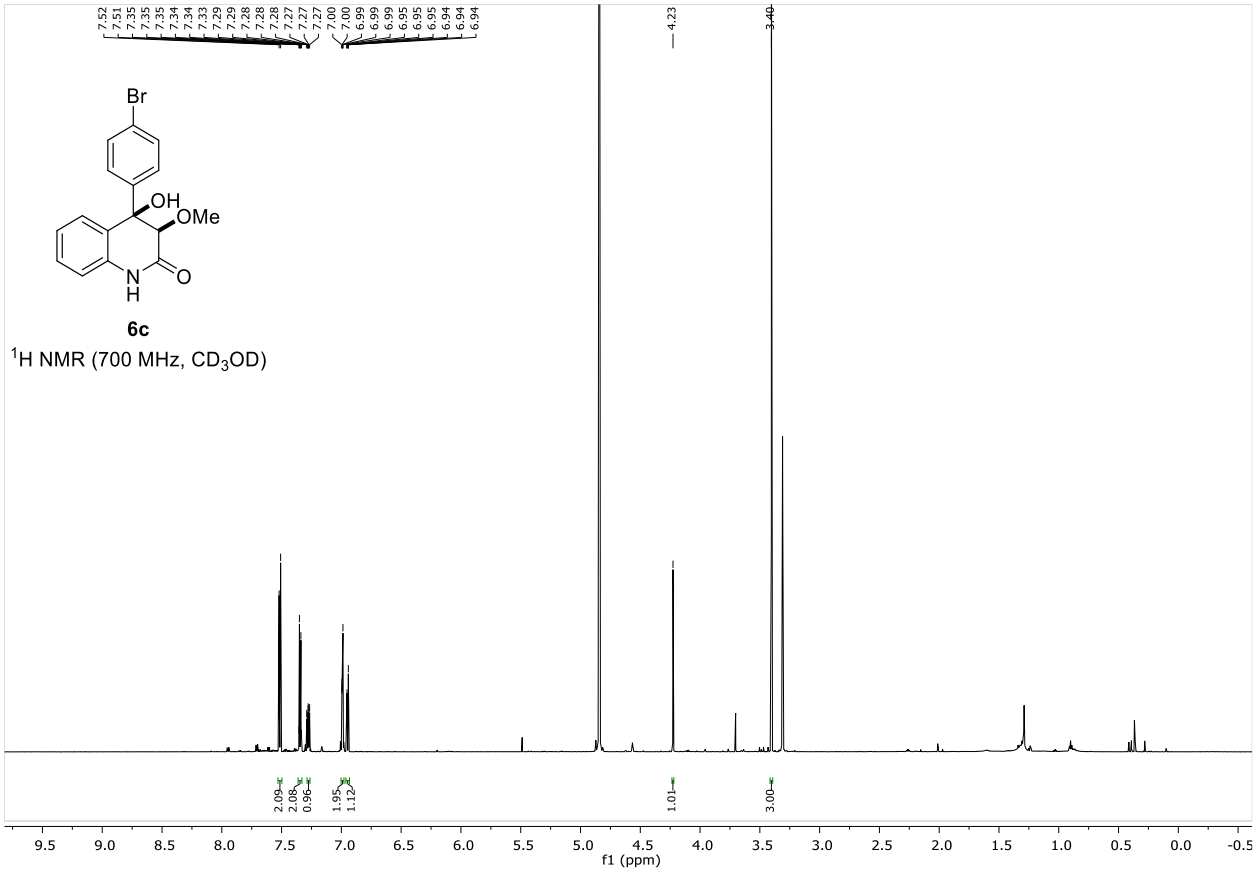
7.52
7.51
7.35
7.35
7.35
7.34
7.34
7.33
7.29
7.29
7.28
7.28
7.28
7.27
7.27
7.27
7.00
7.00
6.99
6.99
6.99
6.95
6.95
6.95
6.94
6.94
6.94
4.23
3.40
Br
OH
OMe
N
H
O
6c
1H NMR (700 MHz, CD3OD)
2.09
2.08
0.96
1.95
1.12
1.01
3.00
f1 (ppm)

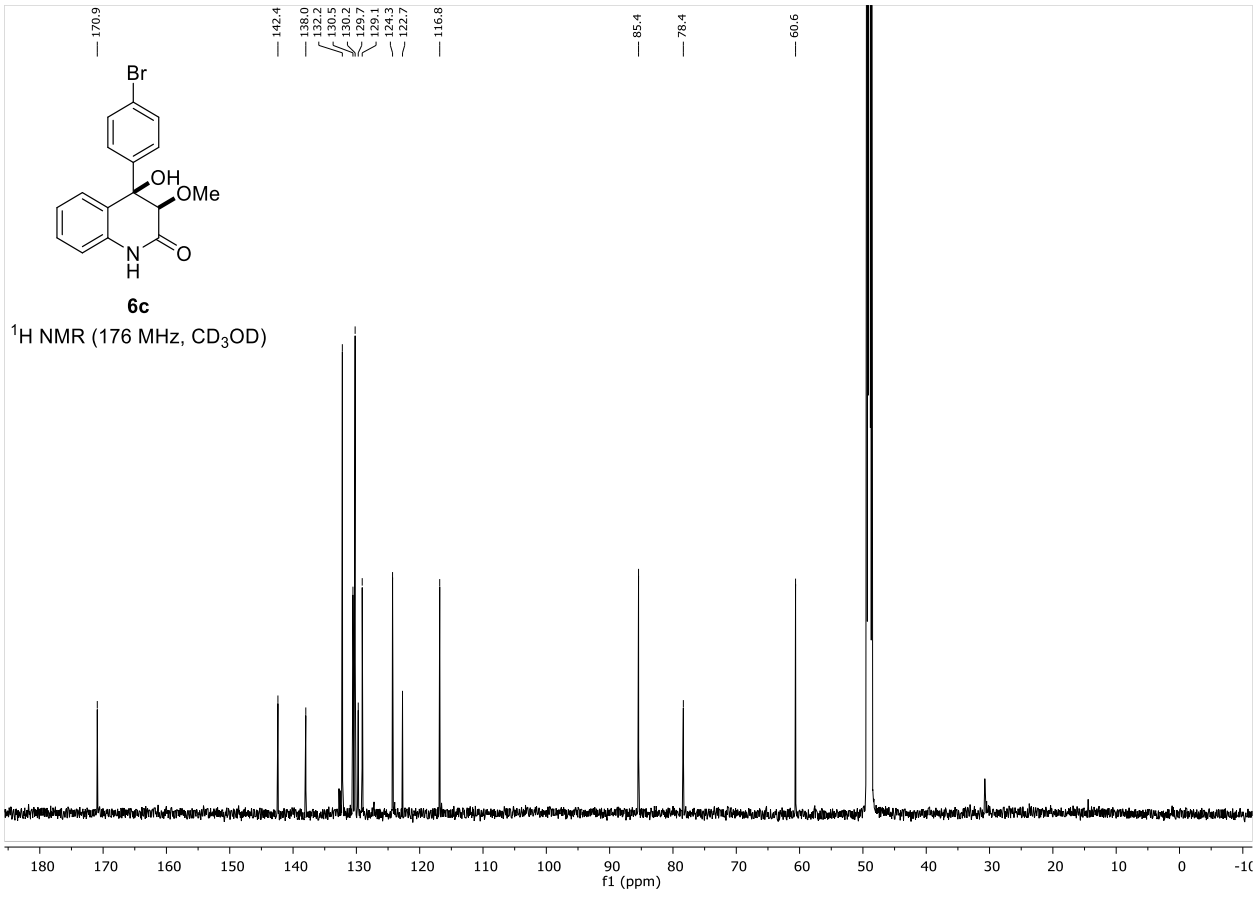
170.9
142.4
138.0
132.2
130.5
130.2
129.7
129.1
124.3
122.7
116.8
85.4
78.4
60.6
Br
OH
OMe
N
H
O
6c
1H NMR (176 MHz, CD3OD)
f1 (ppm)

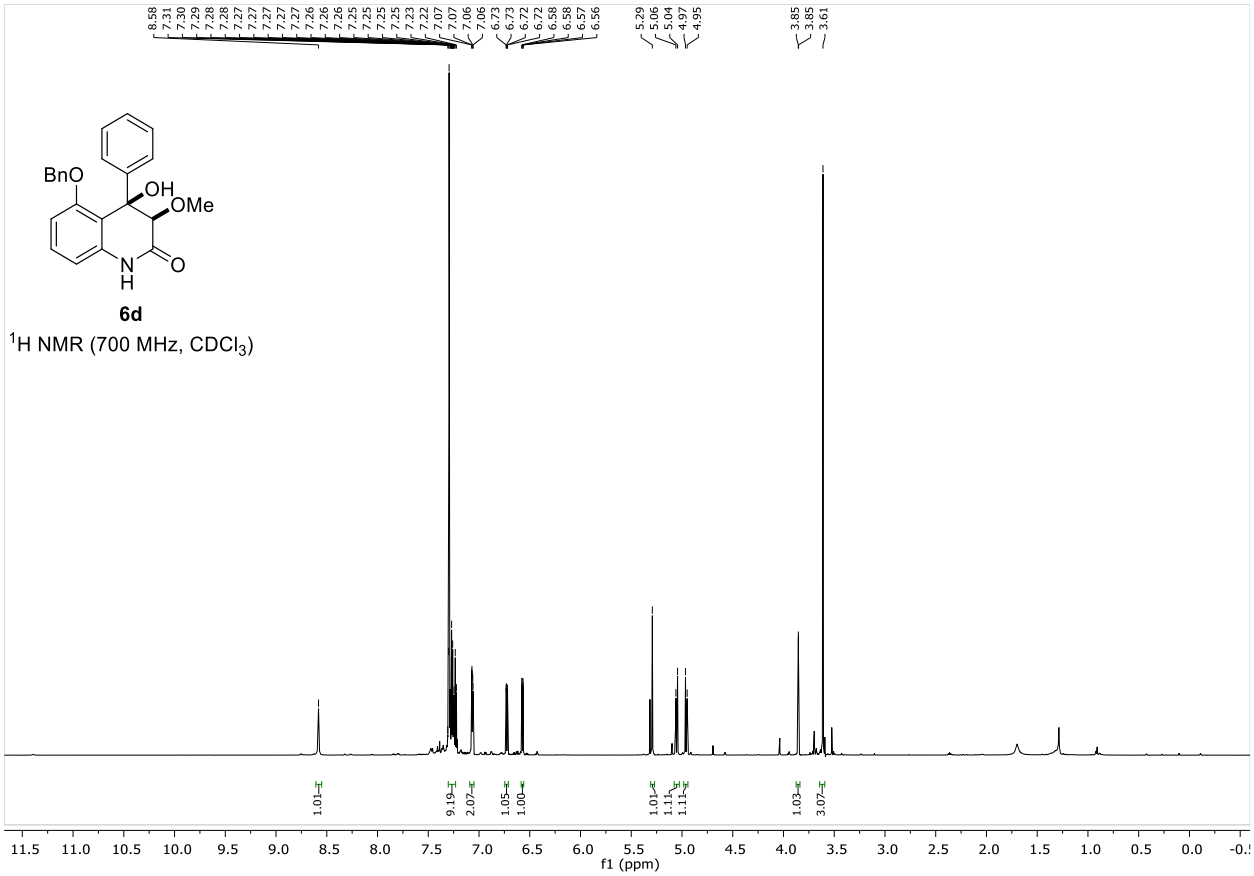
BnO
OH
OMe
N
H
O
6d
1H NMR (700 MHz, CDCl3)
f1 (ppm)

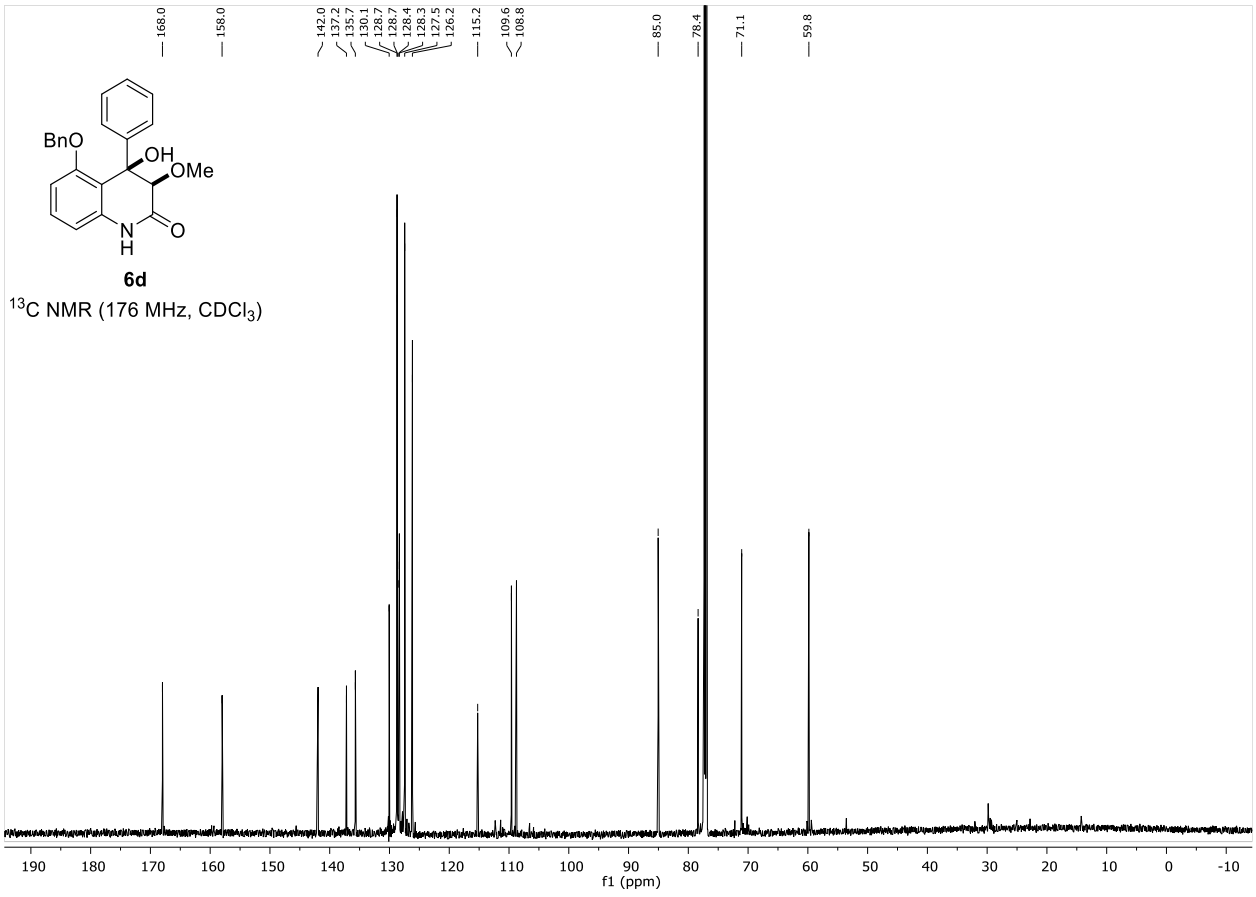
BnO
OH
OMe
N
H
O
6d
13C NMR (176 MHz, CDCl3)
f1 (ppm)

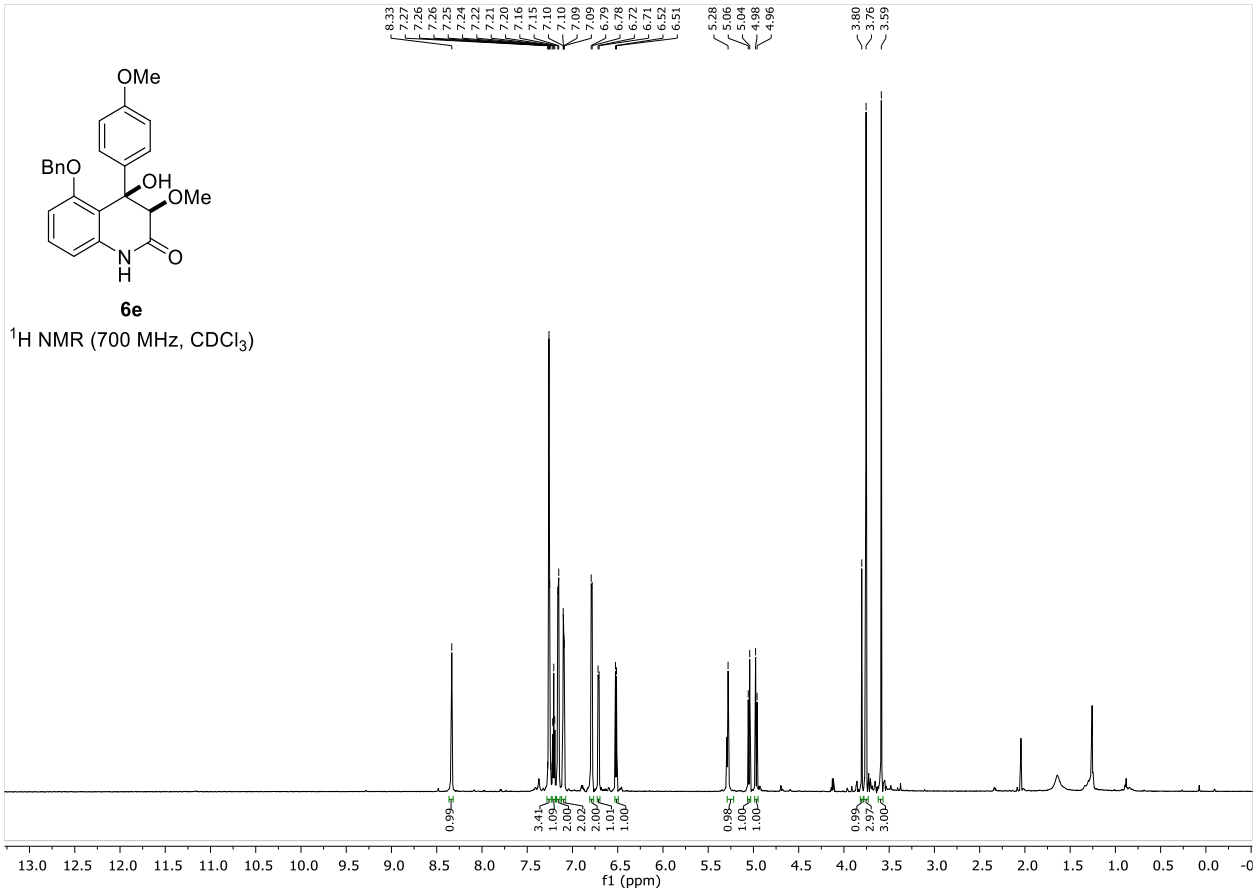
OMe
BnO
OH
OMe
N
H
O
6e
1H NMR (700 MHz, CDCl3)
f1 (ppm)

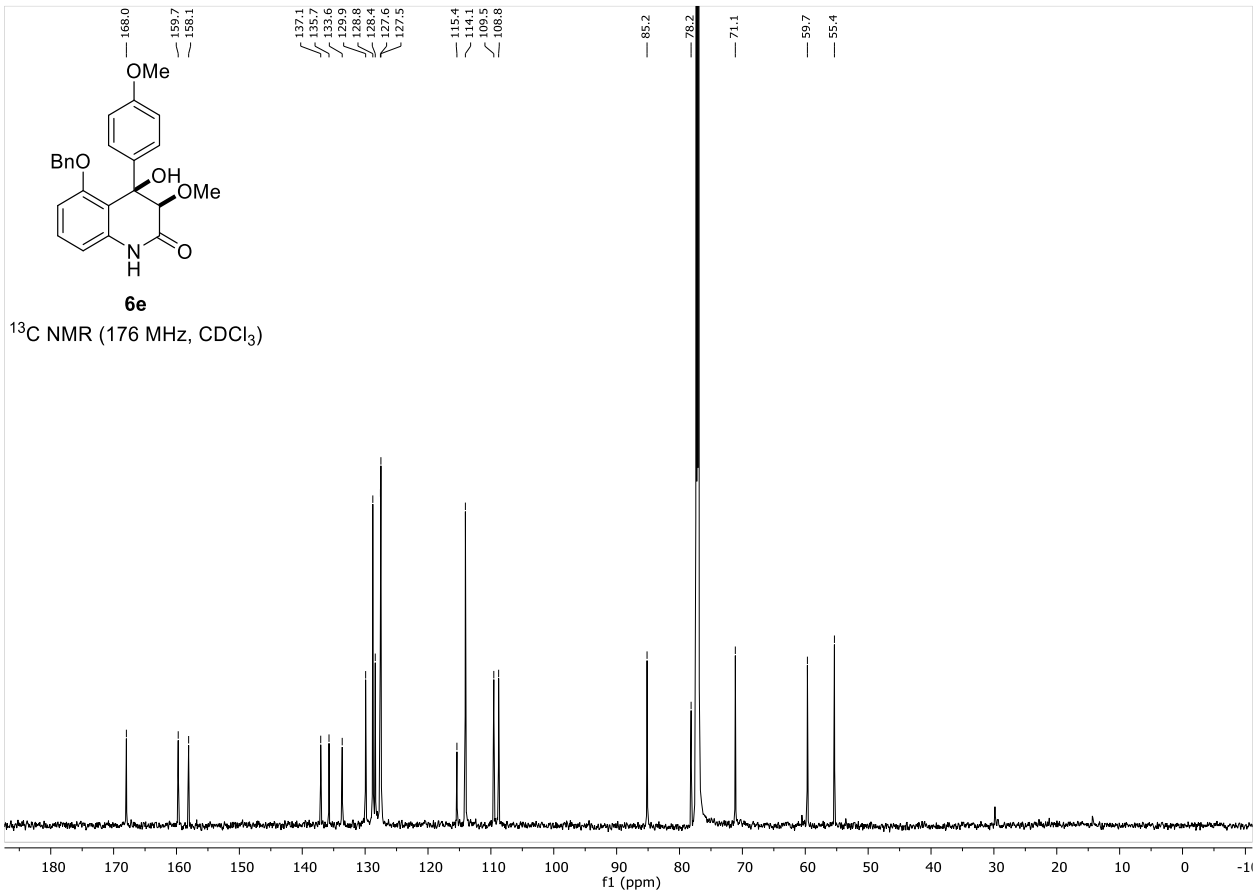
OMe
BnO
OH
OMe
N
H
O
6e
13C NMR (176 MHz, CDCl3)
f1 (ppm)

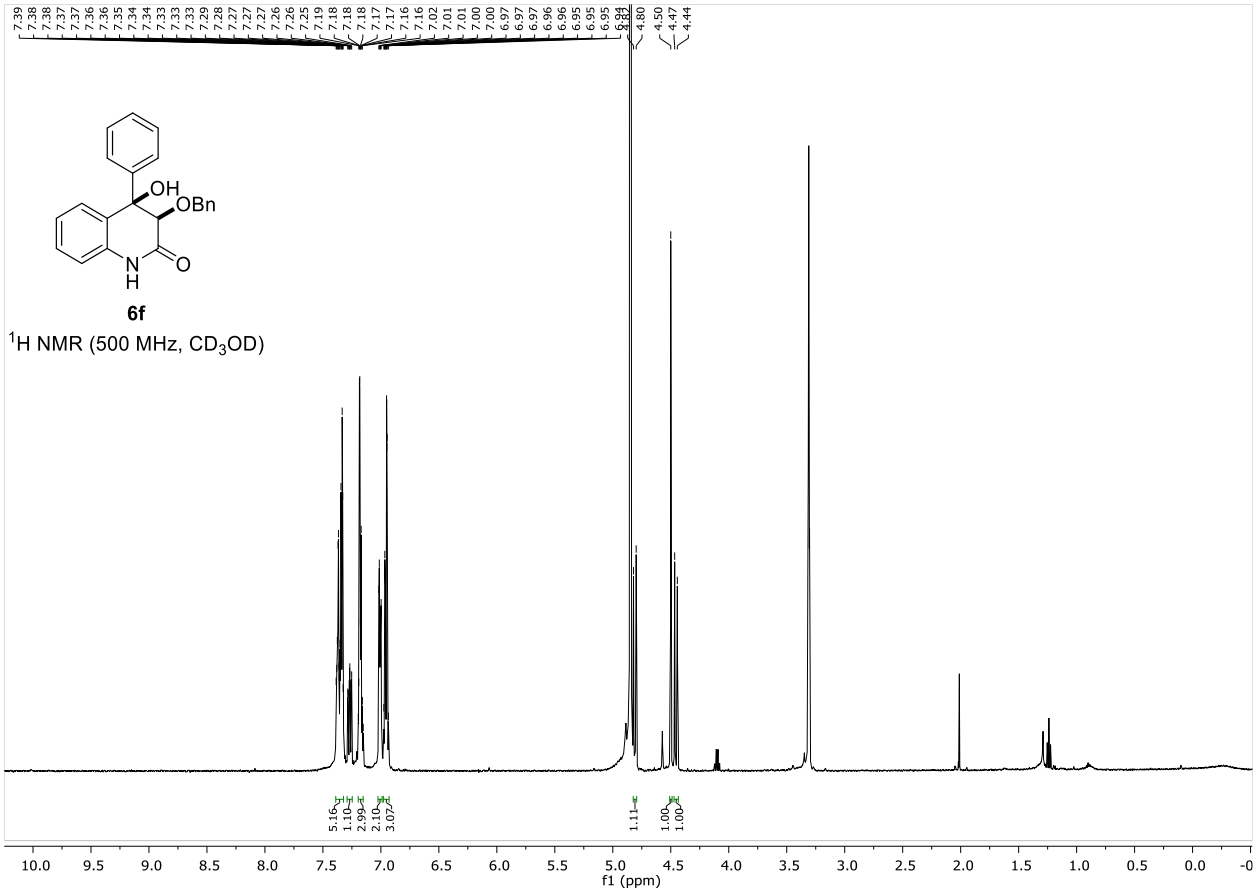

6f

^{1}H NMR (500 MHz, CD_3OD)

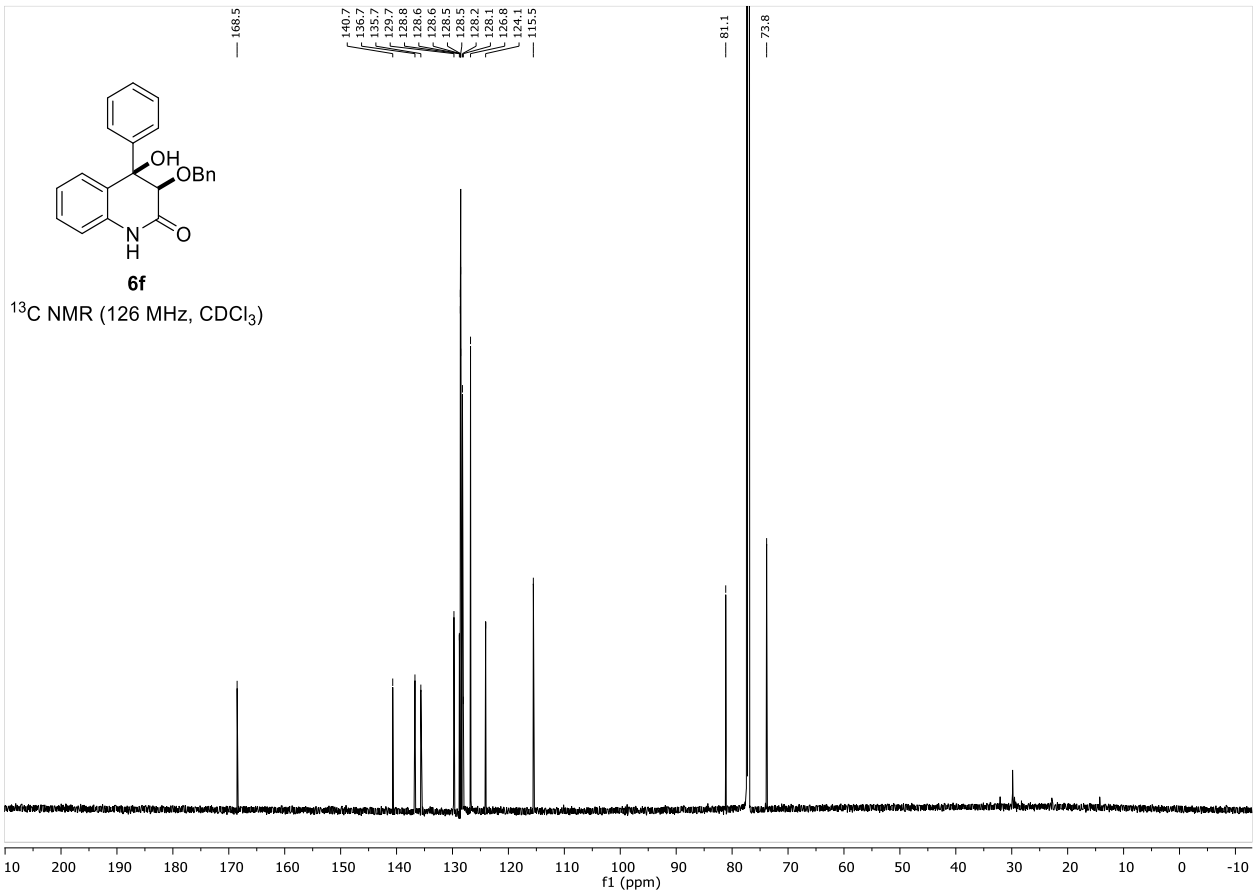

6f

^{13}C NMR (126 MHz, $CDCl_3$)

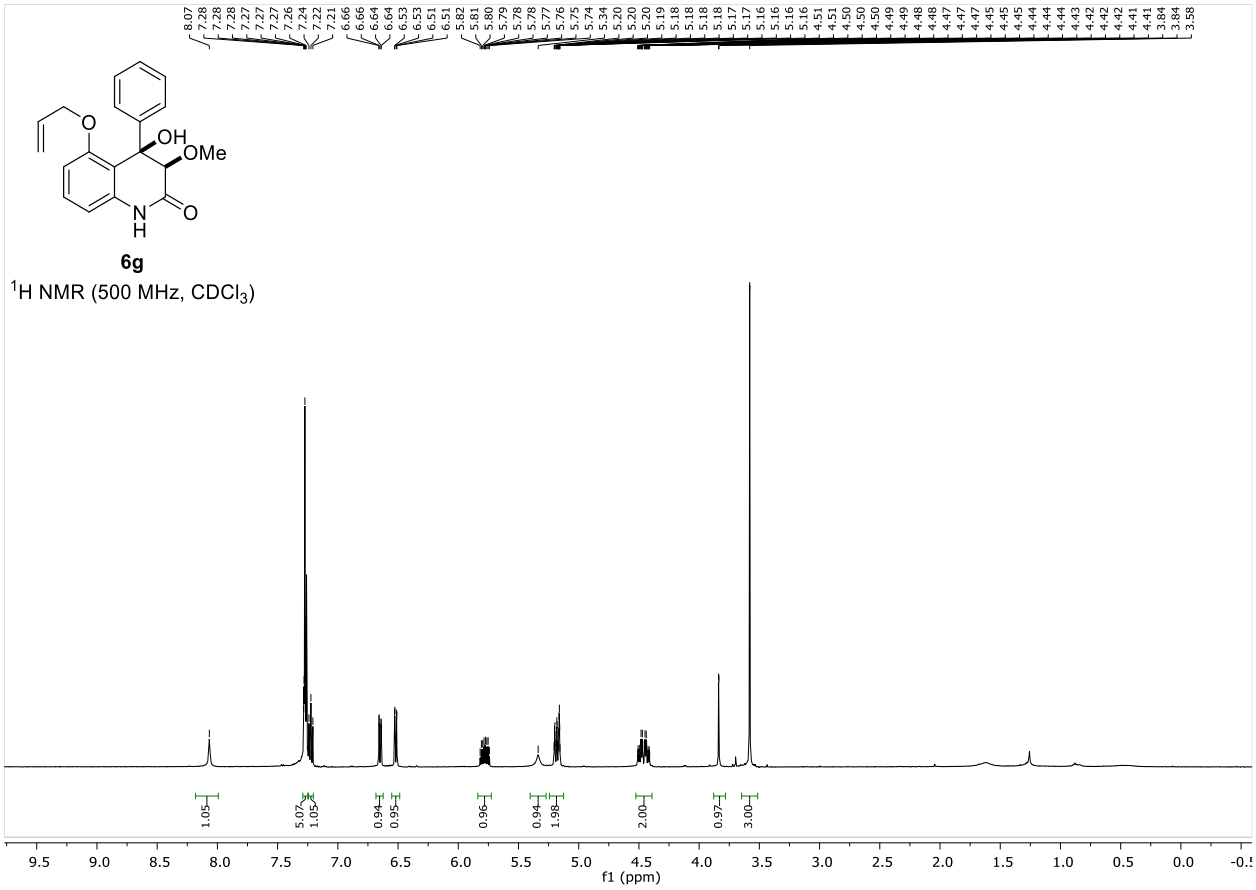
6g
1H NMR (500 MHz, CDCl3)
f1 (ppm)

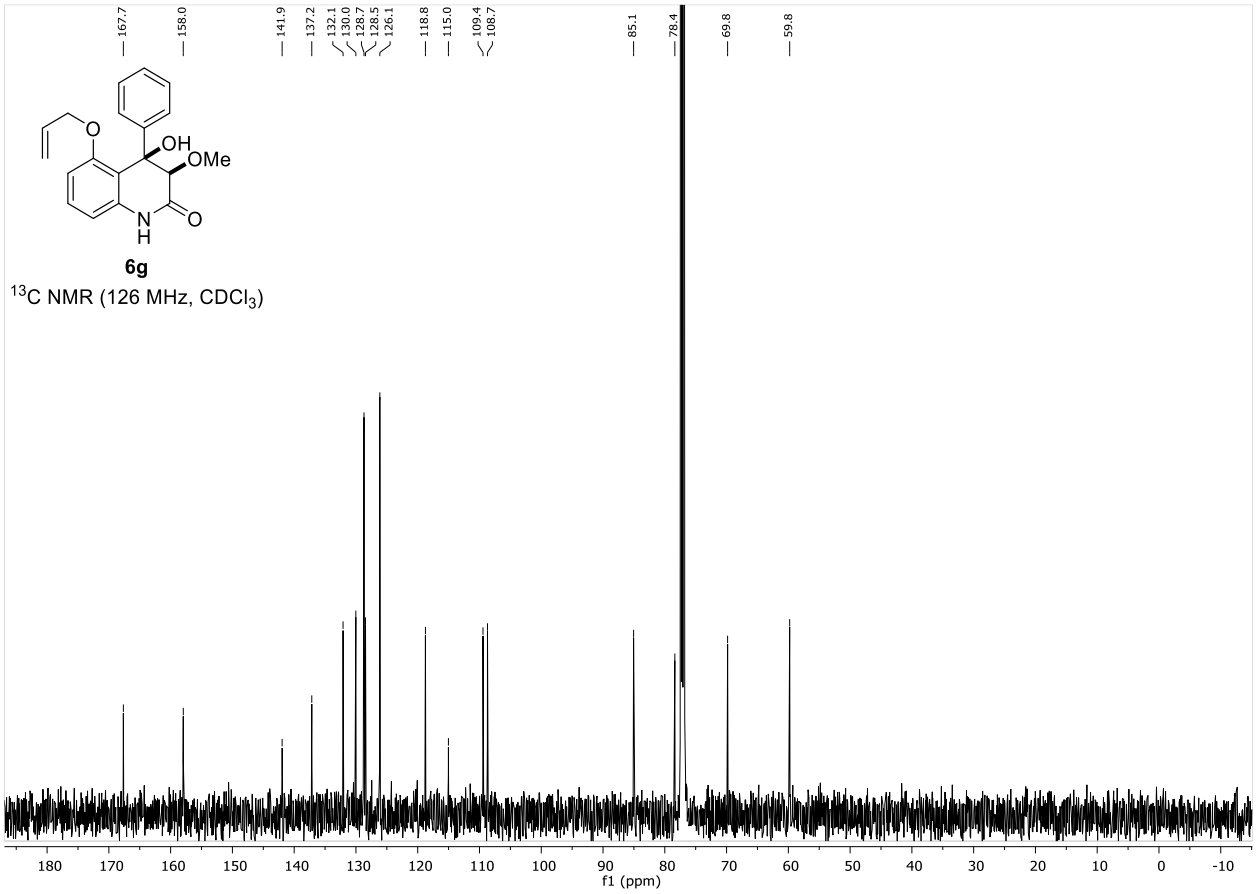
6g
13C NMR (126 MHz, CDCl3)
f1 (ppm)

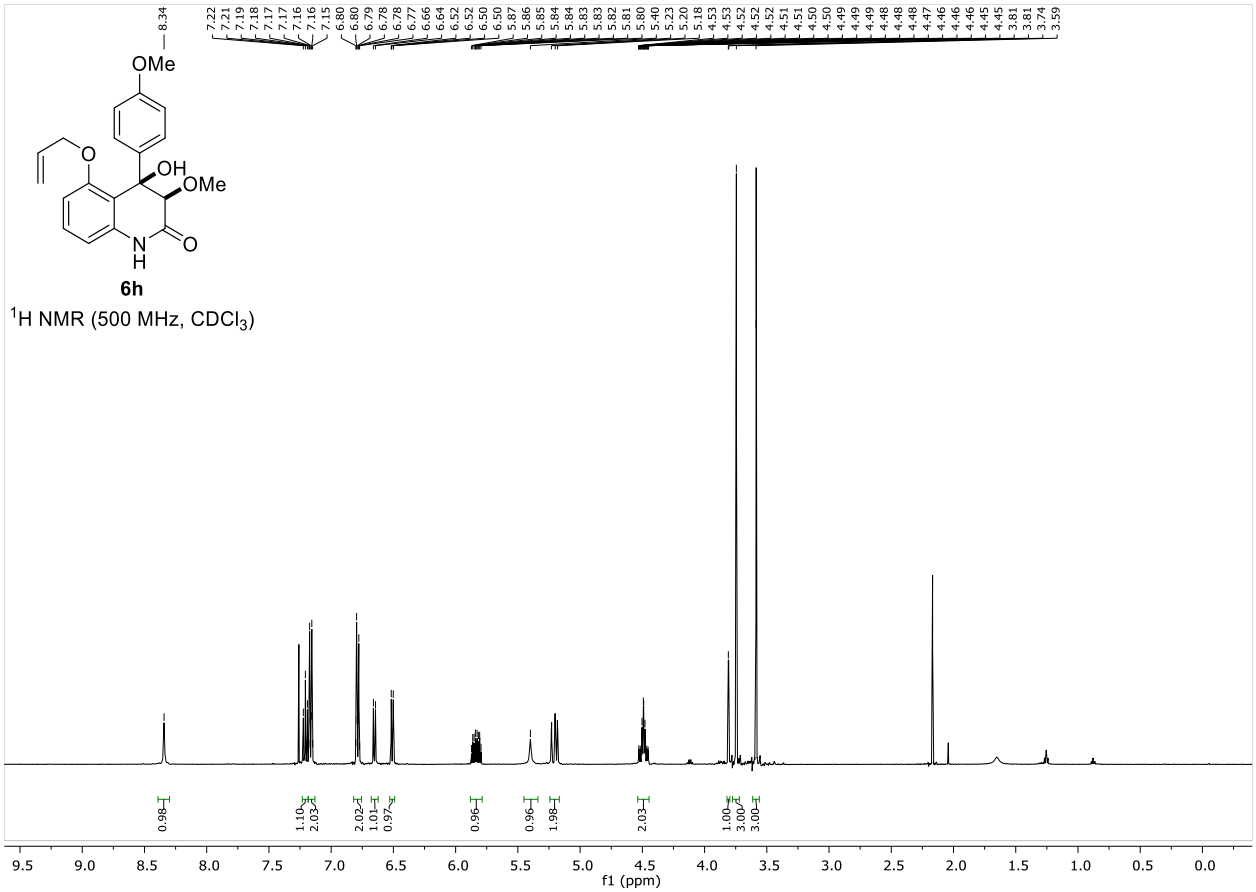
OMe
O
OH
OMe
N
H
O
6h
1H NMR (500 MHz, CDCl3)
f1 (ppm)

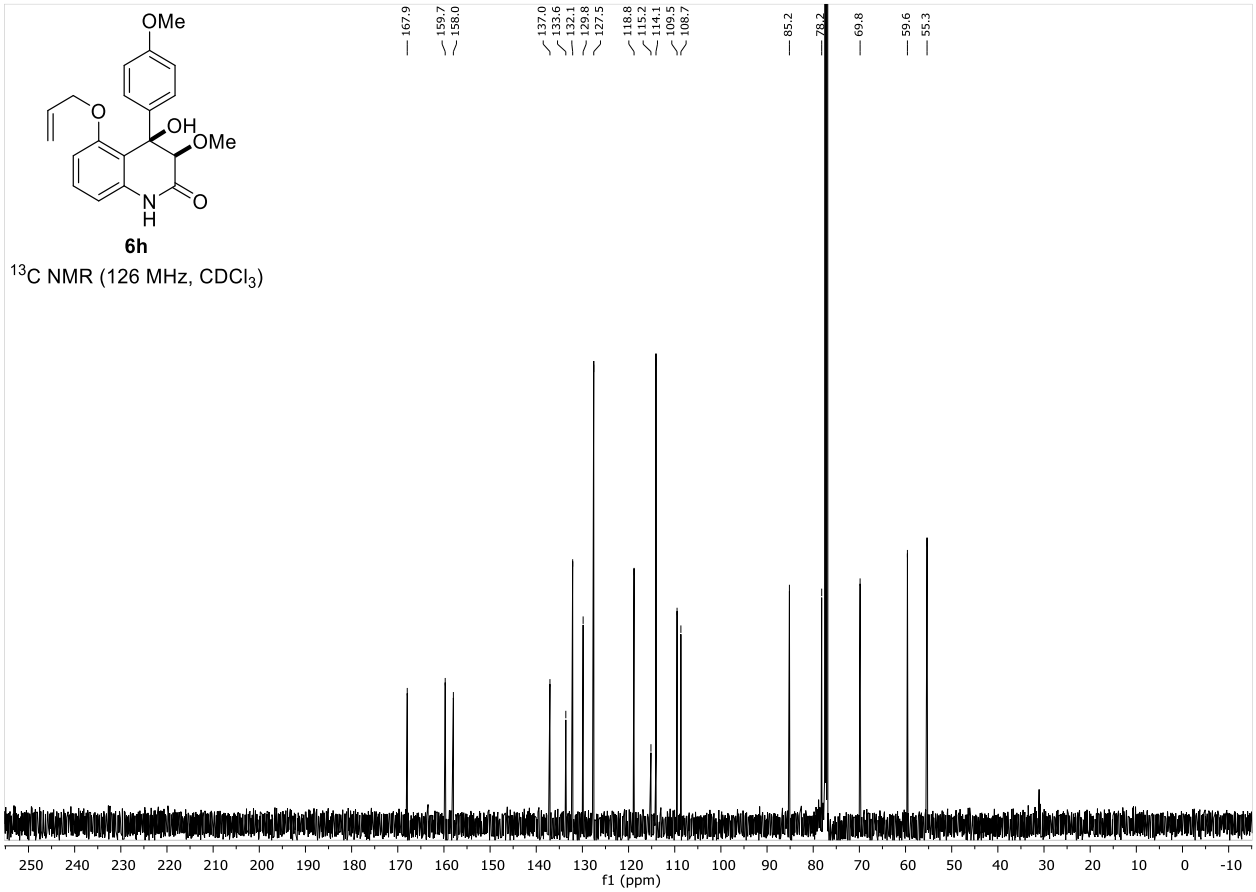
OMe
O
OH
OMe
N
H
O
6h
13C NMR (126 MHz, CDCl3)
f1 (ppm)

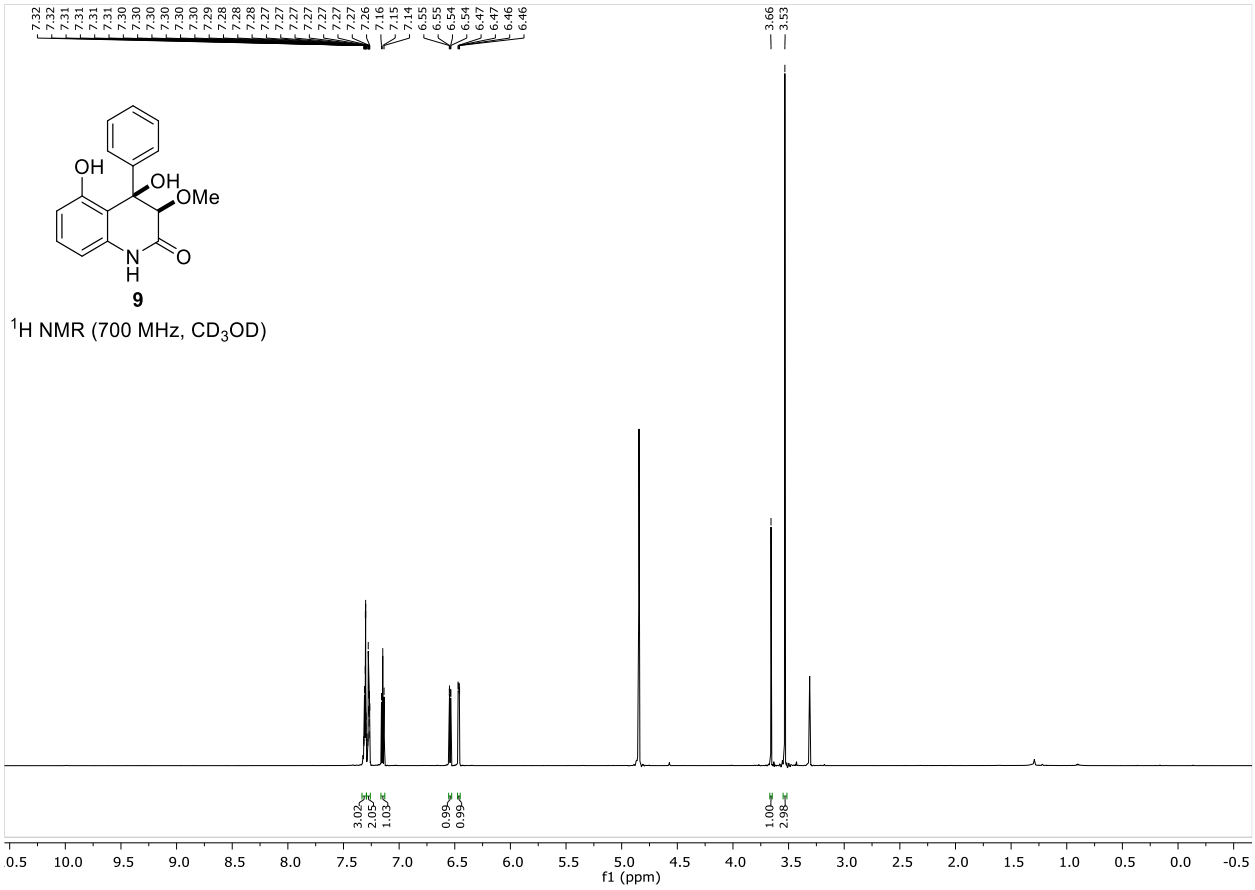
OH
OH
OMe
N
H
O
9
1H NMR (700 MHz, CD3OD)
f1 (ppm)

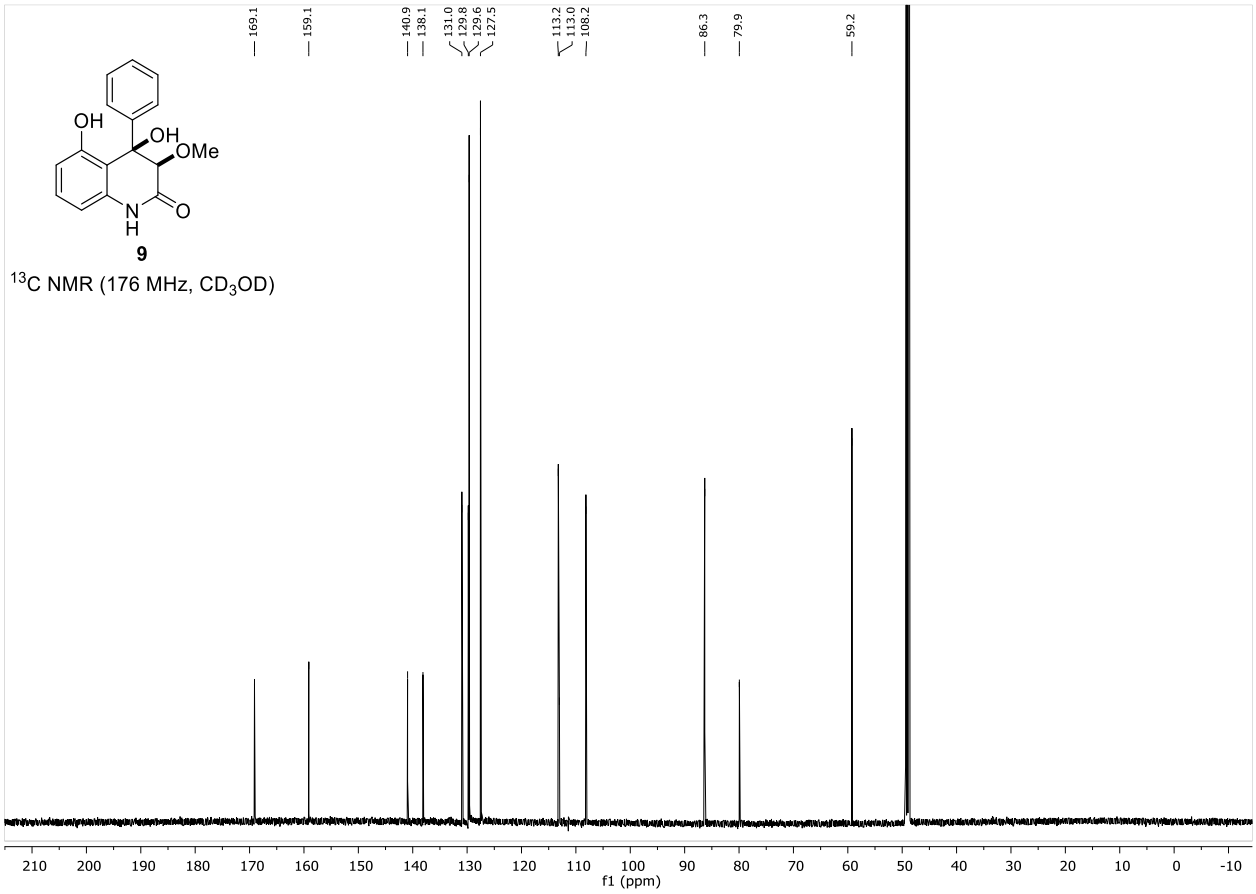
OH
OH
OMe
N
H
O
9
13C NMR (176 MHz, CD3OD)
f1 (ppm)

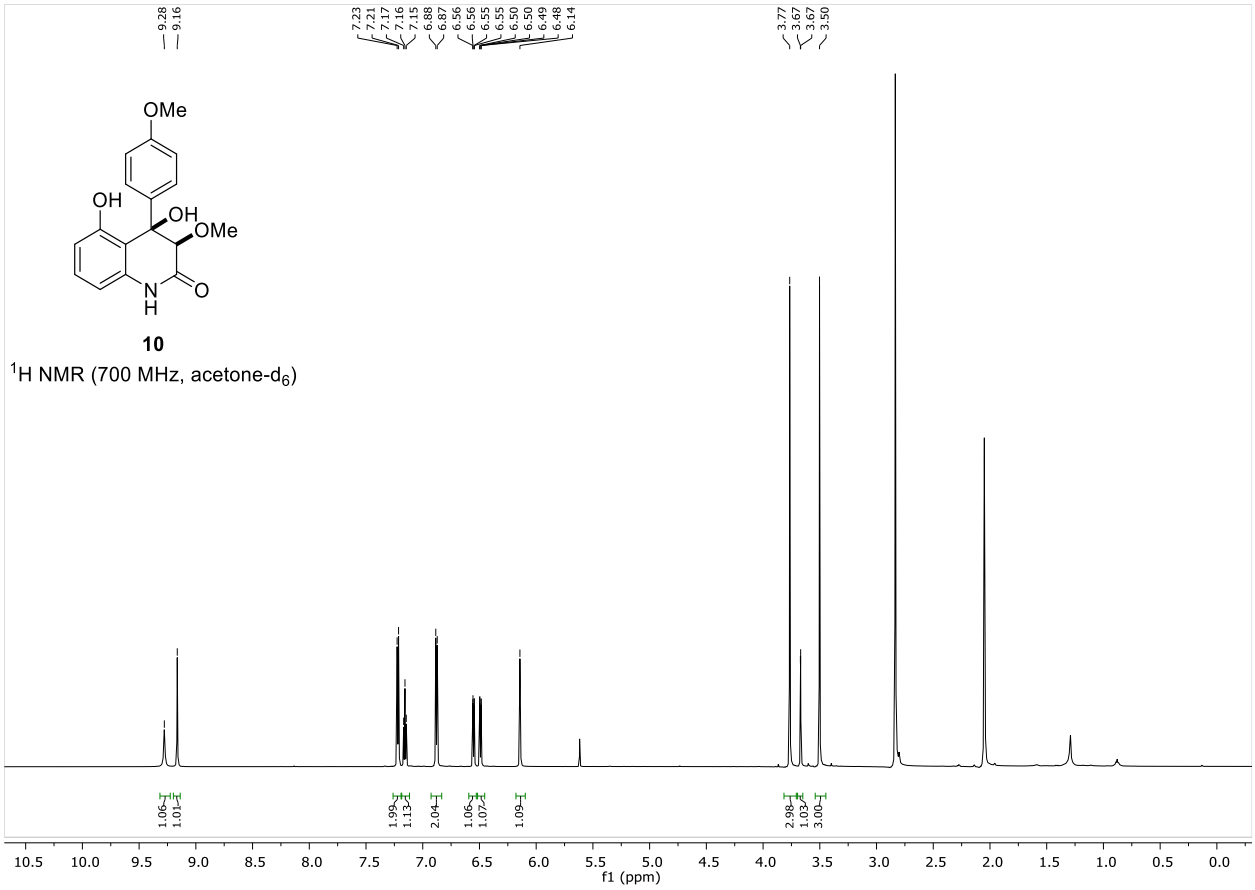

10

^{1}H NMR (700 MHz, acetone-d_6)

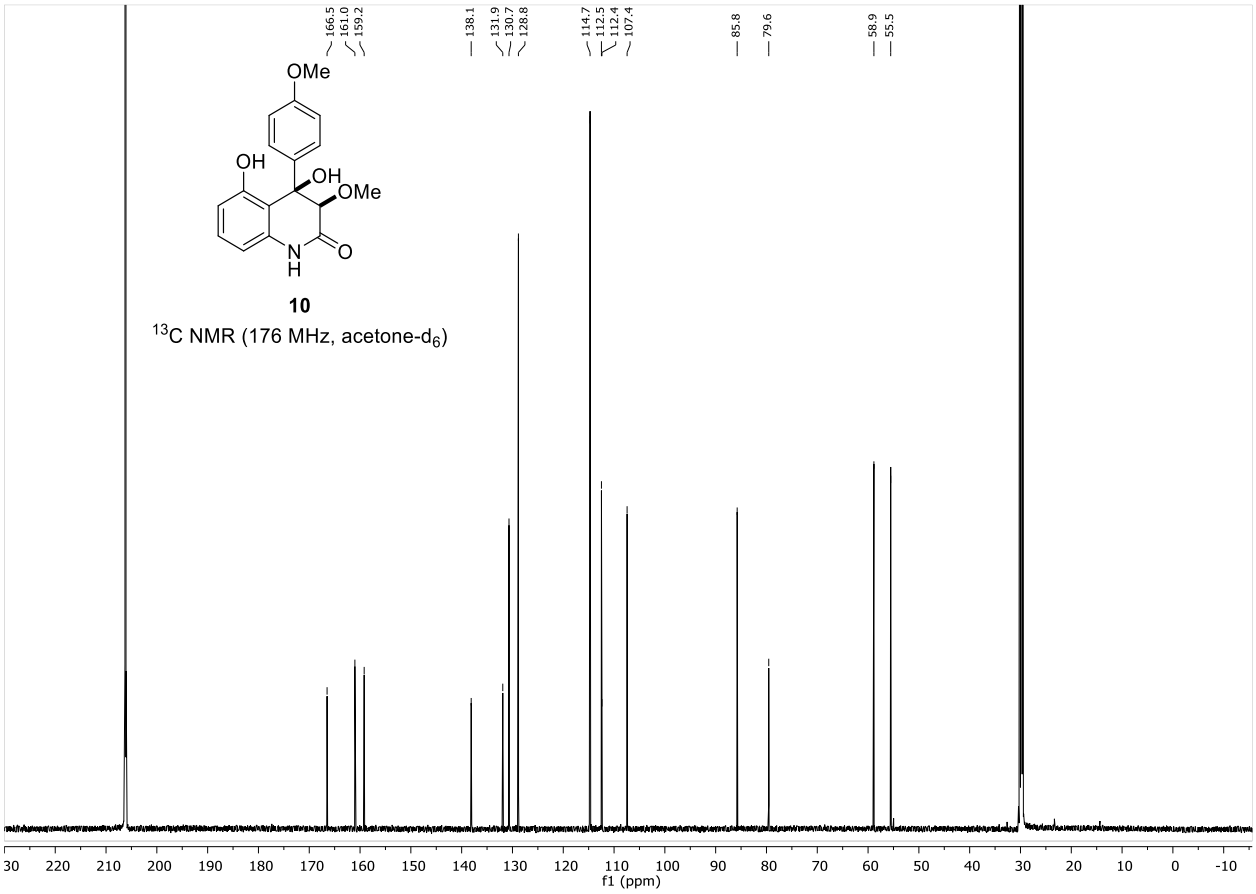

10

^{13}C NMR (176 MHz, acetone-d_6)

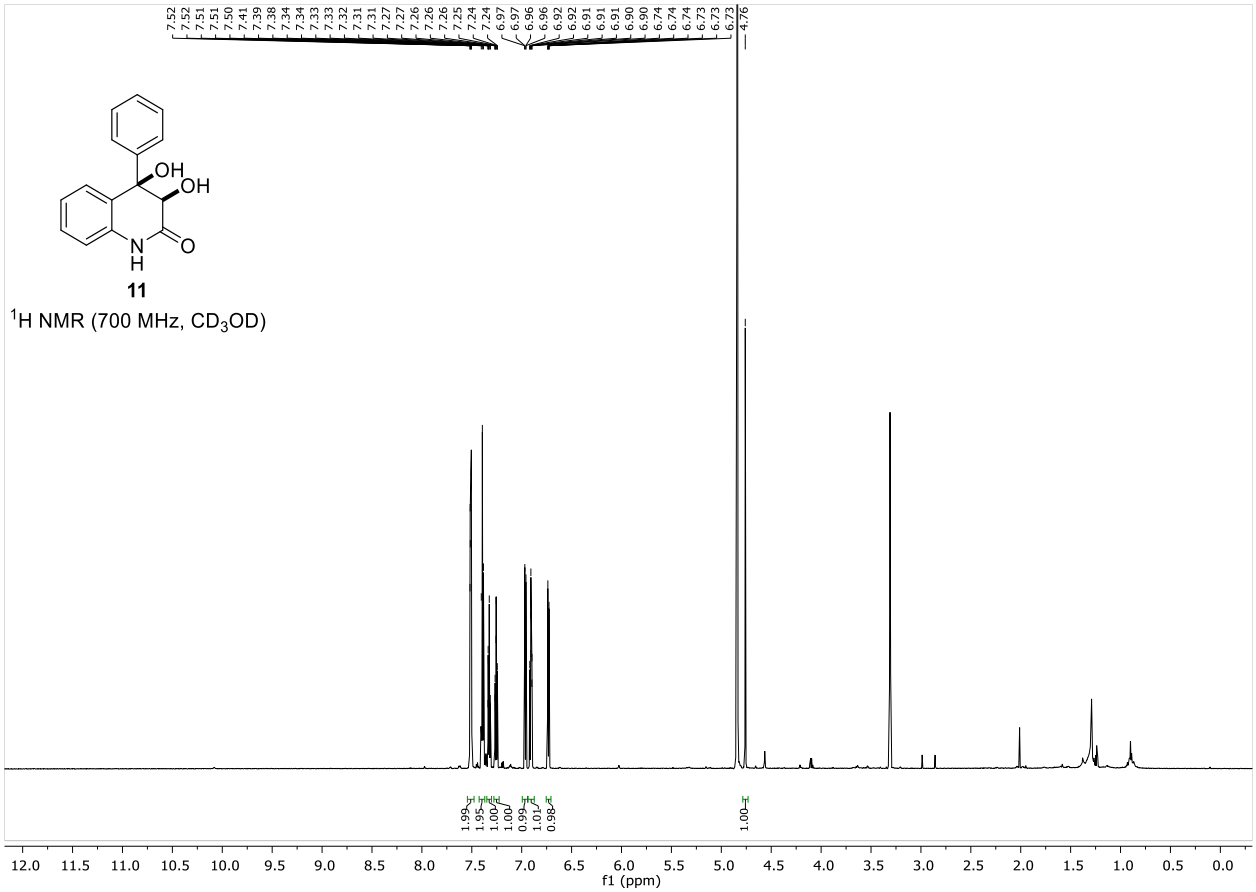
OH
OH
N
H
O
11
1H NMR (700 MHz, CD3OD)
f1 (ppm)

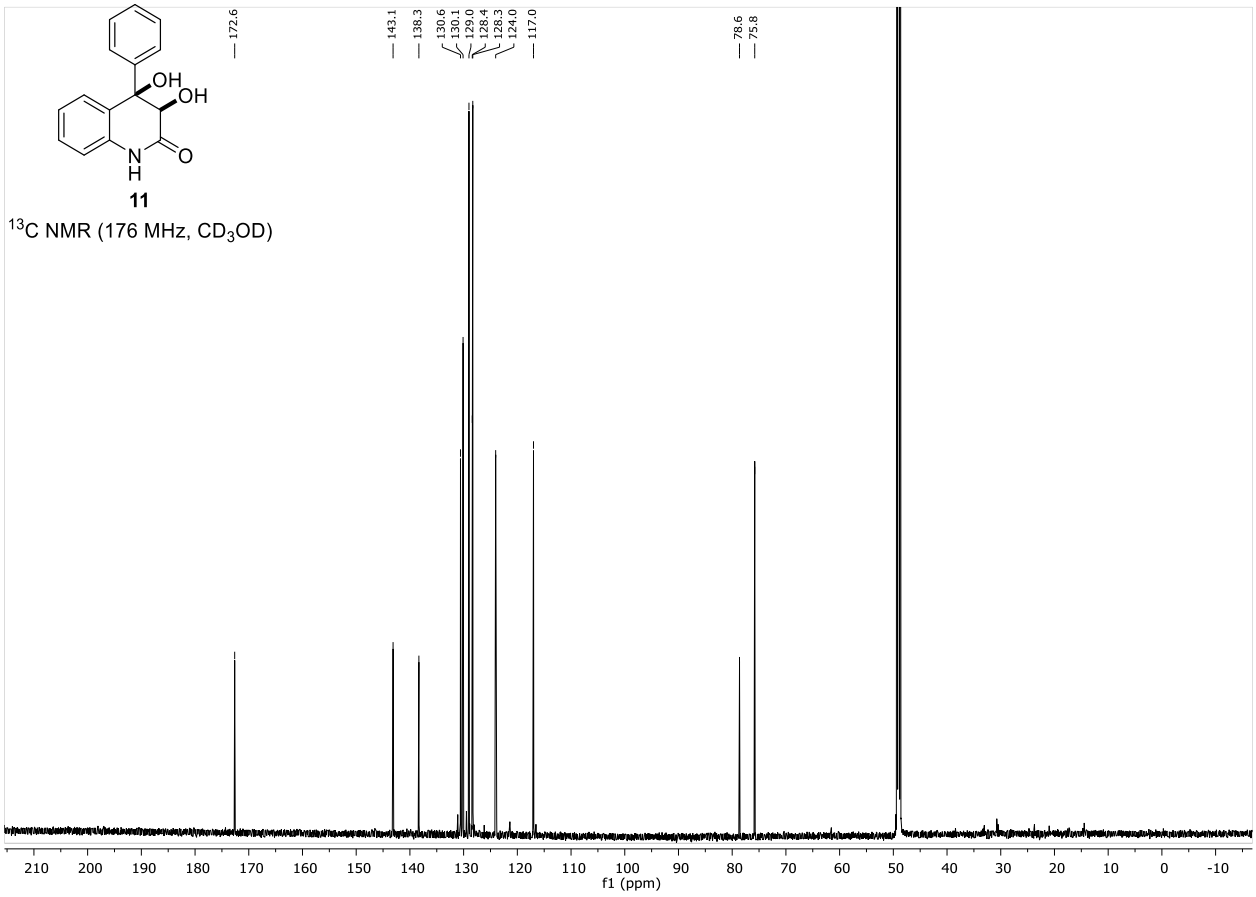
OH
OH
N
H
O
11
13C NMR (176 MHz, CD3OD)
f1 (ppm)

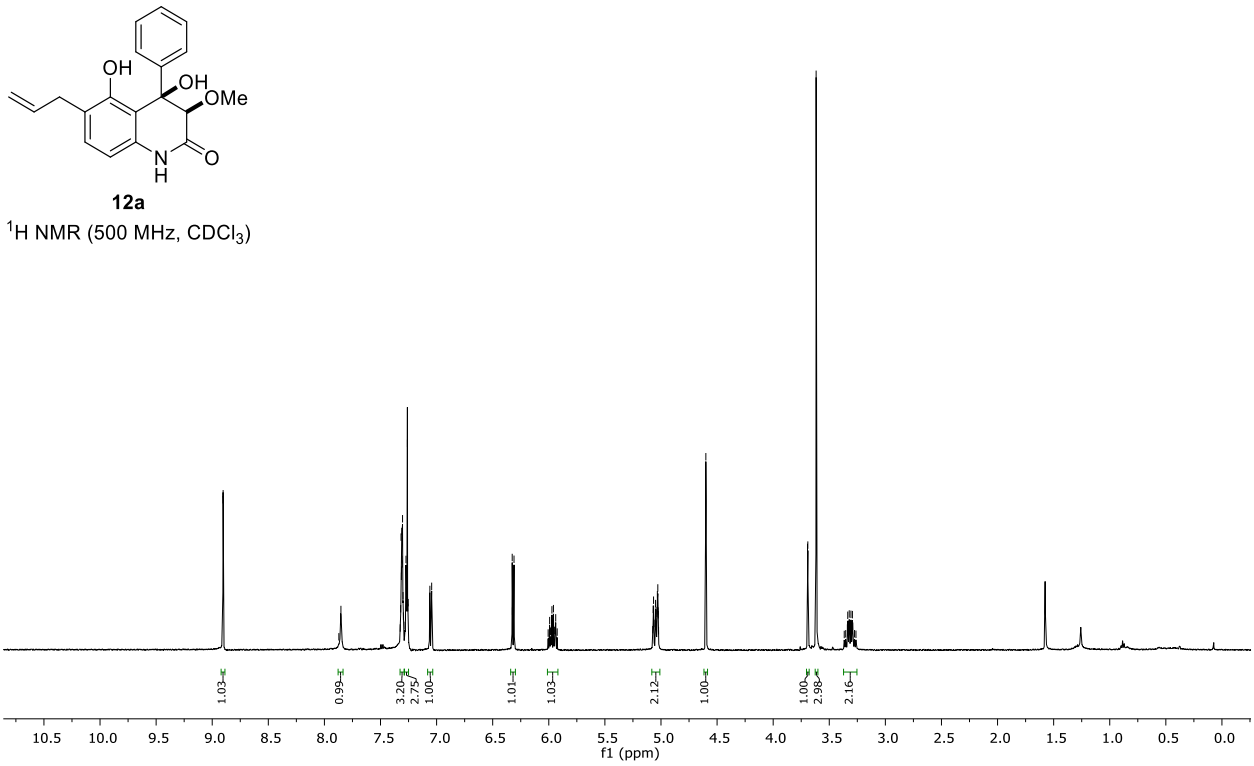

12a

^{1}H NMR (500 MHz, $CDCl_3$)

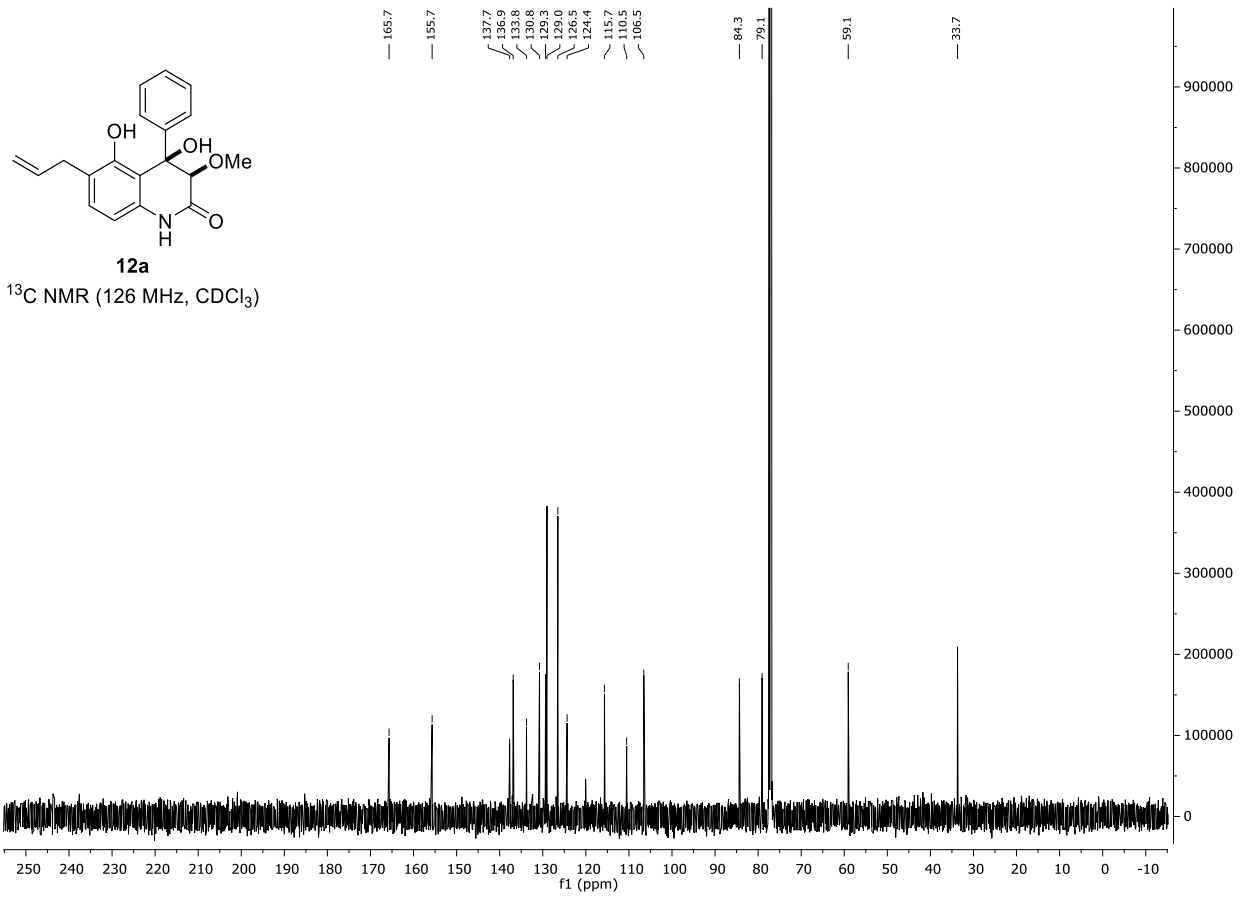

12a

^{13}C NMR (126 MHz, $CDCl_3$)

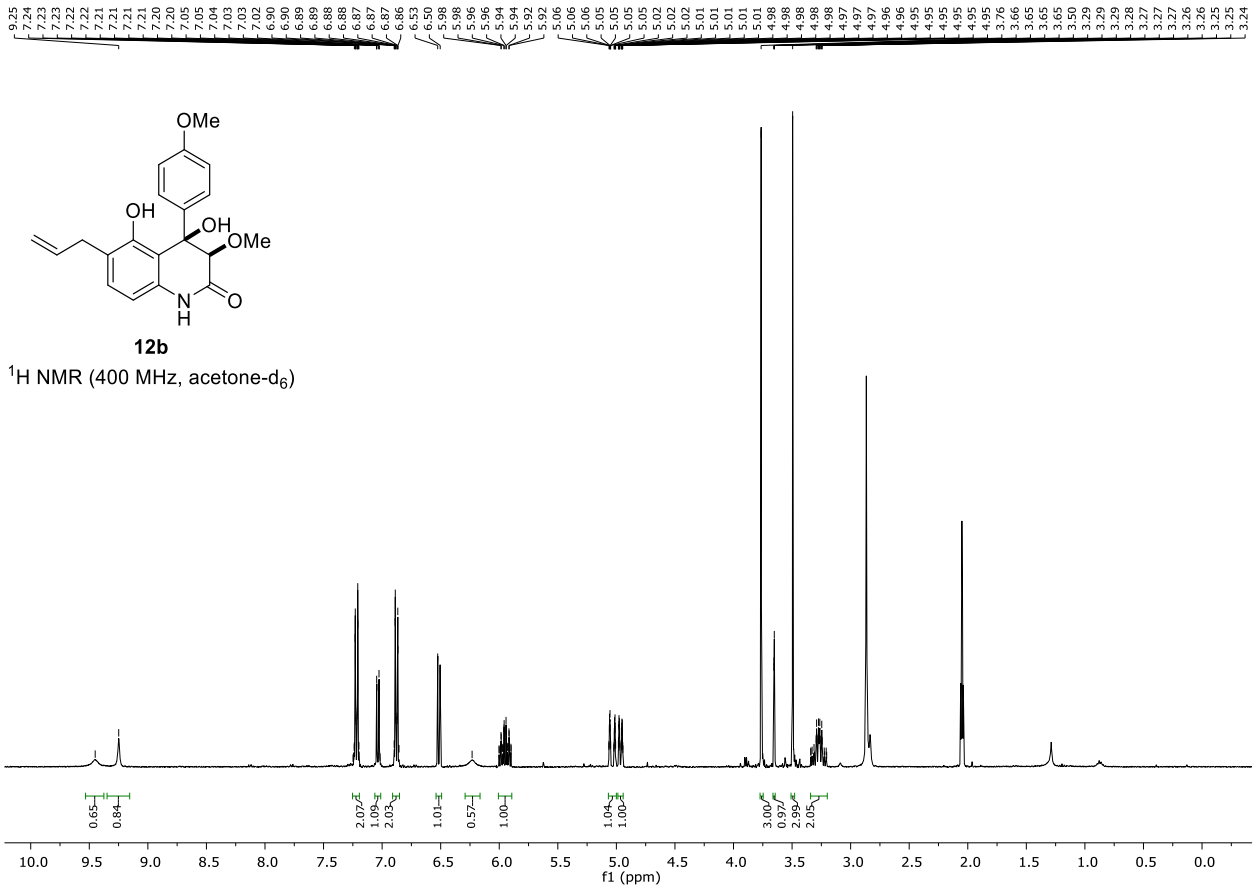
OMe
OH
OH
OMe
N
H
O
12b
1H NMR (400 MHz, acetone-d6)
f1 (ppm)

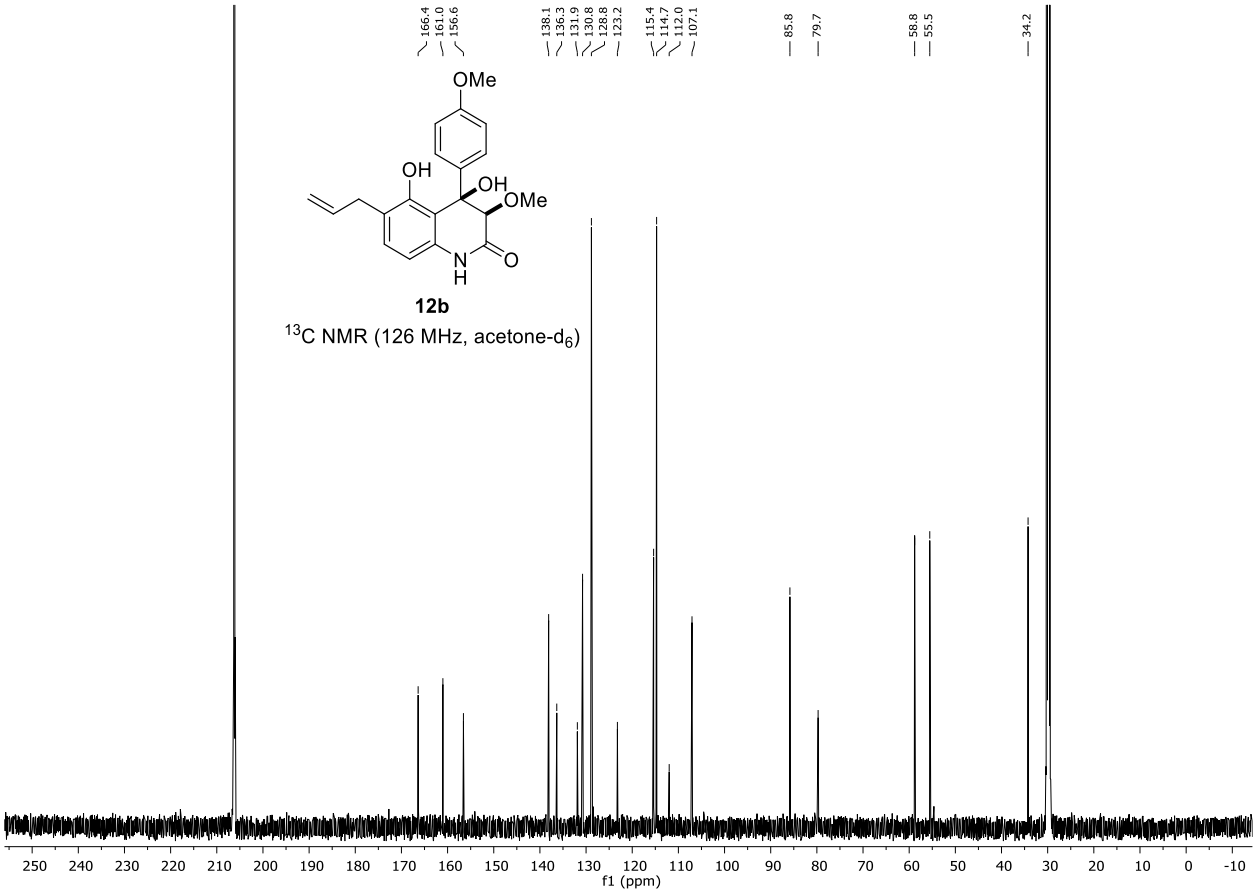
OMe
OH
OH
OMe
N
H
O
12b
13C NMR (126 MHz, acetone-d6)
f1 (ppm)

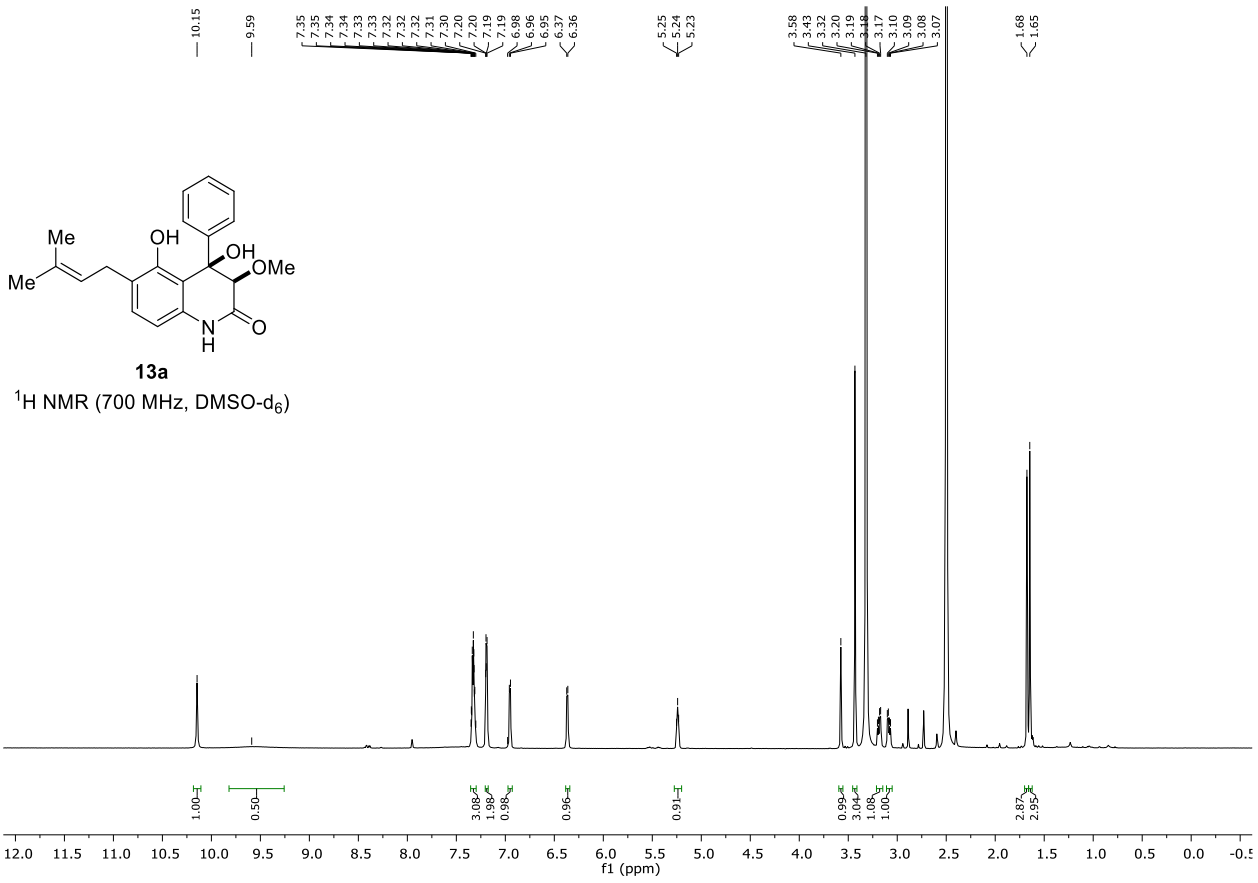

13a

^{1}H NMR (700 MHz, DMSO-d_6)

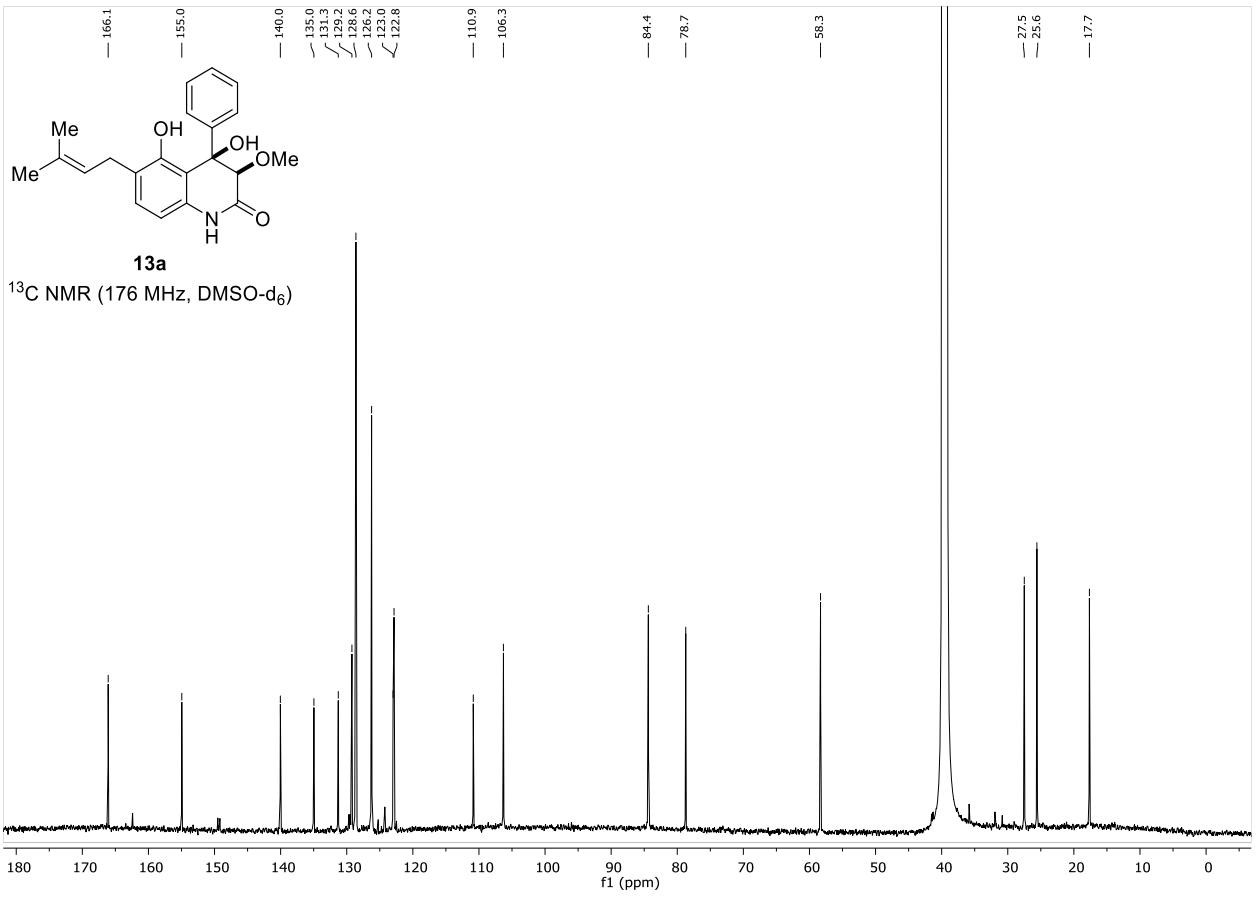

13a

^{13}C NMR (176 MHz, DMSO-d_6)

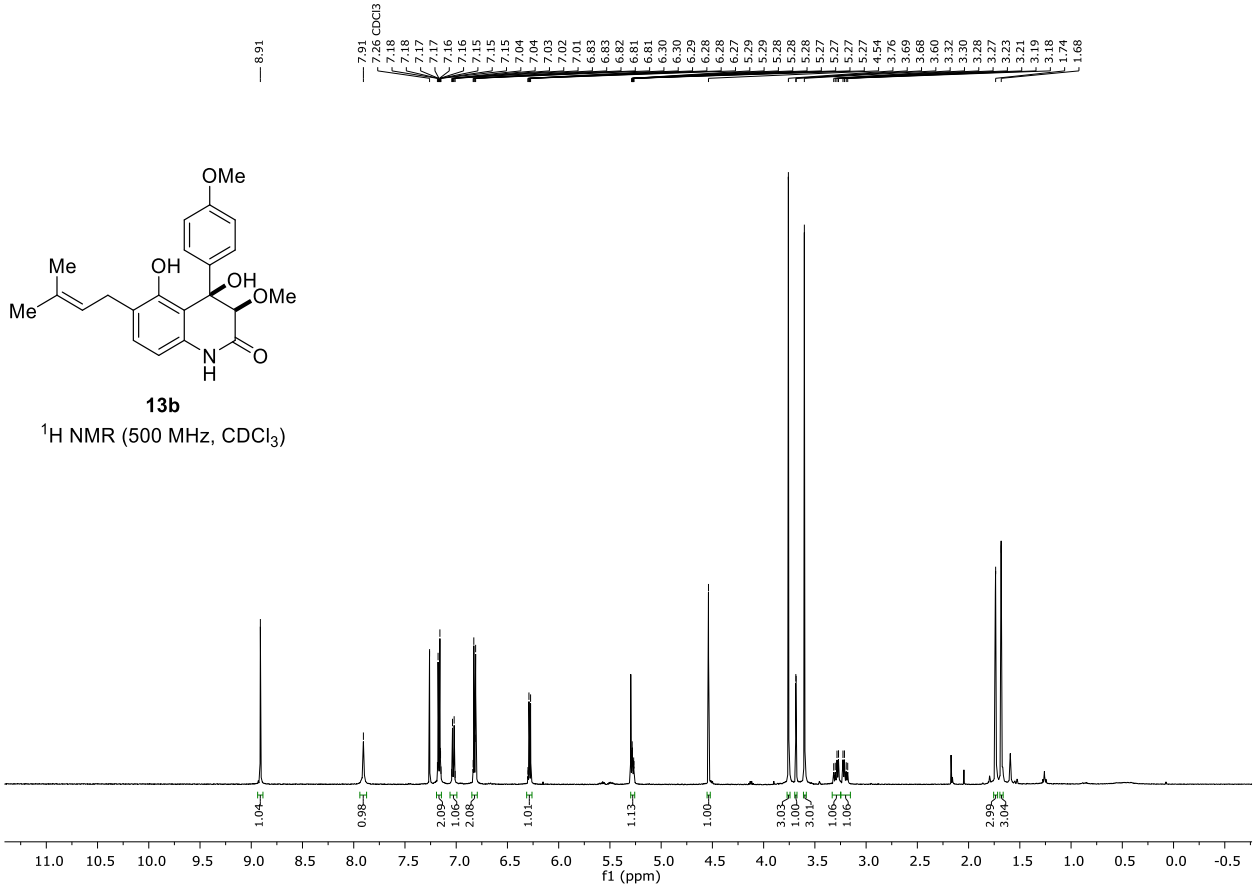
OMe
Me
OH
OH
OMe
Me
N
H
O
13b
^{1}H NMR (500 MHz, CDCl$_3$)
f1 (ppm)

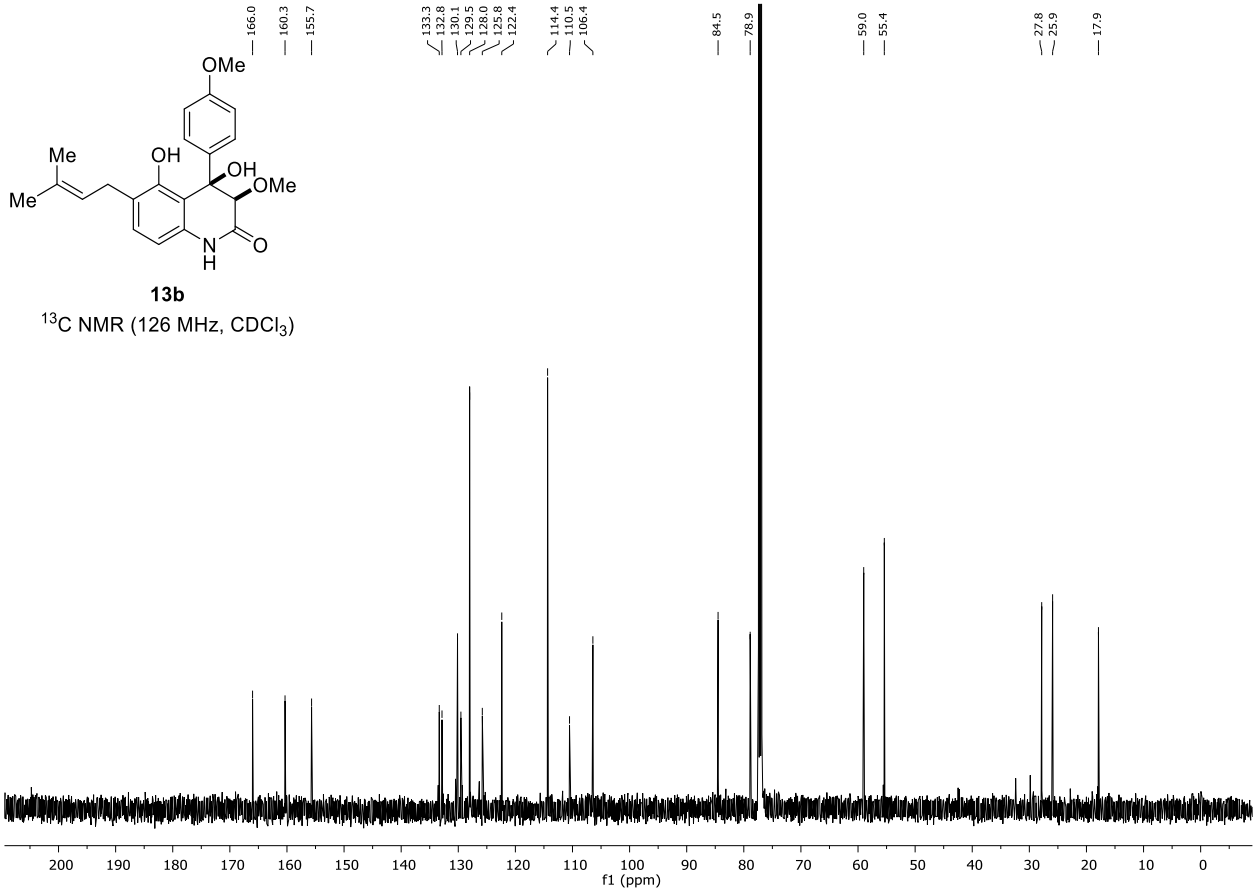
OMe
Me
OH
OH
OMe
Me
N
H
O
13b
^{13}C NMR (126 MHz, CDCl$_3$)
f1 (ppm)

Supporting Information – Five-Step Synthesis of Yaequinolones J1 and J2

Five-Step Synthesis of Yaequinolones J1 and J2

Johannes Schwan, Merlin Kleoff, Philipp Heretsch* and Mathias Christmann*

Freie Universität Berlin, Institut für Chemie und Biochemie, Takustraße 3, 14195 Berlin, Germany

Supporting Information

General Methods

Analytical data were obtained using the following equipment:

NMR spectroscopy: ^{1}H and ^{13}C NMR spectra were acquired on a JEOL ECP 500 (500 MHz), BRUKER Avance 500 (500 MHz), VARIAN Inova 600 (600 MHz), and a BRUKER Avance 700 (700 MHZ) in the reported deuterated solvents. The chemical shifts were reported relative to the deuterated solvents' residual shifts. The multiplicities of the signals are reported using the following abbreviations: s = singlet, d = doublet, t = triplet, q = quartet, p = quintet, br = broad and combinations thereof.

The spectra were processed with the software MESTREC 9.0.

Mass spectra were obtained on a ESI-FTICR-MS: Ionspec QFT-7 (Agilent/Varian)

IR spectroscopy: IR Spectra were recorded on a JASCO FT/IR-4100 spectrometer. Characteristic absorption bands are reported in wavelengths $\tilde{\nu}$ in cm^{-1} and were analyzed with the software Spectral Manager from JASCO.

Flash column and thin layer chromatography: Reaction progress was monitored by thin layer chromatography (silica gel 60 F 254, E. Merck) using UV light (λ = 254 nm) for visualization or vanillin staining agent (170 mL methanol, 20.0 ml conc. acetic acid, 10.0 mL conc. sulfuric acid, 1.0 g vanillin).

Flash column chromatography was performed using silica gel M60 from MACHEREY & NAGEL (particle size: 40–63 μm).

HPLC was conducted on a modular KNAUER HPLC system with a UV detector at 254 nm and differential refractometer. For chiral separations, a ChiralPAK® IA (Daicel) 32 x 250 mm column was used.

MPLC was performed with a TELEDYNE ISCO Combi-Flash Rf or a TELEDYNE ISCO Combi-Flash Rf200 using prepacked SiO_2-columns and cartridges from TELEDYNE. UV response was monitored at 254 nm and 280 nm. As eluents, cyclohexane (99.5%+ quality) and EtOAc (HPLC grade) were used.

Optical rotations were measured on a JASCO P-2000 polarimeter at 589 nm using 100 mm cells and the solvent and concentration (g/100 mL) indicated

Microwave reactions: A BIOTAGE Initiator+ microwave reactor (400 W) was used to perform microwave heated reactions**.** Reactions were conducted in 5 mL glas reactors from BIOTAGE. The temperature was monitored using the IR thermometer of the microwave and power was adjusted automatically to maintain the temperature constant.

Reagents and solvents: Reactions with air or moisture sensitive substances were carried out under an argon atmosphere using standard Schlenk techniques. All reagents and solvents were used as purchased from commercial suppliers unless otherwise noted. Anhydrous solvents were

purified with the solvent purification system MB-SPS-800 (BRAUN). Dry acetonitrile was purchased from ACROS Organics in AcroSeal©-bottles under argon atmosphere with molecular sieves (3 Å). HPLC-grade acetonitrile was purchased from Fischer Scientific. The solvents used for column chromatography (EtOAc, *n*-pentane, *n*-hexane) and work up were purified from commercially available technical grade solvents by distillation under reduced pressure with the help of rotatory evaporators (HEIDOLPH or IKA) at 40 °C bath temperature.

2-Bromoresorcinol was purchased from SIGMA ALDRICH. Imide **4** was prepared according to ref. 1.

Compound names are derived from CHEMDRAW 18.0 and are not necessarily identical with the IUPAC nomenclature.

Room temperature refers to 23 °C.

Synthesis of Compounds

Optimization of the Tandem Knoevenagel-Electrocyclization[a]

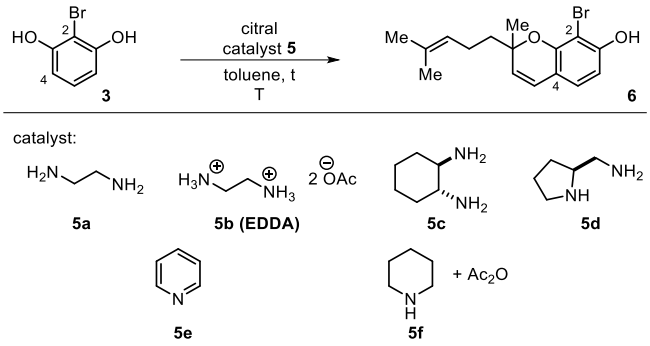

Entry	Catalyst **5** [mol%]	Time [h]	Temp. [°C]	Citral [equiv.]	Yield [%]
1	**a** [30]	0.5	150	1.5	26
2	**b** [30]	0.5	150	1.5	33
3	**c** [30]	0.5	150	1.5	8
4	**d** [30]	0.5	150	1.5	7
5[b]	**e** [200]	18	90	1.0	0
6[b,c]	**f** [220]	40	130	1.0	11
7	**b** [10]	5	140	1.0	29
8	**b** [10]	5	140	1.5	37
9	**b** [10]	5	140	2.0	42
10	**b** [10]	5	140	2.5	23
11	**b** [20]	5	140	2.0	49 (40)[b]

Reactions were performed using general procedure 1. [a] Performed under conventional heating using an oil bath. [b] Pyridine was used as solvent. c Performed according to procedure 2.

Procedure 1:

2-Bromoresorcinol (50 mg, 0.27 mmol, 1.0 equiv.) was dissolved in the solvent stated (3.0 mL). Amine catalyst **5** (0.1 equiv. to 0.2 equiv.) and citral (1.0 to 2.5 equiv.) were added. The mixture was heated to the temperature stated in a sealed tube using microwave or conventional heating for the time stated. After cooling to room temperature, all volatile compounds were removed under reduced pressure. The residue was purified by MPLC (dry loading on Celite®, cyclohexane/EtOAc = 100:0 to 0:100) to yield the title compound **6** as a yellow oil. For characterization data, see detailed procedure of **6**.

Procedure 2:

Citral (282 mg, 1.85 mmol, 1.0 equiv.) and piperidine (0.40 mL, 4.1 mmol, 2.2 equiv.) were dissolved in EtOAc (3.5 mL). Next, acetic anhydride (0.41 mL, 4.3 mmol, 2.3 equiv.) was added dropwise at 0 °C and the mixture was then heated to 90 °C for 1 h. After cooling to r.t., the mixture

was added to a stirred solution of 2-bromoresorcinol (525 mg, 2.78 mmol, 1.5 equiv.) in toluene (7.5 mL) and heated to 150 °C in a sealed tube for 40 h. The reaction mixture was quenched with $NaHCO_3$ (50 mL) and extracted with EtOAc (3 x 50 mL). The combined organic layers were dried ($MgSO_4$), filtered and concentrated under reduced pressure. The residue was purified by MPLC (dry loading on Celite®, cyclohexane/EtOAc = 100:0 to 0:100) to yield the title compound **6** (66 mg, 0.20 mmol, 11% based on citral) as a yellow oil. For characterization data, see detailed procedure of **6**.

8-Bromo-2-methyl-2-(4-methylpent-3-en-1-yl)-2*H*-chromen-7-ol (6)

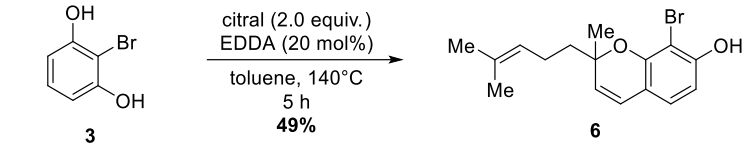

3
$C_6H_5BrO_2$ (189.01)

6
$C_{16}H_{19}BrO_2$ (323.23)

2-Bromoresorcinol (50 mg, 0.27 mmol, 1.0 equiv.) was dissolved in toluene (3.0 mL). Ethylenediamine-*N*,*N*'-diacetic acid (9.5 mg, 0.053 mmol, 0.2 equiv.) and citral (92 µL, 0.53 mmol, 2.0 equiv.) were added. The mixture was heated to 140 °C in a sealed tube using microwave heating for 5 h. After cooling to room temperature, all volatile compounds were removed under reduced pressure. The residue was purified by MPLC (dry loading on Celite®, cyclohexane/EtOAc = 100:0 to 0:100) to yield the title compound **6** as a yellow oil (42 mg, 0.13 mmol, 49%).

R_f = 0.26 (*n*-hexane/EtOAc 95:5); **^{1}H NMR** (600 MHz, $CDCl_3$): δ [ppm] = 6.82 (d, *J* = 8.2 Hz), 6.53 (d, *J* = 8.2 Hz), 6.27 (d, *J* = 9.9 Hz, 1H), 5.45 (d, *J* = 9.9 Hz, 1H), 5.10 (tt, *J* = 7.2, 1.3 Hz, 1H), 2.15 (d, *J* = 8.0 Hz, 1H), 2.12 (d, *J* = 7.7 Hz, 1H), 1.77 – 1.67 (m, 2H), 1.66 (s, 3H), 1.58 (s, 3H), 1.44 (s, 3H); **^{13}C NMR** (151 MHz, $CDCl_3$): δ [ppm] = 153.1, 150.8, 132.0, 127.3, 125.9, 124.1, 122.2, 115.3, 107.3, 99.5, 80.4, 41.3, 26.6, 25.8, 22.7, 17.7; **IR** (neat): $\tilde{\nu}$ [cm^{-1}] = 3506, 3040, 2969, 2921, 2856, 1637, 1604, 1530, 1516, 1499, 1479, 1438, 1384, 1338, 1306, 1246, 1182, 1120, 1077, 1031, 983, 952, 915, 901, 810, 762, 715; **HRMS** (ESI): *m/z* calculated for $C_{16}H_{19}BrNaO_2^+$ ([M+Na]$^+$): 345.0460; found: 345.0461.

2-Methyl-2-(4-methylpent-3-en-1-yl)-8-(trimethylsilyl)-2H-chromen-7-yl trifluoromethanesulfonate (7)

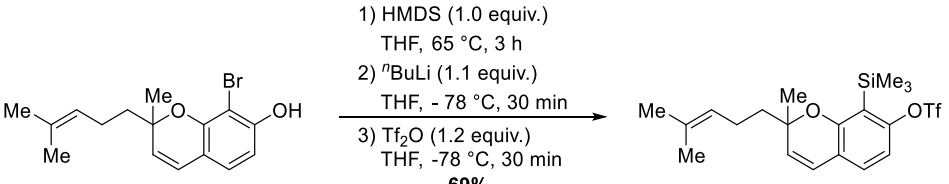

6
$C_{16}H_{19}BrO_2$ (323.23)

7
$C_{20}H_{27}F_3O_4SSi$ (448.57)

Compound **6** (100 mg, 0.309 mmol, 1.0 equiv.) was dissolved in THF (1.0 mL) and hexamethyldisilazane (66 µL, 0.31 mmol, 1.0 equiv.) was added. The mixture was heated to 65 °C for 3 h. After cooling to room temperature, all volatile compounds were removed under vacuum. The residue was dissolved in THF (1.0 mL) and *n*-butyllithium (0.14 mL, 2.5 M, 0.34 mmol, 1.1 equiv.) was added dropwise at –78 °C. After stirring at –78 °C for 30 min, trifluoromethanesulfonic anhydride (62 µL, 0.37 mmol, 1.2 equiv.) was added and stirring was continued for 30 min. $NaHCO_3$ (sat. aq., 10 mL) was added at –78 °C and the mixture was extracted with EtOAc (3x50 mL), dried (Na_2SO_4), and concentrated under reduced pressure. The residue was purified via column chromatography (SiO_2, *n*-pentane/EtOAc 98:2) to yield the title compound **7** (95 mg, 0.21 mmol, 69%) as a colorless oil.

R_f = 0.61 (*n*-hexane/EtOAc 95:5); **^{1}H NMR** (500 MHz, $CDCl_3$): δ [ppm] = 6.98 (d, *J* = 8.3 Hz, 1H), 6.81 (d, *J* = 8.3 Hz, 1H), 6.33 (d, *J* = 9.9 Hz, 1H), 5.58 (d, *J* = 9.9 Hz, 1H), 5.11 (tdd, *J* = 5.7, 2.8, 1.4 Hz, 1H), 2.23 – 2.01 (m, 2H), 1.86 (ddd, *J* = 13.9, 11.6, 5.2 Hz, 1H), 1.68 (s, 3H), 1.67 – 1.61 (m, 1H), 1.59 (s, 3H), 1.40 (s, 3H), 0.40 (s, 9H); **^{13}C NMR** (126 MHz, $CDCl_3$) δ [ppm] = 159.3, 154.2, 132.2, 129.6, 128.5, 123.9, 122.3, 119.9, 119.2, 118.8 (q, *J* = 320.8 Hz), 112.4, 80.2, 42.1, 27.1, 25.8, 23.4, 17.8, 1.2; **^{19}F NMR** (471 MHz, $CDCl_3$) δ [ppm] = –72.8; **IR** (neat): $\tilde{\nu}$ [cm^{-1}] = 2970, 2926, 2858, 1647, 1576, 1445, 1407, 1370, 1341, 1286, 1247, 1206, 1163, 1139, 1076, 1016, 988, 923, 907, 840, 694, 668; **HRMS** (ESI): *m/z* calculated for $C_{20}H_{27}F_3NaO_4SSi^+$ ([M+Na]$^+$): 471.1243; found: 471.1245.

2-Methoxy-N-(8-(4-methoxybenzoyl)-2-methyl-2-(4-methylpent-3-en-1-yl)-2*H*-chromen-7-yl)acetamide (8) and 4-Methoxy-N-(8-(2-methoxyacetyl)-2-methyl-2-(4-methylpent-3-en-1-yl)-2*H*-chromen-7-yl)benzamide (9)

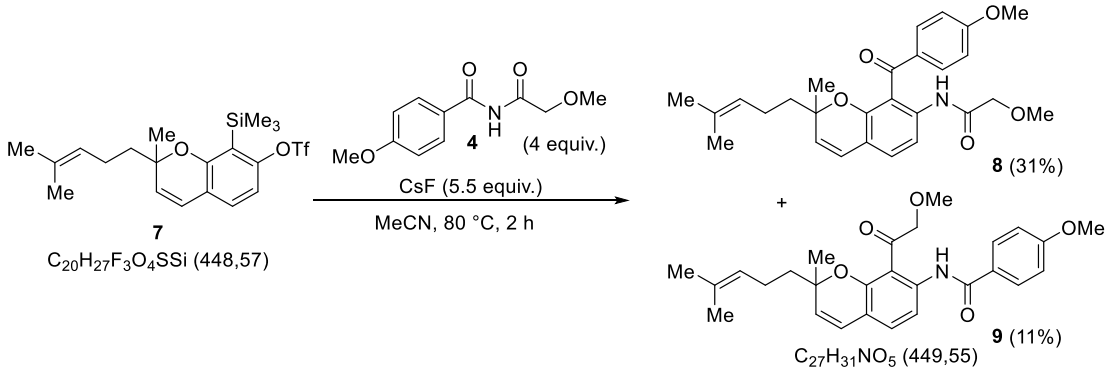

Cesium fluoride (93 mg, 0.61 mmol, 5.5 equiv.) was dried at 10^{-3} mbar and 500 °C for 5 min. After cooling to room temperature, acetonitrile (1.5 mL) and imide **4** (100 mg, 0.45 mmol, 4.0 equiv.) were added. After adding aryne precursor **7** (50 mg, 0.11 mmol, 1.0 equiv.), the mixture was heated to 80 °C for 2 h. After cooling to room temperature, the solvent was removed under reduced pressure and the residue was purified by MPLC (dry loading on Celite®, cyclohexane/EtOAc 100:0 to 0:100), yielding **8** (15 mg, 34 µmol, 31%) and **9** (5.7 mg, 13 µmol, 11%) as yellow oils. The thus

obtained racemic mixture of **8** can be separated into its enantiomers by chiral HPLC (chiralPAK® IA, *n*-hexane/*i*-PrOH 95:5, flow: 18 mL·min^{-1}; 90 bar; *ee* ≥ 99% [HPLC]).

(+)-**8**: $[\alpha]_D^{24}$ = +128.6° (c = 0.22, $CHCl_3$); *(–)*-**8**: $[\alpha]_D^{24}$ = –146.3° (c = 0.19, $CHCl_3$)

R_f = 0.22 (*n*-hexane/EtOAc = 4:1); **^{1}H NMR** (700 MHz, $CDCl_3$) δ [ppm] = 9.25 (s, 1H), 7.83 – 7.78 (m, 3H), 7.06 (d, *J* = 8.3 Hz, 1H), 6.91 – 6.87 (m, 2H), 6.33 (d, *J* = 9.9 Hz, 1H), 5.46 (d, *J* = 10.0 Hz, 1H), 4.90 (ddt, *J* = 7.1, 5.7, 1.4 Hz, 1H), 3.90 (d, *J* = 0.6 Hz, 2H), 3.85 (s, 3H), 3.37 (s, 3H), 1.83 – 1.76 (m, 1H), 1.75 – 1.68 (m, 1H), 1.61 (d, *J* = 1.3 Hz, 3H), 1.45 (d, *J* = 1.4 Hz, 3H), 1.43 – 1.38 (m, 2H), 1.12 (s, 3H); **^{13}C NMR** (176 MHz, $CDCl_3$) δ [ppm] = 195.3, 168.3, 163.8, 151.6, 135.9, 132.0, 131.9, 131.8, 129.0, 128.7, 124.0, 122.1, 118.1, 117.7, 114.1, 113.6, 79.7, 72.3, 59.6, 55.6, 41.5, 26.5, 25.7, 22.5, 17.7; **IR** (neat): $\tilde{\nu}$ [cm^{-1}] = 3356, 2966, 2924, 2852, 1717, 1700, 1683, 1669, 1662, 1653, 1647, 1635, 1596, 1577, 1540, 1533, 1521, 1517, 1507, 1457, 1430, 1418, 1399, 1307, 1285, 1257, 1192, 1170, 1153, 1112, 1083, 1029, 987, 947, 890, 843, 793, 762, 741, 720; **HRMS** (ESI): *m/z* calculated for $C_{27}H_{31}NNaO_5^+$ ([M+Na]$^+$): 472.2094; found: 472.2091.

9:

R_f = 0.35 (*n*-hexane/EtOAc = 4:1); **^{1}H NMR** (700 MHz, $CDCl_3$) δ [ppm] = 12.37 (s, 1H), 8.41 (d, *J* = 8.5 Hz, 1H), 8.06 – 8.02 (m, 2H), 7.17 (d, *J* = 8.5 Hz, 1H), 7.02 – 6.96 (m, 2H), 6.37 (d, *J* = 9.9 Hz, 1H), 5.56 (d, *J* = 9.9 Hz, 1H), 5.12 – 5.08 (m, 1H), 4.74 (d, *J* = 18.0 Hz, 1H), 4.71 (d, *J* = 18.0 Hz, 1H), 3.88 (s, 3H), 3.51 (s, 3H), 2.21 – 2.07 (m, 2H), 1.90 (ddd, *J* = 14.0, 11.1, 5.4 Hz, 1H), 1.73 (ddd, *J* = 14.1, 11.3, 5.2 Hz, 1H), 1.67 (d, *J* = 1.4 Hz, 3H), 1.57 (d, *J* = 1.3 Hz, 3H), 1.49 (s, 3H); **^{13}C NMR** (176 MHz, $CDCl_3$) δ [ppm] = 202.1, 165.6, 162.8, 155.6, 141.9, 132.5, 132.5, 129.6, 127.4, 127.2, 123.5, 122.7, 116.4, 114.2, 113.3, 111.9, 81.6, 80.3, 59.5, 55.6, 42.0, 27.3, 25.8, 23.3, 17.8; **IR** (neat): $\tilde{\nu}$ [cm^{-1}] = 2957, 2924, 2853, 1680, 1650, 1596, 1507, 1454, 1408, 1376, 1306, 1254, 1181, 1124, 1081, 1030, 925, 842, 756; **HRMS** (ESI): *m/z* calculated for $C_{27}H_{31}NNaO_5^+$ ([M+Na]$^+$): 472.2094; found: 472.2080.

Yaequinolone J1 (1) and Yaequinolone J2 (2)

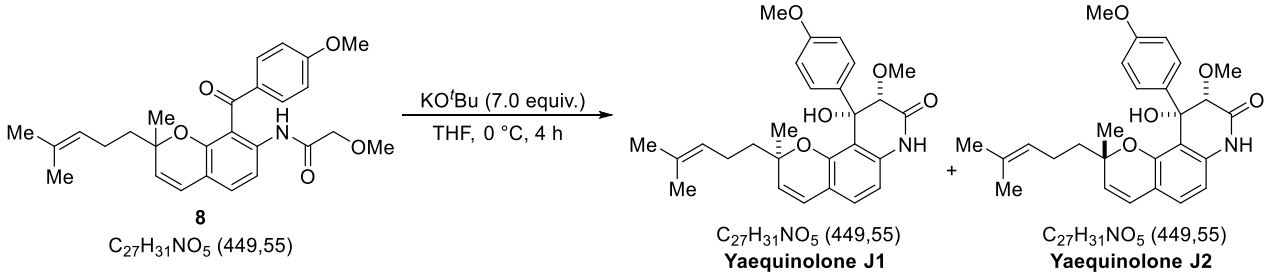

Compound **8** (25 mg, 56 µmol, 1.0 equiv.) was dissolved in anhydrous THF (3.0 mL) and a solution of KO^{t}Bu (0.78 mL, 0.39 mmol, 0.5 M in THF, 7.0 equiv.) was added at 0 °C. The mixture was stirred at 0 °C until complete consumption of starting material was observed via TLC (4 h). The reaction was quenched by addition of water and extracted with EtOAc (3x 50 mL). The combined organic extracts were dried ($MgSO_4$) and concentrated under reduced pressure. The residue was purified

via column chromatography (SiO_2, CH_2Cl_2/MeOH 97:3) to yield a mixture of yaequinolone J1 and J2 (18 mg, 0.41 mmol, *d.r.* = 1 : 1.4 [^{1}H NMR], 74%) as a colorless oil. The two diastereomers were separated by preparative TLC (SiO_2, CH_2Cl_2/MeOH 98:2), to yield pure yaequinolone J1 (7.3 mg, 16 µmol, 29%) and yaequinolone J2 (10 mg, 22 µmol, 40%) as colorless oils.

According to the synthesis of racemic yaequinolones J1 and J2, (–)-yaequinolone J1 (2.5 mg, 5.6 µmol, 30%) was obtained starting from (–)-**8** (8.2 mg, 18 µmol) and KO^{t}Bu (0.26 mL, 0.13 mmol, 0.5 M in THF). (+)-yaequinolone J2 (2.1 mg, 4.7 µmol, 40%) was obtained starting from (+)-**8** (5.3 mg, 12 µmol) and KO^{t}Bu (0.17 mL, 83 µmol, 0.5 M in THF).

(–)-Yaequinolone J1:

$[\alpha]_D^{21}$ = –61.9° (c = 0.21, EtOH) [Lit:[2b] $[\alpha]_D^{23}$ = –65.6° (c = 0.1, EtOH)]; $\mathbf{R_f}$ = 0.37 (CH_2Cl_2/MeOH 95:5); **^{1}H NMR** (700 MHz, $CDCl_3$) δ [ppm] = 7.67 (s, 1H), 7.21 – 7.18 (m, 2H), 6.90 (d, *J* = 7.9 Hz, 1H), 6.80 – 6.76 (m, 2H), 6.34 (d, *J* = 8.0 Hz, 1H), 6.28 (d, *J* = 10.0 Hz, 1H), 5.44 (d, *J* = 10.0 Hz, 1H), 5.34 (s, 1H), 4.72 (tdd, *J* = 6.9, 3.0, 1.5 Hz, 1H), 3.80 (d, *J* = 1.4 Hz, 1H), 3.74 (s, 3H), 3.58 (s, 3H), 1.73 – 1.66 (m, 1H), 1.60 – 1.52 (m, 5H), 1.43 – 1.39 (m, 4H), 1.32 (s, 3H); **^{13}C NMR** (176 MHz, $CDCl_3$) δ [ppm] = 167.5, 159.7, 152.5, 136.4, 133.8, 131.9, 127.9, 127.5, 127.0, 123.6, 122.2, 117.8, 114.4, 114.1, 108.1, 85.1, 80.8, 78.0, 59.6, 55.3, 41.1, 26.7, 25.7, 22.1, 17.5; **IR** (neat): $\tilde{\nu}$ [cm^{-1}] = 3495, 3225, 2965, 2929, 2857, 2836, 1694, 1606, 1510, 1492, 1377, 1252, 1176, 1102, 1046, 827, 742, 716 cm^{-1}; **HRMS** (ESI): *m/z* calculated for $C_{27}H_{31}NNaO_5^+$ ([M+Na]$^+$): 472.2094; found: 472.2092. The spektroscopic data matches those reported for (–)-Yaequinolone J1.[2]

(+)-Yaequinolone J2:

$[\alpha]_D^{21}$ = +176.5° (c = 0.18, EtOH) [Lit:[2b] $[\alpha]_D^{23}$ = +187.1° (c = 0.1, EtOH)]; $\mathbf{R_f}$ = 0.39 (CH_2Cl_2/MeOH 95:5); **^{1}H NMR** (700 MHz, $CDCl_3$) δ [ppm] = 7.81 (s, 1H), 7.21 – 7.18 (m, 2H), 6.91 (d, *J* = 8.0 Hz, 1H), 6.81 – 6.77 (m, 2H), 6.36 (d, *J* = 8.0 Hz, 1H), 6.31 (d, *J* = 10.0 Hz, 1H), 5.50 (d, *J* = 9.9 Hz, 1H), 5.20 (s, 1H), 5.04 (tdd, *J* = 5.7, 2.8, 1.4 Hz, 1H), 3.83 (d, *J* = 1.4 Hz, 1H), 3.76 (s, 3H), 3.58 (s, 3H), 2.09 (dq, *J* = 12.4, 6.6 Hz, 1H), 2.04 – 1.97 (m, 1H), 1.70 – 1.60 (m, 5H), 1.57 (s, 3H), 0.95 (s, 3H); **^{13}C NMR** (176 MHz, $CDCl_3$) δ [ppm] = 167.7, 159.6, 152.6, 136.3, 134.2, 132.4, 128.3, 127.5, 127.0, 123.7, 122.6, 118.3, 114.9, 113.9, 108.2, 85.0, 80.5, 78.0, 59.7, 55.4, 41.4, 25.8, 25.7, 23.1, 17.8; **IR** (neat): $\tilde{\nu}$ [cm^{-1}]= 3507, 3235, 3062, 3043, 2967, 2925, 2853, 2836, 1694, 1641, 1605, 1510, 1491, 1462, 1377, 1303, 1252, 1222, 1175, 1104, 1081, 1046, 998, 916, 883, 830, 753, 734; **HRMS** (ESI): *m/z* calculated for $C_{27}H_{31}NNaO_5^+$ ([M+Na]$^+$): 472.2094; found: 472.2093. The spektroscopic data matches those reported for (+)-Yaequinolone J2.[2]

1H and 13C NMR comparisons (CDCl3)

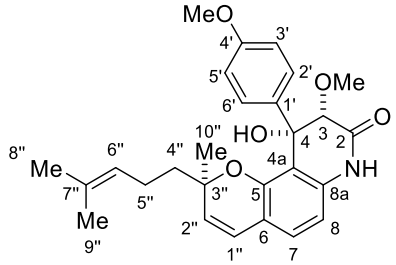

Yaequinolone J1

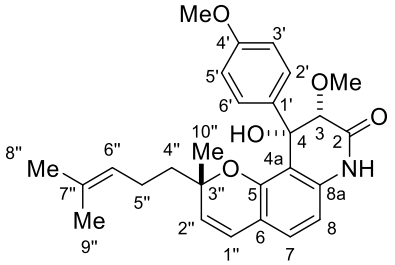

Yaequinolone J2

^{1}H NMR Data	**Synthetic (700 MHz)**	**Natural[2b] (600 MHz)**	**^{1}H NMR Data**	**Synthetic (700 MHz)**	**Natural[2b] (600 MHz)**
Position	**δH (*J* in Hz)**		**Position**	**δH (*J* in Hz)**	
1-NH	7.67, br s	7.40, br s	1-NH	7.81, br s	7.49, br s
3	3.80, d (1.4)	3.80, d (1.1)	3	3.83, d (1.4)	3.83, d (0.9)
7	6.90, d (7.9)	6.90, d (8.0)	7	6.91, d (8.0)	6.93, d (8.0)
8	6.34 (8.0)	6.34, d (8.0)	8	6.36, d (8.0)	6.36, d (8.0)
2', 6'	7.19, m	7.19, d (8.4)	2', 6'	7.19, m	7.19, d (8.8)
3', 5'	6.78, m	6.78, d (8.4)	3', 5'	6.79, m	6.79, d (8.8)
1''	6.28, d (10.0)	6.28, d (9.6)	1''	6.31, d (10.0)	6.31, d (9.7)
2''	5.44, d (10.0)	5.44, d (9.6)	2''	5.50, d (9.9)	5.50, d (9.7)
4''	1.41, m	1.40, m	4''	1.65, m	1.67, m
				1.65, m	1.62, m
5''	1.69, m	1.69, m	5''	2.09, dq (12.4,	2.09, m
	1.56, m	1.56, m		6.6)	
				2.00, m	2.01, m
6''	4.72, tdd (6.9,	4.71, t (7.1)	6''	5.04, tdd (5.7,	5.04, t (7.3)
	3.0, 1.5)			2.8, 1.4)	
8''	1.56, m	1.56, s	8''	1.65, m	1.66, s
9''	1.32, s	1.31, s	9''	1.57, s	1.57, s
10''	1.41, m	1.41, s	10''	0.95, s	0.95, s
3-OMe	3.58, s	3.58, s	3-OMe	3.58, s	3.58, s
4'-OMe	3.74, s	3.74, s	4'-OMe	3.76, s	3.77, s
4-OH	5.34, s	5.36, s	4-OH	5.20, s	5.22, s

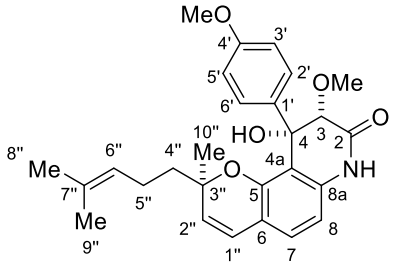

Yaequinolone J1

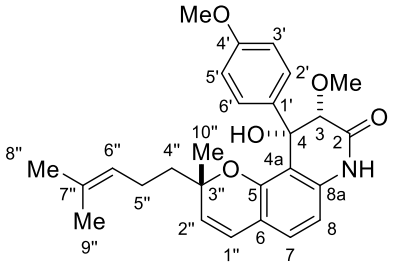

Yaequinolone J2

^{13}C NMR Data	Synthetic (176 MHz)	Natural[2b] (150 MHz)	^{13}C NMR Data	Synthetic (176 MHz)	Natural[2b] (150 MHz)
Position	**δH (*J* in Hz)**		**Position**	**δH (*J* in Hz)**	
2	167.5	167.2	2	167.7	167.4
3	85.1	85.1	3	85.0	85.0
4	78.0	78.1	4	78.0	78.0
4a	114.4	114.3	4a	114.9	114.6
5	152.5	152.5	5	152.6	152.6
6	117.8	118.0	6	118.3	118.5
7	127.0	127.2	7	127.0	127.1
8	108.1	108.1	8	108.2	108.2
8a	136.4	136.2	8a	136.3	136.2
1’	133.8	133.7	1’	134.2	134.1
2’, 6’	127.5	127.5	2’, 6’	127.5	127.4
3’, 5’	114.1	114.2	3’, 5’	113.9	113.9
4’	159.7	159.8	4’	159.6	159.8
1’’	122.2	122.2	1’’	122.6	122.5
2’’	127.9	128.0	2’’	128.3	128.4
3’’	80.8	80.8	3’’	80.5	80.5
4’’	41.1	41.1	4’’	41.4	41.3
5’’	22.1	22.2	5’’	23.1	23.0
6’’	123.6	123.7	6’’	123.7	123.8
7’’	131.9	131.9	7’’	132.4	132.4
8’’	25.7	25.6	8’’	25.8	25.8
9’’	17.5	17.4	9’’	17.8	17.7
10’’	26.7	26.7	10’’	25.7	25.6
3-OMe	59.6	59.5	3-OMe	59.7	59.7
4’-OMe	55.3	55.3	4’-OMe	55.4	55.4

References

(1) Schwan, J.; Kleoff, M.; Hartmayer, B.; Heretsch, P.; Christmann, M. Synthesis of Quinolinone Alkaloids via Aryne Insertions into Unsymmetric Imides in Flow. *Org. Lett.* **2018**, *20*, 7661–7664.

(2) (a) Vece, V.; Jakkepally, S.; Hanessian, S. Total Synthesis and Absolute Stereochemical Assignment of the Insecticidal Methabolites Yaequinolones J1 and J2. *Org. Lett.* **2018**, *20*, 4277–4280. (b) Uchida, R.; Imasato, R.; Shiomi, K.; Tomoda, H.; Ōmura, S. Yaequinolones J1 and J2, Novel Insecticidal Antibiotics from *Penicillium* sp. FKI-2140. *Org. Lett.* **2005**, *7*, 5701–5704.

Appendix

HPLC chromatogram of *rac*-**8** (ChiralPAK IA, 10% IPA/hexane, 34 bar, 0.8 mL/min):

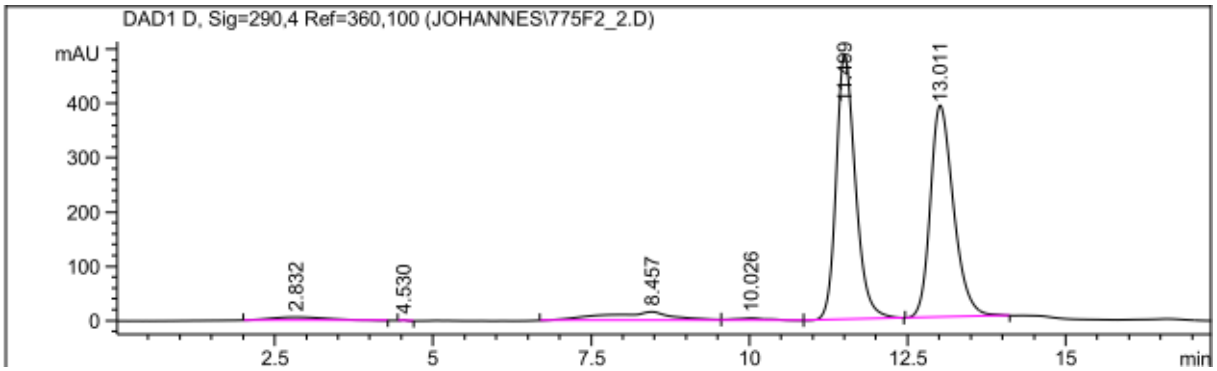

Signal 2: DAD1 D, Sig=290,4 Ref=360,100

Peak #	RetTime [min]	Type	Width [min]	Area [mAU*s]	Height [mAU]	Area %
1	2.832	BB	0.7588	383.23703	5.98713	1.7278
2	4.530	BB	0.0855	7.06715	1.34046	0.0319
3	8.457	BV	0.9825	1241.70569	16.05212	5.5982
4	10.026	VV	0.5045	160.19423	4.16720	0.7222
5	11.499	VB	0.3243	1.03764e4	487.50809	46.7814
6	13.011	BB	0.3911	1.00120e4	390.47000	45.1385

HPLC chromatogram of (+)-**8** (ChiralPAK IA, 10% IPA/hexane, 34 bar, 0.8 mL/min):

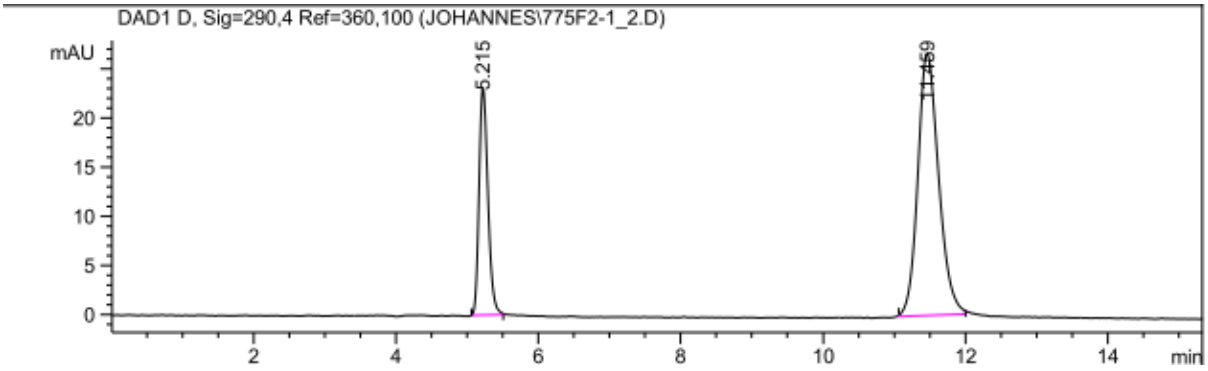

Signal 2: DAD1 D, Sig=290,4 Ref=360,100

Peak #	RetTime [min]	Type	Width [min]	Area [mAU*s]	Height [mAU]	Area %
1	5.215	BB	0.1357	201.69472	23.14871	27.1269
2	11.459	BB	0.3073	541.82794	26.64318	72.8731

HPLC chromatogram of (–)-**8** (ChiralPAK IA, 10% IPA/hexane, 34 bar, 0.8 mL/min):

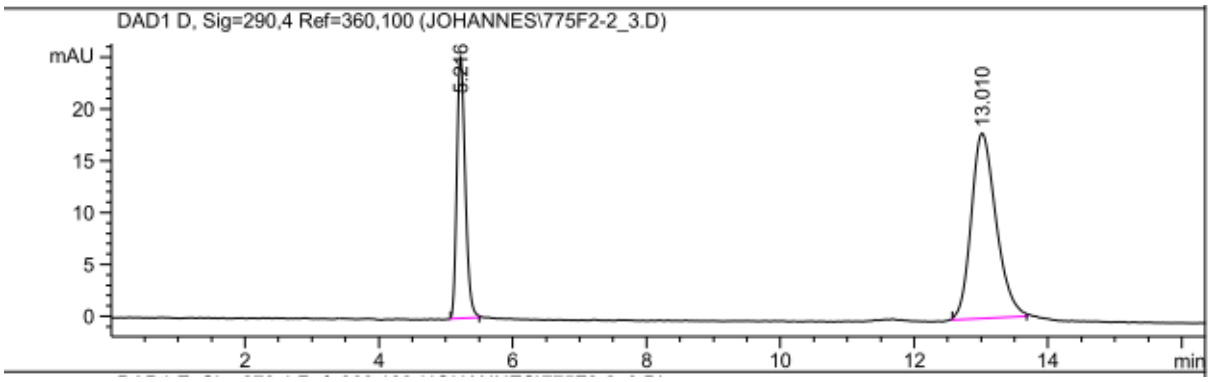

Signal 2: DAD1 D, Sig=290,4 Ref=360,100

Peak #	RetTime [min]	Type	Width [min]	Area [mAU*s]	Height [mAU]	Area %
1	5.216	BB	0.1357	220.38380	25.29259	32.1903
2	13.010	BB	0.3924	464.24362	17.91024	67.8097

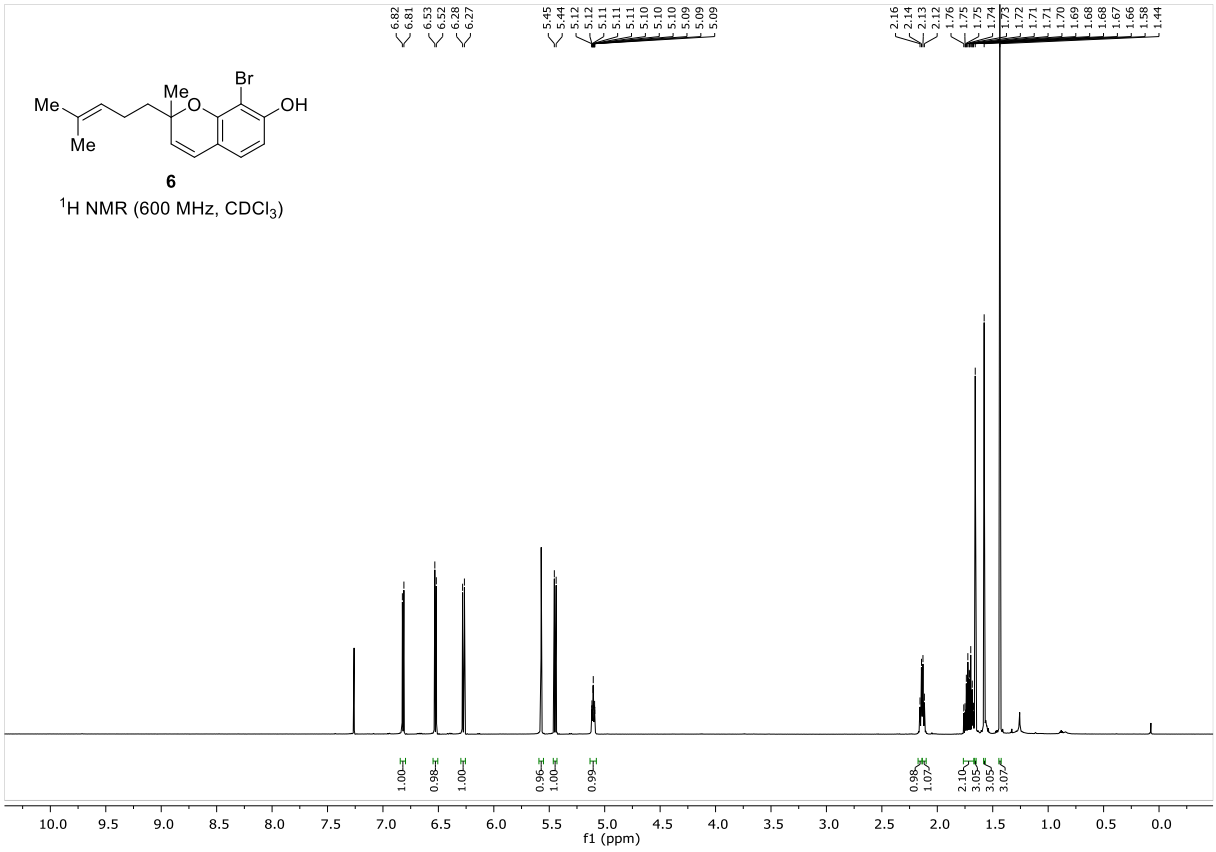
Me
Me
Me
O
Br
OH
6
1H NMR (600 MHz, CDCl3)
f1 (ppm)

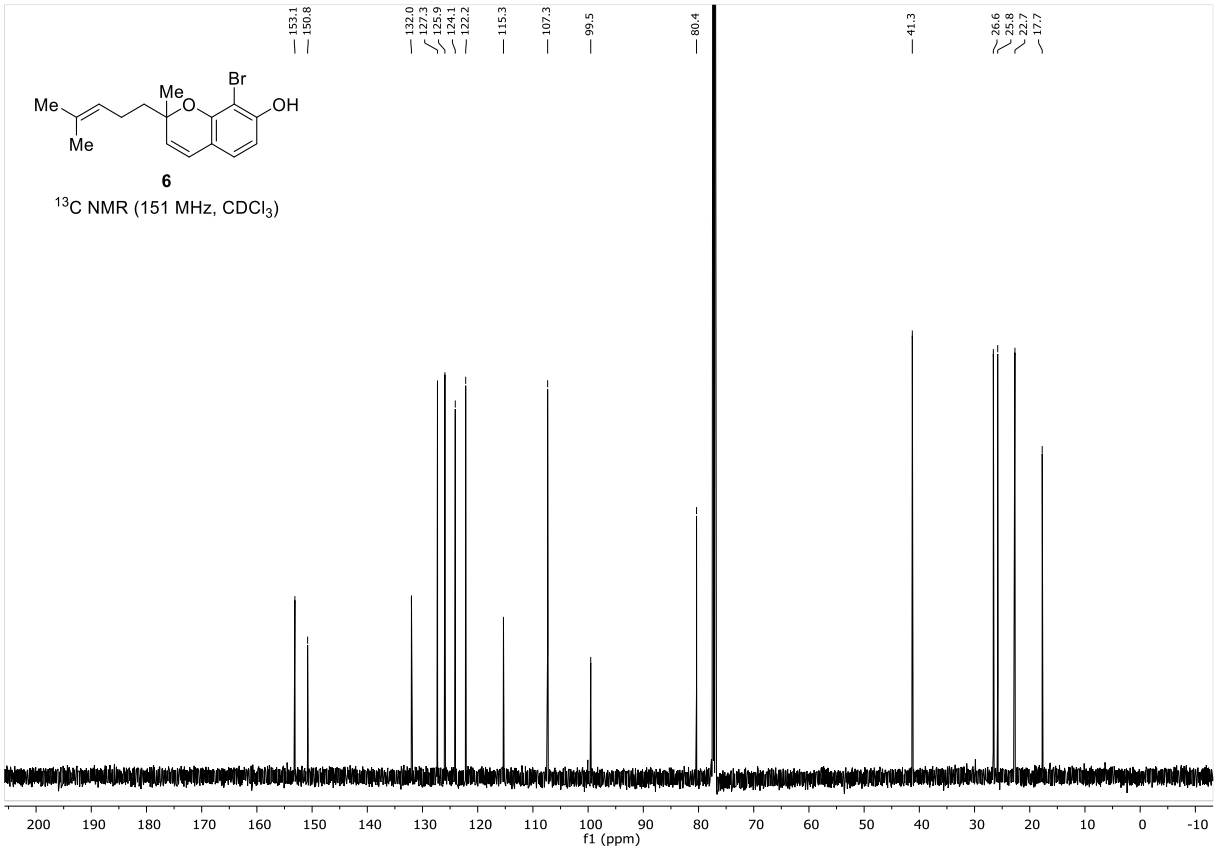
Me
Me
Me
O
Br
OH
6
13C NMR (151 MHz, CDCl3)
f1 (ppm)

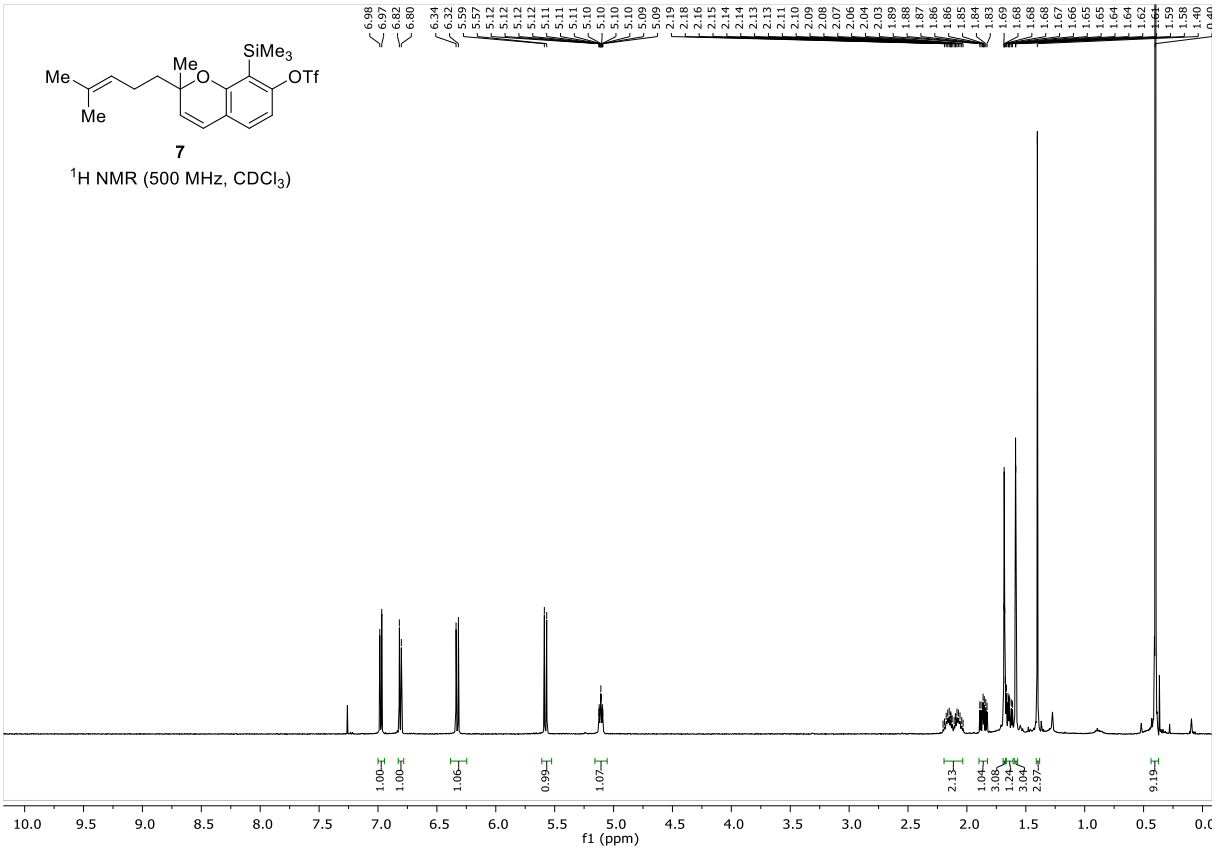
Me
Me
Me
O
SiMe3
OTf
7
1H NMR (500 MHz, CDCl3)
f1 (ppm)

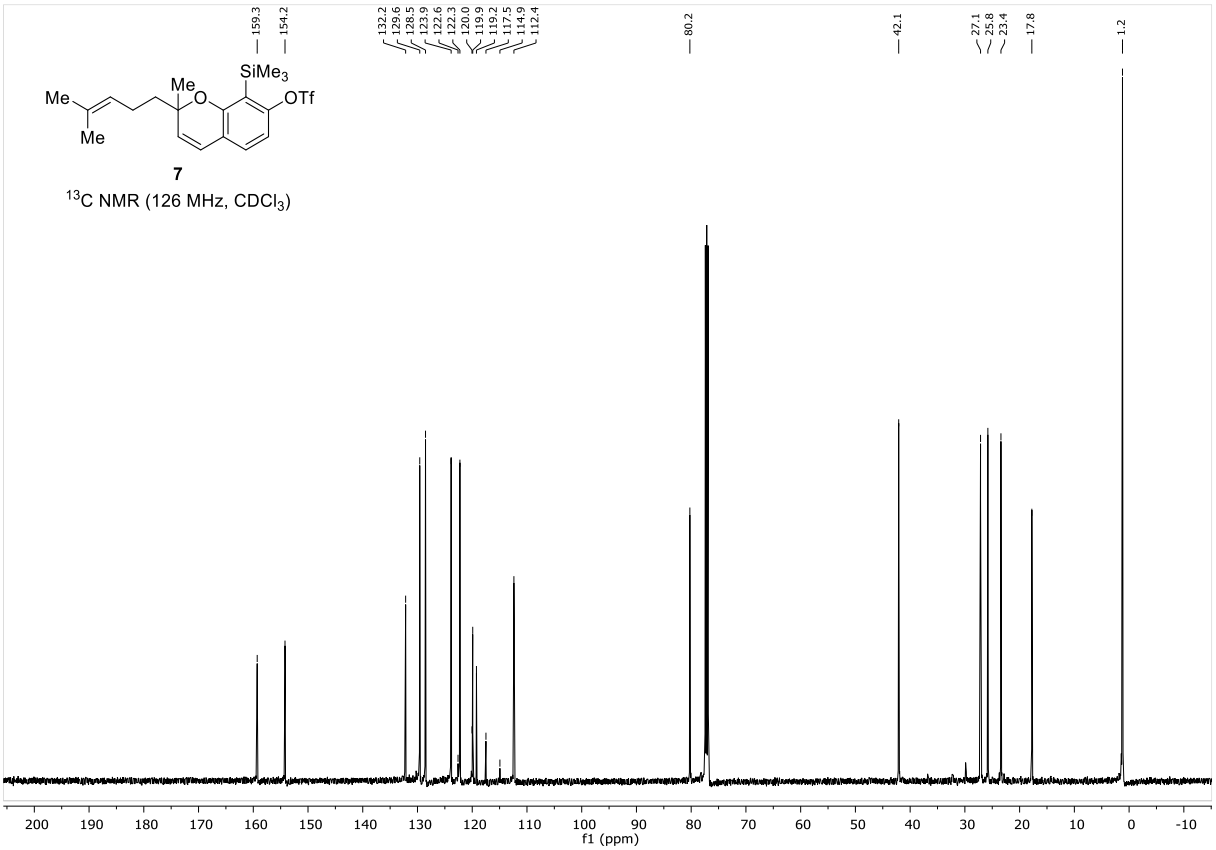
Me
Me
Me
O
SiMe3
OTf
7
13C NMR (126 MHz, CDCl3)
f1 (ppm)

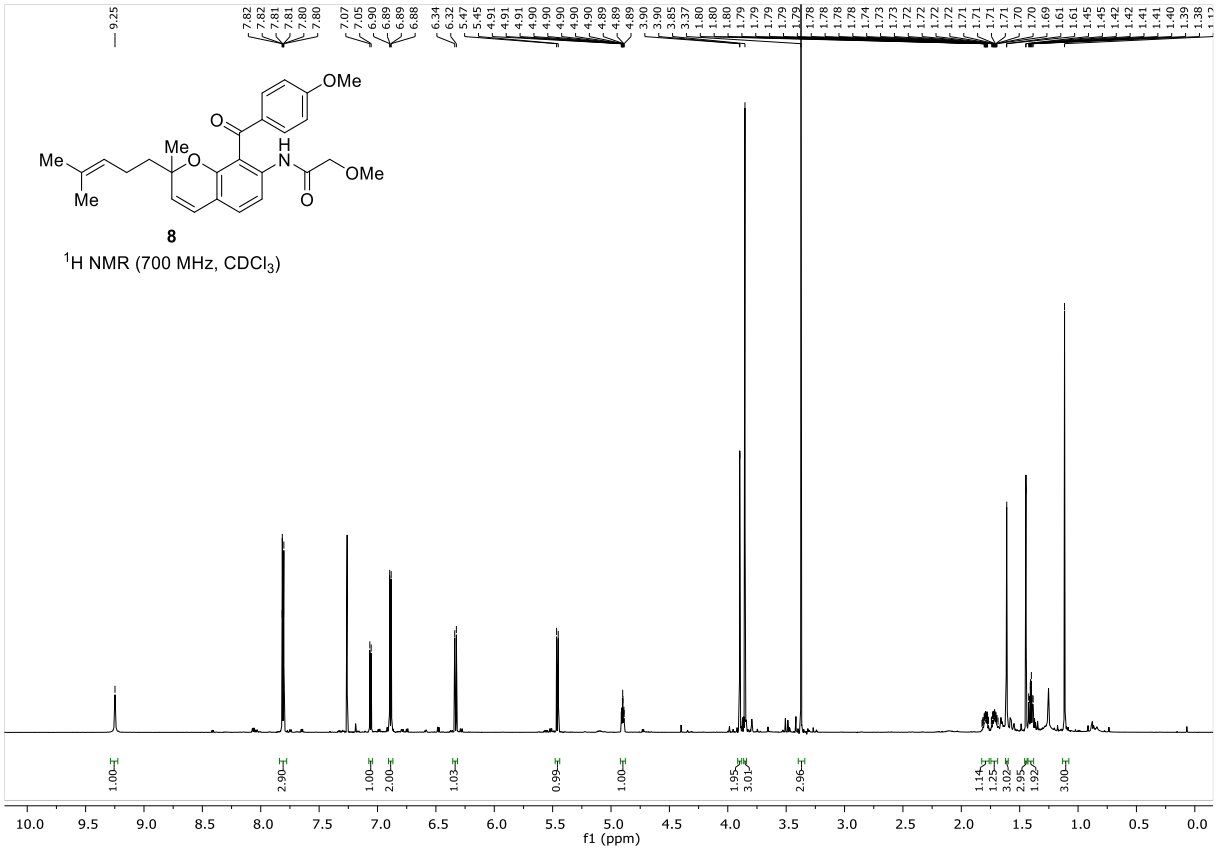
OMe
O
H
N
Me
O
OMe
Me
Me
O
8
1H NMR (700 MHz, CDCl3)
f1 (ppm)

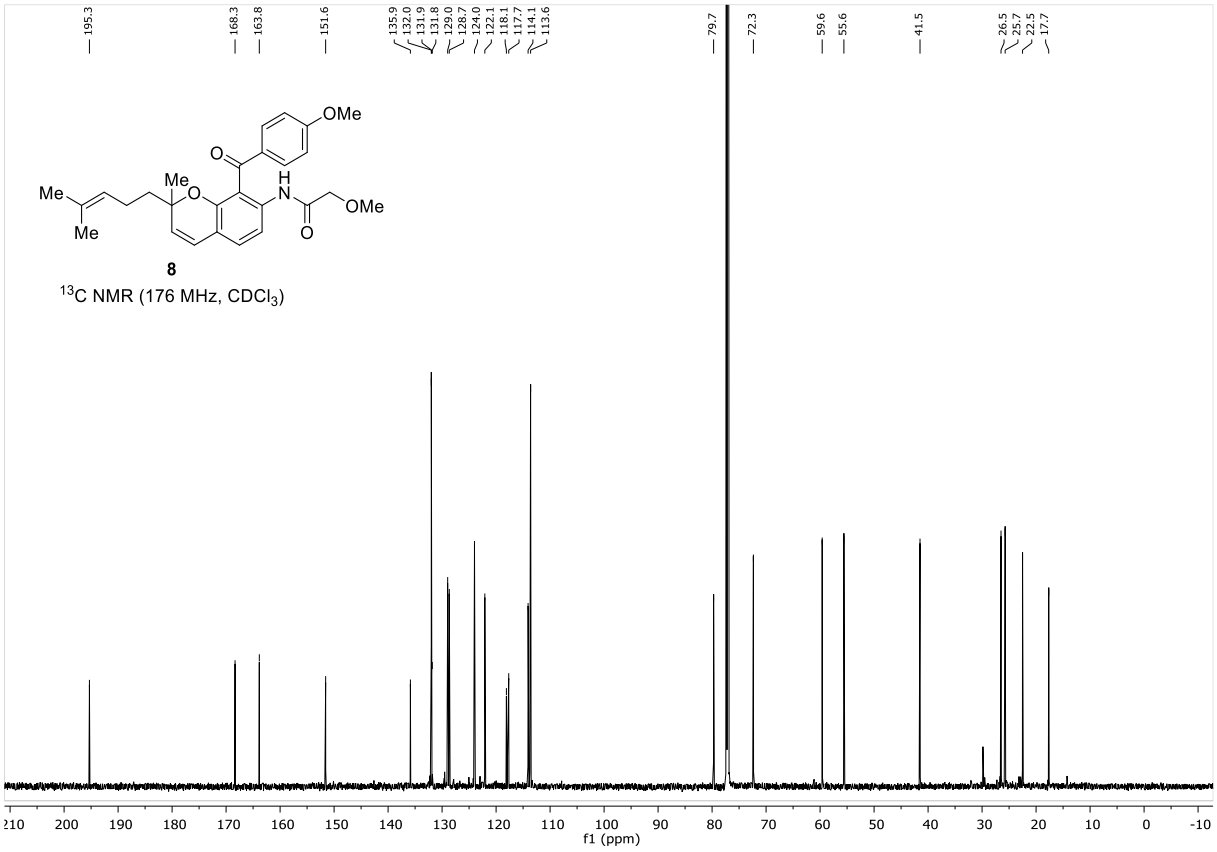
OMe
O
H
N
Me
O
OMe
Me
Me
O
8
13C NMR (176 MHz, CDCl3)
f1 (ppm)

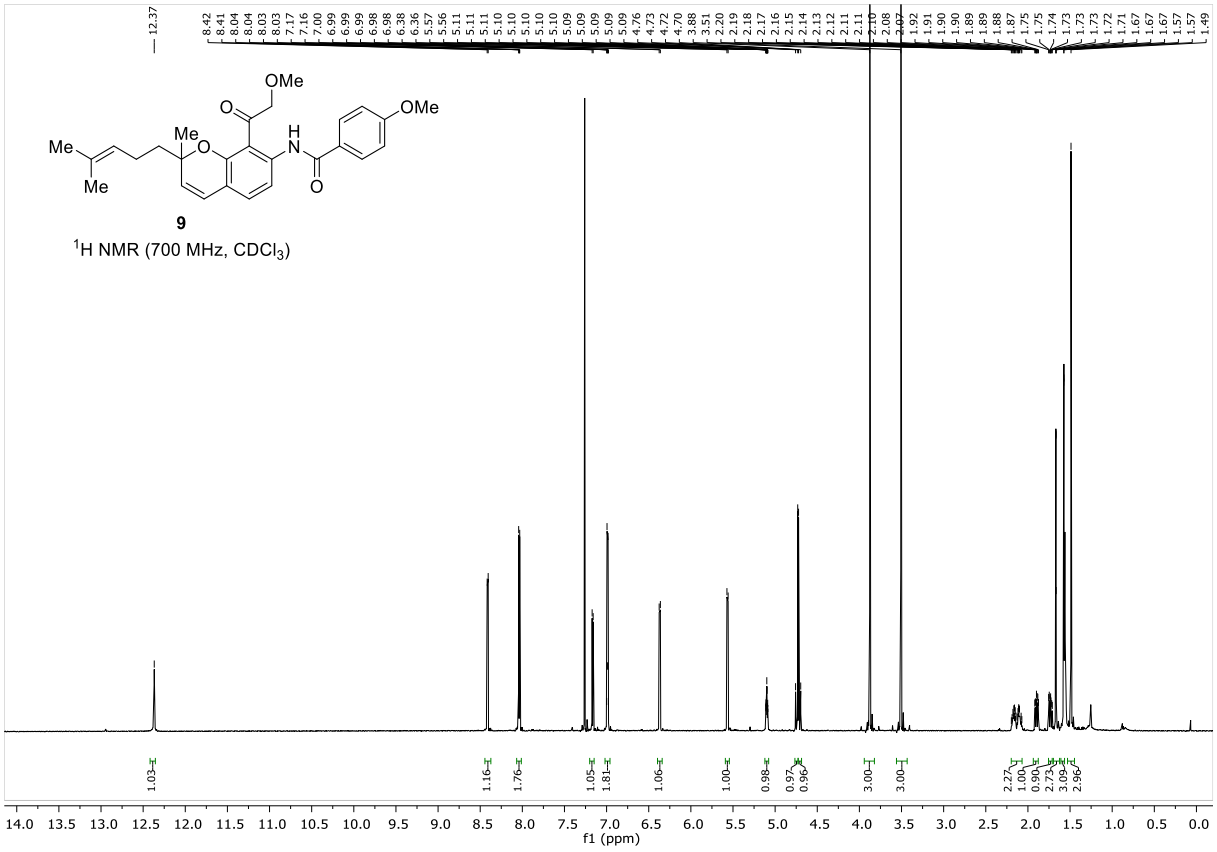
OMe
O
OMe
Me
O
H
N
Me
Me
O
9
1H NMR (700 MHz, CDCl3)
f1 (ppm)

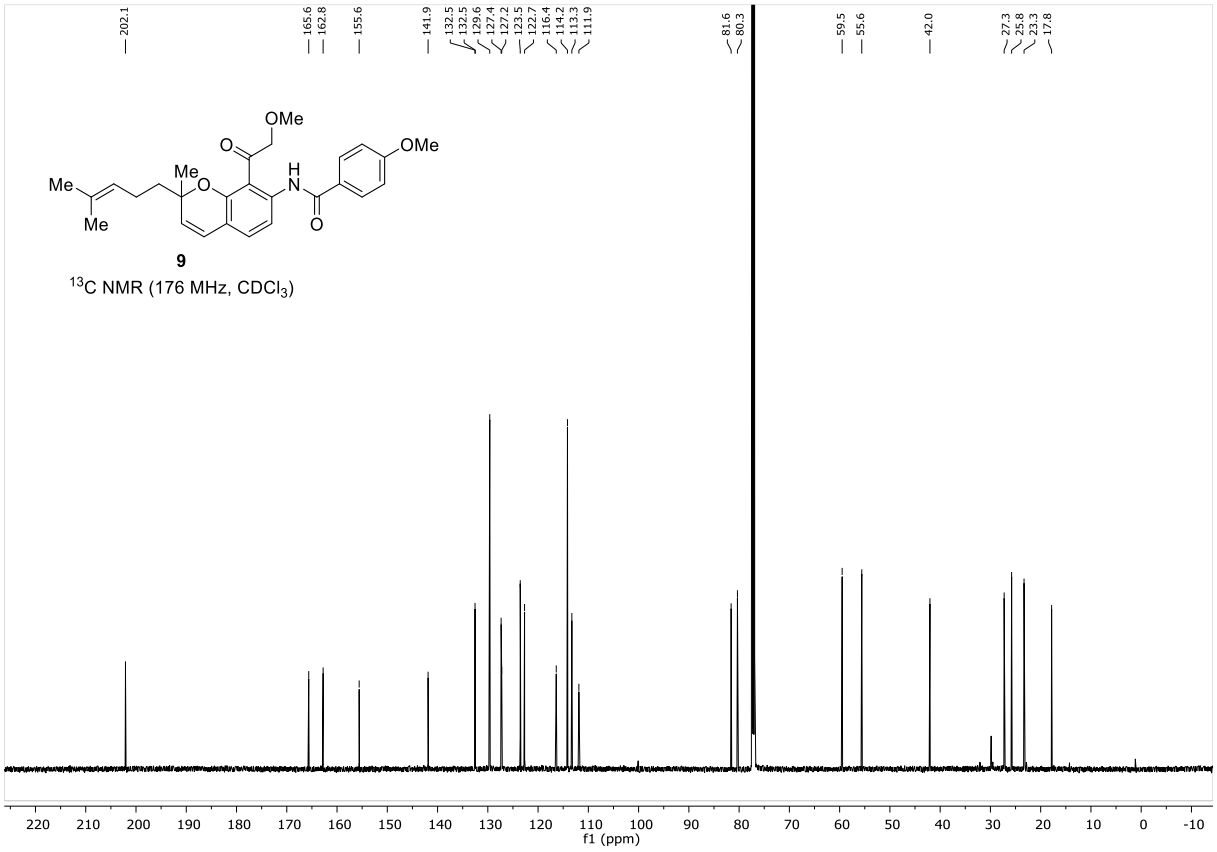
OMe
O
OMe
Me
O
H
N
Me
Me
O
9
13C NMR (176 MHz, CDCl3)
f1 (ppm)

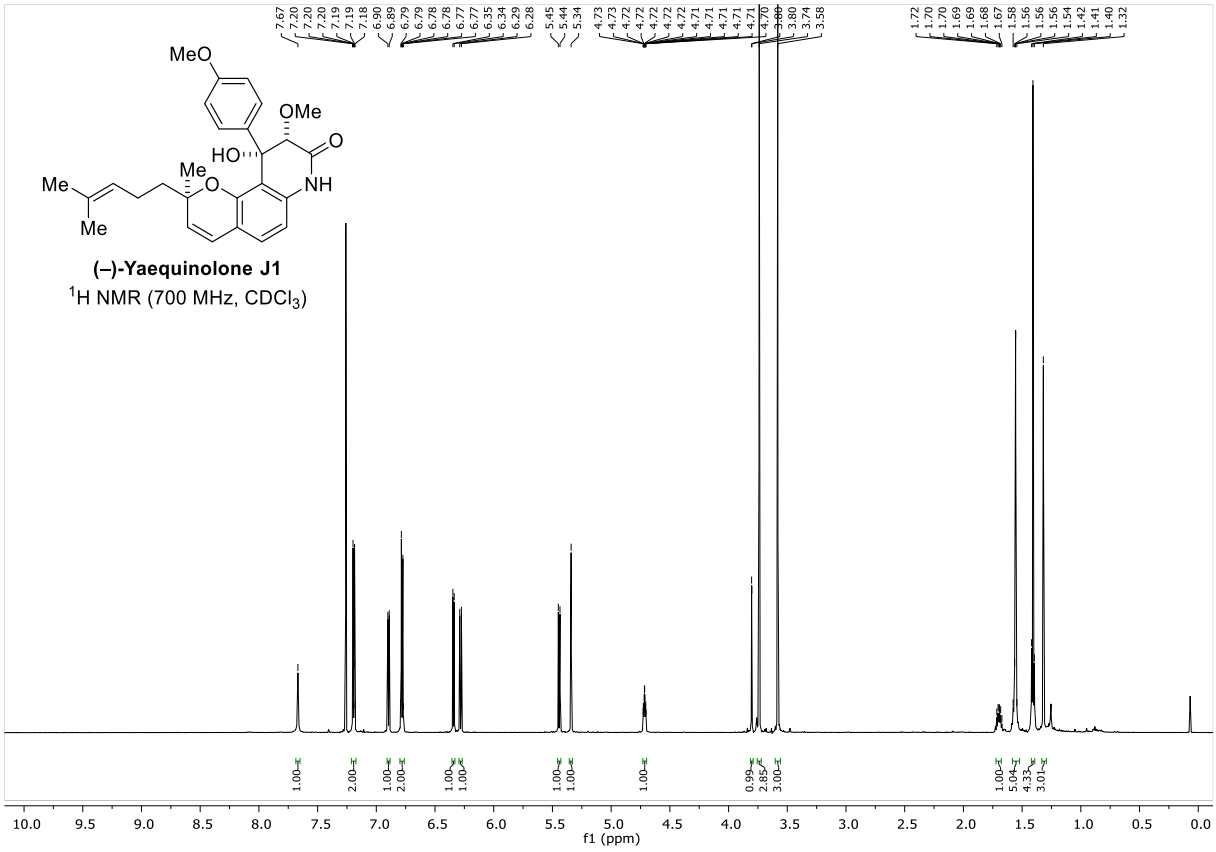
MeO
OMe
HO
O
Me
O
NH
Me
Me
(–)-Yaequinolone J1
1H NMR (700 MHz, CDCl3)
f1 (ppm)

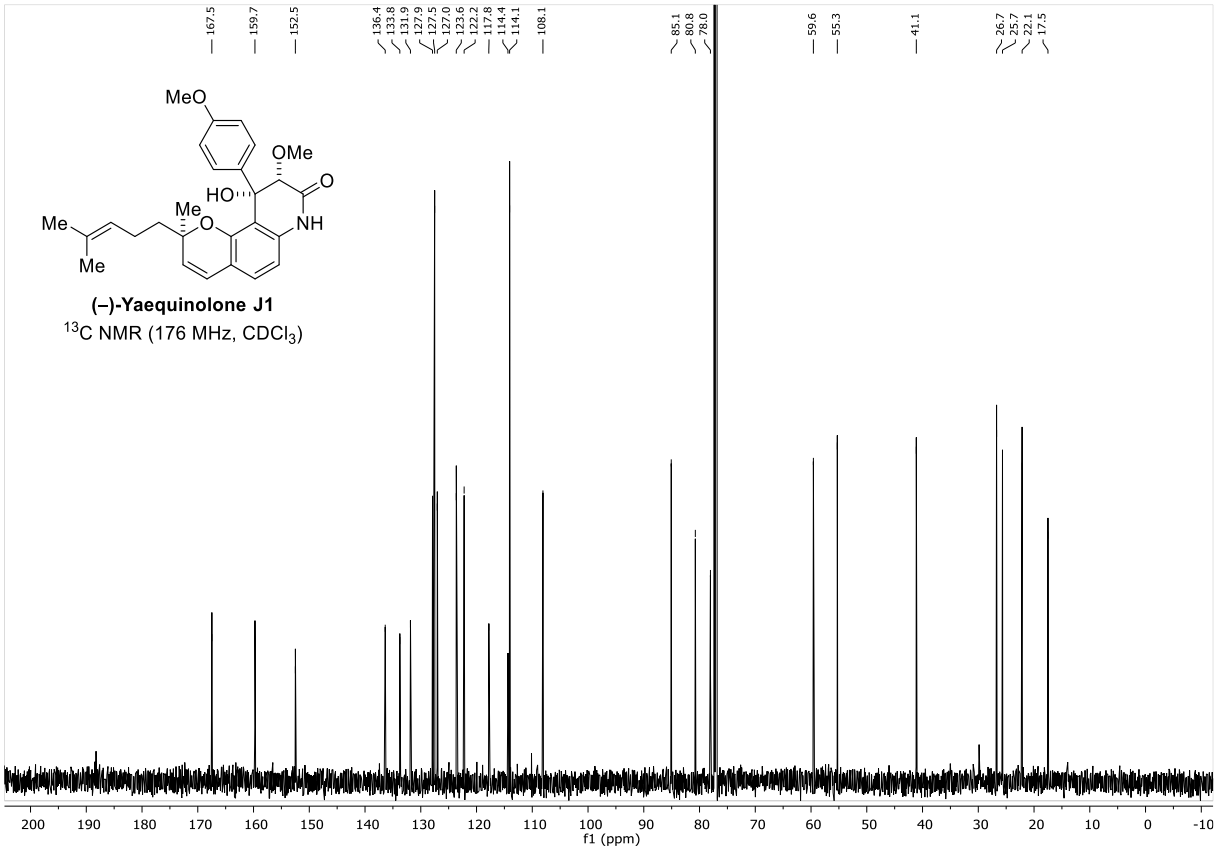
MeO
OMe
HO
O
Me
O
NH
Me
Me
(–)-Yaequinolone J1
13C NMR (176 MHz, CDCl3)
f1 (ppm)

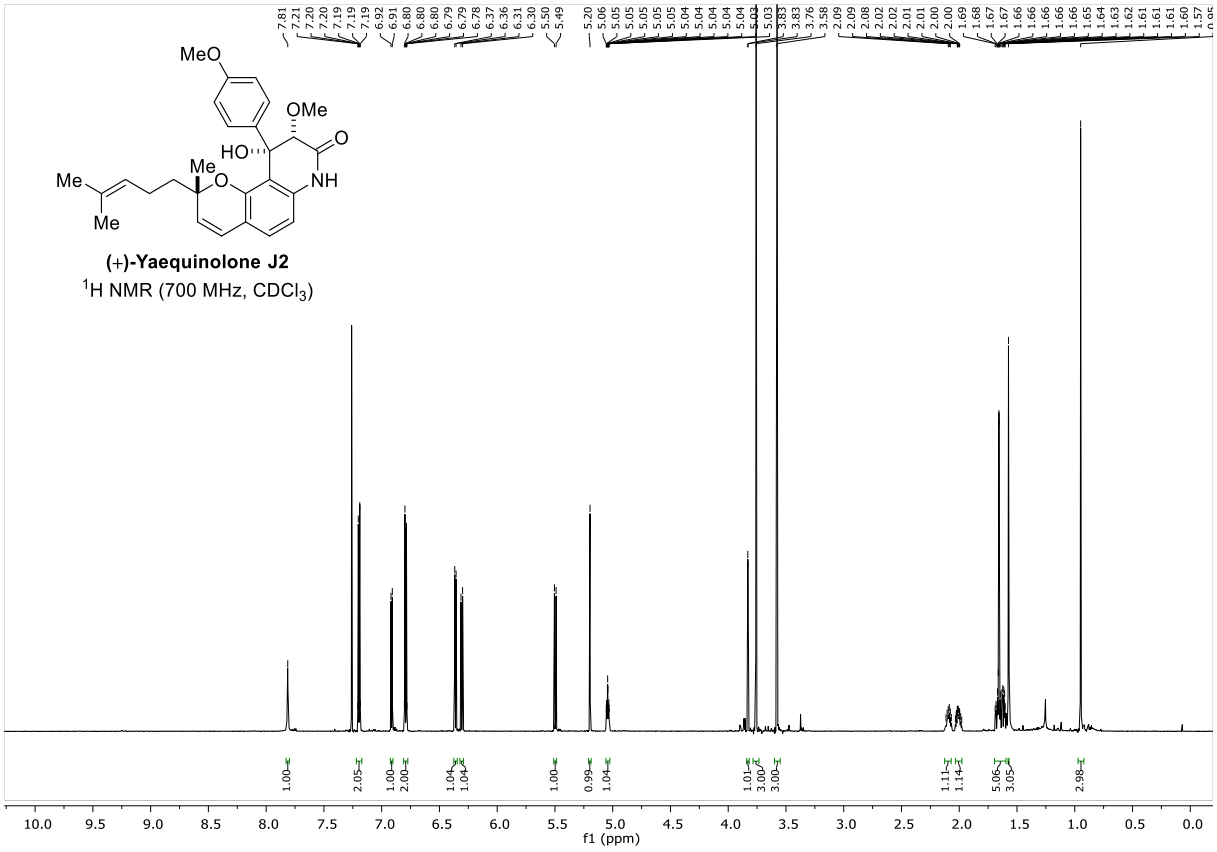
MeO
OMe
HO
O
Me
O
NH
Me
Me
(+)-Yaequinolone J2
1H NMR (700 MHz, CDCl3)
f1 (ppm)

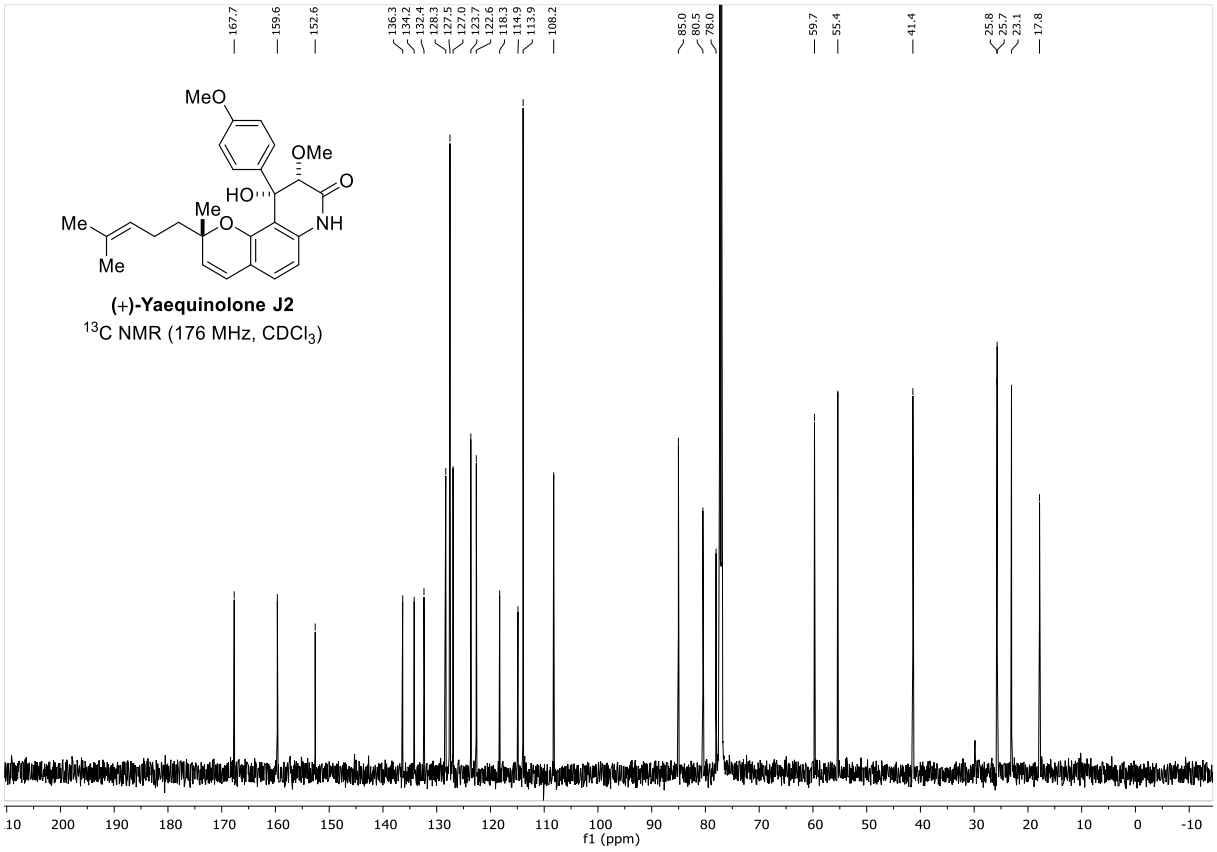
MeO
OMe
HO
O
Me
O
NH
Me
Me
(+)-Yaequinolone J2
13C NMR (176 MHz, CDCl3)
f1 (ppm)